University of Strathclyde

Strathclyde Institute of Pharmacy and Biomedical Sciences

The impact of hypoxia on nanomedicine uptake and efflux in human breast cancer cells

By

William J. Brownlee

A thesis presented in fulfillment of the requirements for the Degree of Doctor of Philosophy

2018

This thesis is the result of the author's original research. It has been composed by the author and has not been previously submitted for examination which has led to the award of a degree.

Signed:

Date:

Acknowledgements

This thesis has only been possible thanks to help from a wide range of people. Firstly, I would like to thank my two supervisors, Dr. Philipp Seib and Prof. Clive Wilson.

I would also like to thank those special people who have enhanced the PhD experience, namely, Sukrut Sumani, Sajjad Ali Khan, Louise Ritchie (Wilson), Partha Laskar, Intouch Sakpakdeejaroen, and any of the many other people who have in their own way improved the research experience**.**

Others to thank, Dr. Mairi Sandison, Graham Mackenzie, Gillian Robb, John Nevin and finally, Richard Pratt (for all the Nitrogen).

Dedication

This work is dedicated to my late mother.

Abstract

In women, breast cancer is the most frequently diagnosed neoplasm, with a recognised high mortality burden. Breast cancer cells adapt to the hypoxic tumoral environment by undergoing changes in metabolism, cell signalling, endo-lysosomal receptor uptake and recycling. The resulting hypoxic cell phenotype has the potential to undermine the therapeutic efficacy of nanomedicines designed for endocytic uptake and specific intracellular trafficking (Chapter 1). The aim of this thesis was to examine the impact of hypoxia and simulated reperfusion on the *in vitro* uptake and release of nanomedicines by human breast cancer cells. Cells were exposed to a hypoxic preconditioning treatment in 1% oxygen for 6 and 24 hours to induce temporal changes in the hypoxic circuit (e.g. HIF1α expression). The preconditioned cells were then dosed with nanoparticles for 45 or 180 minutes emulating nanomedicine access following tumor reperfusion. Hypoxic preconditioning significantly increased nanoparticle retention by up to 10% when compared to normoxic cultures (p<0.001), with the greatest relative difference between normoxic and hypoxic cultures occurring with a 45 minute dosing interval (Chapter 3). Similarly, 24 hours hypoxic conditioning significantly increased nanoparticle uptake, in MDA-MB-231 cells, where HIF1α was partially inhibited by digoxin (p<0.001, Chapter 4). Exocytosis studies indicated that the preconditioned cells had a significantly increased nanoparticle efflux (up to 9%, p<0.001) when compared to normoxic cells (Chapter 3). Overall, this thesis has demonstrated that hypoxic preconditioning regulates both the endocytosis and exocytosis of

nanomedicines in human breast cancer cells (Chapters 3 and 4).

Table of contents

Chapter 1

Chapter 2

Chapter 3

List of figures

List of tables

List of abbreviations

ANOVA	analysis of variance
AP2	Adapter Protein 2
arf6	Adenosine diphosphate ribosylation factor 6
ARNT1	Aryl hydrocarbon receptor nuclear translocator
ATP	Adenosine triphosphate
CAIX	Carbonic anhydrase 9
CBP	Cyclic adenosine monophosphate response element binding protein
cited-2	CbP/p300 interacting transactivator
CLIC	Clathrin and caveolin independent carrier
CoA	Co-enzyme A
$CoCl_2$	Cobalt chloride
DNA	Deoxyribonucleic acid
DU145	Human prostate cancer cell line
E3	Enzyme 3
ECL	Enhanced chemiluminescence
ECM	Extracellular matrix
EGFR	Epidermal growth factor receptor
EMT	Endothelial mesenchymal transition
EPR	Enhanced permeability and retention
ER	Endoplasmic reticulum
FACS	Fluorescence activated cell sorter

FBS	Foetal bovine serum
FDA	United States Food and Drug Administration
FIH1	Factor inhibiting hypoxia inducible factor
FITC	Fluoresceine isothiocyanate
G/A CGTG	Nucleotide sequence, corresponding to guanine/adenine cytosine guanine thymidine guanine
GEEC	Glycosylphosphatidylinositol – anchored protein enriched compartments
GLUT1	Glucose transporter 1
GLUT3	Glucose transporter 3
GTP	Guanine triphosphate
HeLA	Henrietta Lacks human cervical cancer cell line
HER1	Human epidermal growth factor receptor 1
HER2	HER2 receptor
Her2	Her2 receptor
HIF	Hypoxia inducible factor
HIF1	Hypoxia inducible factor 1
HIF1α	The alpha subunit of HIF1
HIF1β	The beta subunit of HIF1 (ARNT)
HIF2	Hypoxia inducible factor 2
HIF2α	Alpha subunit of Hypoxia inducible factor 2
HIF3	Hypoxia inducible factor 3
HIF3α	Alpha subunit of hypoxia inducible factor 3
HRE	Hypoxic response element

HSP60	Heat shock protein 60
HSP70	Heat shock protein 70
IBC	Invasive breast cancer
IC_{50}	Half maximal inhibitory concentration
IUPAC	International Union of Pure and Applied Chemistry
kDa	kiloDaltons
K_m	Michaelis-Menten constant.
L132	Human cell line established from HeLA cells
LDHA	Lactate dehydrogenase A
LDHA	Gene encoding for Lactate dehydrogenase A
LED	Light emitting diode
MCF-7	Michigan Cancer Foundation 7
mmHg	Millimetres of mercury
mRNA	Messenger ribonucleic acid
MTT	(3-(4,5- dimethylthiazol-2-yl)-2,5-diphenyltetrazolium bromide
nab	Nanoparticle albumin-bound
nm	Nanometre
O_2	Oxygen
O_2^-	Superoxide
ODD	Oxygen degradation domain
OR	oestrogen receptor
P300	Adenovirus early region 1A binding protein
P402	Prolyl residue 402 of hypoxia inducible factor 1 alpha

P564	Prolyl residue 564 of hypoxia inducible factor 1 alpha
PAS-B	per-arnt-sim b
PBS	Phosphate buffered saline
PDK1	gene encoding pyruvate dehydrogenase kinase 1
PDK1	pyruvate dehydrogenase kinase 1
PHD	Prolyl hydroxylase domain
PHD2	Proly hydroxylase domain enzyme 2
phosphor p53	Phosphorylated p53
PK1	Prague-Keele 1
PO_2	Oxygen partial pressure
PR	Progesterone receptor
REST	repressor element-1 silencing factor
ROS	reactive oxygen species
RPMI	Rosewell Park Memorial Institute
SD	standard deviation
SDS	sodium dodecyl sulphate
SDS PAGE	sodium dodecyl sulphate polyacrylamide gel electrophoresis
SIRT2	NAD-dependent deacetylase sirtuin – 2
SNJ1	synaptojanin 1
SOD2	mitochondrial superoxide dismutase 2
TBST	tris-buffered saline TWEEN→
VEGF	Vascular endothelial growth factor
vHL	Von-hippel lindau factor

α-KG	alpha keto glutarate

Chapter 1

Introduction

1 Introduction

1.1 Background

Breast cancer is still the most commonly diagnosed cancer, and cause of cancer death in women across Europe and worldwide, making up 25% and 15% of all cancer diagnoses and deaths respectively, in 2012 (Ferlay *et al.* 2013; McGuire, 2016). Here in Scotland, according to comprehensive 2016 data (published 2018) from NHS Scotland (ISDScotland, 2018), it is the highest ranked of all newly diagnosed cancers in women, accounting for 28.7% of total cancer diagnoses.

The heterogeneous nature of breast cancer means it is as with many other cancers, classified via several criteria, based upon progression (clinical stage), size, invasiveness, cellular histology, morphology and gene profiling (Schnitt, 2010; Sotiriou *et al.* 2003). From a molecular therapeutics and treatment regimen perspective however, an important distinction can be made depending upon the tumour cell membrane receptor expression profile. Around 75% of invasive breast cancer express one or several of either oestrogen, progesterone and Her2 receptors (Lal *et al.* 2017; Mitri *et al.* 2012). Those expressing oestrogen or progesterone receptors are termed hormone receptor positive, and first line treatment can include agents like the oestrogen receptor competitive antagonist Tamoxifen→ or (in post menopausal women, and men), aromatase inhibitors. Those overexpressing Her2 receptors may be treated with the Her2 receptor blocking monoclonal

antibody Trastuzumab (Herceptin) (Lal *et al.* 2017; Mitri *et al.* 2012), or Pertuzumab (Perjeta) (De Mattos-Arruda and Cortes, 2013).

Around 15% of invasive breast cancers however, do not express those three hormone based receptors, and are accordingly termed triple negative breast cancer (Brenton *et al.* 2005). Actual morbidity rates for triple negative breast cancer vary by population and ethnicity. For example, in the United States of America, the actual incidence rate across all ethnicities is 15.5 per 100,000 women, yet among non-hispanic black populations, the incidence is much higher at 27.2 per 100,000women (Kohler *et al.* 2015). For treatment of triple negative, late stage and secondary (metastatic) breast cancer, there is still a dependency upon cytotoxic chemotherapeutic agents. Whilst such agents are effective in either limiting or slowing tumour growth, given their non-specific cytotoxicity, they are often akin to a pharmacological 'sledgehammer to crack a walnut'.

A great deal of research therefore, has focused on developing methods for more selective targeting of such agents, and facilitating increased drug delivery to the tumour site, whilst minimizing the often damaging, systemic side effects.

In tandem with this, over recent decades, innovative research has significantly expanded the scientific understanding of tumour biology, metastasis (spread from original tumour site) and oncological mechanisms.

From a pharmacological and drug development perspective, this has opened up the potential of new molecular therapeutic targets in the treatment of all cancers (Wigerup *et al.* 2016). Equally, however, it has thrown up a challenge within drug development, to make best use of this new knowledge, most effectively, and in a time and cost effective manner (Juliano, 2013; Venditto and Szoka, 2013). One major aspect of this challenge, is the recognised need to more fully understand how anticancer therapeutics interact within solid tumors, where cellular behavior and growth demonstrates radical differences from normal physiological healthy tissues and organs (Denison and Bae, 2012). A fundamental driving force of significant changes seen with solid tumour cells, is the characteristic reduction in intracellular oxygen, termed hypoxia (Höckel and Vaupel, 2001). Given the importance of intratumoral hypoxia, and its implications for effective therapeutic drug delivery, there is a considerable interest in fully exploring drug delivery within hypoxic tumour cells. This study aims to develop a better understanding of how intratumoral hypoxia may influence the cellular uptake and efflux of a specific category of anticancer therapeutics. In order to undertake this research, a background understanding of tumour hypoxia and its implications for tumour biology is required.

1.2 The hypoxic tumour environment

Solid tumours do not possess their own inherent vascular system, and as the characteristically sporadic, unregulated, neoplastic growth of a solid tumour increases, the diffusion distances for nutrients and oxygen become greater.

It has been shown that diffusion distances much greater than 100-150 μm (Thomlinson and Gray, 1955) leads to the development of regional or localised hypoxia within tumour cells (Figure 1.1).

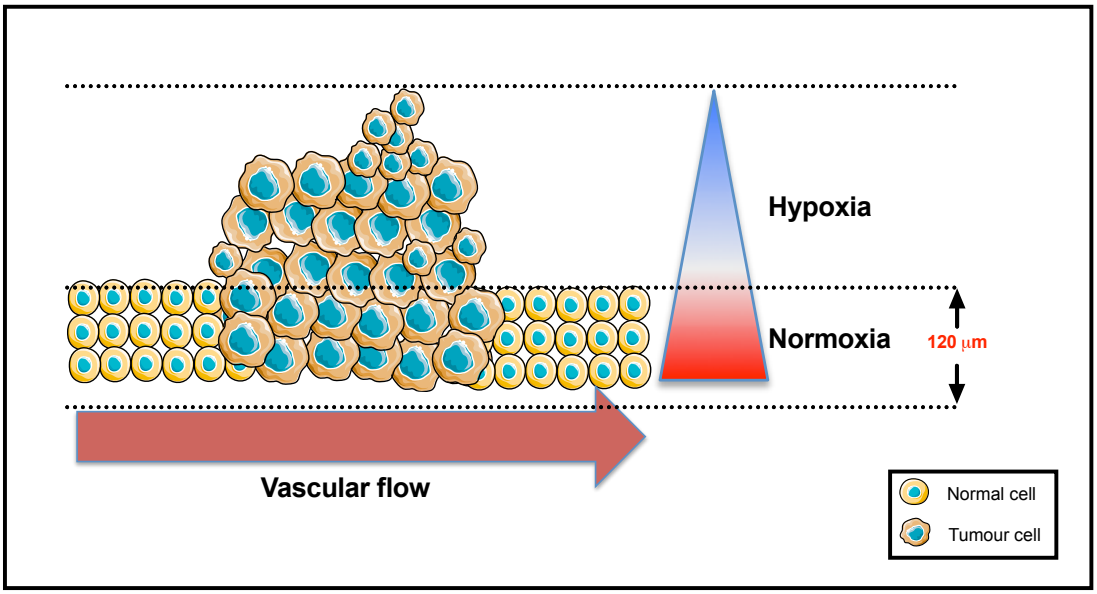

Figure 1.1 Development of diffusion limited intratumoral hypoxia. As rapid tumor growth exceeds oxygen diffusion limits, hypoxic condition develop, leading to a cascade of cellular hypoxic adaptive changes.

As tumour growth progresses, the developing tumour hypoxia leads to the formation of necrotic zones (Brahimi-Horn *et al.* 2007; Harris, 2002). The hypoxia found in such neoplasms is highly variable (Dewhirst *et al.* 2008), depending upon tumour type, extent of growth, and diffusion distances from available blood vessels. Research has demonstrated that diffusion limited hypoxia, depends upon factors such as vascular flow rate, oxygen tension,

tumor density, and vascular integrity (Helmlinger *et al.* 1997; Milotti *et al.* 2017).

There is no strict definition of hypoxia in physiological systems, because between and within different organs and tissue types, the normal physiological oxygen concentration is highly variable (Table 1.1).

Table 1.1 Table of values recorded for normal (and pathological) oxygen levels within various body tissues, exhibiting a high degree of inter and intra organ variability. For reference, standard atmospheric partial pressure is 760 mmHg, and oxygen partial pressure is ≈ 158 mmHg.

Tissue/organ	PO_2 (mmHg)	References
Liver	Periportal cells ≈ 45-50 Perivenous cells ≈ 30-35	(Jungermann and Kietzmann, 2000; Kietzmann, 2017)
Bone	Periosteum ≈ 50 Endosteal sinusoid ≈ 13.5 Bone marrow ≈ 7 - 29	(Spencer *et al.* 2014; Harrison *et al.* 2002; Johnson *et al.* 2017)
Kidney	72	(Müller *et al.* 1998)
Breast (normal)	65 (median)	(Vaupel *et al.* 2007)
Breast (tumor)	10 (median)	(Vaupel *et al.* 2007)

For example, assessing renocortical O_2 partial pressure in living transplant patients, the physiological PO_2 (partial pressure of Oxygen) in the kidney was in the region of 72 mmHg (9.5%) (Müller *et al.* 1998). In another study, normal brain oxygenation levels were recorded as low as 4.4%, but were highly variable depending upon oxygen sensor location (Dings *et al.* 1998; Hoffman *et al.* 1996), and cerebral activity. Similarly, with the liver, physiological oxygenation is highly variable, depending upon physical structure, blood vessel proximity and location of measurements. Hepatic intracellular values range from 45-50 mmHg to 15-20 mmHg, depending upon arterial or venous proximity (Kietzmann, 2017).

Therefore, it is not straightforward to define with certainty what might be termed the physiological 'normoxia' oxygen level, when compared with a hypoxic level within the same or cancerous tissue. One study (Vaupel *et al.* 1991), measured the median and mean PO_2 in normal breast tissue to be 65 mmHg, whereas within breast cancer tissue (stages T1b - T4) the median PO_2 was 28mmHg. From the same study, almost 60% of all the breast tumours tested, possessed a PO_2 less than or equal to 2.5 mmHg within some regions. Further work has shown that hypoxic regions can be found in 25-40% of invasive breast cancer (Lundgren *et al.* 2007). However, more recently, it was demonstrated that those earlier PO_2 measurements could be misleading due to potential misplacement of oxygen electrodes, thereby leading to artificially higher recorded PO_2 measurements within tumour tissue. A subsequent meta-analysis of breast tumour PO_2 measurements

performed using ultrasound-guided oxygen electrodes, demonstrated a median PO_2 of 10 mmHg, within breast tumour tissue (Vaupel *et al.* 2007).

The key aspect regarding understanding of hypoxia within both normal tissue and tumours, is that it is a level of oxygenation which is below that which might be expected under physiological conditions. Most importantly, the level of oxygenation is below the physiological requirements of a given tissue, to the extent that cellular adaptations and metabolic changes are induced. It is that adaptive process to hypoxia within tumour cells, which is of greatest importance to altered tumour biology, with implications for drug delivery, and will be considered next.

1.3 Cellular adaptations to intratumoral hypoxia

For tumour cells to survive in such a stressful hypoxic environment, there is a requirement for considerable alterations to tumour cell metabolism. A cascade of genomic, proteomic and metabolic changes occur, principally driven via the hypoxia inducible factor (Greer *et al.* 2012; Semenza and Wang, 1992; Wang *et al.* 1995) (HIF) family of transcription factors. This results in an altered tumour cell phenotype, able to exist and proliferate at lower oxygen/nutrient levels. This hypoxic tumour cell phenotype has been shown to possess greater metastatic potential (Brizel *et al.* 1996; Gilkes and Semenza, 2013; Semenza, 2015; Vaupel *et al.* 2004), increased resistance to treatment especially via upregulation of the major drug resistance 1 gene

(Comerford *et al.* 2002; Samanta *et al.* 2014), an association with a clinically aggressive breast cancer phenotype (Yamamoto *et al.* 2007) and to be clinically and experimentally more resistant to ionising radiation therapy (Moeller *et al.* 2007; Shannon *et al.* 2003; Vaupel *et al.* 2001).

Of the HIF family of three transcription factors responsible for this hypoxic adaptation, the greatest current knowledge relates to HIF1, and its role in the hypoxic tumour response. In its functional form as a transcription factor, HIF1 exists as a heterodimer, consisting of an α and β subunit (Wang *et al.* 1995). The β subunit (also known as the aryl hydrocarbon receptor nuclear translocator (ARNT1) (Wang and Semenza, 1995), is a constitutively expressed nuclear protein. In contrast, the α subunit, in the presence of oxygen is hydroxylated at two prolyl residues (P402 and P564) located within the N-terminal oxygen dependent degradation domain (ODD). This chemical modification occurs in an oxygen dependent manner via a family of three iron (Fe^{2+}) and α-ketoglutarate dependent dioxygenases, designated prolyl hydroxylase domain enzymes (PHD) 1, 2 and 3. Importantly, since HIF1β is constitutively expressed, it is the presence of the unhydroxylated 1α sub-unit, which is the primary determinant of transcriptional activation of heterodimeric HIF1.

In the presence of oxygen, hydroxylation of HIF1α, allows its binding with von Hippel-Lindau tumour suppressor protein as part of the E3 ubiquitin ligase complex, leading to HIF1α polyubiquitination, and subsequent degradation

via the 26S proteasome (Kaelin and Ratcliffe, 2008). The prolyl hydroxylases (PHDs) involved, principally PHD2 (Berra *et al.* 2003), have an absolute requirement for O_2, α-ketoglutarate, and Fe^{2+} as co-factors (Kaelin and Ratcliffe, 2008), and so, during hypoxia, where oxygen tension is low, degradation of the α subunit may be attenuated.

This inhibition of prolyl hydroxylation of HIF1α, with even short periodic hypoxia, leads to rapid HIF1α accumulation (Yuan *et al.* 2005), translocation to the nucleus (Depping *et al.* 2008), followed by formation of an active dimeric HIF1 complex together with the β sub-unit and recruitment of the transcription cofactors P300 and CBP (Ruas, 2005) . This transcriptionally active HIF1 dimeric complex, then binds to a highly conserved consensus sequence (G/A CGTG) in the promoter region of target genes called the hypoxic response element (HRE) (Semenza *et al.* 1996). A further dioxygenase enzyme, which appears to form part of the HIF1α regulatory circuit, is factor inhibiting HIF1 (FIH1). This can hydroxylyse asparagine 803 in the HIF1α subunit, thereby blocking its interaction with P300 and CBP (Lando, 2002; Mahon *et al.* 2001), and potential transcriptional activity. FIH1 has a higher affinity and therefore lower K_m for oxygen than the prolyl hydroxylase domain enzymes (Hirsilä *et al.* 2003). Therefore, at low oxygen levels, where PHD2 is inhibited, FIH1 may still influence HIF1α transcriptional activity via arginine hydroxylation (Kaelin and Ratcliffe, 2008; Koivunen *et al.* 2004).

Two other members of the HIF family have been documented, HIF 2α and HIF3α, with variable sequence homology to HIF1α. Each forms an active transcriptional factor via binding with HIFβ, as is the case with HIF1. The roles of HIF2 and HIF3, are still under investigation, although it seems that HIF2 has related functionality to HIF1 (Lau *et al*. 2007), with a distinct HIF1 inhibitory role for HIF3 (Makino *et al*. 2007).

Thus, in normoxia, HIF1α is effectively degraded, but in hypoxia, with the failure of PHDs, and other factors, HIF1α and its β subunit, together, act via the HRE to promote key gene transcription, responsible for the cellular response to hypoxia (Figure 1.2).

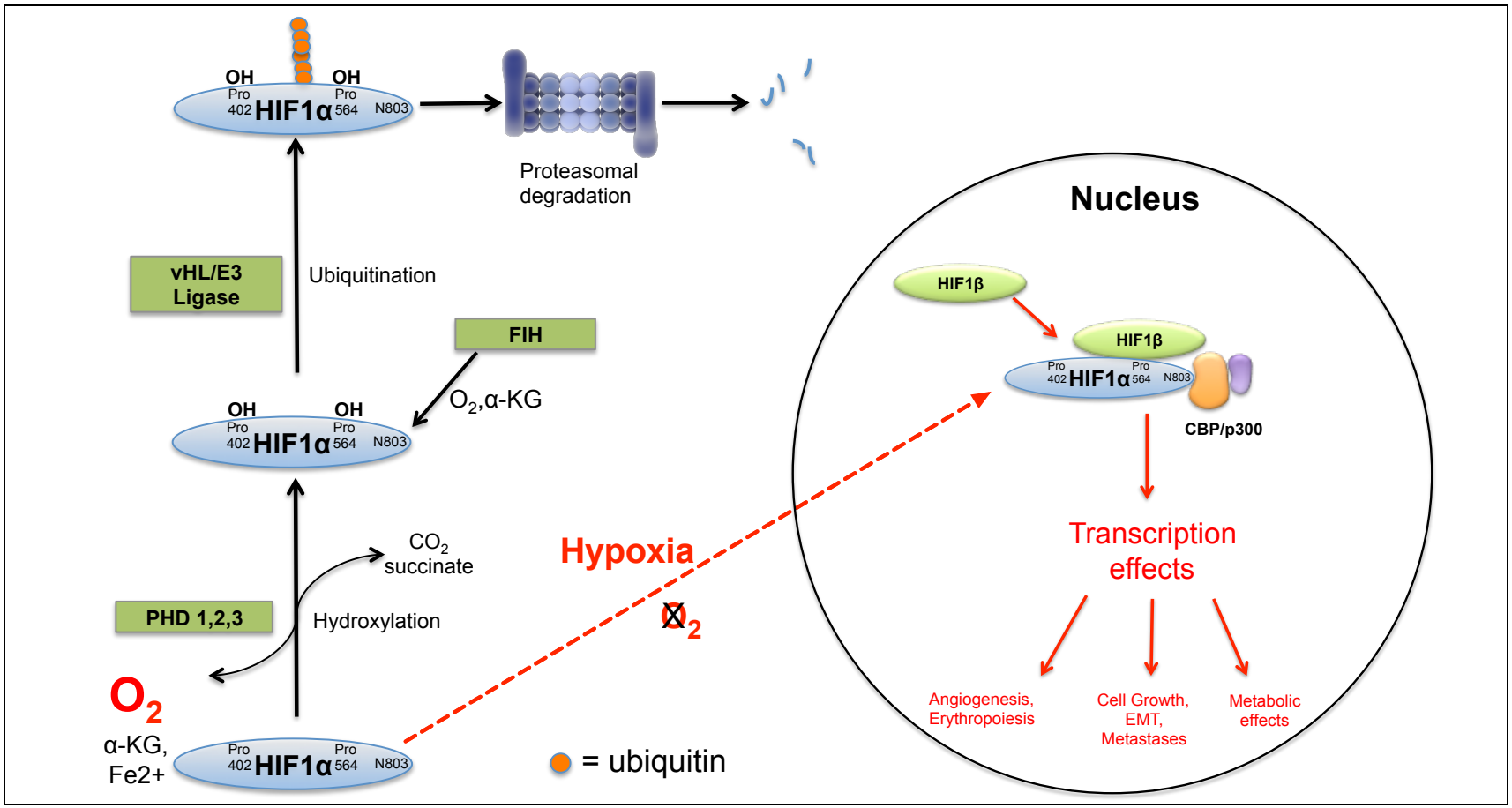

Figure 1.2 The key effector of cellular response to alterations in oxygen level, HIF1α, is continually broken down via the degradation pathway indicated in black arrows. In Hypoxia (red arrows), HIF1α translocates to the nucleus, where in combination with HIFβ, induces cellular adaptations via the hypoxic response element.

It is interesting to note, that the Fe^{2+} which forms part of the catalytic centre of PHDs, can be displaced by cobalt from cobalt chloride, leading to enzymatic inhibition. This inhibition of PHD prolyl hydroxylation activity, prevents proteasomal breakdown of HIF1α, leading to its intracellular accumulation even in the presence of oxygen (Epstein *et al.* 2001; Yuan *et al.* 2003).

There are currently over 800 human genes identified that are influenced by hypoxic induction factors (Schodel *et al.* 2011), and HIF may also influence other genes through its interaction with genes responsible for micro RNA's (Crosby *et al.* 2009). Aside from increasing invasiveness (Chan and Giaccia, 2007), angiogenesis (Liao and Johnson, 2007), cell growth and metastatic potential (Carnero and Lleonart, 2015; Indelicato *et al.* 2010; Sullivan and Graham, 2007), gene expression altered by hypoxia directs major changes to cellular metabolism and energy.

HIF1 achieves changes in tumour cell energy production, via amongst others, altered expression of genes such as *PDK1* that encodes for the enzyme pyruvate dehydrogenase kinase 1(PDK1). This enzyme inactivates pyruvate dehydrogenase via phosphorylation, thereby preventing conversion of pyruvate to acetyl CoA, for entry into the Krebs cycle (Kim *et al.* 2006; Papandreou *et al.* 2006). Similarly, with *LDHA,* which encodes for lactate dehydrogenase A (LDHA), which converts pyruvate to lactate (Semenza *et*

al. 1996). These, in conjunction with several other genes, such as those for the glucose transporters GLUT1 and GLUT3, help shift cellular metabolism further away from O_2 dependent oxidative Phosphorylation, and towards glycolysis, with subsequent potential for less efficient ATP synthesis (Semenza, 2013).

Oxidative phosphorylation with reduced O_2 tension, results in the formation of reactive oxygen species (ROS), such as superoxide (0_2^-). Originally, it was thought that the lack of oxygen during hypoxia provoked the shift from oxidative phosphorylation to glycolysis, although it has been suggested (Semenza, 2012a), that the shift to glycolysis, could be a cellular protective mechanism against superoxide driven cellular damage. Despite descriptions of this glycolytic shift in metabolism having been first described in 1924 (Devic, 2016; Warburg, 1956), the exact nature of these hypoxia induced metabolic changes, is still not entirely clear.

Overall, as the key effector of cellular hypoxic adaptation, and its influence within cancerous cells, elevated HIF1α levels have been shown to be a stand alone negative prognostic indicator in breast cancer, in a number of research studies (Kronblad *et al.* 2006; Trastour *et al.* 2007; Yamamoto *et al.* 2007).

Despite the many cellular adaptations in response to hypoxia, the fundamental imbalance between the molecular demands of rapidly proliferating tumor cells and the deficient oxygen and nutrient supply usually

persists. Indeed, the principle exacerbating factor is rapid tumour cell proliferation and growth, driven partly by hypoxic adaptive changes. The mechanism, angiogenesis, which directly addresses this imbalance via neovascularisation of hypoxic tumor cells, is of great significance. Not only are angiogenesis and neovascularisation influential to tumor survival and proliferation, but also, by their inherent nature, to the development and successful delivery of anti cancer therapeutics.

1.4 Intratumoral angiogenesis

Tumour cells respond to hypoxia via co-ordinated molecular signalling to alter the existing physiological blood supply, amending its growth, leading to angiogenesis and vascular diversion to the tumour tissue. Without this process, solid tumours may not grow much beyond 1-2 mm^3 (Folkman, 2003), and so this angiogenesis, driven by tumour hypoxia is an important step in tumour development. It was Judah Folkman in 1971 (Folkman, 1971), who first elucidated this fundamental aspect of tumor development, demonstrating the close link between vascular development and tumor proliferation. Unlike normal, physiological blood vessel development, which is tightly regulated, tumour angiogenesis is a poorly regulated, uncoordinated process.

The tumoral angiogenesis induced by the hypoxic environment found within solid tumors, has a number of consequences in terms of therapeutic drug

delivery. Tumor angiogenesis, as a consequence of hypoxia, is effected via the release of a number of growth factors from tumor cells including, vascular endothelial growth factor (VEGF) (Forsythe *et al.* 1996; Shweiki *et al.* 1992), platelet derived growth factor β and angiopoeitin – 2 (Kelly, 2003). This produces a defective vascular network which develops around and within solid tumours, characterised by blind ends, tortuous routing, arteriovenous shunts, and irregular vessel structure with ineffective basement membrane and tight junctions (Konerding *et al.* 1999; Vaupel *et al.* 1989). This ineffective angiogenesis, and a lack of hierarchical structure, results in poor perfusion, punctuated by periodic low or negative blood flow (or plasma only flow), stasis and thrombosis, all of which have implications for successful cancer drug delivery.

The inability of tumors to fully develop a co-ordinated, fully functional vascular bed in itself, rather than resolving hypoxia, can excacerbate or lead to a continuation of inadequate, highly variable oxygenation. Within that multifactorial milieu, tumor cell hypoxia is now divided into two distinct categories (Bayer *et al.* 2011). Acute (or cycling) hypoxia is caused by vessel occlusion, or sudden obstruction due to thrombus, or tumor cell growth, whereas chronic hypoxia is due to increasing diffusion distances of tumor cells from an effective blood supply. As a consequence, with acute hypoxia, oxygen delivery can be halted and re-continued from minute to minute producing short periodic reperfusion via so-called vascular bursts. In contrast, chronic hypoxia, due to limited diffusion through tumour cellular

masses, is resolved over a period of days via increased vascular growth and development. These two classifications of tumor hypoxia can be further subdivided, via a number of criteria (Bayer *et al.* 2011), but that is beyond the scope of this research. From a pharmaceutics and drug delivery perspective, it is the way in which this dysfunctional intratumoral vascular development, together with hypoxia may diminish or enhance the delivery of chemotherapeutic agents, which is of most interest.

Possibly the most important opportunity presented by the poorly developed and ineffective tumoral vasculature to enhance drug delivery, is what is termed the enhanced permeability and retention effect.

1.5 Enhanced permeability and retention effect

The highly permeable tumour vasculature can allow the free transit of macromolecules into the tumor interstitium. This can lead to a passive selectivity of tumor tissue for macromolecular drug complexes when compared with normal tissues and organs. This passive process, termed the enhanced permeability and retention effect (EPR) (Matsumura and Maeda, 1986; Maeda *et al.* 2013) , due to the increased endothelial permeability and reduced lymphatic drainage found within the tumour environment, has been shown (Seymour *et al.* 1994) to selectively increase macromolecular drug

delivery and accumulation in the tumour extracellular matric (ECM) compared to normal tissues.

Numerous technologies have been developed for joining or enveloping chemotherapeutic agents, to create macromolecular structures, with the aim of taking advantage of the EPR effect. Ideally such macromolecules would, *in vivo*, exhibit increased retention within tumour tissue when compared to normal tissues, thereby reducing systemic cytotoxicity yet similar or better efficacy, with a lower overall dose. Due to the fact that the dimensions of most macromolecular therapeutics suitable for this fall within the nanometer scale, they are referred to as nanomedicines.

1.6 Nanomedicines

Therapeutic small molecules used to treat cancer are often hydrophobic, with limited aqueous solubility, non-specific cytotoxicity, and non-directed biodistribution. Burdened with narrow therapeutic indices, and severe toxic side effects, such molecules often possess limited potential for prolonged dosing and effective long-term treatment of tumours. A good example of such a scenario, is with the effective anticancer cytotoxic anthracycline, doxorubicin. One of the major limitations of this drug in the treatment of cancer is cardiomyopathy and heart failure which the drug can cumulatively induce (Chatterjee *et al.* 2010; Ewer *et al.* 2004). To an extent this cytotoxic effect is reduced with the pegylated liposomal version of doxorubicin (Muggia

et al. 2018). This nanomedicine called Doxil (Figure 1.3), leads to reduced cardiac side effects principally via selective accumulation of the active drug doxorubicin outside cardiac tissue and in tumour tissue (O'Brien *et al.* 2004). The benefits include increased treatment duration, and potential for repeated dosing over time. However, Doxil itself, has its own, albeit less permanent and damaging, side effects, including severe desquamating dermatitis, commonly referred to as 'foot and hand syndrome' (Barenholz, 2012). Similarly, the successful anticancer compound paclitaxel, with limited solubility, is typically administered together with a toxic excipient, Cremophor (a mixture of ethanol and polyethylated castor oil), to enhance solubility. The severe side effects of this excipient are avoided by the enhanced solubility of the albumin based nanomedicine formulation of paclitaxel, Abraxane (Gradishar *et al.* 2005; Gradishar, 2008; O'Shaughnessy *et al.* 2013).

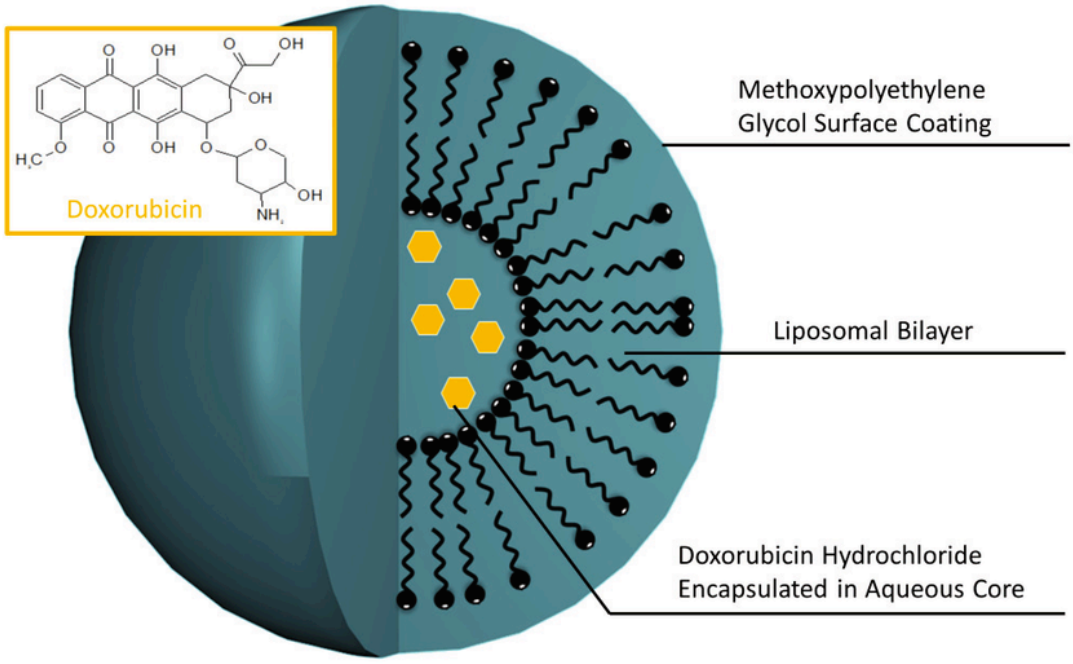

Figure 1.3 Schematic diagram of Doxil. The anticancer anthracycline, doxorubicin, encapsulated within liposomal nano-sized spheres, coated with methoxypolyethylene glycol. Results in enhanced circulatory stability, reduced systemic toxicity and increased intratumoral accumulation. Source; (Engelberth *et al*., 2014).

Nanomedicines, where such small molecule (and other) anticancer therapeutics are incorporated with, or encapsulated in, biocompatible nanoscale particles, liposomes or polymers, have for many years offered potential as alternatives for tumoritropic drug delivery. Rational, evidence based chemical engineering and design of the polymer incorporated into the nanomedicine, can ensure improved biodistribution, pharmacokinetics, and solubility, whilst leaving the small molecule therapeutic unchanged (Duncan and Richardson, 2012). In addition, suitably developed nanomedicines will exhibit improved passive tumour selectivity, taking advantage of the enhanced permeability and retention effect (Prabhakar *et al.* 2013). Based

upon a number of delivery technologies, nanomedicines can be divided into a number of categories (Table 1.2).

Table 1.2 Categories of nanomedicine technologies, and relevant anticancer nanomedicines. Those marked experimental*, currently have no licensed application in cancer therapy. Sources : (Natfji *et al*. 2017; Ventola, 2017)

Nanomedicine category	Licensed anticancer nanomedicine
Antibody-drug conjugates	Trastuzumab
Liposomes	Doxil
Polymeric micelles	Experimental*
Polymer-drug conjugates	Experimental*
Polymer-protein conjugates	Oncaspar (not solid tumours)
Metal nanoparticles	Experimental*

Such nanomedicines have come to the fore in oncology therapeutics in recent years, as they can be engineered to selectively target (active or passive) tumour cells. Good examples of nanomedicines exhibiting passive tumoral selectivity are Doxil and Abraxane. Given, by their nature, the cytotoxicity and poor solubility of many cancer drugs, such an effect is of considerable advantage, reducing systemic toxicity, raising efficacy, increasing the therapeutic index and potentially improving clinical outcomes. There is however, no strict definition of nanomedicines, as discussed by Duncan and Gaspar, (2011). The term nanomedicine, is derived as a

translation of the chemical definition (IUPAC) of nanoparticles, being particles with dimension of 1-100 nm. The term nanomedicine, however, is used with considerably greater flexibility, extending beyond the 100 nm upper dimension, because larger particles may still possess the physico chemical properties and desirable therapeutic characteristics required for drug delivery. In addition, some nanomaterials exhibit extreme aspect ratios, owing to their irregular shape. Gold nanorods, for example, with nanomedicine potential, can have a diameter of 10 nm, yet considerable dimensions to their length, with aspect ratios of 1.5 to 11 (Yu *et al.* 1997). Two authors with an extensive pedigree within this field, Duncan and Richardson, (2012), have gone further in consideration of this ambiguity over terminology, and described nanomedicines as "specifically engineered, nanosized drugs and drug delivery systems composed of at least 2 components (often they have many more)." (Duncan and Richardson, 2012).

Equally important, on a cellular level, the uptake of nanomedicines into individual tumor cells, is principally via the process of endocytosis, and in any discussion of nanomedicine development a basic understanding of this process is required.

1.7 Endocytosis.

Cellular uptake of nanomedicines by tumour cells is almost exclusively via endocytosis. This has the advantage of not relying upon diffusion or active

transport across the plasma membrane, which thereby may alleviate the problem of major drug resistance (Kirtane *et al.* 2013).

In recent years the knowledge base regarding the endocytic process, has expanded considerably, not least due to the understanding that endocytic pathways, rather than merely being transportation mechanisms, actually play an important role within cellular dynamics, molecular organisation and regulation (Conner and Schmid, 2003; Scita and Di Fiore, 2010). This expanded knowledge base regarding endocytosis, has occurred at a time when research into nanomedicines has also increased. Given the nature of such drug design and development, the need for a greater understanding of the intracellular trafficking of drug loaded nanoparticles or nanomedicines within endocytic pathways, is of considerable importance.

Endocytosis is a process whereby select areas of mammalian cell membranes can internalise, taking extracellular, or membrane bound materials, macromolecules, nanoparticles or ligand/receptor complexes with them (Figure 1.4). The terminology used to describe endocytic pathways is cumbersome, with similar aspects described in differing ways. In essence, there are two overall types of cellular uptake, phagocytosis and pinocytosis. Phagocytosis is a process reserved for specialised cell types such as macrophages, and will not be discussed here. Pinocytosis, which literally means ‘cell drinking’, is subdivided into several groupings dependent upon

the molecules involved. From this there are two main groupings, clathrin-mediated and non clathrin-mediated.

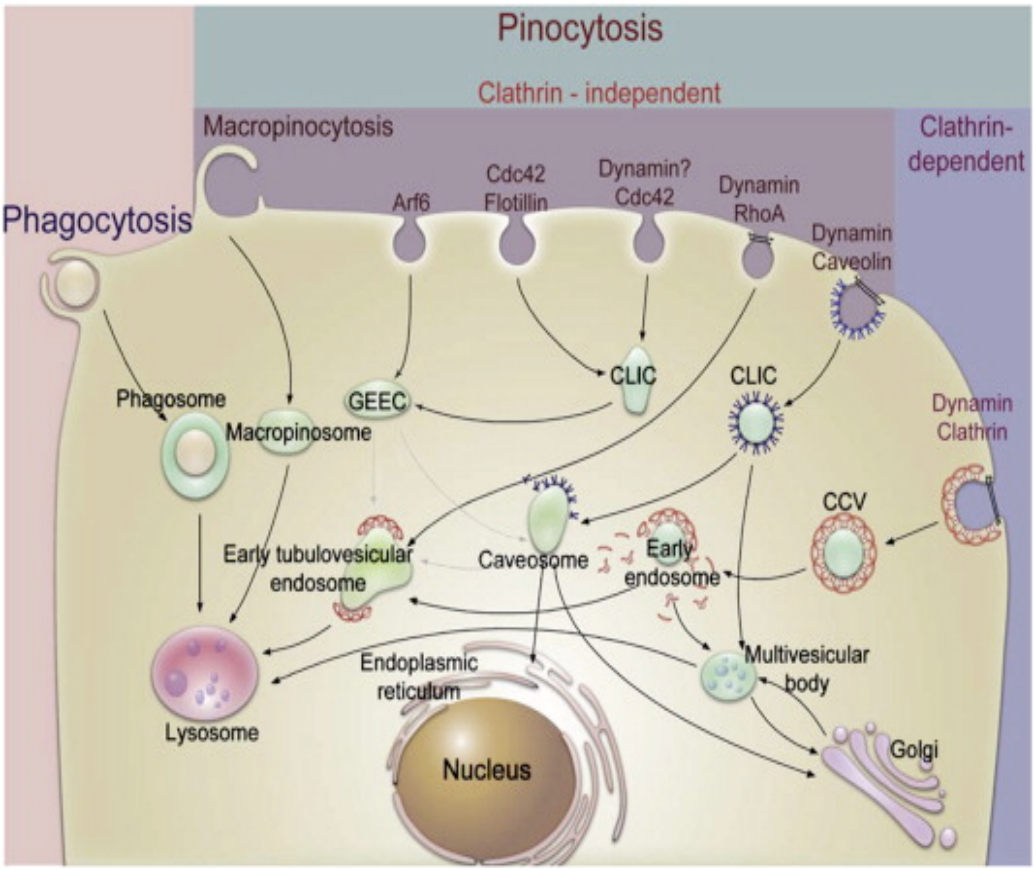

Figure 1.4 A simplified schematic diagram, illustrating cellular uptake mechanisms. Phagocytosis is reserved for specific cell types such as macrophages and neutrophils. Pinocytosis includes several of the uptake mechanisms important to nanomedicine uptake, as described in the text. Abbreviations: CLIC, clathrin independent carriers; ccv, clathrin coated vesicles; MVP, multivesicular body; GEEC, Gpi anchored protein enriched compartment. Source : (Sahay *et al*. 2010).

The endocytic pathway that is to date the best understood, and most studied is clathrin-mediated endocytosis. For this, the protein clathrin from the cytosol, is transferred via mediator proteins to the internal cell membrane, where in triskelion form, it polymerises to form clathrin coated pits (concave invaginations of the plasma membrane) (Doherty and McMahon, 2009; Schmid and McMahon, 2007). As the process continues, the clathrin coated

invagination deepens, and is then released internally from the cell membrane via activity of the helical scission protein, dynamin. This pulls the opposite sides of the membrane invagination together into apposition, ultimately leading to its separation from the plasma membrane in the form of a clathrin coated vesicle, around 50-100 nm in size. These vesicles ultimately may fuse with specialized internal vesicles or organelles, such as the early endosome, then with another type of vesicle, termed the sorting endosome leading to recycling to the cell surface via exocytosis. Alternatively, the clathrin coated vesicle may fuse with the early endosome, which then transitions to form the late endosome, and delivery to the lysosome.

Clathrin-mediated endocytosis, is really an umbrella term for a particularly diverse grouping of internalization mechanisms, with part of that diversity arising from the range of potential adapter proteins that may be involved. Clathrin by itself cannot bind to the plasma membrane, and several adapter proteins are involved (Reider and Wendland, 2011). It is these alternate adapter proteins, such as adapter protein 2 (AP2) or β-arrestin (Gurevich and Gurevich, 2006), Numb (Santolini *et al.* 2000), which are believed to be part responsible for the diversity of cargo uptake and intracellular trafficking which is a feature of clathrin mediated endocytosis (Andersson, 2011). In the specific instance of breast cancer, however, many of these molecular interactions during endocytosis are altered. The adapter protein Numb (Santolini *et al.* 2000), for example, is often found under-expressed in breast

and other tumours, where its absence has been shown to be a negative prognostic indicator (Pece *et al.* 2004).

Other pathways of endocytosis, are less well understood, with the key molecular events not yet fully defined. Caveolae-mediated endocytosis (Drab *et al.* 2001), in a similar manner to CME, also sees concave curving and internalisation of the cell membrane, however, the key protein involved is not clathrin, but caveolin 1. This protein polymerises at the plasma membrane, forming deep concave pits or caveolae ('little caves'), around 60-80 nm in size. These caveolae together with another protein, cavin, are subsequently internalised, and separated from the cell membrane via the scission protein dynamin, as with clathrin mediated endocytosis.

Other endocytic pathways that do not involve clathrin or caveolin such as arf6 dependent endocytosis, GPI-anchored protein enriched early endosomal compartment (CLIC-GEEC) endocytosis, flotillin dependent endocytosis and other (Doherty and McMahon, 2009), are still less well understood.

The important point in relation to nanomedicine development, however, is that such endocytic mechanisms operate continuously, bringing nutrients, hormones and other signaling molecules into the cell, whilst also recycling membrane receptors and other cargoes back to the cell membrane via exocytosis. It is these endocytic pathways, which rational nanomedicine design aims to exploit. Ultimately, the goal is specific direct tumor cell entry,

specific intracellular localisation and compartment/organelle specific drug release.

The key pathways for nanomedicine uptake, according to current knowledge, appear to be mainly clathrin and caveolae mediated, however the situation lacks clarity, especially within tumour cells, where these processes may be distorted. In reality, endocytic mechanisms are much more complex, cell type and cargo dependent processes with a complex interplay of numerous signaling molecules and intracellular structures (Traub, 2011), beyond the scope of this discourse. The process of endocytosis itself is an intensive area of research, and recently a completely new endocytic pathway, which is not reliant on caveolin or clathrin has been described in detail, termed fast endothelin mediated endocytosis (Boucrot *et al.* 2015).

The intracellular trafficking of internalised endocytic vesicles found with endocytosis, involves co-ordinated membrane fusion and budding processes, facilitated principally via a series of GTPases, called Rab (Zerial and Stenmark, 1993). For example, Rab5 and Rab7 play an integrated role in the transition from early to late endosome (Korobko *et al.* 2006). As highlighted earlier, each stage within endocytosis has its own specific characteristics (pH, proteases), which, theoretically, rational nanomedicine design can manipulate and employ for direct targetting to specific intracellular organelles (mitochondria, endoplasmic reticulum, Golgi, nucleus, cytosol).

In the context of cancer therapeutics, however, the fundamental consideration is the development of macromolecular complexes (nanomedicines) in a size range and with physico-chemical properties, which facilitate selective accumulation within the tumour site, via the enhanced permeability and retention effect (EPR). Also desirable is a prolonged circulatory half-life, with minimal renal clearance, and improved water solubility. These overarching goals, which centre around the fundamental premise (and therapeutic potential) of the EPR effect, have been a cornerstone of cancer nanomedicine developmental work and research for several decades, yet with somewhat limited success.

1.8 Strategies for enhancing tumour cell nanomedicine uptake.

A number of strategies have been trialled to increase tumour cell uptake of nanomedicines. Ligand coated nanomedicines designed to actively engage with cognate cell surface receptors which are over expressed in tumours, have also been demonstrated experimentally. Studies have shown that active ligand targeting of nanomedicines directed towards the often overexpressed transferrin receptor in tumour cells, can be more effective (Danhier *et al.* 2010). Such an approach has also been demonstrated with leukaemic cells, using transferrin conjugated to the anticancer therapeutic doxorubicin (Łubgan *et al*. 2008).

Another strategy employed is that of a stimulus - responsive carrier polymer or nanoparticle, which can, following endocytic internalization, release the free drug at specific intracellular locations or in response to a changing cellular environment. This has the benefit of minimising the release of free and active drug outside of target cells, whilst also potentially reducing degradation of the drug whilst within the circulation. This approach often takes advantage of a drug-macromolecular complex which is stable within the circulation, or at physiological circulatory pH (7.4), but which is able to freely dissociate within the acidic endosomal (approx.pH5.5)/lysosomal (approx. pH 4.4-4.8) environment. A further extension of this concept, is the adoption of peptide based drug carriers, where the active chemotherapeutic may only be proteolytically cleaved from the carrier polymer, and thereby rendered active within the protease-rich lysosomal environment. The latter was demonstrated in an early study using the cancer polymer complex, PK1 (Prague-Keele 1). This consisted of a water soluble polymer backbone serving as a carrier with doxorubicin attached via tetrapeptide linker. This linker is susceptible to enzymatic cleavage by cathepsin B, found within lysosomes (Duncan *et al.* 1982). The overall result was effective anthracycline delivery, with a reduced incidence of side effects in patients in Phase I clinical trials (Vasey *et al.* 1999). Many other pH and enzyme responsive nanomedicines have since been designed and explored. For example, silk nanoparticles carrying the potent anticancer anthracycline

doxorubicin can release their drug payload within the lysosome in a pH responsive manner (Totten *et al.* 2017).

Ligand coated, or antibody targeted nanomedicines that actively engage with specific cell membrane receptors, which are over-expressed in tumour cells, have for many years been a subject of research. One such category of nanomedicines, antibody drug conjugates, have been an area of intense research for many years (Lambert and Berkenblit, 2018). Typically these conist of a monoclonal antibody specfic for a (often overexpressed) tumour cell surface antigen, which is attached to an active therapeutic group, via a specific linker molecule. Such tumour membrane antigen targeted nanomedicines could theoretically have greater specific uptake into tumour cells, thereby reducing non-specific systemic side effects. Their have been many experimental actively targetted antibody drug conjugates developed, yet few have performed succesfully in clinical trials (Lambert and berkenblit, 2018).

For example, many tumours overexpress the transferrin receptor up to 100 fold (Danhier *et al.* 2010). This receptor, responsible for cellular iron uptake, upon binding with transferrin, is internalized from the plasma membrane via a clathrin dependent endocytic mechanism (Daniels *et al.* 2012), forming a clathrin coated vesicle. Upon internalisation, this fuses with the early

endosome, where the transferrin dissociates from the receptor, which is then recycled to the cell surface. By conjugating transferrin to the cancer drug doxorubicin, the cytotoxic potency can be increased (Łubgan *et al*. 2008; Singh *et al.* 1998).

Likewise, the coating of nanomedicines with folic acid, will lead to their selective, and preferential receptor mediated endocytic uptake by tumour cells over-expressing the folate receptor (Bhattacharya *et al*. 2007; Low *et al.* 2008; Xia and Low, 2010). Other examples of selective receptor targetting of tumours with nanomedicines, include the transferrin receptor, as mentioned above, or epidermal growth factor receptor, also known as HER1 (Acharya *et al.* 2009; Sreeranganathan *et al.* 2017).

The research here, is concerned with the hypoxia found within solid tumours, and to date, despite the apparent potential of such nanomedicine technology in the active targetting of tumourotropic drug delivery, only one such actively targetted antibody drug conjugate has been licensed for clinical use. Following successful completion of phases I-IV clinical trials, the United States Food and Drug Administration licensed Ado-trastuzumab emtansine (Kadcyla) for Her-2 positive metastatic breast cancer, in 2013 (Verma *et al*. 2012). This compound consists of a monocloncal antibody specific for Her-2, combined to the microtubule inhibitor, DM1, via a non-cleavable linker molecule. Similarly, it is interesting to note, that the world's first actively

targeted controlled-release cancer nanomedicine candidate, Bind 014, failed during phase II clinical trials, despite exhibiting significant pre-clinical and phase I potential. BIND-014 (Hrkach *et al.* 2012), encapsulated the existing United States Food and Drug administration licensed cancer drug docetaxel within a modified poly (lactic glycolic acid) polymeric nanoparticle. Targeting was designed to engage with prostate specific membrane antigen found in prostate tumours and the blood vessels of most other solid tumours. Similarly, there have been many other innovative targetted nanomedicines which have failed to progress beyond phase I/II clinical trials. For example, MBP-426 (liposomal oxaliplatin) which targeted towards over-expressed transferrin receptors in gastric or oesophageal adenocarcinoma). This potential nanomedicine reached phase II (U.S. National Library of Medicine, 2018a), yet has failed to progress further .

1.9 Failure to translate

Despite significant research investment by the pharmaceutical industry, there are still relatively few licensed cancer nanomedicines aimed at solid tumours, and those that do exist do not feature active ligand based targeting to tumour cells (Table 1.2). Abraxane (Nanoparticle albumin-bound (nab) paclitaxel), Myocet→ (liposomal doxorubicin), Doxil (pegylated liposomal doxorubicin), marketed as Caelyx within Europe, Onivyde (pegylated liposomal irinotecan) and Daunoxome (liposomal daunorubicin) are all approved for treatment of solid tumors (Etheridge *et al.* 2013; Venditto and Szoka, 2013). However, within this set of nanomedicines, there are even fewer specifically licensed

for the treatment of breast cancer. These include, Abraxane (O'Shaughnessy *et al.* 2013; Palumbo *et al.* 2015), Caelyx (Rom *et al.* 2014) and Myocet (Batist *et al.* 2001).

What this limited arsenal reflects, is that with each success in cancer nanomedicine development, equally there have been many more unsuccessful nanomedicine formulations. Each of these nanotechnologies, despite excellent *in vitro* potential, failed during clinical translation or earlier in the drug development pipeline (Venditto and Szoka, 2013).

Table 1.3 Anticancer nanomedicines currently licensed by the United States Food and Drug Administration or European Medicines Agency.

Chemotherapeutic	Nano-technology	Drug name (Generic and proprietary)	Clinical application	References
Doxorubicin hydrochloride	Liposomes coated with methoxy polyethylene glycol (PEG)	Pegylated liposomal doxorubicin/Doxil. marketed as Caelyx→ within Europe.	AIDS-related Kaposi's sarcoma, ovarian cancer, metastatic breast cancer.	(Barenholz, 2012; James *et al*., 1994; Sehouli *et al*., 2009; Chuang *et al*., 2010)
Daunorubicin citrate	Lipsomes (non-pegylated)	Liposomal daunorubicin/Daunoxome	AIDS-related Kaposi's sarcoma, other solid tumors, some types of leukaemia	(Petre and Dittmer, 2007; Reinhardt *et al*., 2002; O'Byrne *et al*., 2002; Gong *et al*., 2015)
Doxorubicin hydrochloride	Lipsomes (non-pegylated)	Liposomal doxorubicin/Myocet	Metastatic breast cancer	(Batist *et al*., 2001; Harris *et al*., 2002; Batist *et al*., 2006)
Irinotecan	Liposomes coated with methoxy polyethylene glycol (PEG)	Pegylated liposomal irinotecan/Onivyde	Metastatic pancreatic cancer (2^{nd} line therapy)	(Wang-Gillam *et al*., 2016)
Paclitaxel	Paclitaxel bound to albumin nanoparticles	Nanoparticle albumin-bound (nab) paclitaxel/Abraxane	Metastatic breast cancer, non-small cell lung cancer, pancreatic cancer	(O'Shaughnessy *et al*., 2013; Palumbo *et al*., 2015; Simon, 2014; Bertino *et al*., 2015)

This somewhat limited successful development so far, is attributed to many factors (Duncan and Gaspar, 2011; Duncan and Richardson, 2012; Goldberg *et al.* 2013). Amongst these, is the heterogeneity of tumours and the complex interplay between the constantly changing tumour micro-environment and nanomedicine uptake (endocytosis) into tumour cells.

Clinical delivery of cancer nanomedicines is principally via systemic administration. For successful delivery of nanomedicines into tumours, the two main vascular and interstitial compartments need traversed successfully, with preferential tumorotropic accumulation (via the EPR effect), limited systemic side effects, minimal renal and phagocytic clearance, and minimal immune stimulation. Each of these presents considerable challenges. In addition, the dysregulated vascular system, with consequential periodic acute hypoxia may limit vascular flow on an intermittent and difficult to predict basis, thereby limiting intratumoral access of nanomedicines. Despite the increased vascular permeability found in tumour blood vessels, nanomedicine egress into the tumour stroma may be limited by elevated interstitial pressure (due to reduced lymphatic clearance) opposing vascular flow. Of course researchers have considered these issues for many years. Elevating systolic pressure may effectively counteract elevated interstitial fluid pressure (Nagamitsu *et al.* 2009; Maeda *et al.* 2013). Similarly, researchers are now investigating the use of intermittent vascular flow (vascular bursts) as a mechanism for improving drug delivery (Matsumoto *et*

al. 2016; Miller *et al.* 2017). All of these mechanistic and cellular hurdles which must be overcome, may partially explain why a recent review of nanomedicine studies over a ten year period, found that only 0.7% (median) of systemically administered doses of nanomedicines actually reached tumours (Wilhelm *et al.* 2016). However, whilst all of these developmental challenges are relevant and useful for context, the core focus of this study is the cellular internalization of nanomedicines.

As described above, the cellular uptake of nanomedicines is via endocytosis, yet it is also known that within tumours, that endocytic process is clearly altered, as evidenced by up/down regulated endocytosis-mediated cell surface receptor trafficking, signalling and expression (Mosesson *et al.* 2008). In addition, a core process in hypoxic tumour development, is massive upregulation of certain key transmembrane tyrosine receptor kinases (e.g. epidermal growth factor receptor) vital to increased growth, nutrient uptake, signalling and metabolism. Implicit within increased surface expression of these receptors, is altered endo and exocytosis, facilitating altered receptor signalling, internalisation and recycling to the cell membrane surface. It has been shown in a specific type of tumour cells that hypoxia (1% O_2), via HIF1, can extend epidermal growth factor receptor half-life via down-regulation of endocytosis, leading to extended receptor signaling (Wang *et al.* 2009b). All of this indicates disrupted tumour cell endocytic/exocytic processes due to hypoxia. Given the limited success in nanomedicine therapeutic development, and the critically important endocytic process, there is a real

need to further understand how the hypoxic tumour environment impacts upon not just the endocytic uptake of nanomedicines, but also on the intracellular trafficking and site specific delivery of nanomedicines within tumour cells. Interestingly, whilst many studies have looked at drug delivery under normoxic conditions, there are relatively few which have sought to rigorously quantify the impact hypoxia has upon the cellular internalization and efflux of nanomedicines from cancer cells.

1.10 Impact of hypoxia on tumour cell uptake of nanomedicines or nanoparticles.

A number of studies have investigated the endocytic uptake of certain licensed cancer nanomedicines by a variety of tumor cell types in normoxic environments. Amongst these, is the doxorubicin based cancer nanomedicine, Doxil, shown to be internalized via a caeolae based pathway (Barenholz, 2012), and Abraxane, the paclitaxel based nanomedicine also shown to be internalized via caveolae mediated endocytosis (Bertino *et al.* 2015; Chatterjee *et al.* 2017). However, despite the known impact of hypoxia upon tumor cell metabolism and endocytosis, there is little *in vitro* data exploring the tumour cell uptake of either drug in a hypoxic environment.

Studies into the uptake of nanoparticles such as gold, with potential for use in nanomedicines, have revealed significant differences in endocytic uptake by tumour cells. One study, which examined the endocytic uptake of 1.9 nm

gold nanoparticles, *in-vitro*, by three different cell lines (MDA-MB-231 (a triple negative human breast cancer cell line), DU145 (a cell line derived from prostate cancer brain metastases) and L132 (related to the human HeLa tumour cell line – derived from cervical cancer cells)), found a significant reduction in gold nanoparticle uptake in hypoxic compared to normoxic conditions (Jain *et al.* 2014). A similar study looked at endocytic uptake of three sizes (15, 50 and 70 nm) of gold nanoparticles in an MCF-7 human breast cancer cell line. Uptake of all three sizes of gold nanoparticles was increased in a hypoxic environment, compared with normoxia (Neshatian *et al.* 2014). The same research group also found, more recently, in a separate study, that 50nm gold nanoparticles are taken up to a greater degree by both MCF-7 and HeLa cell lines in a hypoxic environment (Neshatian *et al.* 2015).

The limited research data available, therefore, provides conflicting findings, with either increased or decreased uptake of nanoparticles, following cellular hypoxia. Of course part of this discrepancy may be attributed to tumour cell heterogeneity, and differing experimental methods. Differing periods of hypoxic incubation were used, with different quantification methods. However, it remains the case that there is limited data quantifying the impact hypoxia has upon nanomedicine internalization into tumour cells. In addition, given that cellular efflux (exocytosis) of a nanomedicine may be just as significant as uptake, it is surprising there are no studies that have quantified this following hypoxic exposure. Further complicating matters, some studies have used hypoxic conditions with oxygen concentration as low as 0.1% and

0.2% O_2, which are close to anoxic (0%). This therefore raises questions over which cellular mechanisms were responsible for any observed changes, since it is known that anoxia can trigger alternative transcription factor signaling, independently of HIF1 (Ameri *et al.* 2007; Blais *et al.* 2004). In addition, it has been shown that the cellular hypoxic adaptive response varies with level of oxygenation (Bracken *et al.* 2006; Jiang *et al.* 1996), and whilst 0.1 or 0.2% oxygen may be classed as hypoxic, the question does arise as to whether such values are representative of tumour oxygen levels.

1.11 Thesis aims and objectives

It seems clear that a significant part of the failure to develop effective nanomedicines, has been a lack of understanding of the nanomedicine tumor cell interface, its heterogeneity, and the impact which the intratumoral micro environment imposes upon nanomedicine delivery (Wilhelm *et al.* 2016). Nanomedicines rely upon effective cellular endocytic uptake and intracellular trafficking for therapeutic payload delivery. However, it is known those processes may be disrupted due to hypoxic adaptation in tumour cells, thereby negating the concepts involved in nanomedicine design. There is, therefore, an inherent link between intratumoral hypoxia, re-oxygenation and effective intracellular therapeutic delivery by nanomedicines. Given that hypoxia is a consistent feature of all solid tumours, the lack of solid research data quantifying its impact upon nanomedicine delivery is somewhat surprising.

Given this background, it was hypothesized that hypoxic conditioning and cellular adaptation would have an observable impact upon nanomedicine uptake, *in vitro*, in breast cancer cells. The aim of this thesis, therefore is to rigorously quantify the impact hypoxia may have upon nanomedicine internalization in a human triple negative breast cancer cell line. This will be achieved via three objectives;

1. Quantify the impact of hypoxia upon internalization (endocytosis) and efflux (exocytosis) of a model nanomedicine (fluorescent polystyrene spheres), *in vitro*, in a human triple negative breast cancer cell line (Chapter 3).

2. Confirm the findings from objective 1., in a related human breast cancer cell line, which reflects tumour heterogeneity, *in vitro* (Chapter 3).

3. Determine the role of HIF1α in the findings from objective 1., via chemical inhibition of HIf1α translation (Chapter 4).

Chapter 2

Methods and Materials

2 Methods and Materials

2.1 Chemical reagents

All chemical reagents were of analytical grade, provided by Sigma-Aldrich (Poole, Dorset, UK), and used as supplied, unless otherwise noted.

2.2 Cell culture.

MDA-MB-231 cells (ATCC→ HTB-26™) were purchased from the American Type Culture Collection (Manassas, VA, USA). The 1833 subline was gifted by Dr. Joan Massagué (Memorial Sloan-Kettering Cancer Center, New York, NY, USA) and detailed elsewhere (Kang *et al.* 2003). This cell line was originally derived from the parental MDA-MB-231 cells, which were injected into murine cardiac ventricles, resulting in the formation of metastatic osteolytic bone lesions. Tumour cells from these lesions were expanded via *in-vitro* cell culture, then re-injected into mice. Cells from new osteolytic tumours were then characterised via gene profiling, and their bone metastatic potential assessed. The 1833 subline exhibited the greatest bone metastatic potential, compared to other similarly derived sub populations of the parental MDA-MB-231 cell line, demonstrating enhanced osteolytic metasteses formation.

All cells were cultured in Corning→ T - 75 75 cm^2 cell culture flasks (Corning B.V Amsterdam, The Netherlands) as monolayers in RPMI 1640 media (Life Technologies, UK), supplemented with 10% (v/v) foetal bovine serum (FBS)

and 1 U/mL penicillin streptomycin. Unless otherwise indicated, cells were seeded at 4×10^4 cells/cm^2.

For all experimental work, hypoxic or normoxic culture conditions were achieved using a gas mixture of 5% CO_2, 1% O_2 and 87.8% N_2 (hypoxic) or 5% CO_2, 18.6% O_2 and 70.2% N_2 (normoxic) within a humid 37 $^{\circ}$C incubator. Normobaric conditions were assumed throughout.

For prolonged experimental work, frozen aliquots of each cell line were prepared and reconstituted as required. Briefly, MDA-MB-231 or 1833 cells cultured as detailed above, were detached from cell culture flasks using trypsin, centrifuged, and the pellet re-suspended in 10ml cell culture media, to which 500 μl of molecular grade dimethyl sulphoxide. 1 ml aliquots were dispensed into Starlab→ cryopreservation vessels (Starlab, Milton Keynes, UK), and placed into the -80 $^{\circ}$C freezer, using Nalgene→ progressive freezing chamber 'Mr. Frosty' (Thermo Fisher Scientific, Inchinnan, Scotland), to ensure progressive freezing overnight.

Cells were re-constituted, as required, from frozen aliquots by gentle warming in a water bath. Once thawed, each 1 ml aliquot was rapidly pipetted into 9ml of cell culture media, centrifuged in Corning→ 50ml cenrifuge tubes (Thermo Fisher Scientific, Inchinnan, Scotland), and the pellet re-suspended in fresh culture media.

2.3 Phase contrast imaging of MDA-MB-231 and 1833 cell lines

MDA-MB-231 and 1833 Cells were seeded onto cell culture treated polystyrene Cellstar cell culture dishes (Greiner Bio-One, Kremsmunster, Austria) in normoxic conditions, to achieve approximately 60-70% confluence. Phase contrast imaging was achieved using an inverted Ti-U (Nikon, UK) microscope, with a x 20 phase objective and an orca-flash 4.0 LT sCMOS camera controlled by WinFluor, with 1.5x digital magnification.

2.4 Fluorescent nanoparticles

Sterile Fluoresbrite→ spherical fluorescent polystyrene nanoparticles (diameter 43.4 ± 4.4 nm with an excitation/emission maxima at 441/486 nm), suspended in water, were purchased from Polysciences Europe GmbH, Eppelheim, Germany.

2.5 Pericellular oxygen monitoring

Presens sensor dishes (Presens, Precision Sensing GmbH, Regensburg, Germany) provide real time pericellular oxygen measurement. The principle of measurement, is based around small sensor spots located in the bottom of each well of sterile, 6 well cell culture plates (Figure 2.1).

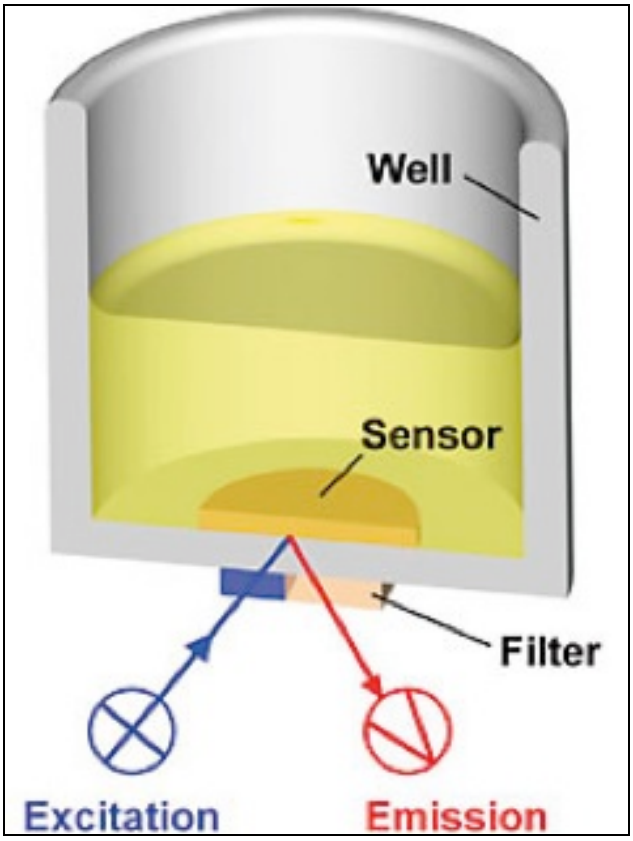

Figure 2.1 Schematic diagram of well in a 6 well Presens cell culture plate. The Presens system illuminates each pre-calibrated sensor by LED. Illuminated sensors then emit fluorescence, which is detected underneath each well. In the presence of oxygen, the fluorescence is quenched, allowing derivation by pre-calibration, of the pericellular oxygen concentration. Sourced from Presens Precision Sensing, GmbH, Germany.

Three wells of Presens Oxohydrodish→ 6 well plates (Presens, Precision Sensing GmbH, Regensburg, Germany) were seeded with MDA-MB-231 cells, as described above. The remaining three wells were filled with an equivalent volume of medium only. Each plate was then placed on the Presens Sensordish→ 24-channel plate reader within the hypoxic incubator. Following temperature equilibration, the in-well oxygen percentage was

recorded for each well, separately, at 10 minute intervals, for a period of up to 26 hours. The mean measurements of three wells per group were collected.

2.6 *In vitro* cytotoxicity studies

2.6.1 Fluorescent nanoparticle cytotoxicity in normoxic and hypoxic conditions

MDA-MB-231 cells were seeded into 96-well tissue culture treated polystyrene plates (TPP Techno Plastic Products AG, Trasadingen, Switzerland) at a density of 3×10^3 cells/cm^2 in 100 μl complete culture medium. The plates were then incubated in either normoxic or hypoxic conditions for 24 hours. The wells were then aspirated and fresh media containing nanoparticles at a range of concentrations up to 1×10^{11} nanoparticles/ml was added, followed by a further incubation in the respective environment for 44 hours. Next, 20 μl of (3-(4,5- dimethylthiazol-2-yl)-2,5-diphenyltetrazolium bromide (MTT; 5 mg/ml in PBS) was added and incubated for 4 hours (Figure 2.2).

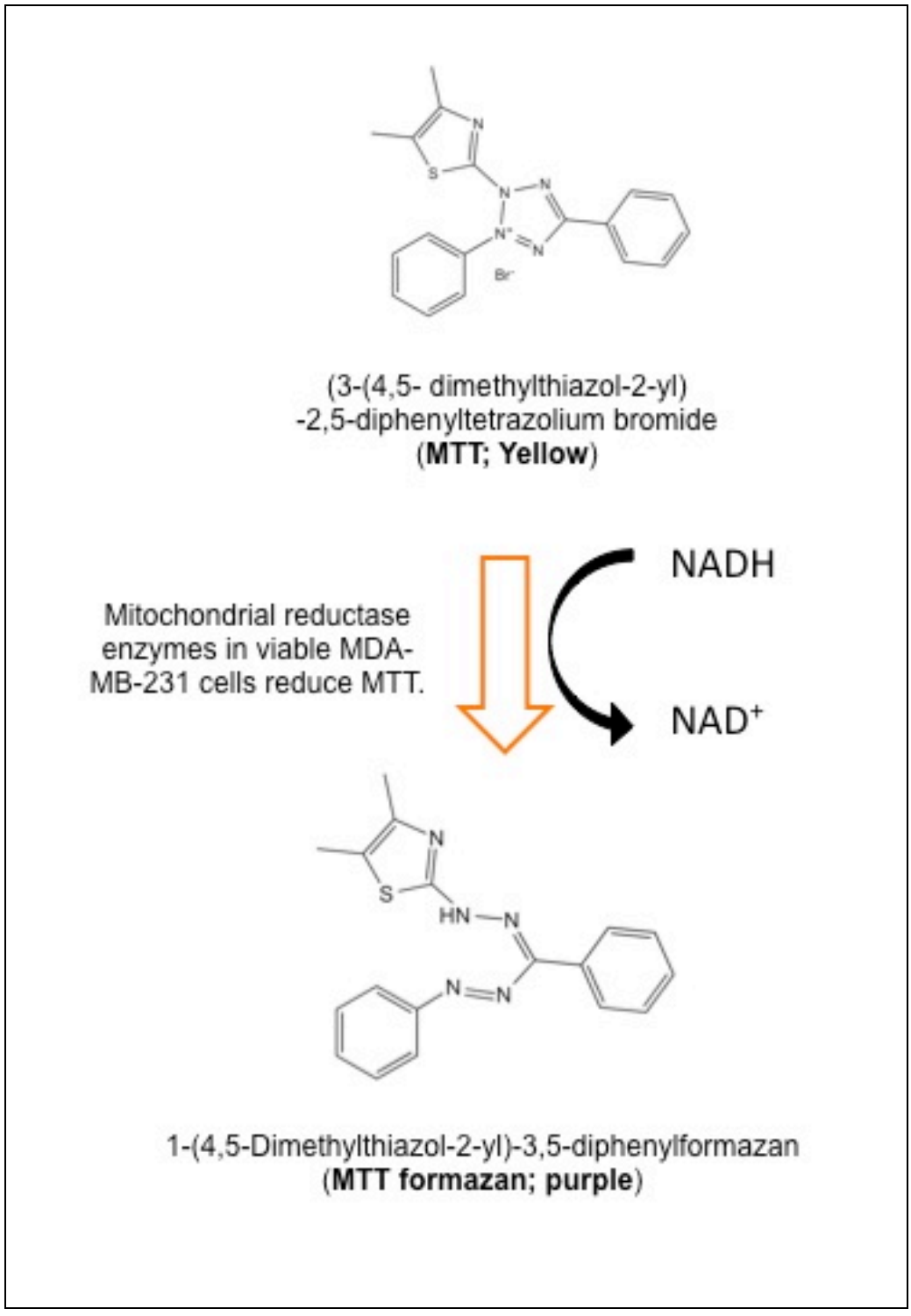

Figure 2.2 The MTT assay. Yellow coloured MTT fluid is reduced by the activity of mitochondrial enzymes in viable cells, to purple coloured formazan crystals.

All wells were then aspirated, formazan crystals solubilised in dimethyl sulphoxide and absorbance read at 570 nm. This process was repeated for a further two biological replicates. Cell viability at each nanoparticle dose was calculated as a percentage of the control (i.e. zero dose).

2.6.2 Cytotoxicity of digoxin in hypoxic MDA-MB-231 cells

MDA-MB-231 cells were seeded into 96-well tissue culture treated polystyrene plates (TPP Techno Plastic Products AG, Trasadingen, Switzerland) at a density of 3×10^3 cells/cm^2 in 100 μl complete culture medium. The plates were then incubated in normoxic conditions for 24 hours. The wells were then aspirated and fresh media containing digoxin solution (1.0 mg/ml in methanol) (Sigma-Aldrich, Dorset, England, UK) at an effective concentration of either 0, 10, 100 or 1000 nmol was added on a column by column basis across each plate. Following a further 20 hour incubation, the MTT protocol and measurements as described above, were performed. This process was repeated for a further two biological replicates.

2.7 *In vitro* trafficking of fluorescent nanoparticles

MDA-MB-231 cells were seeded onto cell culture treated polystyrene Cellstar cell culture dishes (Greiner Bio-One, Kremsmunster, Austria) for 24 hours in either hypoxic or normoxic conditions (as defined above). Next, cells were dosed with fluorescent nanoparticles for either 45 or 180 minutes, placed on ice and washed twice with PBS at 4°C, stored on ice and transferred for confocal imaging immediately. Lysosomal staining was achieved using LysoTracker Red (Thermo Fisher Scientific, Inchinnan, Scotland) according to the manufacturer's instructions. Live cell confocal co-localisation imaging was conducted using a Leica TCS SP5 laser scanning confocal microscope equipped with a 40· liquid immersion objective. Argon laser excitation at 488 (green channel, FITC nanoparticles) and 514nm (red channel, Lysotracker red), were used, focused to 1.0 Airy disk. Images were captured from an average of three line scans at 8-bit resolution, with x and y image dimensions of 1024 x 1024. Confocal slices were assembled into figures, brightness/contrast adjusted using ImageJ v1.0 (National Institutes of Health, Bethesda, Maryland, USA) and imported into Graphpad Prism→ v7.0 (GraphPad Software Inc., La Jolla, CA, USA), for graphical assembly.

2.8 Generation of cell lysates

2.8.1 Preparation of cell lysates for protein array and HIF1α temporal analysis via western blotting.

MDA-MB-231 cells were seeded in Corning→ T - 75 75 cm^2 tissue culture treated polystyrene cell culture flasks (Corning B.V., Amsterdam, The Netherlands) and incubated for 24 hours under normoxic conditions to support cell growth. Next, flasks were split into 4 groups and cultured for a further 24 hours using specific conditioning regimes: (i) normoxic control, (ii) 6 hours of hypoxia (i.e. 18 hours normoxia followed by 6 hours of hypoxia conditioning), (iii) 24 hours of hypoxic conditioning and (iv) positive control using 100 μM $CoCl_2$. The $CoCl_2$ dosing served to chemically block HIF1α breakdown in the presence of oxygen.

At the end of the conditioning regime, culture flasks were immediately immersed in ice. Within 90 seconds, the culture medium was removed and the cell monolayers were washed twice with 5 ml ice cold PBS (pH 7.42), followed by 1.0 ml of ice cold radioimmunoprecipitation buffer (150 mM NaCl, 1.0% IGEPAL CA-630, 0.5% sodium deoxycholate, 0.1% SDS, 50 mM Tris, pH 8.0) containing 40 μl of 25 · Roche Diagnostics Easypack Protease inhibitor cocktail (both from Sigma-Aldrich, Dorset, England, UK). The cells were then harvested using a cell scraper. The lysates were pipetted into ice cold centrifuge tubes and, while maintained at 4 °C, vortexed at full power for 1 minute, shaken at full power for 20 minutes and then centrifuged for 20

minutes at 12,000 · g. Following centrifugation, the supernatant was aliquoted and stored at -80°C until further analysis. Cell lysates were prepared in this way for each treatment group, as biological triplicates.

2.8.2 Preparation of cell lysates of hypoxic conditioned cells, treated with digoxin and normoxic cells treated with cobalt chloride for western blotting.

MDA-MB-231 cells were seeded in 75cm^2 tissue culture treated polystyrene culture flasks and incubated for 24 hours under normoxic conditions to support cell growth. Three flasks were then dosed with 100 μM $CoCl_2$ followed by 100 μl of cell culture media, containing digoxin at an effective concentration of either 10, 100 or 100 nmol/l, and incubated for 24 hours in a normoxic environment. Similarly, 100 μl of cell culture media, containing digoxin at an effective concentration of either 10, 100 or 100 nmol was added to a further three flasks, which were then incubated in normoxia for 18 hours, followed by 6 hours hypoxia.

Following the respective incubation periods, cell lysates were prepared and stored as previously described.

2.9 Protein separation, western blotting and protein arrays

2.9.1 Protein quantification

The total protein concentration of each cell lysate was determined using the Pierce™ bicinchoninic acid colorimetric protein assay kit (Thermo Fisher Scientific, Inchinnan, Scotland). This assay is based upon two chemical reactions, the reduction of Cu^{2+} to Cu^{1+} by protein in an alkaline solution, followed by the binding of two molecules of bicinchoninic acid per Cu^{1+}, in a linear response. The end product absorbs in the wavelength range 540-570 nm.

Briefly, 25 μl of each cell lysate was pipetted in duplicate into the wells of a 96 well cell culture plate (Thermo Fisher Scientific, Inchinnan, Scotland) , together with nine protein (albumin) standards ranging in concentration from 0 to 2000 μg/ml. To each well, 200 μl of bicinchinoic acid in an alkaline buffer (0.1M sodium hydroxide, plus sodium carbonate, sodium bicarbonate and sodium tartrate), mixed in a 1:50 ratio with 4% cupric sulphate were added. Well contents were mixed, and the plate incubated at 37°C for 30 minutes. Absorbance for each well was measured at 570 nm.

Protein concentration was determined by linear Interpolation of meaned sample results from the series of standards (Figure 2.3).

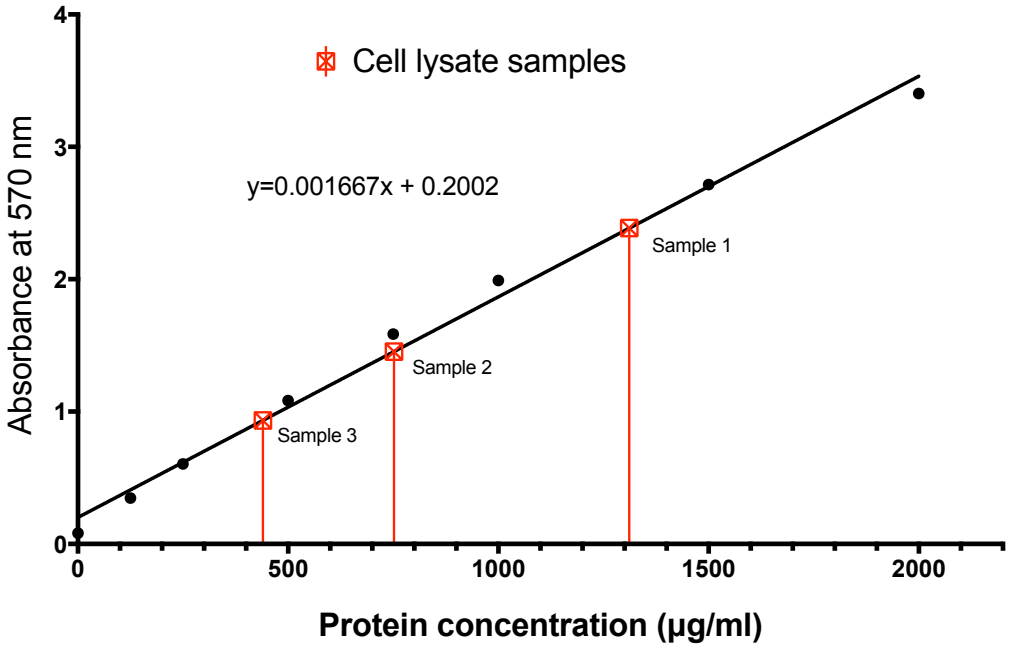

	Protein concentration µg/ml (Interpolated)			A570nm (Entered)
	X	Upper Limit	Lower Limit	Y
Sample 1	1311.540	1389.590	1241.654	2.386
Sample 2	751.712	808.418	694.797	1.453
Sample 3	439.996	501.003	374.120	0.934

Figure 2.3 Representative cell lysate sample protein concentration determination via linear interpolation from a series of known protein standards, using the bicinchoninic acid protein assay.

2.9.2 Polyacrylamide gel preparation

The proteins of interest for separation and detection, were unhydroxylated HIF1α and the loading control, β-actin. These had molecular sizes of 120 and 42 kDa respectively. The polyacrylamide gel was therefore prepared with 8% polyacrylamide content, to allow effective separation within the 25 – 200 kDa range.

The separating gel was prepared by pipetting 4.7 ml of ddH_2O, 2.5 ml of separating gel buffer (1.5 M Tris base, pH 8.8), 0.1 ml of 10% sodium dodecyl sulphate and 2.7 ml of a 30% acrylamide/bis solution (Bio-Rad Laboratories, Hemel Hempstead, UK) into a Sarstedt 50ml centrifuge tube. To catalyse acrylamide polymerisation, 50 μl of freshly prepared 10% ammonium persulphate and 5 μl of N,N,N',N' – tetramethylethylenediamine were added and mixed.

The stacking gel was prepared in the same manner, except 2.5 ml of stacking gel buffer (0.5 M Tris base, pH 6.8) was used. For acrylamide polymerization 10 μl, rather than 5 μl, of N,N,N',N' – tetramethylethylenediamine was used.

2.9.3 Protein separation and western blotting

For western blotting, protein samples were denatured in a 1:1 ratio using Laemmli sample loading buffer [65.8 mM Tris-HCl, pH 6.8, 2.1% (w/v) SDS, 26.3% (w/v) glycerol, 0.01% (v/v) bromophenol blue, and 5% (v/v) 14.2 M β-mercaptoethanol (Bio-Rad Laboratories, Hemel Hempstead, UK)] by heating for 5 minutes at 95°C. Equivalent protein quantities (25 μg) and a Precision Plus Kaleidoscope™ protein ladder (Bio-Rad Laboratories, Hemel Hempstead, UK) were loaded on to an 8% w/v polyacrylamide gel prepared earlier, and separated at a constant 150 V for 55 minutes. Following this, proteins located within the gel were blotted onto a polyvinylidene difluoride membrane (Bio-Rad Laboratories, Hemel Hempstead, UK), for 35 minutes at a constant 75 mA. The following antibodies were used to probe the membrane: rabbit primary antibodies for β-actin (1:10,000) and unhydroxylated HIF1-α (1:1,000) (monoclonal and polyclonal respectively) as well as monoclonal goat anti-rabbit IgG HRP linked secondary antibody (1:2,000) (all from Cell Signalling Technology, Danvers, MA, USA). Primary antibodies were blocked with 5 % w/v bovine serum albumin (Sigma-Aldrich, Dorset, England, UK) in tris-buffered saline Tween (TBST), with secondary antibody blocking achieved with 5% w/v non-fat dry milk powder in TBST. Relevant bands were visualised using Clarity™ western ECL substrate and UltraCruz autoradiography film (Santa Cruz Biotech Inc., Dallas, TX, USA).

HIF1-α and β-actin bands were digitised (Epson Perfection v600 film flatbed scanner, Epson Europe, B.V., Netherlands), and densitometry scans were completed using Image Studio™ Lite software (LI-COR Biotechnology, Lincoln, NE, USA).

2.9.4 Relative expression of cell stress related proteins in cell lysates, determined via protein array.

The relative expression of 11 cell stress-associated proteins was determined using the R&D Proteome profiler™ (catalogue number #ARY018; R&D Systems, Inc., MN, USA), following the manufacturer's instructions. This is a sandwich-based immunoassay, with specific protein capture antibodies bound in duplicate at specific locations on a nitrocellulose membrane (Figure 2.4).

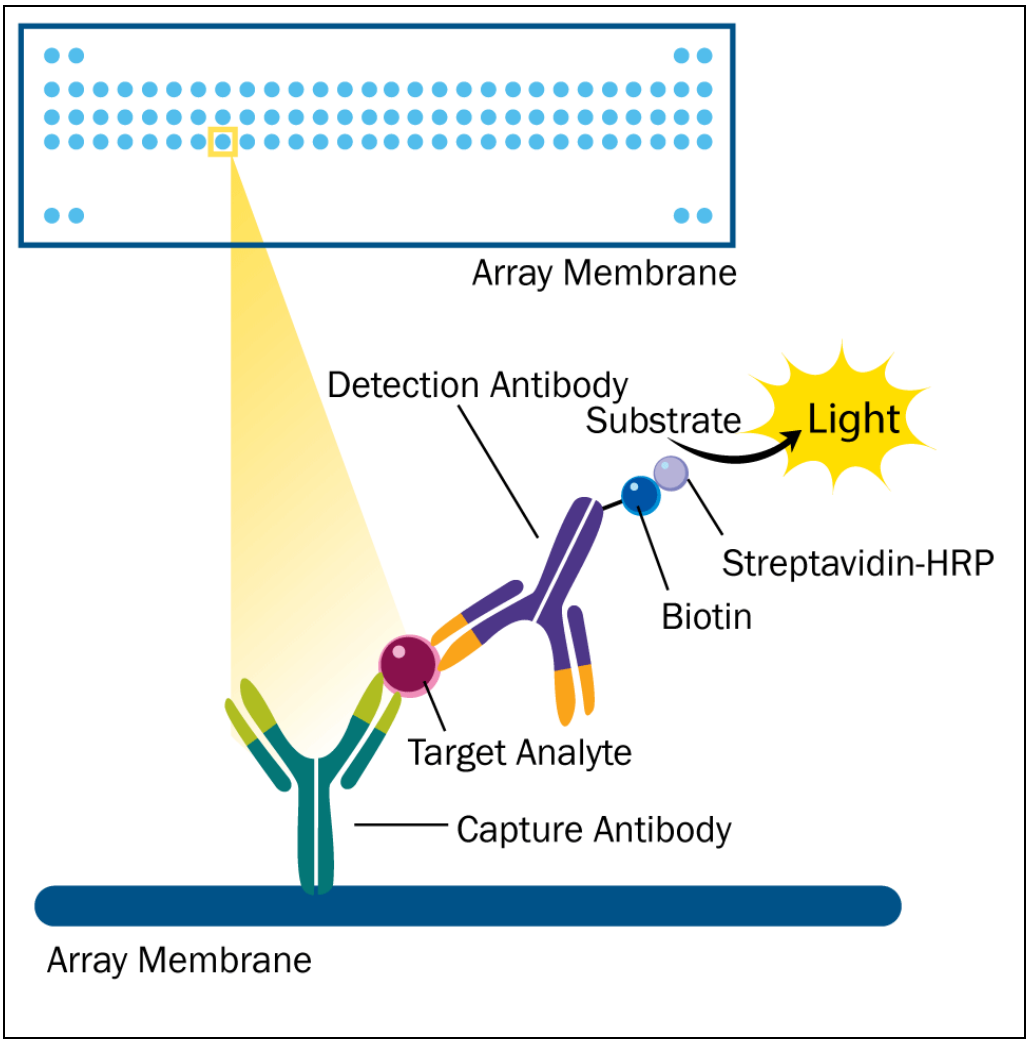

Figure 2.4 Graphical representation of protein array principle (sourced from R&D Systems inc., MN, USA).

Briefly, biological triplicates of MDA-MB-231 cell lysates were prepared as detailed in section 2.8.1., above, and pooled per hypoxic treatment group (0, 6 or 24 hours hypoxic conditioning), with a total of 300 μg protein per sample

used. One array membrane was used per cell hypoxic conditioning group (3 in total). Each of the three pooled lysates were diluted in array buffer 4, and made up to a volume of 1.5 ml with blocking buffer. 20 μl of detection antibody solution was added, mixed and samples incubated at room temperature for one hour. Each of the pooled cell lysates prepared in this way, were then added to one each of the three array membranes, which had been pre-blocked. Arrays were incubated overnight at 2-8°C on a rocking platform. Arrays were aspirated and then washed x 3 with wash buffer, followed by the addition of 2.0 ml of diluted streptavidin – horseradish peroxidase mixture. Arrays were incubated for 30 minutes on a rocking platform at room temperature, washed x 3 as before, and chemiluminescent reagent added. Arrays were then assembled for imaging and densitometry, as detailed in section 2.9.3., above. Relative expression for each specific protein, per pooled lysate was then prepared as a heat map using GraphPad Prism→ v7.0 (Graphpad Software Inc., La Jolla, CA, USA).

2.10 Determination of effective nanoparticle concentration for hypoxic and normoxic uptake comparison

For ongoing normoxic and hypoxic uptake and efflux comparison studies, it was necessary to determine a suitable fluorescent nanoparticle concentration to be used. Preliminary development work had indicated a nanoparticle concentration of 1×10^{10} nanoparticles/ml would provide a measurable

fluorescent signal. To further develop this, dose response experiments were conducted.

Briefly, one Nunc™ 6-well cell culture plate (Thermo Fisher Scientific, Inchinnan, Scotland) was seeded with MDA-MB-231 cells, at a density of 4 x 10^4 cells/cm^2 and incubated for 24 hours in a normoxic environment. Following this respective wells of the plate were dosed with fluorescent nanoparticles at the effective concentrations shown (Table 2.1).

Table 2.1 List of nanoparticle concentrations per well of a 6-well cell culture plate.

Well number	Nanoparticle effective concentration (nanoparticles/ml)
1	$1x10^{10}$
2	$1x10^{10}$
3	$1x10^{10}$
4	$5x10^{9}$
5	$2.5x10^{9}$
6	0 (control)

Cells were then incubated in a normoxic environment for a further 60 minutes. Within the next 15 minute time interval, the cells were washed 3 times with ice cold PBS, detached using trypsin and transferred to flow cytometry tubes for analysis. Flow cytometry was conducted as detailed in section 2.11.1. (below).

A second experiment was conducted to compare nanoparticle concentration and mean FITC fluorescence in both normoxic and hypoxic conditioned MDA-MB-231 cells. Briefly, two Nunc™ 6-well cell culture plates (Thermo Fisher Scientific, Inchinnan, Scotland) were seeded as above, with MDA-MB-231 cells. One plate was incubated in normoxic conditions, the other in hypoxic conditions for 24 hours. Following this, each plate was dosed with nanoparticles (Table 2.2).

Table 2.2 List of nanoparticle concentrations per well of each 6 well cell culture plate.

Well number	Nanoparticle effective concentration (nanoparticles/ml)
1	$1x10^{11}$
2	$1x10^{11}$
3	$1x10^{10}$
4	$1x10^{10}$
5	$1x10^{9}$
6	$1x10^{9}$

Each plate was then returned to its respective environment for a further 180 minutes then processed as before for mean cellular FITC fluorescence measurement by flow cytometry.

2.11 *In vitro* normoxic and hypoxic cell cultures and nanoparticle uptake and release

2.11.1 MDA-MB-231 cell line uptake and efflux studies

MDA-MB-231 cells were seeded into Nunc™ 6-well cell culture plates (Thermo Fisher Scientific, Inchinnan, Scotland). Plates were then incubated for either (i) 24 hours in hypoxic conditions, (ii) 24 hours in normoxic conditions, or (iii) 18 hours under normoxia followed by 6 hours under hypoxia. Cells were then removed from the hypoxic incubator (and exposed to atmospheric oxygen) and wells 1-5, dosed with nanoparticles at an effective concentration of 1×10^{10} nanoparticles/ml, and the plates returned to their respective culture environments for either 45 or 180 minutes, all within a ten minute interval. Within the next 15 minute time interval, the cells were washed 3 times with ice cold PBS, detached using trypsin and transferred to flow cytometry tubes for analysis. Comparison of nanoparticle uptake between normoxic and hypoxic treatments were conducted, per hypoxic incubation interval, two 6-well plates per experiment, in parallel. Per comparison, one 6-well plate from hypoxic conditions, and one 6-well plate from normoxic conditions were run in parallel, and this was repeated on three separate occasions, with separate cultured cell populations on different days, to create three biological experiments. Per 6-well plate, 5 wells were dosed with nanoparticles, with the sixth well in each case acting as blank. This gave a total of 15 comparison measurements, across three biological replicates. The limiting factor in conducting these experiments, was the

inability to have more than one hypoxic conditioned plate in use in any given experiment (as opening the incubator destroyed the hypoxic environment within a few seconds, thereby negating the possibility of a second or third plate undergoing hypoxic incubation). These comparisons were therefore conducted in the same way, for all the hypoxic conditioning periods and nanoparticle dosing intervals, as indicated above.

For normoxic efflux studies, 2 x Nunc™ 6-well cell culture plates (Thermo Fisher Scientific, Inchinnan, Scotland) labelled baseline and release respectively, were seeded with MDA-MB-231 or 1833 cells as before. Following 24 hours normoxic incubation for both plates, wells 1-5 of the plate labelled release were dosed with nanoparticles as above, and returned to normoxic incubation. The normoxic and hypoxic comparison studies for both baseline and efflux plates in both normoxia and hypoxia, were conducted in parallel, as for the uptake studies Fifteen minutes later the 6-well plate labelled baseline was similarly dosed and returned to incubation. Further processing of both plates was then conducted as per the schedule shown (Table 2.3).

Table 2.3 Summary of 6-well cell culture plate processing following normoxic or hypoxic incubation, to enable comparison of nanoparticle efflux with both the MDA-MB-231 and 1833 cell lines. *Preparation of cells for flow cytometry was conducted as with the earlier nanoparticle uptake studies.

Minutes post 24 hour incubation	Plate	Step performed
0	Release (2)	Dose with nanoparticles
15	Baseline (1)	Dose with nanoparticles
45	Plate 2	wash x 3 with PBS
60	Plate 1	Wash and process for flow cytometry*
75	Plate 2	Wash and process for flow cytometry*

The same procedure was used for hypoxic efflux studies, where 24 hours hypoxic incubation was employed for both plates instead.

Flow cytometry was performed using a FACS Canto™ II FACS analyser (Becton Dickinson, Oxford, England, UK) by assessing mean cell-associated fluorescence with an argon laser (excitation 488 nm, emission 525 nm) and gating for 10,000 events (Figure 2.5). For all hypoxic measurements normoxic control groups were run in parallel. Mean FITC fluorescence values were determined from the derived FCS 3.0 files using FlowJo→ v10.3 software (FlowJo LLC, Oregon, USA). Mean FITC fluorescence values were converted to percentages of the respective normoxic control mean, to calculate relative differences.

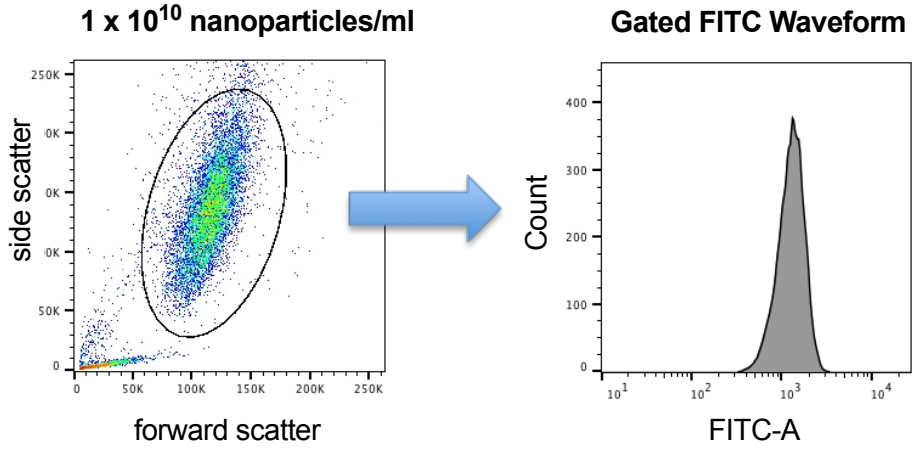

Figure 2.5 Representative FACS scatter plot from MDA-MB-231 cells dosed with nanoparticles. Left hand side panel shows cellular gating used and right hand side shows typical derived FITC waveform from which mean FITC fluorescence values were calculated. Scatter plot colours denote event frequency.

2.11.2 1833 cell line nanoparticle uptake and efflux studies

Nanoparticle uptake and efflux studies were undertaken with the 1833 cell line in a similar manner, as that with the MDA-MB-231 cell line. However, comparison of normoxic with hypoxic conditioning was only conducted with hypoxia of 24 hours duration. Nanoparticle dosing (1 x 10^{11} nanoparticles/ml) was conducted over a 45 minute period only.

2.11.3 Impact of digoxin upon nanoparticle uptake by normoxic MDA-MB-231 cells.

MDA-MB-231 cells were seeded into 2 x Nunc™ 6-well cell culture plates (Thermo Fisher Scientific, Inchinnan, Scotland). All the wells of one plate were dosed with digoxin at an effective concentration of 100 nmol. Both plates were then incubated for 24 hours in normoxic conditions. Cells were then dosed with nanoparticles at an effective concentration of 1×10^{10} nanoparticles/ml, and the plates returned to their respective culture environments for 45 minutes. Within the next 15 minute time interval, the cells were washed 3 times with ice cold PBS, detached using trypsin and transferred to flow cytometry tubes for analysis, as detailed above.

2.11.4 Impact of digoxin upon nanoparticle uptake by hypoxia-conditioned MDA-MB-231 cells, compared to untreated normoxia-conditioned control cells.

MDA-MB-231 cells were seeded into 2 x Nunc™ 6-well cell culture plates (Thermo Fisher Scientific, Inchinnan, Scotland). All the wells of one plate were dosed with digoxin at an effective concentration of 100 nmol/l. The digoxin treated plate was then incubated for 24 hours in normoxic conditions, with the untreated plate incubated in normoxic conditions for an equivalent period. Following incubation, cells were dosed with nanoparticles at an

effective concentration of 1×10^{10} nanoparticles/ml, and the plates returned to their respective culture environments for 45 minutes. Within the next 15 minute time interval, the cells were washed 3 times with ice cold PBS, detached using trypsin and transferred to flow cytometry tubes for analysis, as detailed above.

2.12 Statistical analyses

Statistical analyses were performed using GraphPad Prism→ v7.0 (Graphpad Software Inc., La Jolla, CA, USA). All significance tests used unpaired two tailed Student's *t* tests, except for cytotoxicity measurements, where a one-way unpaired ANOVA with Sidak multiple comparisons test was used ($\alpha = 0.05$). Asterisks denote statistical significance as follows: $*p < 0.05$, $**p < 0.01$ and $***p < 0.001$. All data are presented as mean values ± standard deviation (SD), unless otherwise stated.

Chapter 3

Impact of hypoxia on nanoparticle uptake and efflux in a human breast cancer cell line.

3 Impact of hypoxia on nanoparticle uptake and efflux in a human breast cancer cell line.

3.1 Introduction

Cancer nanomedicines are typically macromolecular drug delivery systems in the nanometer size range that are developed to reduce systemic toxicity but that also have the potential to exploit key features of solid tumor pathophysiology namely, leaky blood vessels and reduced lymphatic drainage to enhance passive tumor accumulation (Duncan and Gaspar, 2011; Shi *et al.* 2016). Despite decades of research (Duncan and Gaspar, 2011; Duncan and Richardson, 2012), only a few anticancer nanomedicines are currently in routine clinical use; for example, Abraxane (nanoparticle albumin-bound paclitaxel), Myocet (liposomal doxorubicin), Doxil (PEGylated liposomal doxorubicin), marketed as Caelyx within Europe, Onivyde (PEGylated liposomal irinotecan) and Daunoxome (liposomal daunorubicin) are approved for treatment of solid tumors (Venditto and Szoka, 2013). Specifically, Abraxane (Palumbo *et al.* 2015), Caelyx (Rom *et al.* 2014) and Myocet (Batist *et al.* 2001) are licensed for the treatment of advanced metastatic breast cancer no longer responsive to estrogen, progesterone and ERBB2 (Her2/neu) targeted therapies. The primary motivation for the development of these nanomedicine formulations has been the improvement in side effect profiles (e.g. reduction in doxorubicin-associated cardio toxicity) enabling the use of these cytotoxic drugs in heavily pre-treated patients (Rom *et al.* 2014). However, the overall small number of this anticancer nanomedicine arsenal generally, reflects the difficulties encountered in the

successful development of anticancer nanomedicines from concept through clinical practice (Barenholz, 2012; Goldberg *et al.* 2013).

Many anticancer nanomedicine designs currently in preclinical and clinical development exploit the leaky vasculature and reduced lymphatic drainage of solid tumors as these tumor features favour the passive accumulation of nanomedicines at the tumor sites. This phenomenon was first described in 1986 and is now commonly referred to as the “enhanced permeability and retention” (EPR) effect (Matsumura and Maeda, 1986). This arises due to a number of factors, including intratumoral hypoxia. Hypoxia in turn triggers angiogenesis and neo-vascularisation principally via vascular endothelial growth factor (Forsythe *et al.* 1996; Shweiki *et al.* 1992), platelet derived growth factor β and angiopoeitin-2 (Kelly, 2003). The result is dysregulated and chaotic vascular growth, which commonly lacks stabilising smooth muscle cells. These abnormal blood vessels are heterogeneous but typically characterised by defective, irregular vascular endothelial cell coverage (Hashizume *et al.* 2000). These defective endothelial cells exhibit enlarged intercellular fenestrations, which facilitate the (passive) tumorotropic transit and accumulation of nanomedicines (or macromolecules) within solid tumors (i.e. the EPR effect) (Maeda, 2015); acting against this trend is the raised internal tumor pressure (Jain, 2014). Exploitation of the EPR effect in a clinical setting has proven difficult, and emerging evidence calls for better EPR-positive patient stratification using image-guided approaches; this has

now been pioneered in advanced metastatic breast cancer patients (Lee *et al.* 2017b).

Both tumor vascular development and density (Torosean *et al.* 2013) as well as perfusion and hypoxia, are key regulators of nanomedicine distribution because nanomedicines are typically administered intravenously and must therefore successfully complete their journey from the injection site to the tumor. Intratumoral hypoxia can be intermittent or transient (Bennewith and Durand, 2004; Vaupel and Mayer, 2014) which means that the physical access of a nanomedicine to hypoxic breast cancer tumor cells may be restricted to short, transient periods of vascular reperfusion. During reperfusion, the nanomedicine must navigate physical barriers, such as the extracellular matrix and immune and cancer-associated cells (e.g., fibroblast, macrophages etc.), and must overcome physiological factors (e.g., high interstitial fluid pressure) to reach the core of solid (breast) tumors (Sriraman *et al.* 2014).

Hypoxia within the solid tumor itself is of particular importance. Typically, survival of tumor cells under hypoxic stress requires adaptation via a series of hypoxic induction factors (HIF), principally HIF1 (Semenza and Wang, 1992; Semenza, 2009). These factors consist of a constitutively expressed β subunit (ARNT; aryl hydrocarbon receptor nuclear translocator) and one of three oxygen-labile α subunits (denoted 1, 2 and 3). During periods of hypoxia, HIF1α, rather than undergoing normal proteasomal degradation

(Kaelin and Ratcliffe, 2008), translocates to the nucleus, where it combines with the HIFβ subunit to act on the conserved consensus sequence 5'-(A/G) CGTG-3' (Wenger *et al.* 2005), the hypoxic response element, in the promoter region of over 1,000 genes (Bando *et al.* 2003; Mole *et al.* 2009). This triggers a cascade of cellular changes, with the overall result being clinically aggressive, highly metastatic (Brizel *et al.* 1996; Sundfør *et al.* 2009) and treatment resistant (Rohwer and Cramer, 2011; Mao *et al.* 2016) tumor growth.

However, of potentially greater significance from a nanomedicine perspective is that hypoxic adaptation also alters key cellular processes, including energy metabolism (Eales *et al.* 2016; Frezza *et al.* 2011; Sun and Denko, 2016), endocytic receptor internalization (Mosesson *et al.* 2008), transmembrane receptor recycling, trafficking (Wang *et al.* 2009b) and signaling (King *et al.* 2012). Nanomedicines designed for intracellular activation in cancer cells rely on endocytosis and correct intracellular trafficking for effective therapeutic payload delivery. The energy dependence of endocytic uptake of nanomedicines means that these hypoxia-induced changes have the potential to directly undermine fundamental nanomedicine design principals. Therefore, an inherent link exists between hypoxic status, re-oxygenation of hypoxic tumor cells and the cellular presentation and internalisation of nanomedicines. However, few if any studies have sought to rigorously quantify the impact of these biological changes upon nanomedicine uptake and retention. Given the dynamic nature of the hypoxic response and the

myriad changes observed within hypoxic tumor cells, the aim of this study was to quantify, *in vitro*, the impact of hypoxia exposure, simulated reperfusion and dosing interval on nanomedicine internalisation and retention in triple negative, clinically aggressive human breast cancer cells. The MDA-MB-231 cell line was selected, because it is representative of the most difficult to treat breast cancer subtype (triple negative breast cancer) (Brenton *et al.* 2005), which is deficient in estrogen, progesterone and ERBB2 (Her2/neu) receptors (Lal *et al.* 2017), MDA-MB-231 cells are therefore unresponsive to hormone (e.g., Tamoxifen) or receptor based therapies (e.g., Herceptin) which are typically used to treat other breast cancer types. Therefore to make progress with triple negative breast cancer there is the urgent need to better understand the performance of nanomedicines (e.g. nanoparticles) in the presence of hypoxia. This study quantified the uptake and efflux of nanoparticles in hypoxic conditioned MDA-MB-231 breast cancer cells and the bone metastatic subpopulation. In parallel, expression of key biological markers of the hypoxic cell stress response, including HIF1-α, was assessed.

3.2 Results

3.2.1 Phase contrast imaging of MDA-MB-231 and 1833 cell lines.

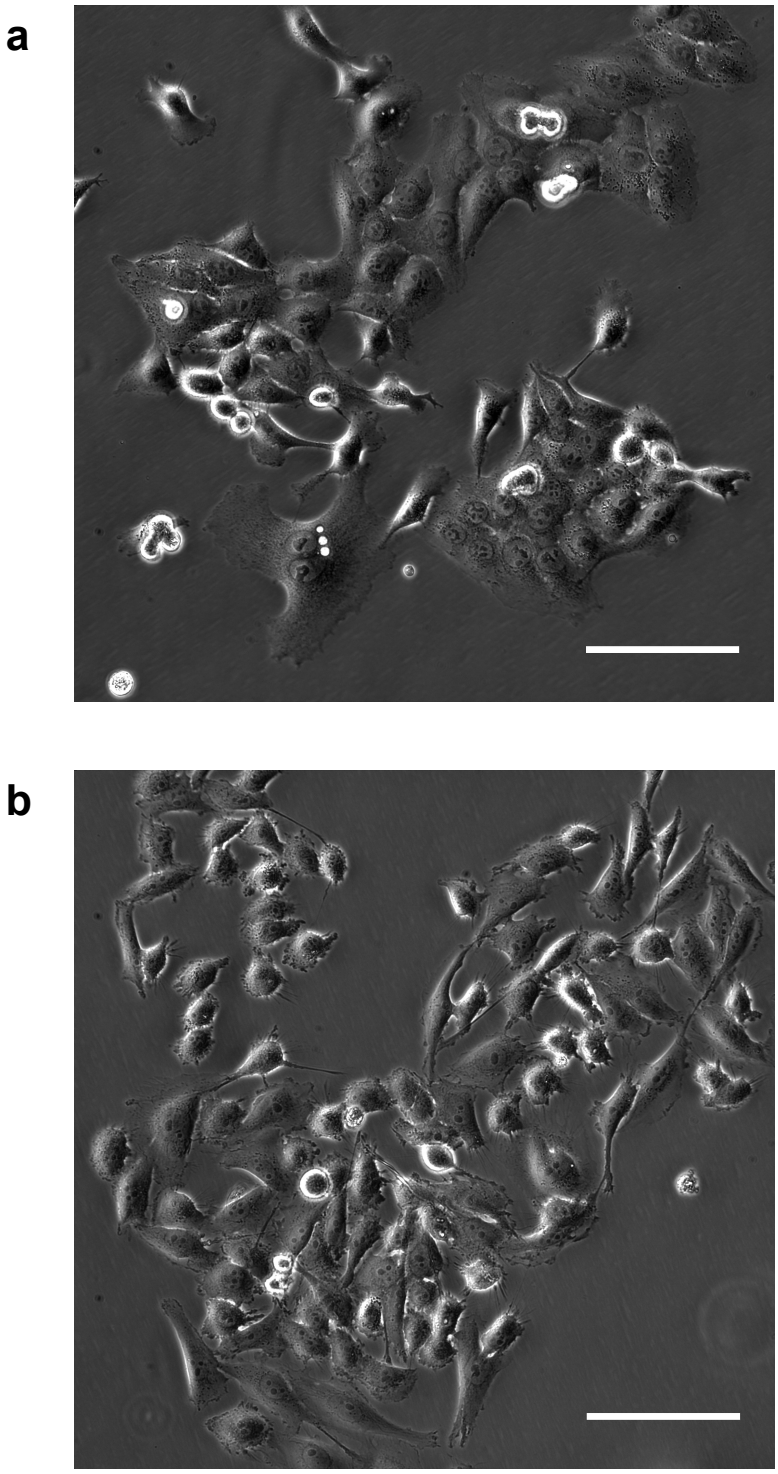

Figure 3.1 Phase contrast imaging of **a**. MDA-MB-231 and **b**. 1833 cell lines, exhibiting morphological differences. Magnification 30x. Scale bar 100 μm.

Phase contrast imaging (Figure 3.1) demonstrated the morphological differences between the MDA-MB-231 and 1833 cell lines, when cultured *in vitro*. The 1833 cell line exhibited a more mesenchymal-like appearance.

3.2.2 Comparison of pericellular oxygen with or without cells in a controlled hypoxic environment.

Mean pericellular oxygen was measured at each time point, for wells with media only or media plus MDA-MB-231 cells over a 26 hour period. Monitoring of pericellular oxygen levels, measured within cell culture wells, allowed an evaluation of the actual oxygen levels cultures were exposed to, as opposed to the regulated 1% oxygen environment in which they were conditioned. Following 30 minutes hypoxic exposure the mean percentage pericellular oxygen level for wells containing cells was lower than those with media only (2.3% ± 0.50 *vs*. 6.3% ± 0.38; $p < 0.01$, respectively) (Figures 3.2 and 3.3). In wells containing cells, mean pericellular oxygen reached 1.33%, following 1 hour incubation (Figures 3.2 and 3.3). There was a continuous decline in mean pericellular oxygen in both cell populations, ultimately falling below the 1% oxygen threshold. During the relatively stable conditions between 10 and 20 hours of hypoxic incubation, a statistically significant differential was maintained in the mean pericellular oxygenation ($\%O_2$) of wells with and without cells (0.44% ± 0.02 *vs*. 0.78% ± 0.07; $p < 0.01$, respectively)

Exposure to atmospheric oxygen at 24 hours conditioning, resulted in transient elevation of pericellular oxygen levels, emulating the intermittent reperfusion seen with hypoxic tumors. Values returned to ≤ 1% within 50 minutes of resumption of hypoxic conditions.

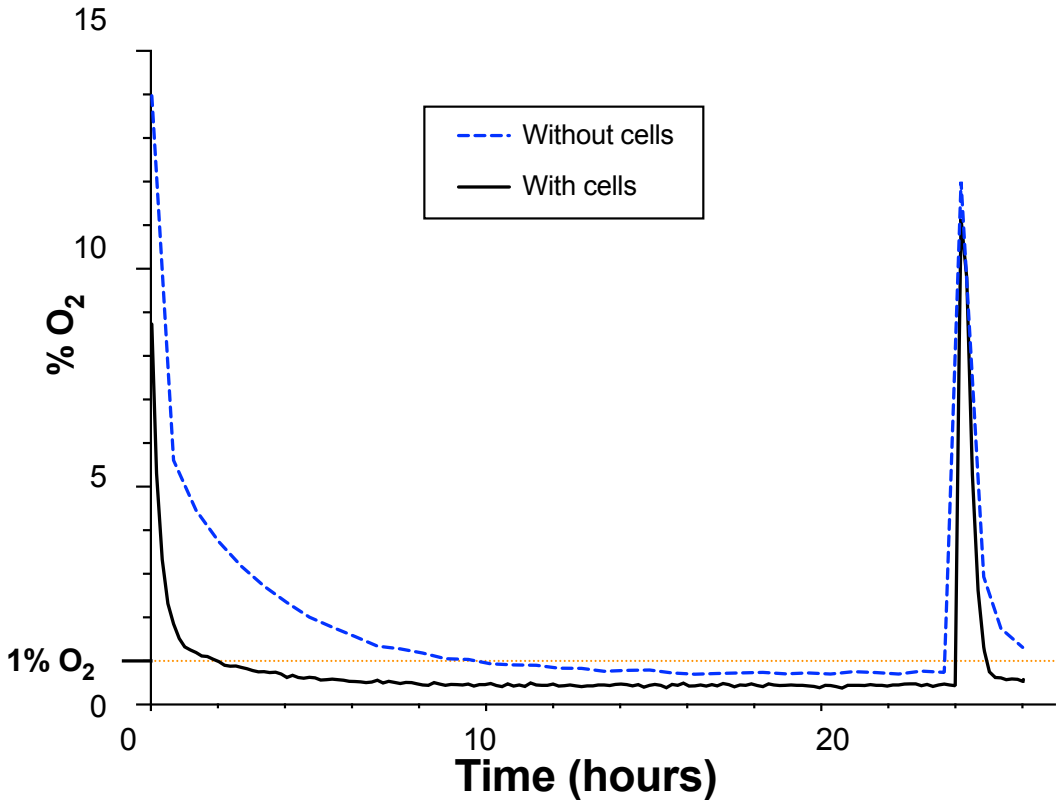

Figure 3.2 Pericellular oxygen monitoring to emulate transient intratumoral reperfusion of breast tumor. Mean pericellular oxygen recorded at ten minute intervals in the presence or absence of MDA-MB-231 cells. *n* = 3 per group from three technical replicates.

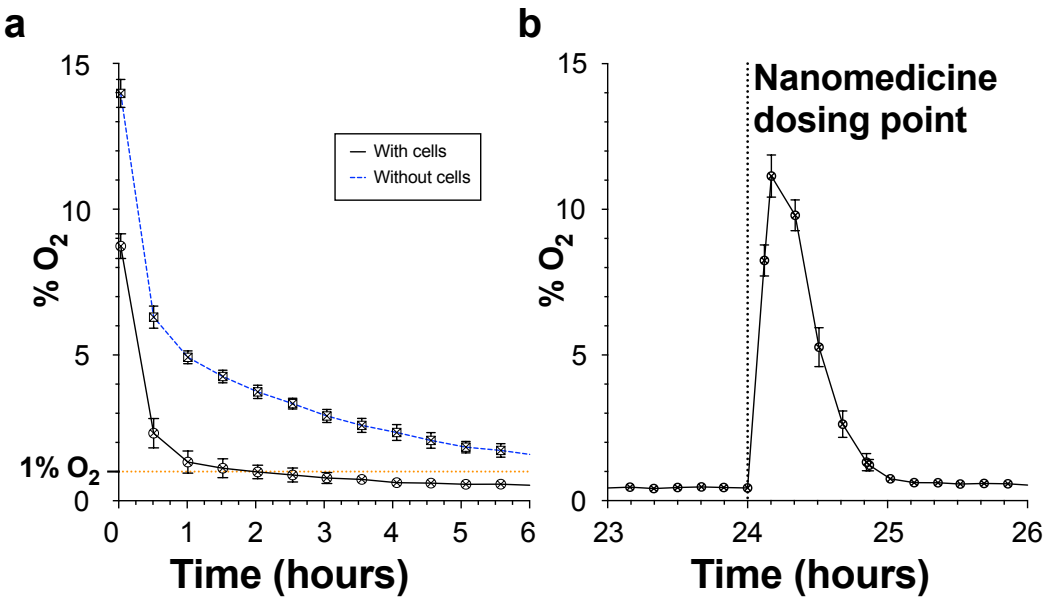

Figure 3.3 Detailed data plots derived from full 26 hour pericellular monitoring (Figure 3.2). **a.** Detailed data plot from recorded data over the first 6 hour period, showing clear distinction in pericellular oxygen between wells with cells (black) and wells without cells (blue). b. Detailed data plot between 23 and 26 hours, showing the period of simulated reperfusion, and point at which the model nanomedicine was added. For each data point, *n* = 3 ± SD, from a single biological experiment.

Having established the parameters of hypoxic conditioning for experimental work, the next step was to ensure recovery of HIF1α from cell lysates, and assessing its expression via SDS PAGE and western blotting.

3.2.3 Initial testing of HIF1α recovery, hypoxic conditioning and western blotting protocols

The protocol used throughout this thesis for the recovery of HIF1α from cell lysates, and its subsequent separation and quantification, was developed through a series of stages. This included modifying separation voltage, protein transfer duration and current, together with specific changes to both primary and secondary antibody titres. Recovery of HIF1α required a specific protocol, developed to take accord of the relatively short half-life (2 – 4 minutes) of HIF1α upon exposure to oxygen.

To consolidate (and demonstrate) successful development of these protocols, a western blot probing for HIF1α, with β actin as loading control, was prepared with cell lysates pre-treated as shown (figure 3.4). Results demonstrated effective and consistent lysate preparation containing HIf1α. Cobalt chloride treatment of cells, which blocks HIF1α breakdown, leading to its accumulation, was used as a positive control. A cobalt chloride concentration of 100 μM over 24 hours had proven effective in preliminary work, therefore here the impact of higher doses was compared. It was interesting to note that there was little difference in the HIF1α expression, following 24 hours dosing with 200 or 400 μM cobalt chloride. The exposure of MDA-MB-231 cells to either 24 or 48 hours of hypoxia, produced very little difference in relative expression of HIF1α. HIF1α was clearly detected across all wells, with reduced HIF1α levels in diluted samples, when

compared with their undiluted counterparts. In order to maximize HIF1α recovery, total protein loading per well was uncontrolled (i.e., maximum protein loading), as shown by the uneven β actin expression.

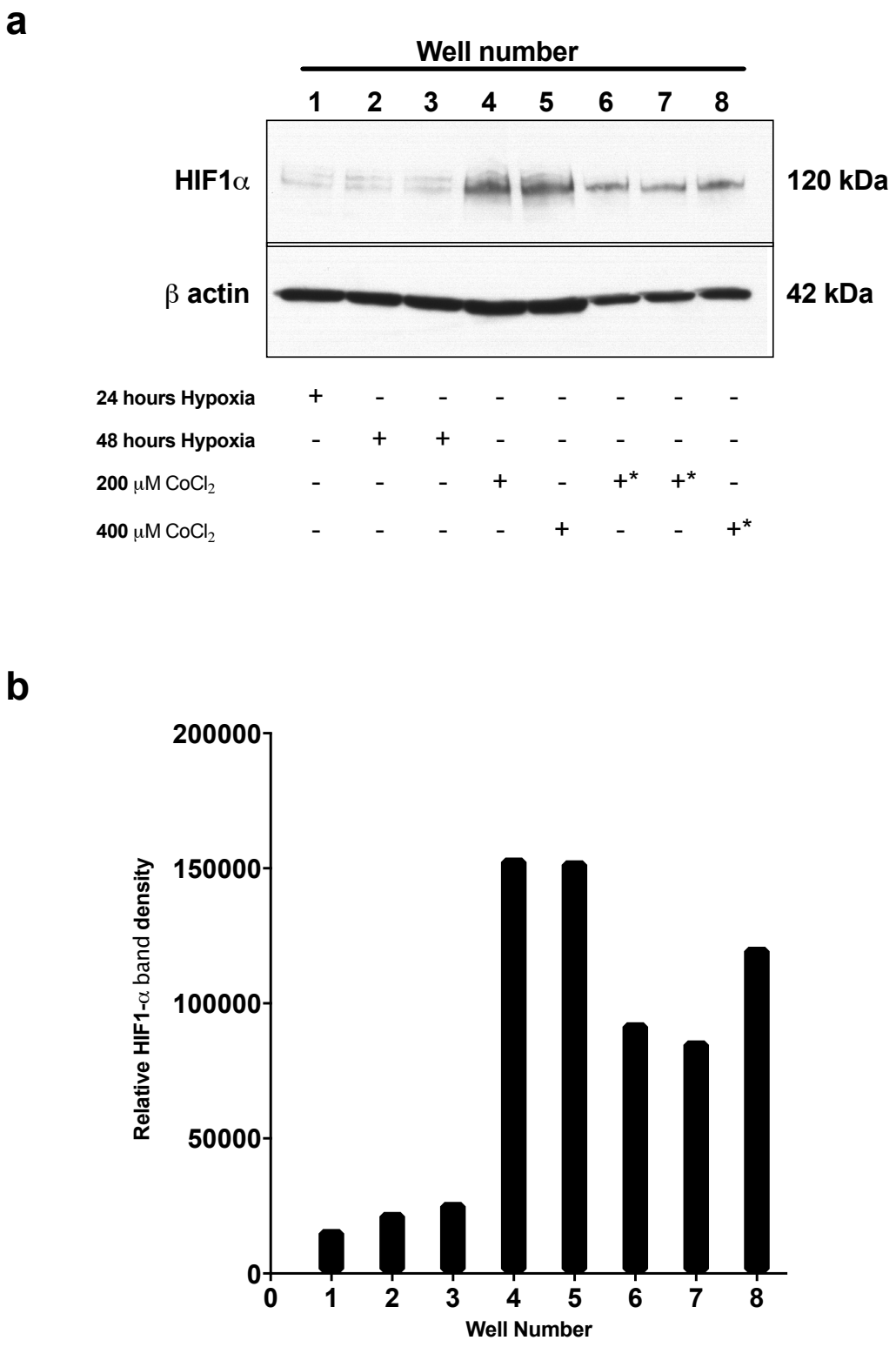

Figure 3.4 Western blot and subsequent densitometry analysis of MDA-MB-231 cell lysates pre-treated as shown. **a**. * denotes cell lysates pre-diluted 1 in 3 prior to gel loading, to assess HIF1α detection at lower concentrations. **b**. Densitometry of **a**.

As the methodology for HIF1α extraction from cell lysates and its effective detection had been demonstrated, measurements were subsequently undertaken of changes to key cell stress proteins (including HIF1α), following hypoxic conditioning.

3.2.4 Assessment of the hypoxic phenotype of MDA-MB-231 cells

The phenotypic adaptation of MDA-MB-231 cells exposed to hypoxia was monitored by assessing the expression of 11 cell stress related proteins, including HIF1α, the key effector of hypoxic adaptation, after 0, 6 and 24 hours of hypoxic conditioning (Figure 3.5). In order to afford better comparison, mean data generated from the arrays was assembled as a heat map (Figure 3.6).

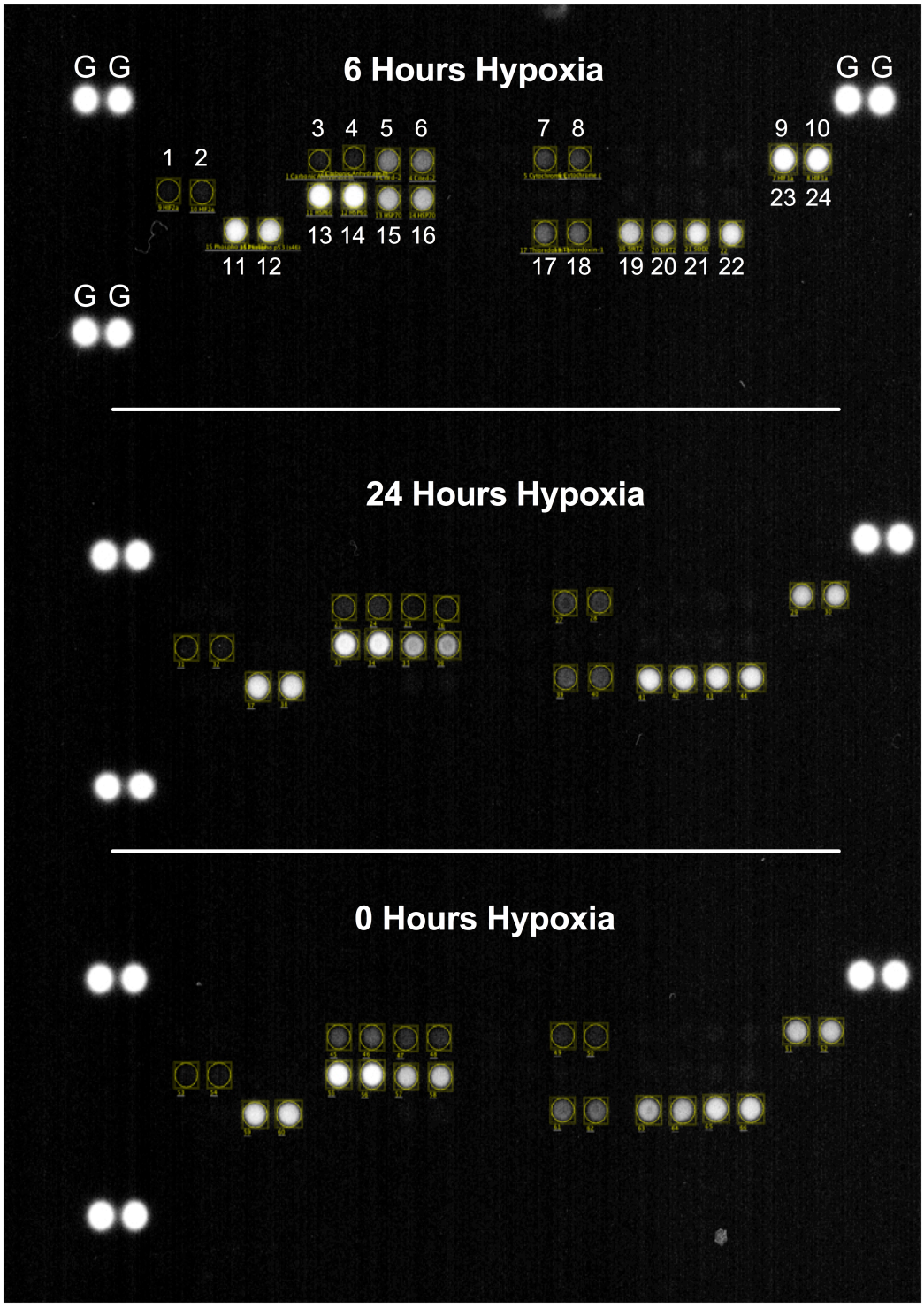

Figure 3.5 Protein array scanned fluorescent images, assembled into a single image, showing relative specific protein expression. For all three treatment groups, the numbering is the same. Protein key; spot numbers (duplicates), 1, 2 HIF2α; 3, 4 CAIX; 5, 6 Cited-2; 7, 8 Cytochrome c; 9, 10 HIF1α; 11, 12 Phospho p53; 13, 14 HSP60; 15, 16 HSP70; 17, 18 Thioredoxin-1; 19, 20 SIRT2; 21, 22 SOD2; 23, 24 p27. G = guide marker.

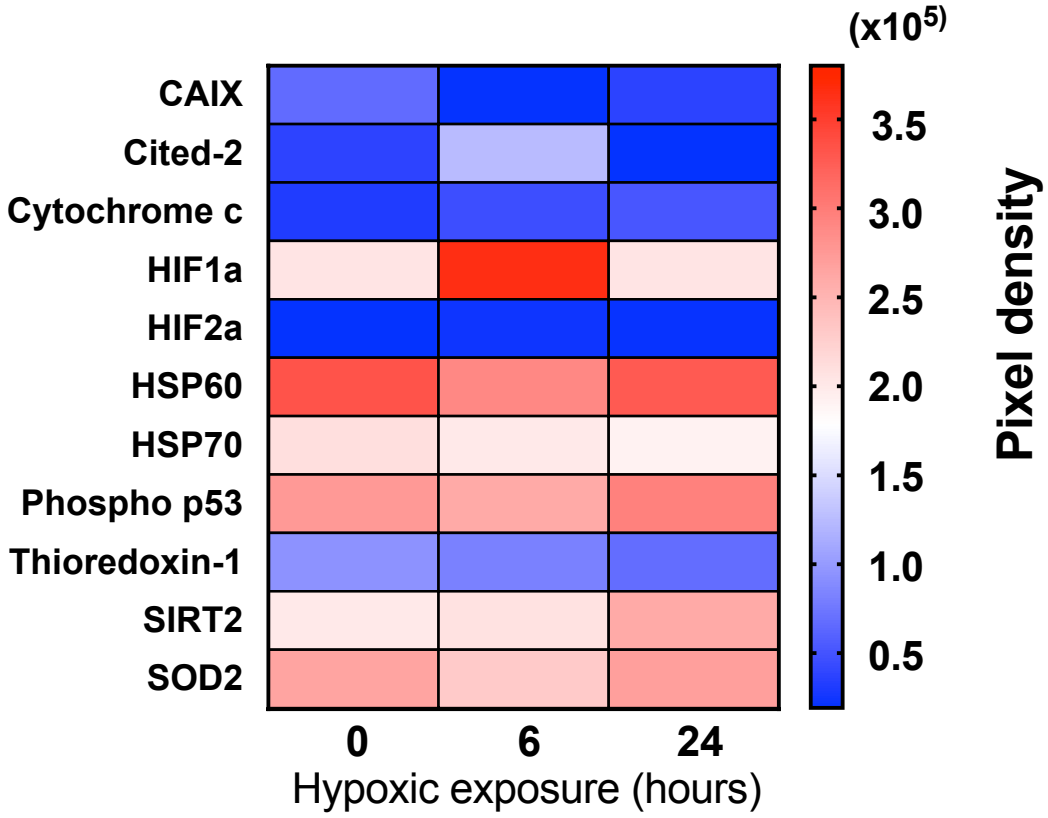

Figure 3.6 Relative expression of MDA-MB-231 key cell stress proteins in response to varying periods of hypoxic conditioning. Whole cell lysates from three biological replicates at each of the *in vitro* hypoxic incubation periods shown, were pooled and relative expression of 11 cell stress related proteins determined via protein array. Protein key; *CAIX, Carbonic Anhydrase 9; Cited-2, CbP/p300 – interacting transactivator – 2; Cytochrome c; HIF1α, α subunit of hypoxic induction factor 1; HIF2α, α subunit of hypoxic induction factor 2; HSP60, heat shock protein 60; HSP70, heat shock protein 70; Phospho p53 (s46), Phosphorylated p53; Thioredoxin-1; SIRT2, NAD-dependent deacetylase sirtuin-2; SOD2, Mitochondrial superoxide dismutase 2 (Mn-SOD).*

The protein array results from pooled cell lysates demonstrated differentially regulated cell stress associated proteins. For example, HIF1α levels were highest after 6 hours of hypoxia returning to normoxic levels after 24 hours of

hypoxia when. Carbonic anhydrase 9 expression showed a close to 2 fold increase from 6 hours to 24 hours (relative measured fluorescence 21003 and 39116, respectively). Cited-2 (CbP/p300 – interacting transactivator – 2) exhibited a similar expression profile, with elevated levels following 6 hours hypoxia, whereas Thioredoxin-1 increased progressively across the 24 hours hypoxic period (Figure 3.6). HIF1α is a master regulator of the hypoxic response; therefore, given its importance, the protein array results were verified by SDS PAGE and western blotting to determine the relative HIF1α expression in a series of biological triplicates (Figure 3.7).

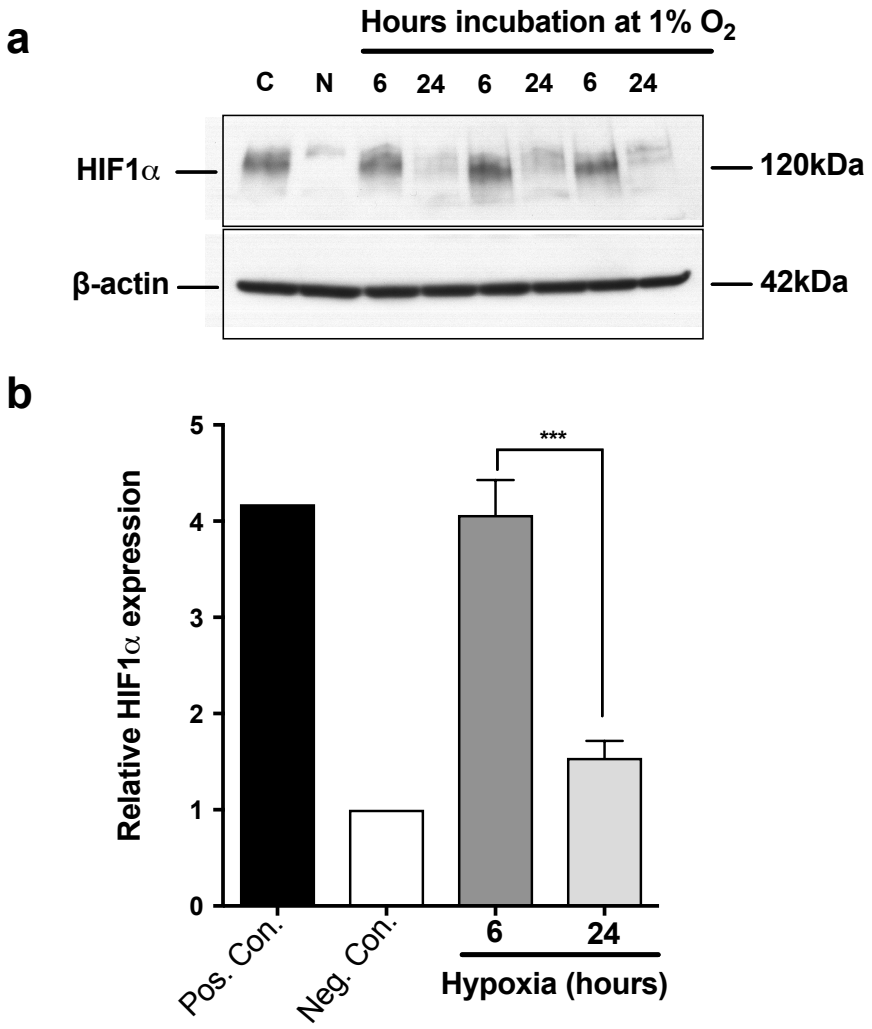

Figure 3.7 (a) SDS PAGE and immunoblotting of MDA-MB-231 whole cell lysates, stained for unhydroxylated HIF1α, with β actin as internal loading control. (b) Densitometry of (a), expressed as fold change relative to negative control (N) (normoxia), set to 1.0. For both hypoxic incubation periods, *n* = 3 from three separate biological experiments. Equivalent cells incubated for 24 hours in normoxia alone or in the presence of 100 μM $CoCl_2$, were used as negative (N) and positive (C) controls respectively. *** denotes $p < 0.001$. Error bars denote SD.

The immunoblotting results confirmed the HIF1α expression pattern observed with the protein arrays (Figures 3.5 and 3.6); namely, the HIF1α expression levels were highest after 6 hours of hypoxic incubation (a 4.10-fold increase) and lower at 24 hours (a 1.54-fold increase), whereas the control cultures showed no substantial change in HIF1α (1.0-fold). Having established the nature of the hypoxic response, and its variation depending upon duration of hypoxia, the next stage involved detection and measurement of fluorescent nanoparticles via FACS analysis.

3.2.5 Impact of fluorescent polystyrene nanoparticles on cell viability

The potential confounding effects from reduced cell viability due to nanoparticles were excluded by assessing cell viability first. Cell viability over a 48 hour period was similar under either hypoxic or normoxic incubation conditions following exposure to the range of nanoparticle concentrations (Figure 3.8); no biologically significant reduction of cell viability was observed ($IC_{50} > 10^{11}$ nanoparticles/ml). It is important to observe, however, that there was a small but statistically significant reduction in relative cell viability within the normoxic cell population, following 48 hours exposure to 1×10^{11} nanoparticles/ml.

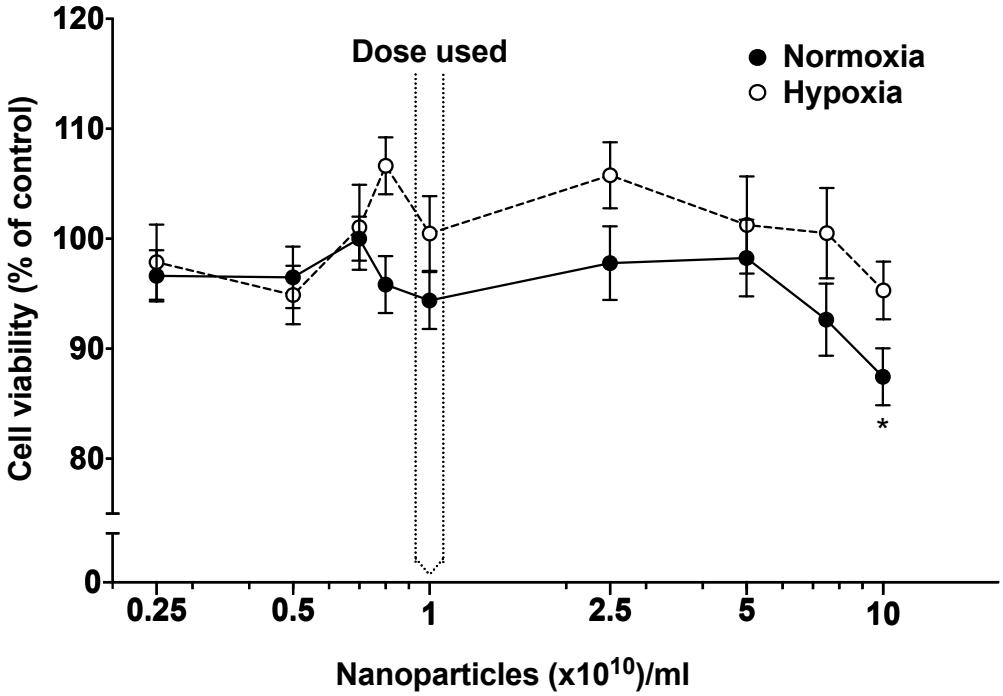

Figure 3.8 Cytotoxicity and uptake of nanoparticles in response to normoxia and hypoxia. (a) *In vitro* cytotoxicity of fluorescent nanoparticles in the MDA-MB-231 human breast cancer cells. Cells were dosed with fluorescent nanoparticles and subsequently cultured in either hypoxia (1% O_2) or normoxia. At 48 hours cell viability was assessed using the MTT assay. Dotted lines indicate the nanoparticle dose used for subsequent studies (*n* = 18 at each dosing point, from three biological replicates; ± SD). The dose, as shown, selected for subsequent studies, 1 x 10^{10} nanoparticles/ml, corresponds to 7 x 10^{-2} mg/ml polystyrene.

3.2.6 Imaging the Endolysosomal trafficking of fluorescent nanoparticles via dual wavelength confocal microscopy

Dual wavelength confocal imaging of live MDA-MB-231 cells revealed co-localisation of the fluorescent nanoparticles (green) with acidic intracellular vesicles (red), indicating endolysosomal uptake for both control (normoxic) and hypoxic cultures (Figures 3.9 and 3.10). The overall trafficking pattern was similar for both normoxic and hypoxic cultures following a 45 minutes or 180 minutes exposure to nanoparticles (Figures 3.9 and 3.10). Importantly, nanoparticles were also found distributed throughout the interior of the cell following both normoxic and hypoxic conditioning. No increased membrane binding of nanoparticles was observed with hypoxic conditioned cells, compared to normoxic equivalents.

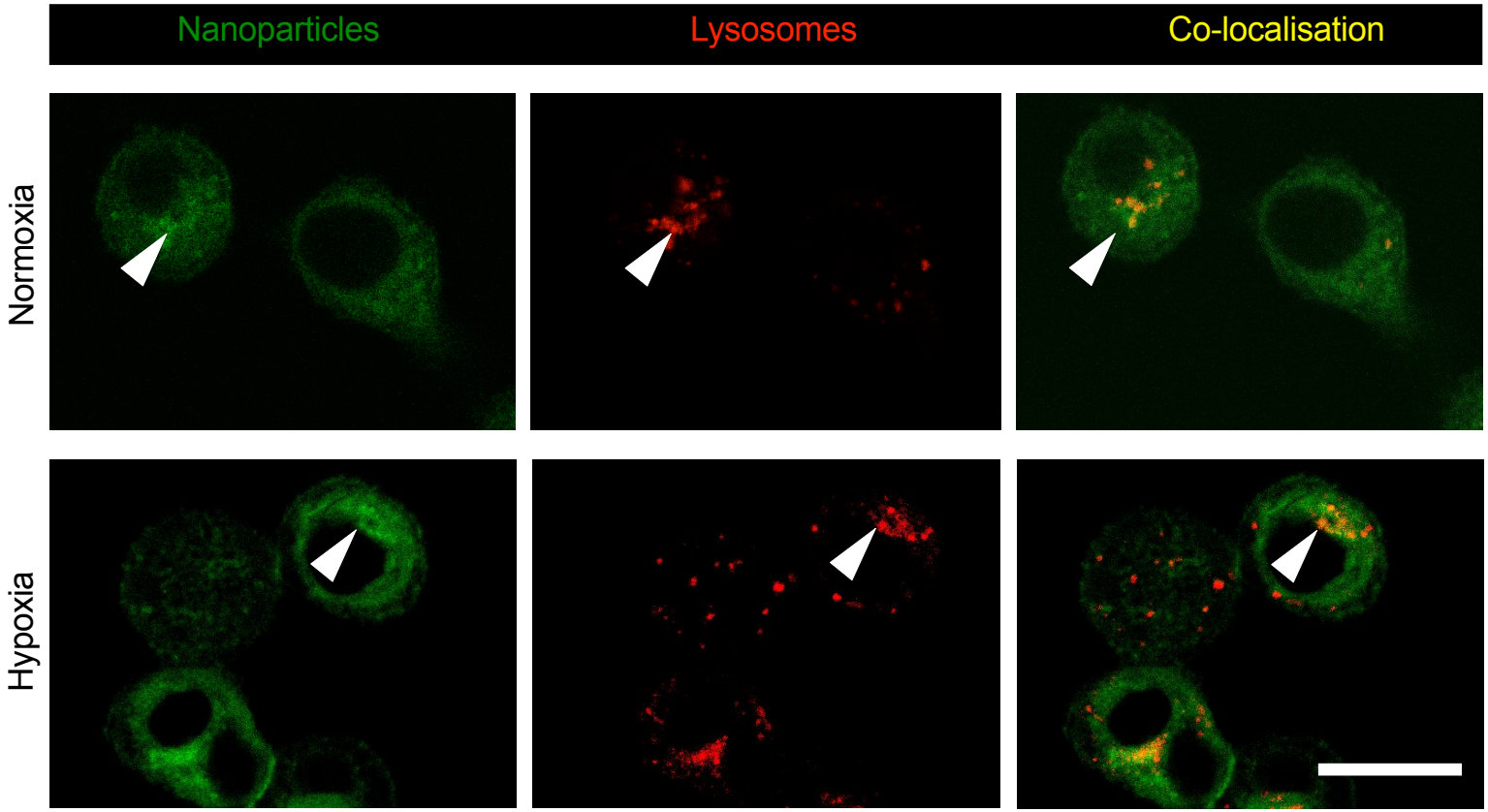

Figure 3.9 Representative live cell confocal imaging of cells exposed for 24 hours to normoxia or hypoxia and subsequently dosed for 45 minutes with nanoparticles (green). Acidic vesicles were stained using LysoTracker Red. Arrows show nanoparticle co-localisation in acidic vesicles. Scale bar 20 μm.

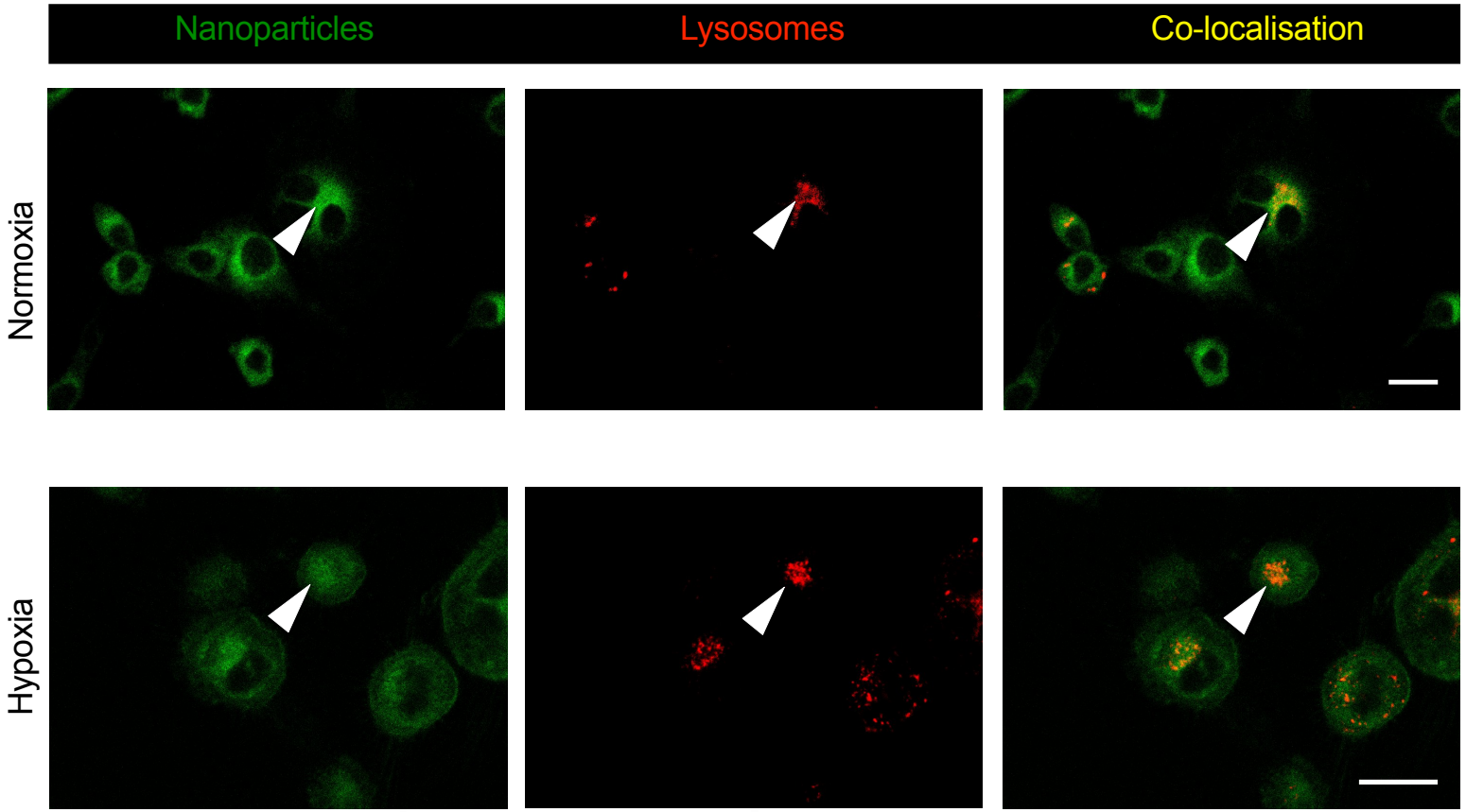

Figure 3.10 Representative live cell confocal imaging of cells exposed for 24 hours to normoxia or hypoxia and subsequently dosed for 180 minutes with nanoparticles (green). Acidic vesicles were stained using LysoTracker Red. Arrows show nanoparticle co-localisation in acidic vesicles. Scale bar 20 μm

3.2.7 *In vitro* assessment of the uptake of varying concentrations of nanoparticles by MDA-MB-231 cells

In order to determine the most appropriate concentration of fluorescent nanoparticles to use for comparing uptake or efflux in MDA-MB-231 cells, several initial experiments were conducted. MDA-MB-231 cells, conditioned in a normoxic environment were dosed with varying concentrations of fluorescent nanoparticles, as shown, and mean cellular FITC fluorescence determined (Figure 3.12). Results showed that measured mean cellular FITC fluorescence varied with effective nanoparticle concentration (Figure 3.11).

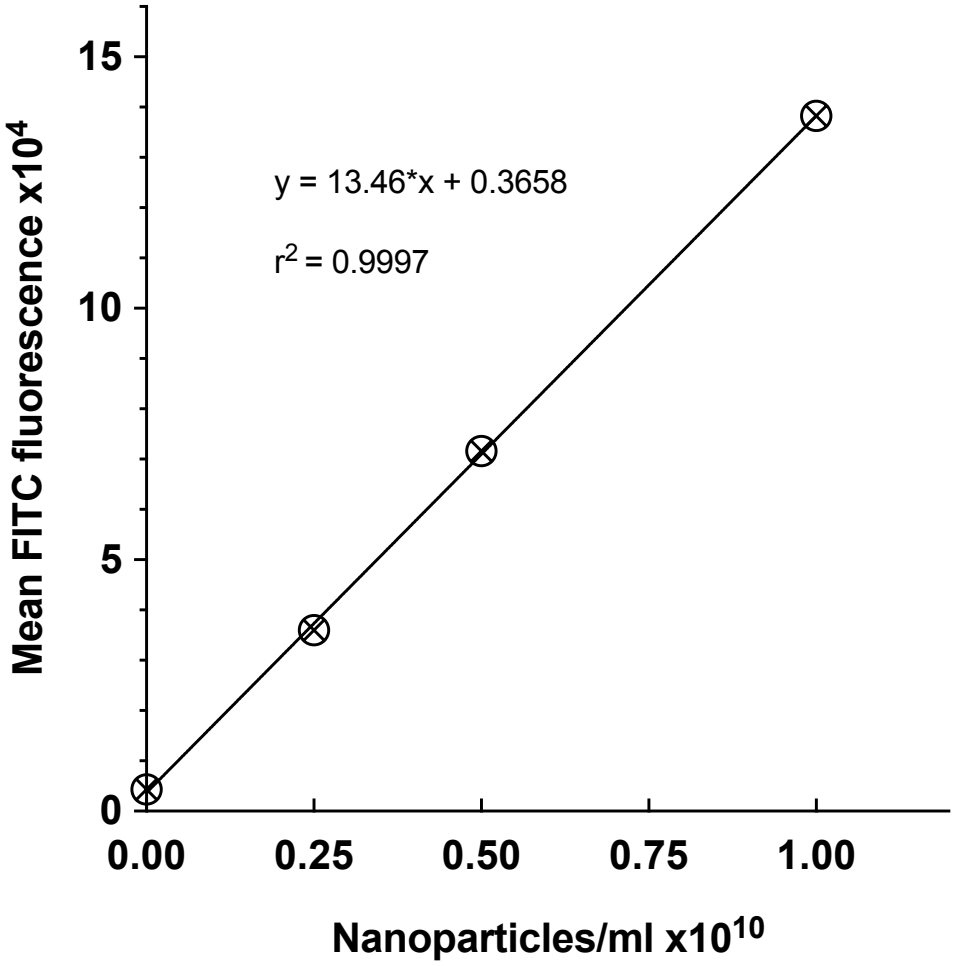

Figure 3.11 Linear relationship of FITC fluorescence and nanoparticle concentration in MDA-MB-231 cells. At all concentrations *n* = 1, except 1 x 10^{10} nanoparticles/ml, where *n* = 3 technical replicates, from a single biological experiment.

To further explore measured mean cellular FITC fluorescence, and its relationship with nanoparticle concentration, MDA-MB-231 cells were conditioned in normoxic or hypoxic conditions, then dosed with three different nanoparticle concentrations. The results demonstrated (Figures 3.13) clear differentiation in measured mean cellular FITC fluorescence, which consistently varied with nanoparticle concentration in both normoxic and hypoxic conditioned MDA-MB-231 cells.

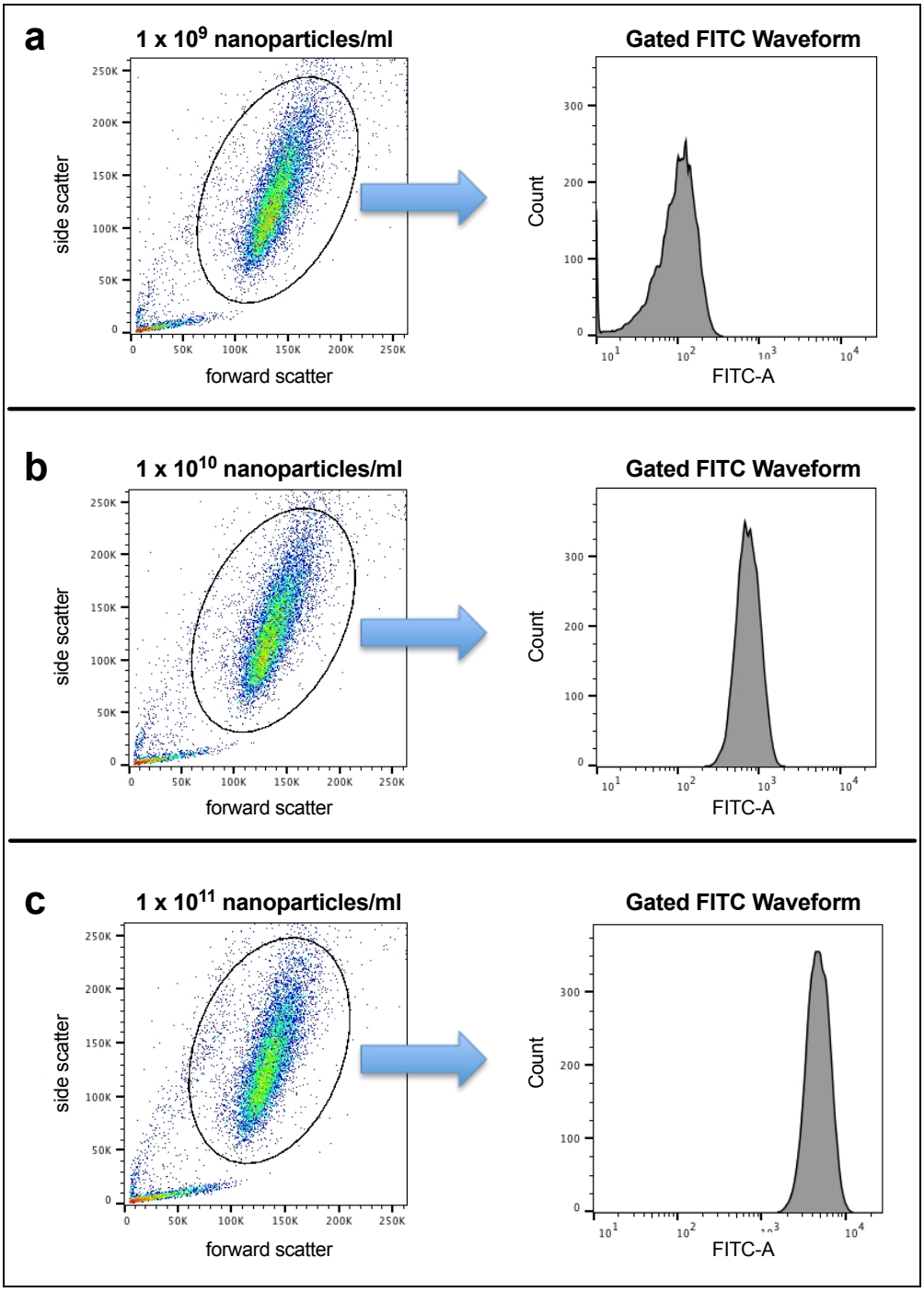

Figure 3.12 Representative FACS plots from three cell lysates, at each of three nanoparticle concentrations used. Scatter dot plots (left panel) represent gating for MDA-MB-231 cells (≥10,000 events), in either normoxic (c), or hypoxic (a and b) conditions, at nanoparticle concentrations shown. Right panel; gated FITC waveforms, from which mean FITC fluorescence was calculated for each sample. Colouring on scatter plots represent event frequency.

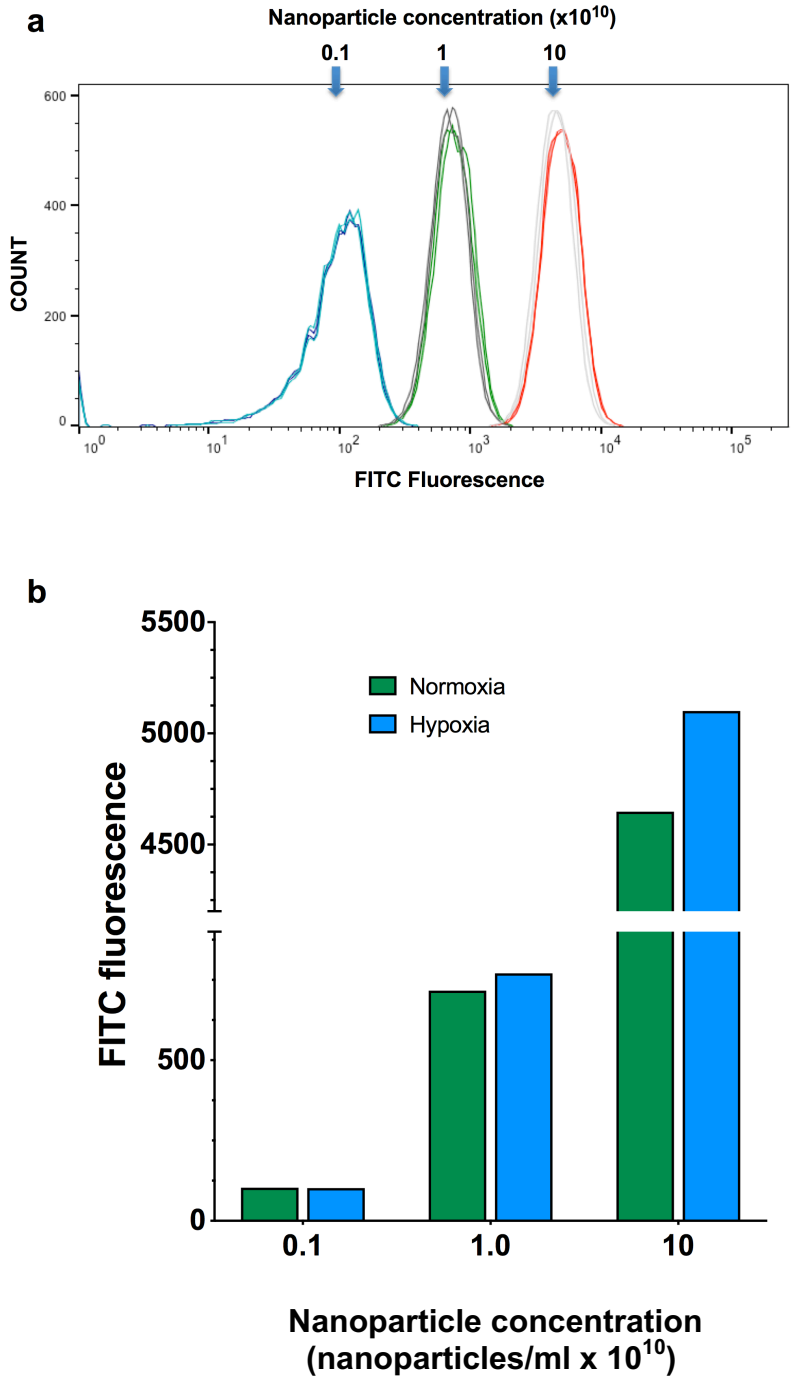

Figure 3.13 FITC fluorescence measurements from MDA-MB-231 cells pre-conditioned for 24 hours in either normoxic or hypoxic conditions and dosed with fluorescent nanoparticles at the concentrations shown for 180 minutes. **a.** Mean FITC fluorescence waveform overlay derived from all 12 samples measured. **b**. Mean FITC fluorescence values. *n* = 2 technical replicates per treatment group, and nanoparticle concentration, providing 12 measurements in total, generated from a single biological experiment.

Based upon these results, the concentration of nanoparticles used in further experimental work with the MDA-MB-231 cell line was 1 x 10^{10} nanoparticles/ml.

The next step was to compare nanoparticle uptake by MDA-MB-231 cells under normoxic or hypoxic (of varying duration) conditions, and with varying nanoparticle dosing intervals.

3.2.8 *In vitro* comparative measurement of nanoparticle uptake by the MDA-MB-231 cell line, following normoxic or hypoxic incubation

The relative expression of cell stress related proteins, and in particular, the differential expression of HIF1α observed after 6 or 24 hours of hypoxic conditioning (Figures 3.6 and 3.7) led to the choice of these same time points for uptake studies in MDA- MB-231 human breast cancer cells. The experimental protocol used, is summarized in figure 3.14.

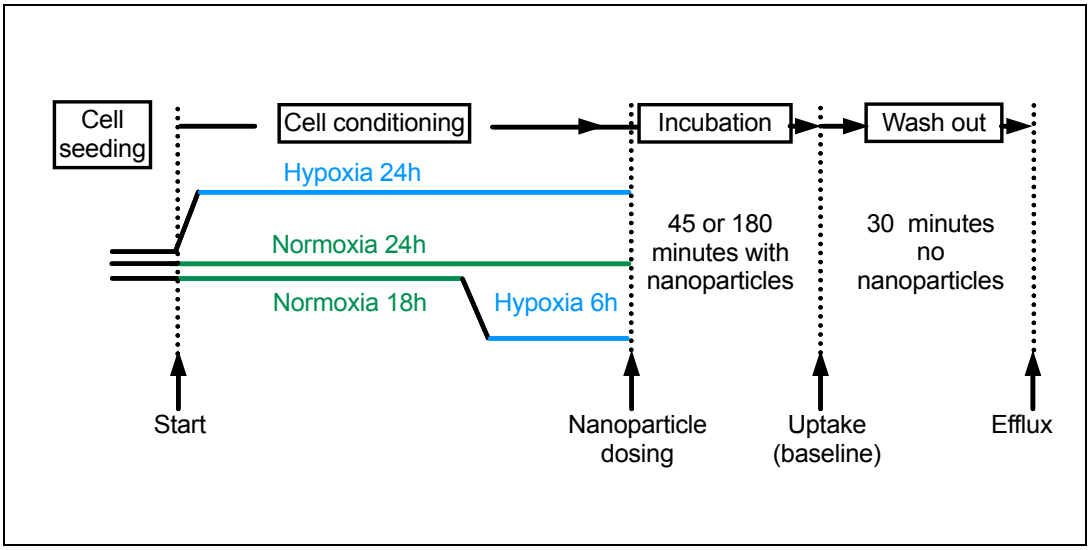

Figure 3.14 Schematic overview of uptake and efflux studies conducted using the human MDA-MB-231 and 1833 cell lines. 1883 cell uptake/efflux studies, were conducted following 24 hours normoxic or hypoxic incubation, with a nanoparticle dosing interval of 45 minutes only.

Following the respective hypoxia conditioning, MDA-MB-231 cells were exposed to nanoparticles for either 45 or 180 minutes. When compared to the respective normoxic controls, nanoparticle uptake at 45 minutes was significantly increased (100.0 ± 4.76 *vs*. 108 ± 4.35; $p < 0.001$, respectively) in cells exposed to 6 hours of hypoxic conditioning (Figures 3.15 and 3.16). With the same hypoxic conditioning regime, nanoparticle uptake was substantially upregulated (100.0 ± 2.71 *vs*. 101.56 ± 3.71; $p = 0.2$) at 180 minutes (Figures 3.15 and 3.16). By contrast, cells conditioned for 24 hours under hypoxia showed significantly increased nanoparticle uptake at both the 45 and 180 minute dosing intervals when compared to normoxic control cultures. The largest overall upregulation of nanoparticle uptake (10%) was observed at the 45 minute dosing interval in cells conditioned under hypoxia for 24 hours (Figure 3.16)

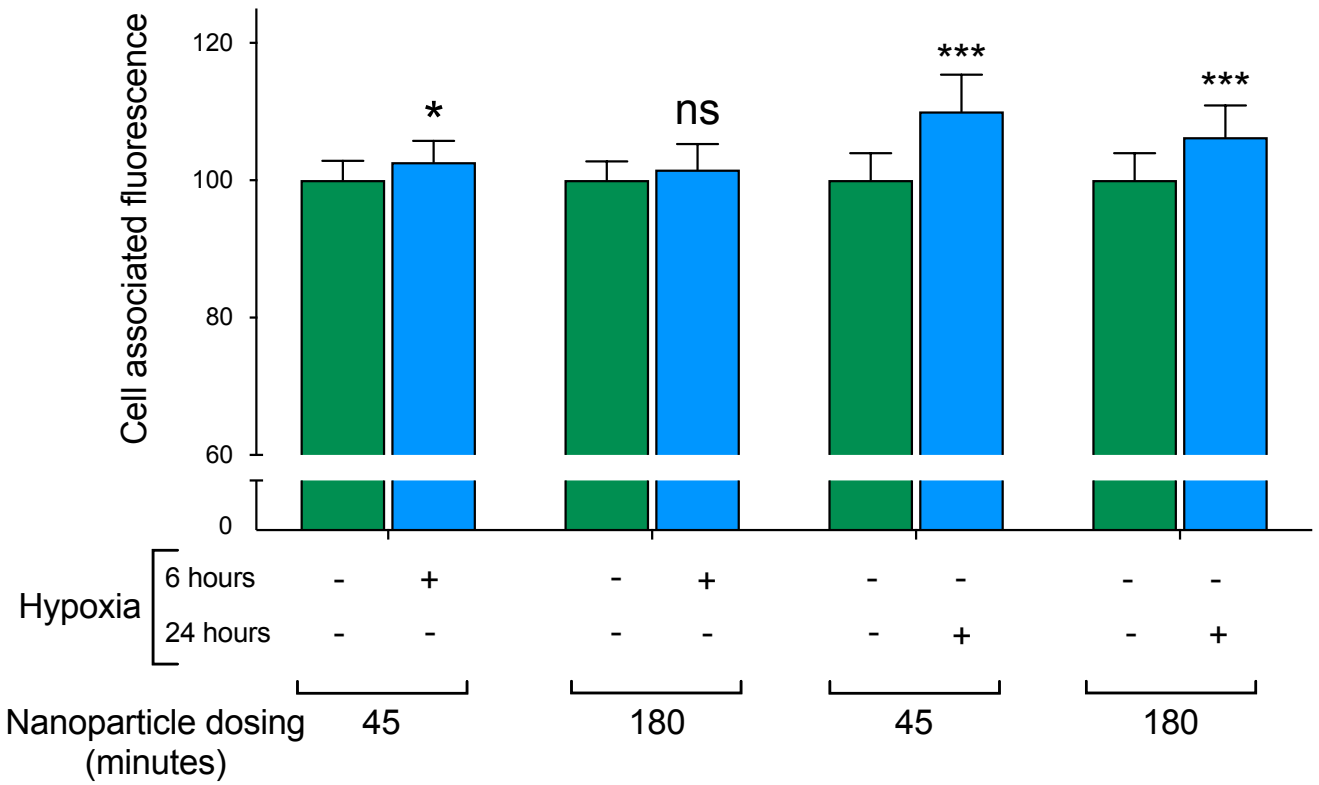

Figure 3.15 Impact of hypoxic preconditioning on the uptake of nanoparticles by human MDA-MB-231 breast cancer cells. Cells were conditioned in hypoxia (1% O_2) for either 6 or 24 hours and then dosed with nanoparticles for either 45 or 180 minutes. Uptake of fluorescent nanoparticles was assessed by measuring mean single cell-associated fluorescence by flow cytometry; ≥10,000 events and. For each hypoxic treatment interval and dosing interval, *n* = 3 biological experiments, consisting of fifteen technical replicate comparisons (5 wells x 3, from 3 x 6-well plates in normoxia, and 5 wells x 3, from 3 x 6 – well plates in hypoxia) per treatment group and dosing interval ± SD. (Experimental scheme also shown in figure 3.14).

In order to better compare the relative differences in nanoparticle uptake (Figure 3.15), mean percentage change (normoxia vs. hypoxia) in cellular FITC fluorescence was calculated and plotted below (Figure 3.16).

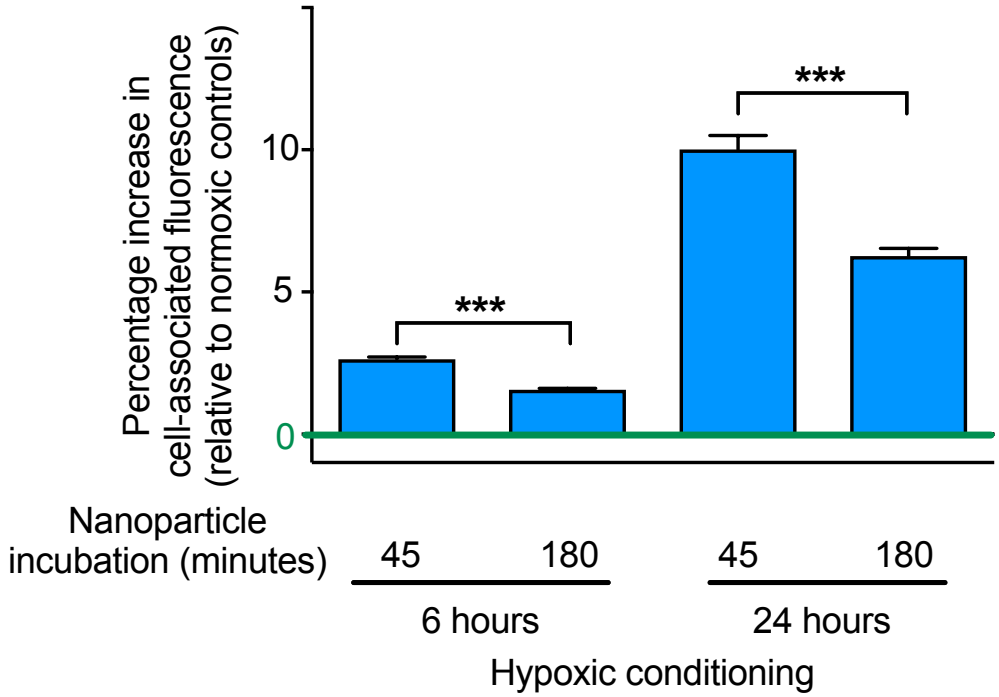

Figure 3.16 Impact of hypoxic preconditioning on the uptake (endocytosis) of nanoparticles by human MDA-MB-231 breast cancer cells. Mean percentage change in FITC fluorescence recorded, per dosing interval and hypoxic conditioning duration, relative to normoxic controls. Green bar represents normoxic baseline. *n* = 3 biological experiments for each dosing group and treatment period ± SD. This data was generated from the detailed experimental data shown in figure 3.15.

3.2.9 *In vitro* comparative measurement of nanoparticle uptake by the 1833 cell line, following normoxic or hypoxic incubation

As the largest observed increase in nanoparticle uptake with the MDA-MB-231 cell line was found with 24 hours hypoxic incubation, followed by 45 minutes dosing with nanoparticles, those conditions were used for confirmation studies with the 1833 breast cancer bone metastatic subline. 1833 cells conditioned for 24 hours in hypoxia and dosed with nanoparticles for 45 minutes also resulted in a significantly increased (7.96%) nanoparticle uptake (Figure 3.17), when compared with normoxic equivalents. Similar to Figure 3.16, the results were calculated and plotted as mean percentage change in FITC fluorescence.

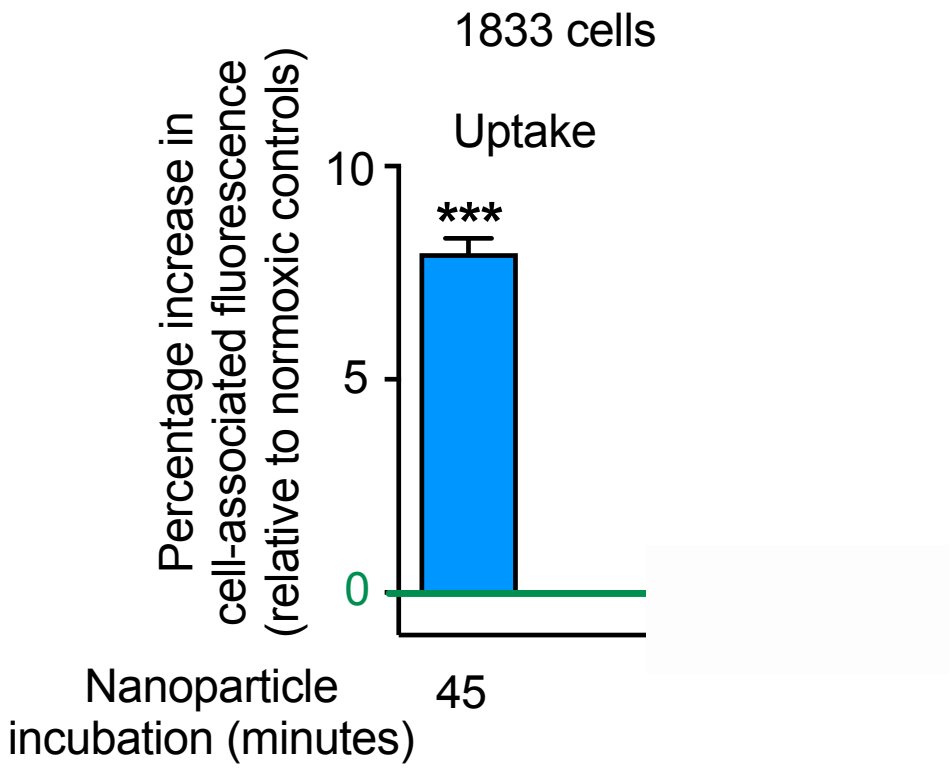

Figure 3.17 Impact of hypoxic preconditioning on the uptake (endocytosis) of nanoparticles by human 1833 breast cancer cells. 1833 cells, were incubated in normoxic or hypoxic conditions for 24 hours, followed by dosing with fluorescent nanoparticles (1 x 10^{10} nanoparticles/ml) for 45 minutes. Mean percentage change in FITC fluorescence, relative to normoxic controls was then calculated as before. Green bar represents normoxic baseline. *n* = 3 independent biological experiments, consisting of fifteen technical replicate comparisons (5 wells x 3, from 3 x 6-well plates in normoxia, and 5 wells x 3, from 3 x 6-well plates in hypoxia) ± SD.

3.2.10 *In vitro* comparative measurement of nanoparticle efflux (exocytosis) by the MDA-MB-231 and 1833 cell lines, following normoxic or hypoxic incubation

The observation that hypoxic conditioned MDA-MB-231 and 1833 cells showed consistently increased nanoparticle uptake raised the possibility that this response was due to (i) increased endocytosis (i.e. uptake), (ii) reduced exocytosis (i.e. recycling) or (iii) a combination of both (i) and (ii). This question was addressed by performing pulse chase experiments with normoxic and hypoxic conditioned cells. These studies were conducted with MDA-MB-231 and 1833 cells which were conditioned for 24 hours to hypoxia and pulse dosed for 45 minutes, as this treatment gave the greatest relative increase in nanoparticle uptake (Figures 3.15, 3.16 and 3.17). After this treatment, the cells were chased for 30 minutes and then analysed. Comparison of the baseline cell-associated fluorescence with post chase cell-associated fluorescence demonstrated a post-chase drop in the MDA-MB-231 cells which was significantly greater following hypoxic conditioning than following normoxic conditioning (81.13% ± 2.18, n =15 and 72.14% ± 4.94, n = 15, respectively) (Figure 3.18). Similarly, the post-chase drop in the 1833 cells was also significantly greater following hypoxic conditioning than with normoxic conditioning (52.09% ± 4.85, n = 10 and 43.74% ± 2.39, n =10, respectively) (Figure 3.19).

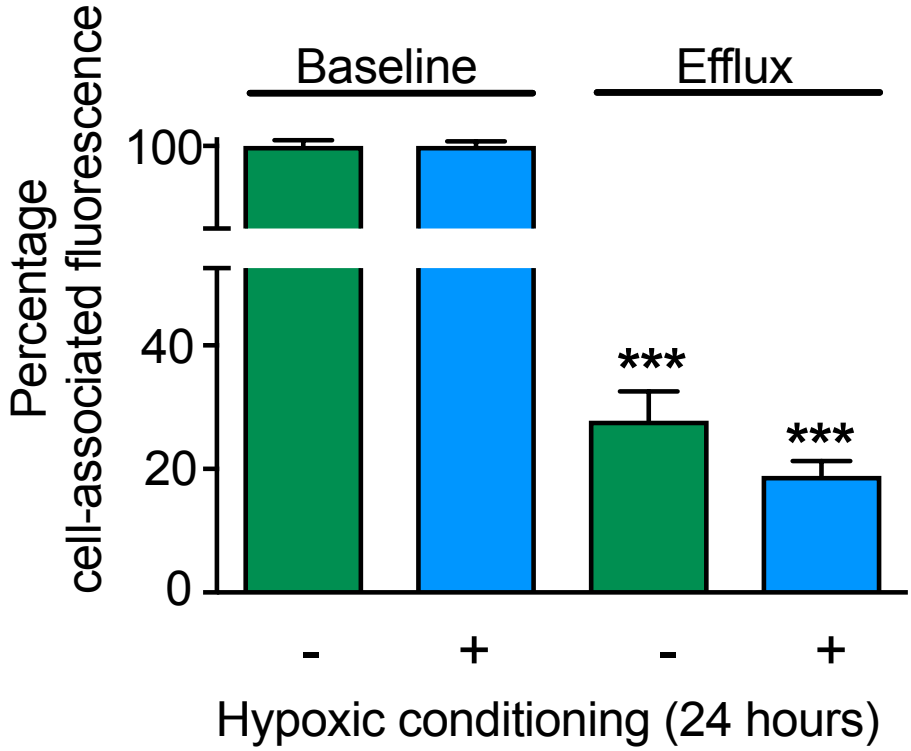

Figure 3.18 Impact of hypoxic preconditioning on the recycling (exocytosis) of nanoparticles by human MDA-MB-231 breast cancer cells. Cellular uptake of fluorescent nanoparticles was assessed for baseline and efflux by measuring mean single cell-associated fluorescence via flow cytometry, gating for ≥ 10,000 events; For baseline and efflux comparison, in either normoxic or hypoxic conditions, *n* = 3 biological experiments, consisting of fifteen technical replicate comparisons (5 wells x 3, from 3 x 6-well plates for baseline measurements (normoxia and hypoxia) and 5 wells x 3, from 3 x 6 – well plates for efflux measurements (normoxia and hypoxia)) ± SD. Experimental scheme also shown in Figure 3.14.

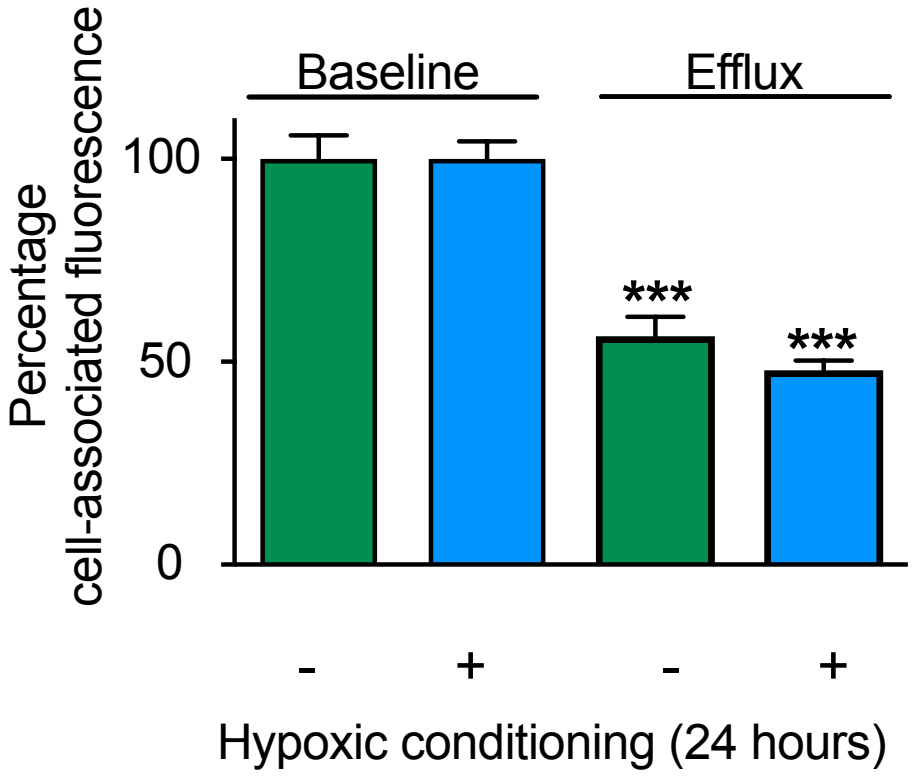

Figure 3.19 Impact of hypoxic preconditioning on the recycling (exocytosis) of nanoparticles by the human 1833 breast cancer cell bone metastatic subline. Cellular uptake of fluorescent nanoparticles was assessed for baseline and efflux by measuring mean single cell-associated fluorescence via flow cytometry, gating for ≥ 10,000 events; For baseline and efflux comparison, in either normoxic or hypoxic conditions, *n* = 2 biological experiments, consisting of ten technical replicate comparisons (5 wells x 2, from 2 x 6-well plates for baseline measurements (normoxia and hypoxia) and 5 wells x 2, from 2 x 6 – well plates for efflux measurements (normoxia and hypoxia)) ± SD. Experimental scheme also shown in Figure 3.14.

3.3 Discussion

This is believed to be the first quantitative study on human breast cancer cells that assesses the impact of hypoxic adaptation on both nanomedicine internalisation and recycling whilst also taking into account the temporal changes in key elements of the hypoxic adaptation circuit itself. Recent mechanistic insights into nanomedicine access to tumor cells includes transient vascular bursts (Harney *et al.* 2015; Matsumoto *et al*. 2016) and a combination of radiotherapy and tumor associated macrophages (TAM) that show the potential to enhance therapeutic delivery of nanomedicines via the characteristically short periodic vascular reperfusion (Miller *et al.* 2017) found in tumors. In experimental xenografts these vascular bursts were dependent on blood flow, were intermittent and facilitated nanomedicine distribution into large areas of the tumor (100 sμ^2) (Matsumoto *et al*. 2016). The uptake studies were therefore designed so that nanomedicine dosing occurred at the start of short periods of re-oxygenation, followed by hypoxia. This reflected the current understanding of transient tumor vascular reperfusion (Michiels *et al.* 2016), and the subsequent access of nanomedicines to the intratumoral space.

This study examined the impact of hypoxia on nanoparticle endo- and exocytosis using a simple, but yet effective and well-controlled two-dimensional *in vitro* culture system. The merit of this system is the ability to both monitor pericellular oxygen levels non-invasively and to quantify

nanoparticle uptake and efflux. Unlike three-dimensional organotypic culture models this model system reduced the complexity thus eliminating confounding factors such as mass transport limitations (of both nanoparticles and oxygen) and permitting rapid sample processing and analysis. Rapid sample handling is important to ensure that endocytosis and exocytosis is arrested (here by placing samples on ice). While this study demonstrates the basic role of hypoxia in nanoparticle uptake and efflux, many other factors are likely to impact nanomedicine performance. A number of normoxic studies have considered factors like stability of the carrier, cargo release and particle size and elasticity (Akinc and Battaglia, 2013). However, this study was designed specifically to exclude as many of these confounding factors as possible. The particle size of 43.4 ± 4.4 nm, was selected because clinically used nanomedicines are typically within the 10 to 100 nm size range (Shi *et al.* 2016; Duncan and Gaspar, 2011). Furthermore, particles with a nominal diameter of 50 nm have no restrictions with respect to uptake routes into cells, which is encountered at larger particle sizes (e.g. >100 nm limited caveola uptake) (Duncan and Gaspar, 2011). Furthermore, polystyrene nanoparticles were selected to minimize any confounding effects (e.g. alternations of plasma membrane/endocytic membrane compositions) (Duncan and Gaspar, 2011).

The results showed that nanomedicine internalisation is altered in a dynamic fashion in response to varying periods of hypoxic conditioning and dosing intervals (Figures 3.16 and 3.17). These findings paralleled the altered

expression of key proteins within the hypoxic adaptation circuit itself. MDA-MB-231 cells increased their capacity for internalisation of nanoparticles in response to hypoxic conditioning for 6 or 24 hours, with the greatest difference observed following 24 hours hypoxia. In addition, following all hypoxic conditioning periods, the greatest relative increase in internalisation was observed over a 45 minute nanoparticle dosing interval (Figures 3.15 and 3.16). The MDA-MB-231 parent cell line is heterogeneous and contains adapted, highly metastatic sub-populations (Kang *et al.* 2003; Minn *et al.* 2005). The performance of nanoparticles in the bone metastatic subline 1833 was therefore examined, because bone metastasis is common in triple negative breast cancer (Massagué and Obenauf, 2016). The cellular response in MDA-MB-231 and 1833 cells (classified as mesenchymal-like) was also examined to make inroads into the effects of tumor heterogeneity (within the same patient) on nanomedicine uptake and efflux in hypoxia. However, gene expression analysis of triple negative breast cancer has identified six main subtypes (mesenchymal-like cells are one of them) (Abramson and Mayer, 2014). It thus remains to be seen how all these different subclasses of triple negative cells respond to hypoxia.

Similarly to the parent cell line, 24 hour hypoxic conditioning of 1833 cells followed by a 45 minute dosing interval showed a significant increase in nanoparticle uptake (Figure 3.17). Furthermore, both the MDA-MB-231 and 1833 cell lines conditioned to hypoxia for 24 hours increased their exocytosis of nanoparticles (Figures 3.18 and 3.19). It is therefore speculated that

hypoxic endocytic uptake and recycling are similar in both these mesenchymal-like breast cancer cell lines. However, systematic studies examining potential differences in such mechanisms between these lines have not been reported.

Overall, these results demonstrate that intratumoral hypoxia has the potential to alter nanomedicine uptake by tumor cells, thereby modifying intracellular trafficking and confounding effective therapeutic payload delivery.

A key aspect of the hypoxic response is the shift from energy-efficient oxidative phosphorylation to the less productive, yet oxygen conserving, glycolytic pathway (Kim *et al.* 2006; Papandreou *et al.* 2006; Semenza, 2013). As a consequence, hypoxic tumor cells may enter a lower energy state associated with reduced ATP synthesis. Because nanomedicine internalisation via endocytosis is an active, energy-dependent process, the expectation would be a reduction in nanomedicine internalisation, yet here, a significant increase was observed. There are however, few studies available for comparison with this work. One study reported a reduction in the cellular uptake of 1.9 nm gold nanoparticles in MDA-MB-231 cells under hypoxic conditions (Jain *et al.* 2014). However, that study employed a very low (0.1%) oxygen environment for hypoxic conditioning and the conditioning was only for 4 hours prior to dosing with nanoparticles. Some cellular hypoxic adaptations would be expected over that short duration of hypoxia, but no validations of molecular changes were reported and pericellular oxygen

levels were not determined. For this research, therefore, *in situ* pericellular oxygen monitoring was adopted and 11 stress related proteins were tracked (including the master hypoxic effector, HIF1α) as markers of hypoxic cellular conditioning and the cellular hypoxic response, respectively. By contrast, in a different study, (Neshatian *et al.* 2014) the results demonstrated elevated internalisation of gold nanoparticles (sizes: 15, 50 and 70 nm) in human MCF-7 breast cancer cells following 18 hours of hypoxic pre-conditioning in a very low 0.2% oxygen environment. For this study, a hypoxic oxygen level of 1% was selected. This was because meta-analysis (Vaupel *et al.* 2007) of *in vivo* ultrasound guided hypoxia measurements within human breast tumors indicated that the median pO_2 was 10 mmHg. Using normobaric assumptions, this approximates to around 1.0 to 1.3% oxygen. As expected, a lower pericellular oxygen was found in the presence of cells than in cell-free media (Figure 3.1). This suggests that an incubation environment as low as 0.2 or 0.1% O_2, as used in the previous published studies, could lead to anoxic, as opposed to hypoxic, conditions within the cells themselves (Place *et al.* 2017). This is important, because anoxia is known to trigger alternative cellular responses (e.g. activating transcription factor 3 and 4) that are not mediated via HIF (Ameri *et al.* 2007; Blais *et al.* 2004). This raises concerns about the relevance of these previously published studies in the context of nanomedicines and limits the ability to compare these findings with them.

Overall, nanomedicine retention within cells is the sum of both uptake (i.e. endocytosis) and efflux (i.e. exocytosis) (Duncan and Richardson, 2012) and

requires a mechanism for regulation of cellular homeostasis (e.g. cell volume, plasma membrane economics) (Duncan and Pratten, 1977) and for response to and modulation of cell signalling (e.g. receptor recycling versus down regulation). Therefore, assessment of the endocytic index of nanomedicines must include both endocytosis and exocytosis (Duncan and Richardson, 2012). The current results showed that 24 hour hypoxic preconditioning increased nanomedicine uptake, but it also increased exocytosis. The degree and speed of recycling under normoxic conditions observed here is similar to that noted in previous work (albeit, under differing experimental conditions) (Seib *et al.* 2007; Fiorentino *et al.* 2015).

The observed upregulation of the energy dependent processes of endo- and exocytosis, in what is ostensibly a low energy hypoxic cellular state, would appear to be counterintuitive. However, tumor cell hypoxic adaptation involves well-established changes to endocytic receptor uptake and signalling (Franovic *et al.* 2007; Mosesson *et al.* 2008; Wang *et al.* 2012) and altered intracellular trafficking (Wang *et al.* 2009b). Recent *in vitro* research has shown that MDA-MB-231 and HeLa cells undergo a generalised reduction in overall internalisation of the tumor cell surface proteome in response to hypoxia, with a parallel selective upregulation of specific endocytic pathways, mediated via caveolin 1 (Bourseau-Guilmain *et al.* 2016)). Further, the recycling of transmembrane proteins may also be influenced by interaction with proteins like Caveolin 1, among others (Christianson *et al.* 2017). Interestingly, constitutive *in vitro* expression of

Caveolin 1 is markedly higher in MDA-MB-231 cells than in many other tumor cell lines (Nehoff *et al.* 2014; Kang *et al.* 2016), suggesting its potential for a greater influence in this cell line. Similarly, upregulation of exocytotic release of exosomes or vesicles from tumor cells during hypoxia is known to play a significant role in tumor development and signaling (King *et al.* 2012; Wang *et al.* 2014), with implications for altered or upregulated exocytosis. Thus, the results may reflect these types of specific upregulated endocytic and exocytic processes, which deserve further investigation.

This study also measured relative expression of HIF1α, the master effector of hypoxic adaptation, to assess how the cellular hypoxic response might change with the duration of hypoxic exposure. Unhydroxylated HIF1α expression was increased approximately four fold when compared to normoxic levels after 6 hours of hypoxia, but returned to near normoxic levels following 24 hours of hypoxia. Similar temporal patterns of HIF1α expression have been demonstrated in MDA-MB-231 cells exposed to similar *in vitro* hypoxic conditions (Cavadas *et al*. 2015). The regulation of this cyclical HIF1α expression is multifactorial, but it appears to be driven principally by a variety of cellular factors, including REST (repressor element 1- silencing transcription factor) (Cavadas *et al*. 2015). In the context of these results, it is interesting to note that the greatest differences in nanoparticle internalisation were observed following 24 hours of hypoxic conditioning, where it was also found that HIF1α had returned to near normal levels.

The relative expression of ten other key cell stress proteins in the MDA-MB-231 cells was also assessed and the results demonstrated that their altered expression depended on the duration of hypoxia. Whilst all these proteins are relevant to the cellular stress response to hypoxia, of particular note are those known to form part of the HIF1 regulatory circuit. For example, CbP/p300 – interacting transactivator – 2 (Cited 2) is a known HIF1 negative regulatory element that exhibits preferential binding of CBP/p300 co-factors required for HIF1 transcriptional activity (Wang *et al.* 2016). Similarly, the NAD dependent deacetylase Sirtuin2 (SIRT2) has been shown, through deacetylation, to increase proteasomal breakdown of HIF1 via enhanced affinity for PHD2 (Seo *et al.* 2014). The results demonstrated that the relative expression of Cited 2 peaked following six hours of hypoxia, whereas Sirtuin2 exhibited the highest relative expression following 24 hours of hypoxic conditioning. Taken within the overall context of this research, these results underline the dynamic nature of hypoxic adaptation within tumor cells and its impact on the uptake and efflux of nanomedicines during hypoxia.

3.4 Conclusions

The objective of this work was to quantify the difference that tumor cell hypoxic adaptation might make to *in vitro* nanomedicine uptake and recycling. This research has demonstrated that both uptake and recycling of the model nanomedicine were increased following hypoxic incubation in both the MDA-MB-231 and 1833 cell line (Figure 3.20).

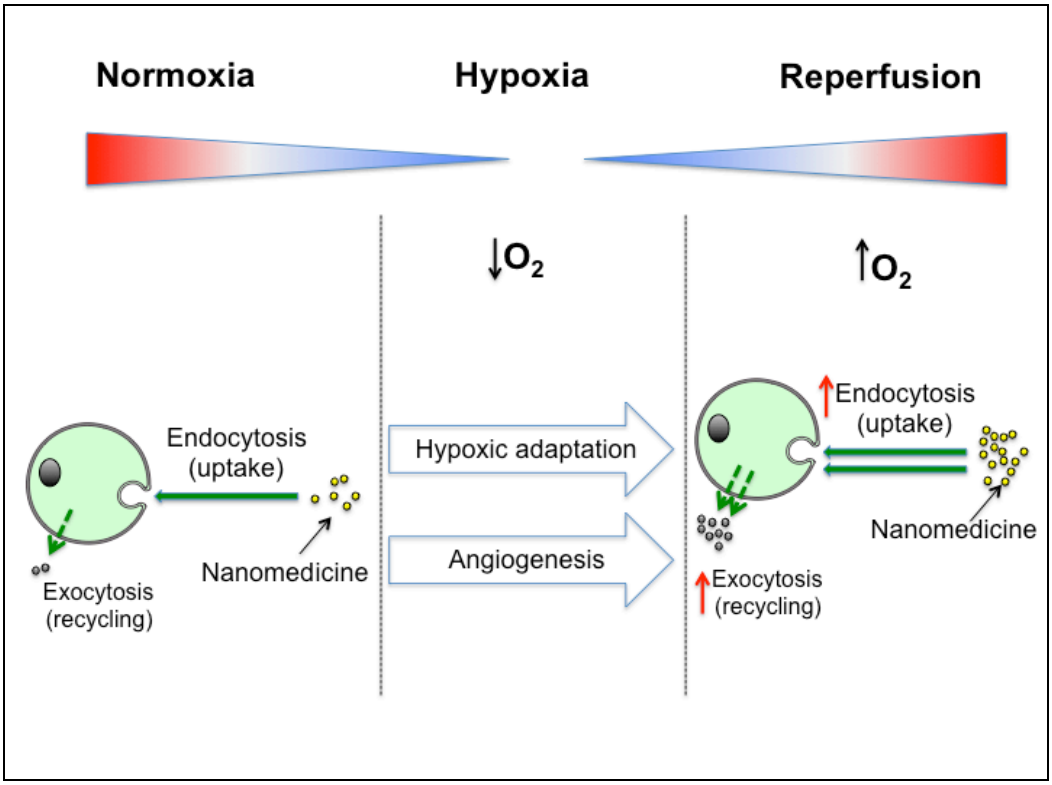

Figure 3.20 Schematic summary of key findings: Hypoxic conditioning of breast cancer cells increases nanomedicine uptake and efflux.

Further, it was also demonstrated with the MDA-MB-231 cell line, that the magnitude of these changes depended on the duration of the hypoxic exposure and the dosing interval. Overall, these results expand the existing knowledge of how the hypoxic tumor microenvironment can potentially alter nanomedicine internalisation, with implications for effective therapeutic delivery and design.

Chapter 4

Influence of HIF1α on nanoparticle uptake

4 Influence of HIF1α on nanoparticle uptake

4.1 Introduction.

The results from the work documented in chapter 3 of this thesis, demonstrated that *in vitro* hypoxic conditioning of both MDA-MB-231 and 1833 cells, results in increased nanoparticle uptake and efflux. Interesting questions arise from those results however, regarding the mechanism that leads to altered cellular nanoparticle processing. Whilst HIF1 is the recognised major transcriptional effector in cellular hypoxic adaptation, research also shows a number of other factors involved, especially in hypoxic gene repression (Cavadas *et al.* 2017). It is the combination of hypoxia driven gene promotion and repression, which leads to the phenotypic changes involved in cellular hypoxic adaptation. A specific example of this is the repressor element-1 silencing factor (REST) (Cavadas *et al.* 2015). This transcriptional repressor has been shown to decrease HIF1α transcription during hypoxia (Cavadas *et al.* 2015), suggesting a regulatory role in the hypoxic cellular response. In addition, REST has been demonstrated in human embryonic kidney 293 cells to also regulate approximately 20% of the genes repressed during hypoxia (Cavadas *et al.* 2016). This includes *SNJ1*, encoding for synaptojanin 1, implicated in clathrin mediated membrane trafficking (Cavadas *et al.* 2016).

There are other transcriptional factors, which may operate independently of HIF, in order to either increase or suppress gene expression in response to

hypoxia (Cummins and Taylor, 2005; Elvidge *et al.* 2006). A number of other factors may also act indirectly, in response to hypoxia or specific characteristics (pH, Reactive oxygen species, nitric oxide etc..) of the intracellular hypoxic environment. Each one of these may, either alone or in combination, be responsible for inducing the changes in nanoparticle uptake and efflux that was observed earlier (chapter 3).

Therefore, whilst the observed alterations to nanoparticle uptake and efflux shown earlier were in response to hypoxia, it is not clear whether the changes were directly mediated via HIF1 alone, in conjunction with other cellular changes, or via an unrelated, as yet unexplored, mechanism.

In order to demonstrate the role that HIF1 may have played in the observed changes to nanoparticle uptake (chapter 3), similar experiments could be conducted whilst inhibiting HIF1.

There are a variety of techniques that have been demonstrated for HIF1 inhibition. From a cell biology perspective, HIf1α and HIF2α, have both been selectively inhibited via short interfering RNA, and related techniques (Bartholomeusz *et al.* 2009; Wang *et al.* 2009a; Liu *et al.* 2012; Malamas *et al.* 2016). However, the focus of this thesis was chemical inhibition of HIF1α expression.

Given the significant role which HIF1α and HIF1 play within tumour development and survival, there is considerable ongoing research work into the development of chemical HIF1 blocking agents as cancer therapeutics (Semenza, 2012b). In addition, from the pharmaceutical industry perspective, there is an interest and financial motivation, in the re-purposing of existing approved drugs (Shim and Liu, 2014), as HIF1 blocking agents. Not only is their potential for altering tumour growth via HIF1 inhibition, but manipulation of HIF1 may also be useful in kidney disease associated aneamia (Joshua Kaplan *et al.* 2018) and cardiology(Ong *et al.* 2014). These topics are extensively reviewed here (Masoud and Li, 2015).

Chemical agents can inhibit HIF1 via a diverse array of mechanisms. This includes either interfering with the endogenous hypoxic HIF1/HIF1α regulatory pathway, or working directly to alter or influence the HIF1 molecule itself (Figure 4.1). There are many known chemicals which may inhibit the activity or expression of HIF1 or HIF1α, however, the focus here, is on those with the greatest associated research data. Selecting the most appropriate inhibitor for use in this research was therefore important, and ultimately dependent upon its proposed mechanism of action.

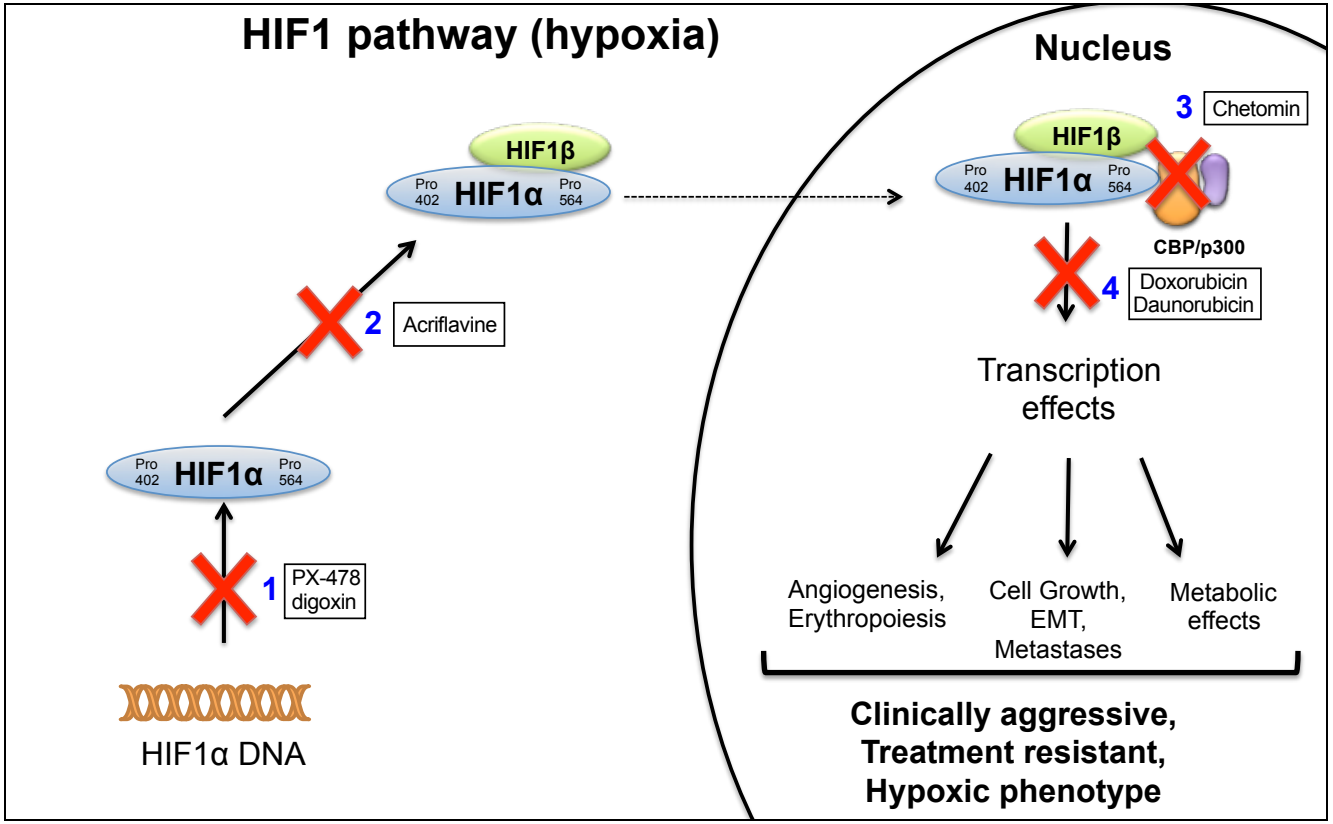

Figure 4.1 There are 4 major targets of chemical inhibition of HIF1/HIF1α, during hypoxic conditions. **1**. Transcription/translation of HIF1α. **2**. Dimerization of HIF1α with HIF1β. **3**. The heterodimeric form of HIF1 requires the CBP/p300 co-factor complex for transcriptional activity. **4**. HIF1 exerts transcriptional activity via the conserved 5'-CGTG-3' consensus sequence (hypoxic response element (HRE)) in the promoter region of target genes.

There are several inhibitors that have been shown to inhibit or influence HIF1α mRNA translation. One of these, PX-478, is a compound which has been shown to inhibit HIf1α *in vitro* (Palayoor *et al.* 2008) and *in vivo.* It has also been the subject of a phase 1 clinical trial (U.S. National Library of Medicine, 2018b). This molecule is understood to work via a variety of mechanisms (Lee and Kim, 2011), but its principal effect appears mediated by inhibition of HIF1α mRNA translation (Koh *et al.* 2008; Jacoby *et al.* 2010; Welsh *et al.* 2004).

Seemingly working in a similar fashion, cardiac glycosides, and in particular, digoxin, have been studied for their ability to inhibit the hypoxic cellular adaptive response in cancer cells. Digoxin is a clinically approved cardiac inotrope, prescribed for increasing myocardial contractility in heart failure patients (Abdul-Rahim *et al.* 2018; van Veldhuisen *et al.* 2018). This makes it a particularly attractive drug to study for HIF1 inhibition, because it is already in clinical use, is readily available and its cardiac therapeutic range and side effect profiles have been well studied. Its ability to inhibit HIF1, *in vitro* has been documented (Wei *et al.* 2013; Wong *et al.* 2012), exerting its effect via inhibition of HIF1α mRNA translation (Zhang *et al.* 2008). In addition a number of studies have suggested its efficacy in reducing tumour growth *in vivo* (Lin *et al.* 2009; Svensson *et al.* 2005). Other researchers have demonstrated the potential for digoxin as adjuvant therapy to pre-existing cytotoxic anticancer therapies (Smolarczyk *et al.* 2018) – many of which are

currently, or have potential to be, administered in nanoparticulate formulations. It is therefore interesting to note that there is little published research examining the impact that chemical inhibitors of HIF/HIF1α such as digoxin may have upon nanomedicine uptake and efflux dynamics.

An important inhibitor of HIF1α dimerization, and thereby transcriptional activity, is the compound acriflavine. Already known as a chemical dye and topical antibacterial agent, with anti-malarial potential (Dana *et al.* 2014), its HIF1 dimerization blocking ability was Identified via a cell based screening assay (Lee *et al.* 2009b). Further work identified this compound as binding to a specific (PAS-B) domain of both HIF1α and HIF2α, thereby inhibiting dimerization and transcriptional activity (Lee *et al.* 2009b). Importantly, this compound has been shown via prostate cancer xenograft modeling to reduce tumour growth and vascularization (Lee *et al.* 2009b). More recently, this compound has also been shown to effectively induce tumour cell death, apoptosis and a reduction of VEGF *in vitro*, within a number of brain cancer cell lines via HIF1 inhibition, with similar findings using *in vivo* glioblastoma modeling (Mangraviti *et al.* 2017).

Another compound, with a similar mode of action – yet only acting on HIF2α, PT2385 (Peloton Therapeutics, inc.), is currently being investigated in clear cell renal cell carcinoma (U.S. National Library of Medicine, 2018c).

Preventing heterodimeric HIF1 interacting with the transcriptional co-factors CBP/p300 (Arany *et al.* 1996), has been shown to block HIF transcriptional activity at the hypoxic response element on target genes (Kung *et al*. 2000). High throughput screening identified the fungal metabolite chetomin, as an effective CBP/p300 blocker, shown to inhibit tumour growth (Kung *et al.* 2004). Yet despite its proven ability as a potent inhibitor of HIF1 transcriptional activity, further development was not conducted due to its plethora of cytotoxic effects (Onnis *et al.* 2009).

Even if HIF1 is fully functional, its blockade at the hypoxic response element in target genes, essentially inhibits the HIF mediated hypoxic response. A variety of molecules have been shown to work directly in this manner. The anthracycline cancer therapeutics, doxorubicin and daunorubicin, are potent inhibitiors of HIF1 activity at the hypoxic response element, blocking HIF1 binding to target gene DNA (Lee *et al.* 2009a). Working in a related manner, the bacterial peptide, echinomycin, has been shown to inhibit HIF1 activity by competitively binding to the hypoxic response element on target genes (Kong *et al.* 2005).

From a number of potential candidate compounds, digoxin was therefore selected as Hif1 inhibitor for the work in this chapter. Aside from its ability to inhibit HIF1α mRNA translation, there were two other important reasons for this choice:

1. This is a drug that is already in routine clinical use, has global regulatory approval, and has been documented in other studies, both *in vitro* and *in vivo* for inhibition of HIF1.

2. Digoxin is a drug in which there is a great deal of interest as a possible chemotherapeutic adjuvant, owing to its HIF1α inhibitory qualities (Zhang *et al.* 2008; Wong *et al.* 2012). It has been the subject of evidence from a number of clinical trials in that role, and, partly due to conflicting and equivocal results, is currently the subject of a pharmacodynamic clinical trial (U.S. National Library of Medicine, 2018d), to help assess the ability of digoxin at non-toxic therapeutic doses to actively inhibit HIF1α in breast cancer tissue. This study has a completion date of July 2018.

Digoxin has low aqueous solubility, typically prepared via co-solvation in either dimethyl sulphoxide or methanol for *in vitro* use. Therefore, for these *in vitro* studies, digoxin pre-dissolved in methanol was used, and diluted in phosphate buffered saline as required. Three concentrations of digoxin which aligned with those successfully deployed in previously published studies (Wei *et al.* 2013; Zhang *et al.* 2008), were initially assessed for cytotoxicity and HIF1 inhibitory ability. The most appropriate concentration of digoxin, exhibiting a balance between HIF1 inhibitory qualities and cytotoxicity, was then deployed for nanoparticle uptake comparison experiments. As the greatest *in vitro* increase in nanoparticle uptake by

MDA-MB-231 cells had been previously demonstrated following 24 hours hypoxic conditioning and a 45 minute dosing interval (chapter 3 Figures 3.15 and 3.16), those same parameters were adopted for these experiments.

The objective of this chapter was to repeat comparison of nanoparticle uptake in MDA-MB-231 cells following normoxic or hypoxic incubation, but with the addition of a suitable chemical HIF1 inhibitor. To accomplish this there was the need to, (i) Demonstrate *in vitro* inhibition of HIF1α expression by digoxin in both hypoxia conditioned and cobalt chloride treated MDA-MB-231 cells, (ii) Determine whether digoxin inhibition of HIF1α *in vitro*, alters the previously observed increased nanoparticle uptake in MDA-MB-231 cells.

By employing a chemical inhibitor that acted via blockade of HIF1α mRNA translation as opposed to any other subsequent point in the HIF1 pathway, the extent of inhibition (and reduction in HIF1α protein expression) could be assessed in hypoxic or cobalt chloride treated cell lysates via SDS PAGE and western blotting.

4.2 Results

4.2.1 Digoxin cytotoxicity.

The *in vitro* cytotoxicity of digoxin upon hypoxic MDA-MB-231 cells over a 24 hour period was assessed via the MTT assay (Figure 4.2). The results showed that at concentrations of 100 and 1000 nmol/l digoxin, hypoxic MDA-MB-231 cell viability was significantly reduced (reduction of 14.78 and 19.09 %, respectively), when compared with untreated cells.

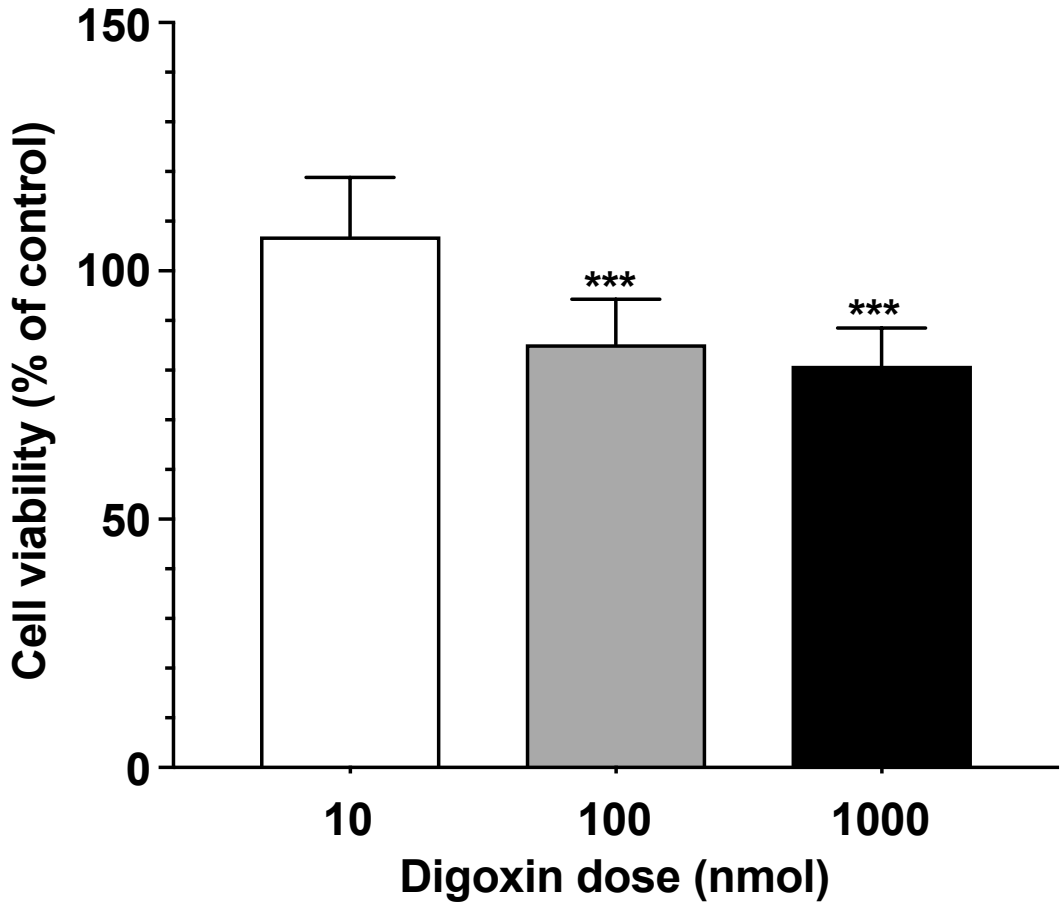

Figure 4.2 *In vitro* cytotoxicity of digoxin in MDA-MB-231 cells. Cells were exposed to digoxin for 24 hours in hypoxia (1% O_2). For untreated and 10 nmol digoxin treated cells, number of data points = 51 and 34, respectively. For all others, number of data points was 36. At each digoxin dosing level, data was derived from three separate biological experiments. Error bars denote SD.

4.2.2 HIF1α translation inhibition by digoxin

Given the relative cytotoxicity of digoxin observed at higher doses, it was necessary to assess the ability of digoxin to inhibit HIF1α expression in MDA-MB-231 cells at each of the three digoxin dosing levels, to enable selection of the most appropriate inhibitory dose. HIF1α inhibition was demonstrated in either hypoxic or cobalt chloride (positive HIF1α control) treated normoxic MDA-MB-231 cells. Western blot and densitometry scan data demonstrated that in the case of cobalt chloride treated cells (Figure 4.3), near complete inhibition of HIF1α expression was observed at the highest digoxin dose (1000 nmol) (well 2). Lesser inhibition was observed in those same cells at the two lower doses (wells 3 and 4, corresponding to 100 and 10 nmol respectively), over a 24 hour incubation period. Importantly, the loading control β - actin, demonstrated consistent expression, with or without digoxin.

Interestingly, with MDA-MB-231 cells conditioned with 6 hours of hypoxia (1% O_2) the highest dose of digoxin (1000 nmol) did not completely inhibit HIf1α expression. The degree of inhibition in hypoxia conditioned cells did not differ markedly with digoxin dose. The results showed more effective, dose related, inhibition of HIF1α with cobalt chloride treated normoxic cells, than with hypoxic cells.

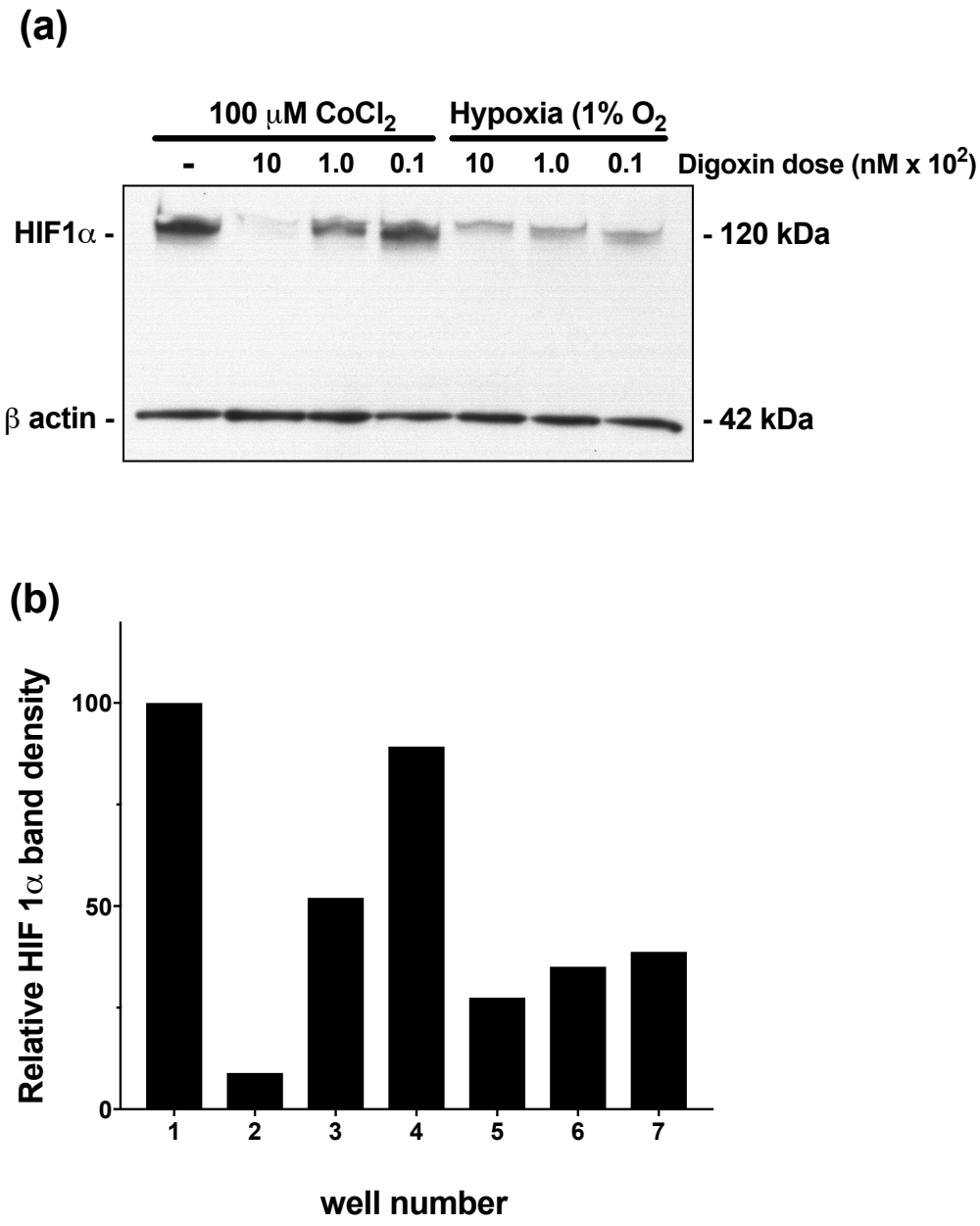

Figure 4.3 HIF1α inhibition by digoxin in MDA-MB-231 cells. Cell lysates were prepared as follows; **(i)** wells 1-4, MDA-MB-231 cells dosed with 100 μM $CoCl_2$ followed by 100 μl of cell culture media, containing digoxin at an effective concentration of either 0, 10, 100 or 100 nmol, and incubated for 24 hours in a normoxic environment, **(ii)** wells 5 – 7, 100 μl of cell culture media, containing digoxin at an effective concentration of either 10, 100 or 100 nmol was added to MDA-MB-231 cells, followed by 18 hours in normoxic, then 6 hours hypoxic incubation. **(a)** SDS PAGE and western blotting of corresponding cell lysates from independent experiments, probed for unhydroxylated HIF1α, with β actin as loading control. **(b)** Relative HIF1α band densitometry of **(a)**, expressed as percentage change relative to untreated positive control (well 1).

4.2.3 Comparison of *in vitro* nanoparticle uptake by normoxic MDA-MB-231 cells, following 24 hours incubation with or without 100 nmol/l digoxin.

As earlier work (chapter 3, Figures 3.15 and 3.16) had demonstrated that the largest overall increase in nanoparticle uptake occurred over a 45 minute dosing period following 24 hours hypoxic incubation, those same experimental parameters were used for HIF1α inhibition studies. In consideration of the ability of digoxin to inhibit HIF1α at varying doses, for further work, a digoxin dose of 100 nmol was used. First the base line nanoparticle uptake was assessed in normoxia. Due to the relative *in vitro* cytotoxicity of digoxin at a concentration of 100 nmol, a comparison was conducted to assess its impact upon nanoparticle uptake by MDA-MB-231 cells in normoxic conditions. The results (Figure 4.4) showed no significant difference in nanoparticle uptake by normoxia conditioned MDA-MB-231 cells, compared to that of digoxin treated normoxic cells (normalised mean FITC fluorescence 100.0 ± 2.93 *vs*. 97.91 ± 2.08; $p = 0.56$).

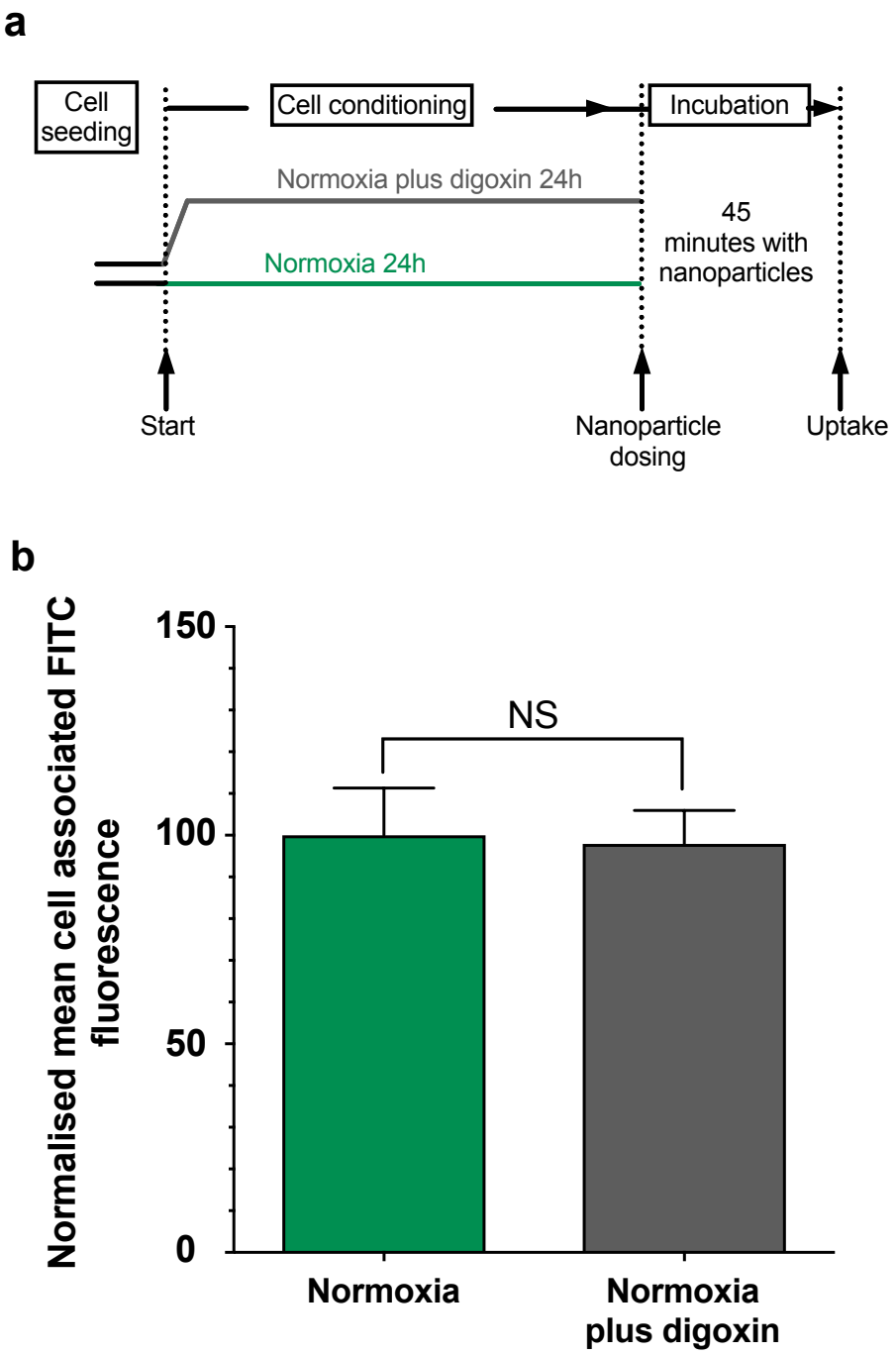

Figure 4.4 Impact of digoxin upon nanoparticle uptake by normoxic conditioned MDA-MB-231 cells. a. Schematic overview of experimental work. **b**. *In vitro* measurement of nanoparticle uptake by digoxin (100 nmol) treated, normoxic conditioned, human MDA-MB-231 breast cancer cells, compared to normoxic controls. *n* = 2 from two biological experiments consisting of ten technical replicate comparisons (5 wells x 2 from 2 x 6-well plates in normoxia and 5 wells x 2 from 2 x 6 – well plates in normoxia plus digoxin) per treatment group ± SD.

4.2.4 *In vitro* nanoparticle uptake by Normoxia conditioned MDA-MB-231 cells compared to uptake by equivalent hypoxia conditioned cells dosed with digoxin.

Earlier results (chapter 3) demonstrated a significant increase in nanoparticle internalisation by hypoxic conditioned MDA-MB-231 cells, compared to their normoxic conditioned equivalents. In order to determine the role of HIF1α, nanoparticle uptake by hypoxic MDA-MB-231 cells in the presence and absence of the HIF1α inhibitor digoxin (100 nmol), was measured. The results (Figure 4.5) showed significantly elevated nanoparticle uptake in hypoxic MDA-MB-231 cells treated with digoxin, when compared with normoxic conditioned cells (normalised mean FITC fluorescence 113.3 ± 6.42 *vs*. 100.00 ± 6.30; $p<0.001$).

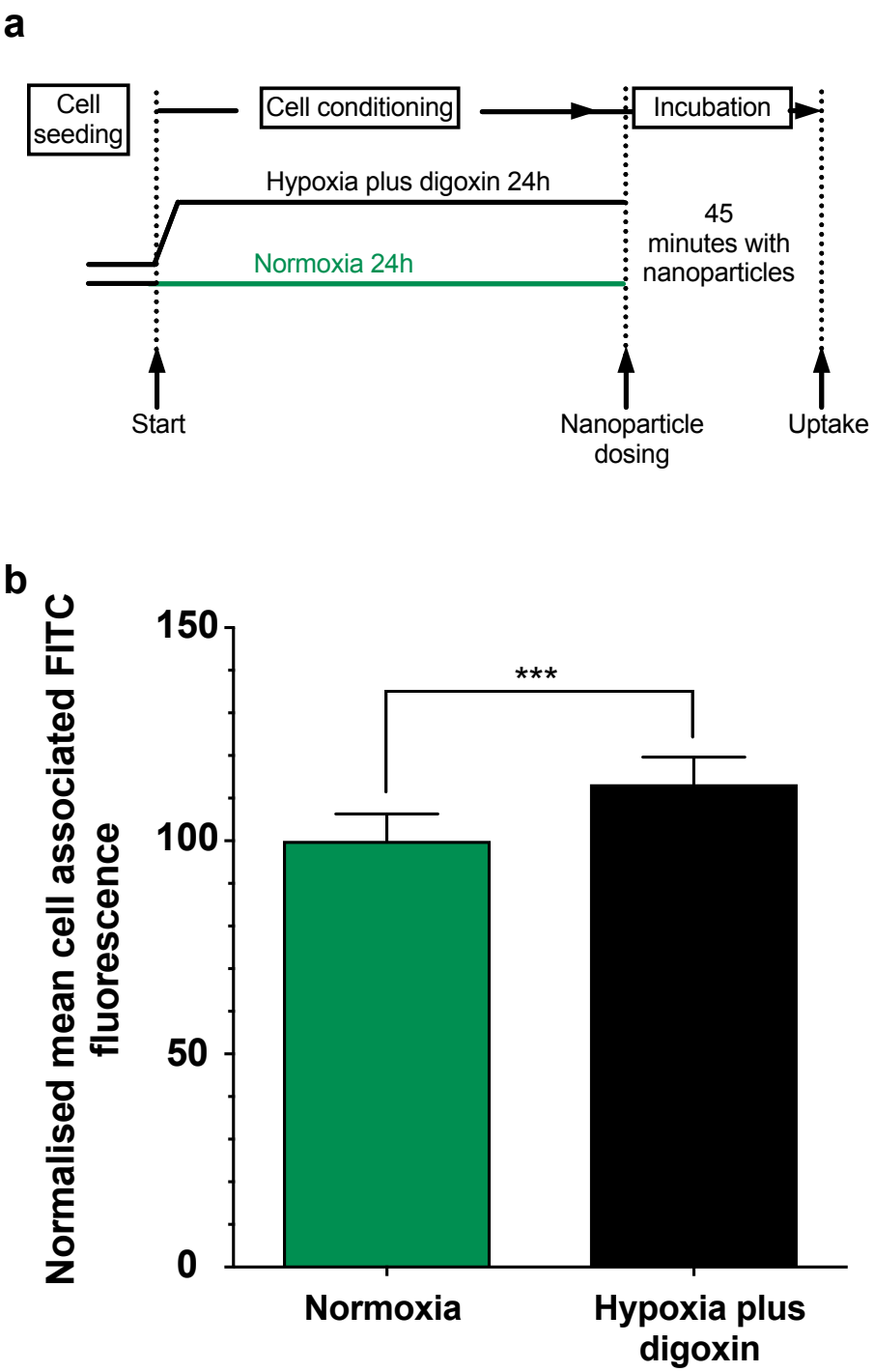

Figure 4.5 Impact of digoxin upon nanoparticle uptake by hypoxic conditioned MDA-MB-231 cells. a. Schematic overview of experimental work. **b**. *In vitro* measurement of nanoparticle uptake by digoxin (100 nmol) treated hypoxic human MDA-MB-231 breast cancer cells, compared to normoxic controls. *n* = 2, from two biological experiments consisting of ten technical replicate comparisons (5 wells x 2 from 2 x 6-well plates in normoxia and 5 wells x 2 from 2 x 6 – well plates in hypoxia plus digoxin) per treatment group ± SD.

4.3 Discussion

The earlier results in chapter 3 demonstrated that hypoxic conditioned MDA-MB-231 cells exhibited significantly increased uptake (endocytosis) (Figures 3.15 and 3.16) and efflux (exocytosis) (Figure 3.18) of nanoparticles *in vitro*, when compared with equivalent normoxic cells. The research in this chapter was designed to further investigate these findings, and determine the role of HIF1α in the altered nanoparticle trafficking seen following hypoxic conditioning.

The results from this chapter also produced results that are relevant to understanding the role of digoxin and how it may act to inhibit HIF1α. Researchers describing the mechanism of digoxin-mediated HIF1α inhibition often cite a single data source (Zhang *et al.* 2008). This paper first described the HIF1α inhibitory effect and its effect on HIF1α translation, following 24 hours hypoxic exposure. Other *in vitro* studies where digoxin mediated inhibition of HIF1α has been demonstrated (Wei *et al.* 2013), also used 24 hour incubation periods. One study examining digoxin mediated inhibition of HIF1α, specifically in hypoxic MDA-MB-231 cells, demonstrated inhibition of HIF1α expression with a digoxin concentration of 400 nmol. However, this was, as with other studies, observed after a full 24 hour hypoxic (1% O_2) incubation (Wong *et al.* 2012). Yet it is known, and I have demonstrated earlier (Chapter 3, Figures 3.5, 3.6 and 3.7), that MDA-MB-231 cells exhibit a temporal peak in HIF1α at around 6 - 8 hours within a 24 hour time period *in*

vitro (Cavadas *et al*. 2015). Therefore in this work I intentionally sought to demonstrate the inhibitory effect of digoxin on HIF1α expression following 6 (rather than 24) hours hypoxic exposure (i.e. at, or near, its peak level).

The results (Figure 4.3) demonstrated that digoxin mediated HIF1α inhibition was incomplete at all three digoxin concentrations (10, 100 and 1000 nmol), in hypoxic conditioned MDA-MB-231 cells. In contrast, in equivalent normoxic cells treated with 100 μM cobalt chloride, HIF1α was almost completely inhibited at the highest concentration (1000 nmol) of digoxin, and partially inhibited at all other concentrations. Further, there appeared to be a concentration related reduction in HIF1α levels observed with the cobalt chloride treated cells - a finding which was not replicated in hypoxic conditioned cells (Figure 4.3).

The nature of the distinction between the inhibition of HIF1α in cobalt chloride or hypoxia treated cells, as observed in this study, is potentially related to the different mechanisms responsible for HIF1α accumulation in either treatment group (Figure 4.6).

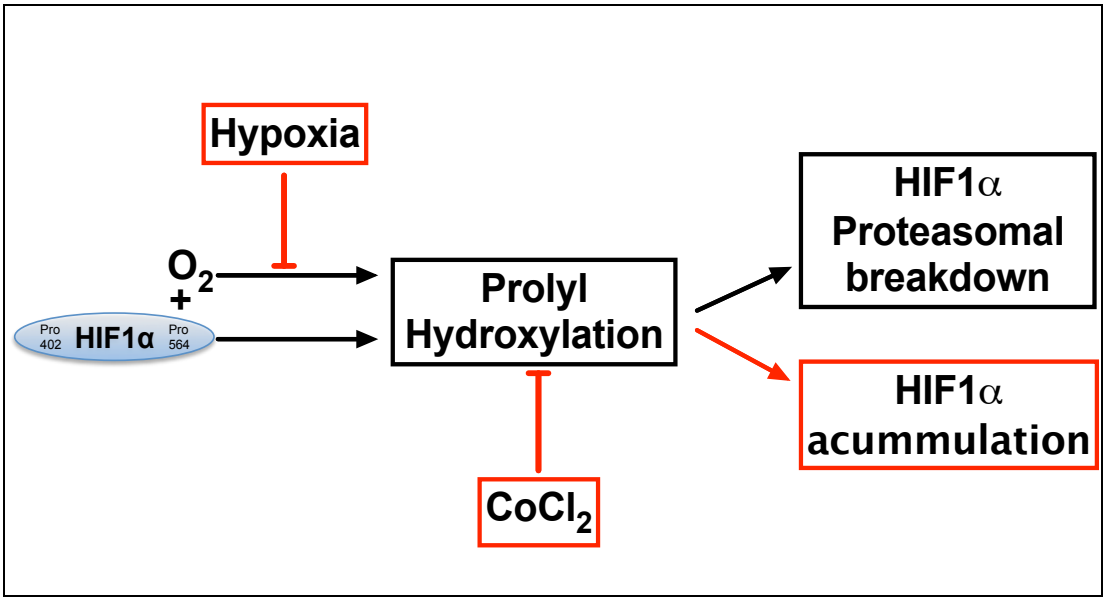

Figure 4.6 Hypoxia and cobalt chloride can both inhibit (red) the hydroxylation of HIF1α, via different mechanisms, leading to HIF1α accumulation.

Cobalt chloride displaces the Fe^{2+} at the catalytic centre of the PHD enzymes, responsible for the hydroxylation, subsequent polyubiquitination and proteasomal breakdown of HIF1α in normoxic conditions. This leads to HIF1α accumulation within cells, which cannot be broken down, even in the presence of oxygen. By contrast, HIF1α accumulation occurs with hypoxia, since those same PHD enzymes responsible for its hydroxylation and breakdown, have an absolute requirement for oxygen. Both mechanisms, which exert their influence downstream of HIF1α translation, result in an accumulation of HIF1α. There are of course many other factors that can influence HIF1/HIF1α levels (Semenza, 2017), but the distinct difference in the HIF1α inhibitory effect of digoxin observed here (Figure 4.3) does raise

further questions. Is the current understanding of HIF1α accumulation incomplete, or is it the mechanism of digoxin-mediated HIF1α inhibition that is incomplete? It is interesting to note, that the evidence relating to the use of digoxin as an effective HIF1α inhibitor, or a cancer therapeutic has been challenged. Some of the findings, for example from the original research detailing the mechanism of digoxin mediated HIF1 inhibition (Zhang *et al.* 2008), have been questioned. In particular, mouse xenograft studies which demonstrated enhanced tumour resolution in the presence of digoxin, may have been due to the markedly different sensitivity to digoxin of human and mouse cells (Lopez-Lazaro, 2009; Zhang and Semenza, 2009).

There do not appear to be any published studies that have performed similar digoxin mediated inhibition, at the temporal peak (6-8 hours) of HIF1α specifically in hypoxic MDA-MB-231 cells, as has been done here. It is interesting to note, however, that recent research (Lee *et al.* 2017a) demonstrated near complete inhibition of HIF1α accumulation in hypoxic gliomal stem cells *in vitro*, using relatively low doses of digoxin (400 nmol/l). In addition, a clear dose related inhibitory effect was demonstrated. This was achieved following what appears to have been eight hours hypoxia (1% O_2), although the timing is not clear in the published manuscript. There are however, two important caveats to that work. Firstly, it is not clear whether the experimental conditions were the same as used in this thesis. Secondly, and perhaps most importantly, gliomal stem cells are a very specific sub-

population of human neural tumour tissue, distinct from human breast tumour cells, making direct comparison with the results in this thesis difficult.

It would have been useful to replicate these experiments, to confirm the HIF1α expression patterns seen in both treatment groups, in the presence of varying concentrations of digoxin. However, time restrictions precluded such a course of action. Further experimentation might also benefit from supplementation with an alternative HIF1α translation inhibitor (e.g., the compound PX-478 (Palayoor *et al.* 2008; Jacoby *et al.* 2010)) for comparison.

Having considered the ability of digoxin to inhibit HIF1α expression in hypoxic MDA-MB-231 cells at several concentrations, *in vitro*, it was then essential to determine the cytotoxic potential of digoxin at those same doses. Digoxin like many other chemical inhibitors of HIF1α, can exert a wide variety of non-HIF1α related effects upon cells. These effects, depending upon concentration, may prove cytotoxic. In addition, when deployed clinically as a cardiac inotrope for treatment of congestive heart failure, digoxin has a narrow therapeutic plasma concentration range (van Veldhuisen *et al.* 2018; Abdul-Rahim *et al.* 2018). As a consequence, therapeutic drug monitoring is conducted on patients treated with digoxin, ensuring the plasma concentration stays within the range 1.02 - 2.56 nmol (0.8 – 2.0 ng/ml) (Hauptman *et al.* 2013). All of the digoxin concentrations that have previously been used in peer-reviewed studies to inhibit HIF1 *in vitro*, were

well above the upper threshold (typically 2.56 nmol) of this range (i.e., supratherapeutic), creating potential for cytotoxicity. It was therefore essential to determine cytotoxic effects of digoxin upon hypoxic MDA-MB-231 cells, at the same concentrations as used for HIF1α inhibition.

Results from the MTT study, demonstrated (Figure 4.2) a significant reduction in hypoxic MDA-MB-231 cell viability, at both 100 and 1000 nmol digoxin concentrations. Having established this cytotoxicity, and in consideration of both previous published research and relative HIF1α inhibitory ability, it was decided to use an effective digoxin concentration of 100 nmol for further nanoparticle uptake comparison work.

One concern for the nanoparticle uptake comparison studies was that digoxin might by itself influence nanoparticle uptake, even in normoxic MDA-MB-231 cells. Therefore, prior to comparing nanoparticle uptake in hypoxic and normoxic MDA-MB-231 cells treated with digoxin, a comparison was made of nanoparticle uptake in normoxic and normoxic plus digoxin treated cells. The results (Figure 4.4) demonstrated that there was no significant difference in nanoparticle uptake between normoxic plus digoxin and untreated normoxic cells, over a 45 minute dosing interval. Having established that an effective digoxin concentration of 100 nmol did not adversely influence nanoparticle uptake in non-hypoxic cells, experimental work to compare nanoparticle uptake in digoxin treated hypoxic cells was conducted.

Comparison of nanoparticle uptake (endocytosis) by normoxic MDA-MB-231 cells with equivalent hypoxic digoxin-treated cells, showed a significant increase in nanoparticle uptake in the latter. Indeed, whereas in earlier experimental work in chapter 3 (Figures 3.15 and 3.16), there was a 10% increase in nanoparticle uptake by the same cell line conditioned in hypoxia, these results showed a slightly greater increase in uptake. This was a somewhat counterintuitive result, because it could be anticipated that even partial HIF1α inhibition would reduce cellular hypoxic changes, thereby minimising the increased nanoparticle uptake as observed previously.

These results could suggest that HIF1α does not play a significant role in the increased nanoparticle uptake previously observed (Chapter 3), but such a conclusion is tempered by the fact that inhibition of HIF1α was incomplete. More plausible however, is that it is a more complex interplay between several factors beyond the scope of these results. Given that the pharmacological action of digoxin is effected via altered intracellular calcium concentration, it is worth noting that calcium itself plays a very significant role in tumour development and progression (Monteith *et al.* 2017). Importantly, however, within the context of this study, it is also relevant that calcium signalling plays a role in HIF1α mRNA levels and activity within breast cancer cells (Tosatto *et al.* 2016). Thus, understanding the results both for nanoparticle uptake and HIF1α inhibition in the presence of digoxin in this study, may involve further work.

In chapter 3, both the uptake (endocytosis) and efflux (exocytosis) of nanoparticles was compared between normoxic and hypoxic conditioned cells. This provided greater clarity on the mechanisms involved, because it was the combined effect of both of these aspects of cellular trafficking, which indicated what was happening in the cell. One of the limitations of the results in this chapter, is the fact that it was not possible to conduct both efflux (exocytosis) and uptake (endocytosis) experimental work within the time frame of this thesis. Therefore, from the results obtained, it may not be determined whether the increased uptake found in hypoxic digoxin treated cells was due to altered efflux, altered uptake, or a combination of both.

4.4 Conclusion

This chapter has demonstrated that digoxin may not completely inhibit HIF1α translation in hypoxic MDA-MB-231 cells, when HIF1α levels might nominally be at their highest. The results also showed that digoxin could inhibit HIF1α accumulation in cobalt chloride treated MDA-MB-231 cells, in a concentration related manner. In addition, nanoparticle uptake by a human breast cancer cell line was increased in hypoxic cells, when compared to normoxic equivalents, whilst HIF1α was partially inhibited by digoxin.

Chapter 5

Key findings, future work and conclusion

5 Key findings, future work and conclusion

5.1 Key findings

Chapter 1 of this thesis, provided background information describing how hypoxic adaptation significantly alters fundamental aspects of tumour cell structure, blood supply, metabolism and protein expression. The inherent link that exists between those hypoxic adaptations observed in tumour cells, and nanomedicine internalization pathways was then described.

Given this background, it was hypothesized that hypoxia would alter the uptake (endocytosis) and the efflux (exocytosis) of a model nanomedicine in a human breast cancer cell line. In order to pursue this, three objectives were established for this work,

1. Quantify the impact of hypoxia upon internalization (endocytosis) and efflux (exocytosis) of a model nanomedicine, *in vitro*, in a human triple negative breast cancer cell line (Chapter 3).

2. Confirm the findings from objective 1., in a related human breast cancer cell line, which reflects tumour heterogeneity, *in vitro* (Chapter 3).

3. Determine the role of HIF1α in the findings from objective 1., via chemical inhibition of HIf1α expression (Chapter 4).

This chapter is a summary of the key findings from the research conducted towards this thesis. It also outlines the potential for further development of this research.

Chapter 3 results demonstrated significantly increased *in vitro* endocytic uptake of nanoparticles by MDA-MB-231 cells incubated in a hypoxic environment, when compared with equivalent cells incubated in normoxia. In addition, it was found that this altered uptake varied depending upon duration of hypoxic exposure. These results have now been published (Appendix 1) (Brownlee and Seib, 2018).

5.2 Future work

A limitation of this work, however, was that it only considered hypoxic exposure over two time periods – 6 hours and 24 hours. Similarly, it was found that the nanoparticle dosing interval impacted the difference in nanoparticle uptake seen between normoxic and hypoxic cells. Whilst small differences in nanoparticle uptake between normoxic and hypoxic conditioned cells were observed with a 180 minute nanoparticle dosing interval, the differences were markedly greater over 45 minutes. Those

findings raise a further question, would altering the hypoxic exposure periods for cells, lead to different findings, when comparing nanoparticle uptake with normoxic incubated cells? This question could potentially be addressed by repeating some of the experimental work employing longer or shorter hypoxic incubation periods.

In addition, a further question arises related to nanoparticle dosing interval. The findings in this thesis already suggest that the magnitude of difference in nanoparticle uptake between normoxic and hypoxic conditioned cells is greater over shorter nanoparticle dosing intervals. Would a much shorter nanoparticle dosing interval result in a greater degree of difference between both cell populations? It is known that endocytosis can be very rapid, with rapid changes in cargo selectivity(Seib *et al.* 2007; Watanabe and Boucrot, 2017), therefore the ability to measure nanoparticle uptake over much shorter time intervals could help future understanding of the nanoparticle uptake dynamics in both hypoxic or normoxic cells. However, due to the nature of the protocol developed for nanoparticle uptake measurements in this thesis, the minimal dosing interval technically possible was 45 minutes. Using different laboratory equipment, a laboratory protocol could potentially be developed for fluorescent nanoparticle uptake analysis, based around a 96 well cell culture plate assay (or similar). Employing an automated plate reader equipped to enable very short duration automated nanoparticle dosing, cell washing and measurement of fluorescence in a controlled normoxic or hypoxic environment. Such an approach might allow much

tighter control of short nanoparticle dosing interval, cellular environment and repeated measurements over time.

The work in chapter 3 of this thesis set out to rigorously quantify the difference between nanoparticle uptake and efflux in normoxic and hypoxic human breast cancer cells. Following the additional work described above, a logical next step would be to identify the endocytic mechanisms responsible for the differences in nanoparticle uptake that were observed. This might help to answer the question, why is uptake and efflux higher in hypoxic cells, when compared to normoxic incubated cells? The knowledge gained from addressing this question could then be useful in future rational nanomedicine design, ensuring more effective cellular delivery, or in development of new therapeutic targets. In the discussion section of chapter 3 (chapter 3, page 109 and 110), I suggested that the increased endocytic uptake of nanoparticles as demonstrated in this thesis, could be related to research findings by Bourseau-Guilmain *et al*. (2016). This demonstrated that hypoxia reduced generalised cellular internalization of surface proteins, yet increased internalization (endocytosis) of specific transmembrane receptors or proteins in several cancer cell lines, including MDA-MB-231.

In order to explore this further, and develop the work of this thesis, a number of experimental approaches could be used. Earlier in this thesis, fluorescent confocal microscopy co-localisation studies (chapter 3, section 3.2.6) were used to demonstrate that MDA-MB-231 cells internalized nanoparticles via

an active endo-lysosomal route following normoxic or hypoxic incubation. This methodology could be adapted such that instead of only co-localising internalized nanoparticles with acidic intracellular vesicles, they could also be co-localised with fluorescent specific transmembrane receptors or pathway specific cargoes. This would help clarify the endocytic pathways involved, and potential differences between normoxic or hypoxic conditioned cells. For example, fluorescent caveolin 1 (a fundamental participant in caveolae mediated endocytosis) (either through transfection or using labeled antibodies) could be used to track or co-localise caveolae based nanoparticle uptake (Hayer *et al.* 2010). In a similar manner, fluorescent transferrin, internalized via clathrin mediated endocytosis or fluorescent CD44 (Howes *et al.* 2010; Eyster *et al.* 2009), indicative of the clathrin and caveolin independent carrier GPI-anchored protein enriched early endosomal compartment (CLIC-GEEC) pathway, could be used. A number of markers of intracellular endocytic vesicles might also be adopted, for tracking progression from early to late endosome and then to lysosome. Green fluorescent labeled Rab5 (Sandin *et al.* 2012) and Rab7 (Majzoub *et al.* 2015), as markers of early and late endosomes respectively, could be combined with work using fluorescent lysosome-associated membrane glycoprotein 1 to indicate co-localisation with lysosomes or phagolysosomes (Sandin *et al.* 2012). A further extension of this type of approach to identify internalization pathways of nanoparticles has been demonstrated (Vercauteren *et al.* 2011), whereby an algorithm based approach was used to quantify nanoparticle uptake.

Complementary to this experimental approach, selective endocytic pathway inhibition could be employed. There are numerous ways this can be achieved, examples include selective short interfering RNA mediated knockdown of adapter protein 2 (Motley *et al.* 2003; Boucrot *et al.* 2010), which is essential for clathrin mediated endocytosis. Or in a similar manner, caveolin 1 knockdown via short interfering (Yamaguchi *et al.* 2009) or short hairpin (Diaz *et al.* 2014) RNA transfection. Of course no single endocytic inhibitor or cargo is completely pathway specific or devoid of pleiotropic effects (Vercauteren *et al.* 2010). A well structured approach employing several of those techniques was described by Boucrot *et al*. (2015) in order to delineate a complete new endocytic pathway. The use of such techniques might enable better understanding of differences between normoxic and hypoxic nanoparticle internalization in this cell line.

To further investigate the increased nanoparticle uptake demonstrated in hypoxic MDA-MB-231 and 1833 cells, gene expression studies might also be conducted. Microarray or RNA-seq comparison of relative fold gene expression could be conducted between normoxic and hypoxic conditioned cells. These data sets might then enable identification of differences relating to regulatory or structural endocytic proteins involved in nanoparticle uptake and efflux in hypoxia and normoxia. In addition, if properly conducted (Edgar and Barrett, 2006), these results might enable comparison with those of previous research groups via online electronic warehousing tools such as the

gene expression omnibus (National Center for Biotechnology Information, 2018). However, there are two factors that might confound gene data interpretation in hypoxic cells. Firstly, the impact of HIF1α as a gene transcription factor is known to act upon different sets of genes (repressing or up regulating), dependent upon duration of hypoxia (Bando *et al.* 2003; Cavadas *et al.* 2017). Secondly, during hypoxia, translation is selectively inhibited (Liu *et al.* 2006; Connolly *et al.* 2006). Therefore, gene up regulation occurring following, say, 6 hours of hypoxia may result in increased gene transcription, but translation and subsequent protein assembly may be prevented, until re-oxygenation. Therefore, in any case, comparative protein expression studies would also be required, in a similar manner to those conducted as part of this thesis (Chapter 3, Figures 3.5, 3.6 and 3.7). It is interesting to note that ordinarily, translation of HIF1α itself, does not appear to be inhibited during hypoxia (Braunstein *et al.* 2007).

The exocytosis (efflux) of nanoparticles was found to be increased in MDA-MB-231 cells post hypoxic conditioning for 24 hours, when compared with their equivalents incubated in normoxia. In the discussion section of chapter 3 (Page 110), it was suggested this could be related to the already understood increased exosome and exocytic vesicle release and intercellular signaling found with hypoxic tumour cells (King *et al.* 2012; Wang *et al.* 2014). To pursue this further, two different approaches could be used. Firstly, explore the relationship between the elevated exocytosis of nanoparticle in hypoxic conditioned cells in relationship to exosome or exocytic vesicle

release. Specific protein markers for both have already been documented, such as CD63 as a marker for exosomes (King *et al.* 2012; Dutta *et al.* 2014) or Rab22A (Wang *et al.* 2014) in the case of microvesicles. These could be used to track and co-localise fluorescent nanoparticle exocytosis. Secondly, adaptation of some of the approaches described above for endocytosis, to explore both the exocytic pathways involved and specific alterations to exocytic gene and protein expression could be used.

Whilst the majority of cellular work in this thesis has involved the MDA-MB-231 triple negative human breast cancer cell line, additional research was conducted with the bone metastatic 1833 sub line derived from the same patient. Only some of the experimental schedule undertaken with the MDA-MB-231 cell line was conducted with the 1833 cell line. This demonstrated that the increased nanoparticle uptake and efflux found with the MDA-MB-231 cell line could also be demonstrated in the 1833 cell line. Further work could therefore be conducted, replicating the full experimental schedule already conducted with the MDA-MB-231 cell line. This would determine if the 1833 cell line also exhibited the same differences in relation to nanoparticle dosing interval and duration of hypoxic exposure as seen with the parental MDA-MB-231 cell line. In addition, further nanoparticle uptake and efflux comparison studies could be undertaken to determine if the findings reported here with hypoxic conditioned cells, are found in other related breast cancer cell lines such as MCF-7 (Holliday and Speirs, 2011).

The hypoxic work in this thesis was conducted in a 1% oxygen atmosphere. However, it has long been understood that cellular expression and accumulation of HIF1α varies with oxygen concentration (Bracken *et al.* 2006). Therefore, it could also be informative for future work to replicate some of the work undertaken in this thesis at different oxygen levels.

In chapter 4, the research was further developed, and there were two important findings. The first related to the use of digoxin as a HIF1α inhibitor. The results demonstrated a distinct difference between digoxin-mediated inhibition of HIF1α accumulation in cobalt chloride treated cells when compared to hypoxic cells. However, the data set available was limited in scale, and the experiments may need repeating to confirm this. As HIf1α expression was assessed via protein expression, the choice of digoxin inhibitor to be used was restricted to those whose activity is upstream of HIF1α translation. An expansion of this work might therefore encompass the use of different inhibitors targeting different elements of the HIF1α pathway. This might then enable a better understanding of the role of HIF1α in altered hypoxic nanoparticle uptake and efflux.

The second finding from the research in chapter 4, was that in the presence of partial digoxin mediated HIF1α inhibition, MDA-MB-231 cells incubated in hypoxia demonstrated increased nanoparticle uptake, when compared to equivalent untreated normoxic cells. Further work, including comparison of nanoparticle efflux may need to be undertaken, given the limitation of the

data sets. This might distinguish between changes in efflux or endocytosis in hypoxic digoxin treated cells.

5.3 Conclusion

Since the first description of the enhanced permeability and retention effect in 1986 (Matsumura and Maeda, 1986), researchers have tried to develop better cancer nanomedicines which minimize damaging side effects, whilst enhancing therapeutic response. In reality, despite a great deal of research in this field, progress has been slow. A search of published research into nanomedicines over a ten-year period (Figure 5.1), reveals a large number of publications in this field, yet the number of licensed cancer nanomedicines is at present still limited. This discrepancy was dissected in some detail by Venditto and Szoka (2013).

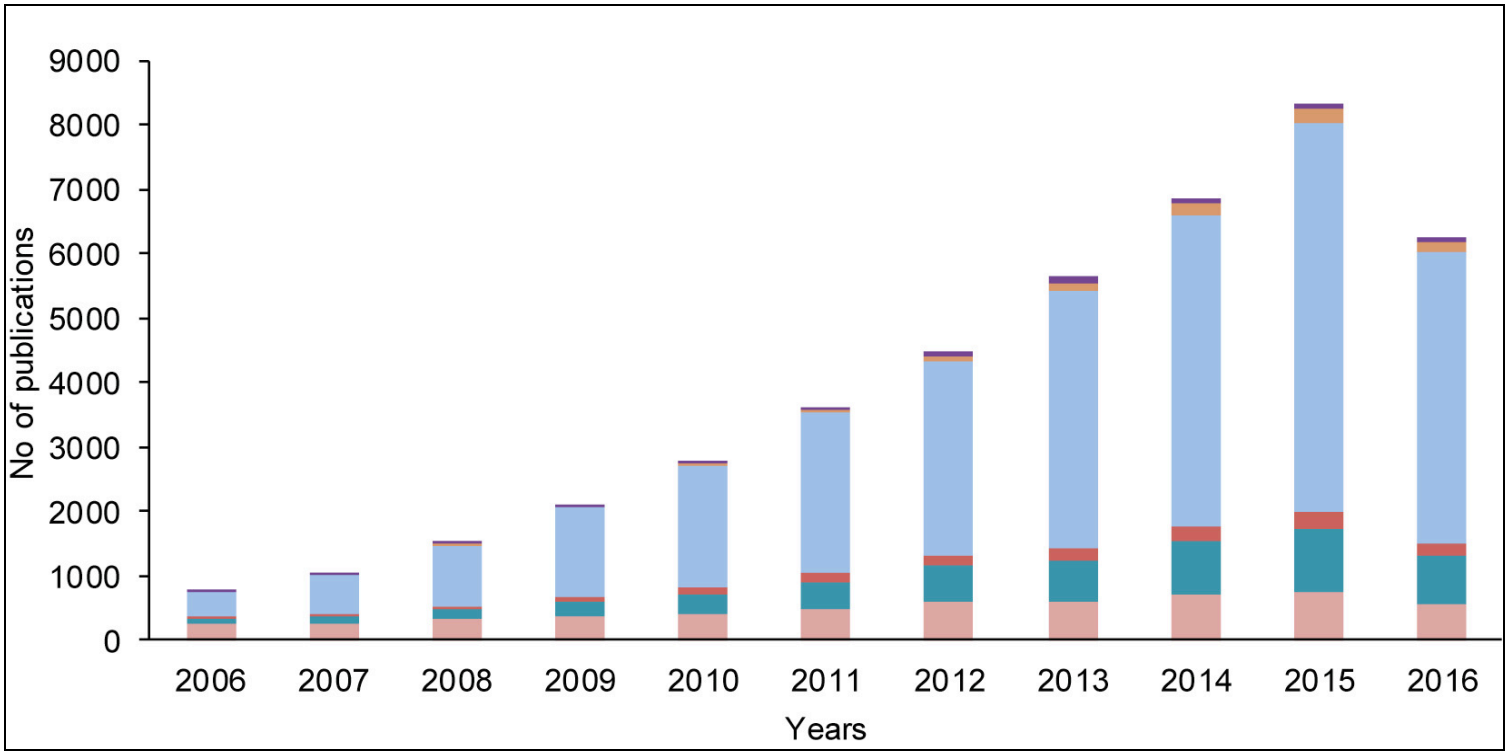

Figure 5.1 Number of studies from 2006 to 2016 related to nanomedicines for cancer, obtained from Web of Science→. Colours from bottom up indicate the following search terms; pink, “liposomes and cancer”; teal, “micelles and cancer”; dark red, “polymer-drug conjugates and cancer”; light blue, “nanoparticles and cancer”; orange, “antibody drug conjugates and cancer”, violet, “PEGylated proteins and cancer” (Source: Natfji *et al.*, 2017).

In the specific case of metastatic breast cancer, the number of cancer nanomedicines licensed by the United States food and drug administration or European medicines agency is even more restricted (Chapter 1, Table 1.2). As further evidence of the difficulty developing new cancer nanomedicines, some of those cancer nanomedicines currently in use were developed more than 20 years ago. Doxil for example, was developed in 1994 specifically to address the surge in opportunistic Kaposi's sarcoma infections seen at the height of the AIDS epidemic and was the first United States food and drug administration approved cancer nanomedicine in 1995 (Barenholz, 2012; Gabizon *et al.* 2003; Gabizon *et al.* 1994; Northfelt *et al.* 1998). Since then, progress in cancer nanomedicine development has been slow for a variety of reasons. Many academic reviews and opinion papers have been published (Shi *et al.* 2016; Wilhelm *et al.* 2016; Anchordoquy and Simberg, 2017) outlining these difficulties. A recurring theme is the challenge of developing nanomedicine formulations within the context of the heterogeneous biology of tumour cells, and the biological compartments which need traversed for successful nanomedicine delivery. Of course, from a clinical standpoint, better use of existing or new nanomedicines in cancer can be achieved through, for example, patient stratification for the enhanced permeability and retention effect (Natfji *et al.* 2017; Lee *et al.* 2017b) itself. However, from a primary research perspective, better understanding of how nanomedicines interact at the cell membrane, and how the hypoxic tumour microenvironment can alter such interactions, could also be beneficial. Given its significance,

the effects of hypoxia – a key feature of solid tumours – is worthy of additional consideration, particularly in light of the significant findings in this thesis.

A great deal of primary research into new nanomedicine formulation employs *in vitro* monolayer cell culture at least in the early development work. Typically, incubation of such cultures is in an incubator environment of humid air, supplemented with 5% CO_2 at 37°C. This thesis has demonstrated the significant impact which hypoxia and its duration has upon *in vitro* nanomedicine internalization and efflux in a human breast cancer cell line.

I have demonstrated, *in vitro*, that hypoxia can significantly increase nanoparticle uptake and efflux in a triple negative breast cancer cell line, and that the observed altered uptake varies with duration of hypoxic exposure. These findings, if replicated in other cell lines, suggest that greater priority should be given to hypoxic culture as a core component of *in vitro* cancer nanomedicine primary research work. In addition, due consideration of the degree of hypoxia and its duration may be equally important. Better standards of oxygen monitoring, such as pericellular oxygen as performed in this thesis would allow better understanding and scientific reporting of experimental conditions. This might then help facilitate better reproducibility and relevance of primary nanomedicine research work, potentially leading to enhanced development and translation of nanomedicines.

References

Abdul-Rahim, A. H., Shen, L., Rush, C. J., Jhund, P. S., Lees, K. R., McMurray, J. J. V., on behalf of the VICCTA-Heart Failure Collaborators (2018). Effect of digoxin in patients with heart failure and mid-range (borderline) left ventricular ejection fraction. *Eur J Heart Fail* 20, 1139–1145.

Abramson, V. G., and Mayer, I. A. (2014). Molecular Heterogeneity of Triple-Negative Breast Cancer. *Curr Breast Cancer Rep* 6, 154–158.

Acharya, S., Dilnawaz, F., and Sahoo, S. K. (2009). Targeted epidermal growth factor receptor nanoparticle bioconjugates for breast cancer therapy. *Biomaterials* 30, 5737–5750.

Akinc, A., and Battaglia, G. (2013). Exploiting Endocytosis for Nanomedicines. *Cold Spring Harbor Perspectives in Biology* 5, a016980–a016980.

Ameri, K., Hammond, E. M., Culmsee, C., Raida, M., Katschinski, D. M., Wenger, R. H., Wagner, E., Davis, R. J., Hai, T., Denko, N., et al. (2007). Induction of activating transcription factor 3 by anoxia is independent of p53 and the hypoxic HIF signalling pathway. *Oncogene* 26, 284–289.

Anchordoquy, T. J., and Simberg, D. (2017). Watching the gorilla and questioning delivery dogma. *Journal of Controlled Release* 262, 87–90.

Andersson, E. R. (2011). The role of endocytosis in activating and regulating signal transduction. *Cell. Mol. Life Sci.* 69, 1755–1771.

Arany, Z., Huang, L. E., Eckner, R., Bhattacharya, S., Jiang, C., Goldberg, M. A., Bunn, H. F., and Livingston, D. M. (1996). An essential role for p300/CBP in the cellular response to hypoxia. *Proc. Natl. Acad. Sci. U.S.A.* 93, 12969–12973.

Bando, H., Toi, M., Kitada, K., and Koike, M. (2003). Genes commonly upregulated by hypoxia in human breast cancer cells MCF-7 and MDA-MB-231. *Biomedicine & Pharmacotherapy* 57, 333–340.

Barenholz, Y. C. (2012). Doxil — The first FDA-approved nano-drug: Lessons learned. *Journal of Controlled Release* 160, 117–134.

Bartholomeusz, G., Cherukuri, P., Kingston, J., Cognet, L., Lemos, R., Leeuw, T. K., Gumbiner-Russo, L., Weisman, R. B., and Powis, G. (2009). In vivo therapeutic silencing of hypoxia-inducible factor 1 alpha (HIF-1α) using single-walled carbon nanotubes noncovalently coated with siRNA. *Nano Res.* 2, 279–291.

Batist, G., Harris, L., Azarnia, N., Lee, L. W., and Daza-Ramirez, P. (2006). Improved anti-tumor response rate with decreased cardiotoxicity of non-pegylated liposomal doxorubicin compared with conventional doxorubicin in first-line treatment of metastatic breast cancer in patients who had received prior adjuvant doxorubicin: results of a retrospective analysis. *Anticancer Drugs* 17, 587–595.

Batist, G., Ramakrishnan, G., Rao, C. S., Chandrasekharan, A., Gutheil, J., Guthrie, T., Shah, P., Khojasteh, A., Nair, M. K., Hoelzer, K., et al. (2001). Reduced cardiotoxicity and preserved antitumor efficacy of liposome-encapsulated doxorubicin and cyclophosphamide compared with conventional doxorubicin and cyclophosphamide in a randomized, multicenter trial of metastatic breast cancer. *J Clin Oncol* 19, 1444–1454.

Bayer, C., Shi, K., Astner, S. T., Maftei, C.-A., and Vaupel, P. (2011). Acute Versus Chronic Hypoxia: Why a Simplified Classification is Simply Not Enough. *International Journal of Radiation Oncology*Biology*Physics* 80, 965–968.

Bennewith, K. L., and Durand, R. E. (2004). Quantifying transient hypoxia in human tumor xenografts by flow cytometry. *Cancer Research* 64, 6183–6189.

Berra, E., Benizri, E., Ginouvès, A., and Volmat, V. (2003). HIF prolyl-hydroxylase 2 is the key oxygen sensor setting low steady-state levels of HIF-1α in normoxia. *The EMBO Journal 22 (16), 4082-4090.*

Bertino, E. M., Williams, T. M., Nana-Sinkam, S. P., Shilo, K., Chatterjee, M., Mo, X., Rahmani, M., Phillips, G. S., Villalona-Calero, M. A., and Otterson, G. A. (2015). Stromal Caveolin-1 Is Associated With Response and Survival in a Phase II Trial of nab-Paclitaxel With Carboplatin for Advanced NSCLC Patients. *Clin Lung Cancer* 16, 466–474.e4.

Bhattacharya, R., Patra, C. R., Earl, A., Wang, S., Katarya, A., Lu, L., Kizhakkedathu, J. N., Yaszemski, M. J., Greipp, P. R., Mukhopadhyay, D., et al. (2007). Attaching folic acid on gold nanoparticles using noncovalent interaction via different polyethylene glycol backbones and targeting of cancer cells. *Nanomedicine: Nanotechnology, Biology, and Medicine* 3, 224–238.

Blais, J. D., Filipenko, V., Bi, M., Harding, H. P., Ron, D., Koumenis, C., Wouters, B. G., and Bell, J. C. (2004). Activating transcription factor 4 is translationally regulated by hypoxic stress. *Mol. Cell. Biol.* 24, 7469–7482.

Boucrot, E., Ferreira, A. P. A., Almeida-Souza, L., Debard, S., Vallis, Y., Howard, G., Bertot, L., Sauvonnet, N., and McMahon, H. T. (2015). Endophilin marks and controls a clathrin-independent endocytic pathway. *Nature* 517, 460–465.

Boucrot, E., Saffarian, S., Zhang, R., and Kirchhausen, T. (2010). Roles of AP-2 in clathrin-mediated endocytosis. *PLoS ONE* 5, e10597.

Bourseau-Guilmain, E., Menard, J. A., Lindqvist, E., Indira Chandran, V., Christianson, H. C., Cerezo Magaña, M., Lidfeldt, J., Marko-Varga, G., Welinder, C., and Belting, M. (2016). Hypoxia regulates global membrane protein endocytosis through caveolin-1 in cancer cells. *Nat Commun* 7, 11371.

Bracken, C. P., Fedele, A. O., Linke, S., Balrak, W., Lisy, K., Whitelaw, M. L., and Peet, D. J. (2006). Cell-specific Regulation of Hypoxia-inducible Factor (HIF)-1α and HIF-2α Stabilization and Transactivation in a Graded Oxygen Environment. *Journal of Biological Chemistry* 281, 22575–22585.

Brahimi-Horn, M. C., Chiche, J., and Pouysségur, J. (2007). Hypoxia and cancer. *J Mol Med* 85, 1301–1307.

Braunstein, S., Karpisheva, K., Pola, C., Goldberg, J., Hochman, T., Yee, H., Cangiarella, J., Arju, R., Formenti, S. C., and Schneider, R. J. (2007). A Hypoxia-Controlled Cap-Dependent to Cap-Independent Translation Switch in Breast Cancer. *Molecular Cell* 28, 501–512.

Brenton, J. D., Carey, L. A., Ahmed, A. A., and Caldas, C. (2005). Molecular Classification and Molecular Forecasting of Breast Cancer: Ready for Clinical Application? *JCO* 23, 7350–7360.

Brizel, D. M., Scully, S. P., Harrelson, J. M., Layfield, L. J., Bean, J. M., Prosnitz, L. R., and Dewhirst, M. W. (1996). Tumor oxygenation predicts for the likelihood of distant metastases in human soft tissue sarcoma. *Cancer Research* 56, 941–943.

Brownlee, W. J., and Seib, F. P. (2018). Impact of the hypoxic phenotype on the uptake and efflux of nanoparticles by human breast cancer cells. *Sci. Rep.* 8, 12318.

Carnero, A., and Lleonart, M. (2015). The hypoxic microenvironment: A determinant of cancer stem cell evolution. *Inside the Cell* 1, 96–105.

Cavadas, M. A. S., Cheong, A., and Taylor, C. T. (2017). The regulation of transcriptional repression in hypoxia. *Experimental Cell Research* 356, 173–181.

Cavadas, M. A. S., Mesnieres, M., Crifo, B., Manresa, M. C., Selfridge, A. C., Keogh, C. E., Fabian, Z., Scholz, C. C., Nolan, K. A., Rocha, L. M. A., et al. (2016). REST is a hypoxia-responsive transcriptional repressor. *Sci. Rep.* 6, 31355.

Cavadas, M. A. S., Mesnieres, M., Crifo, B., Manresa, M. C., Selfridge, A. C., Scholz, C. C., Cummins, E. P., Cheong, A., and Taylor, C. T. (2015). REST mediates resolution of HIF-dependent gene expression in prolonged hypoxia. *Sci. Rep.* 5, 17851.

Chan, D. A., and Giaccia, A. J. (2007). Hypoxia, gene expression, and metastasis. *Cancer Metastasis Rev.* 26, 333–339.

Chatterjee, K., Zhang, J., Honbo, N., and Karliner, J. S. (2010). Doxorubicin Cardiomyopathy. *Cardiology* 115, 155–162.

Chatterjee, M., Ben-Josef, E., Robb, R., Vedaie, M., Seum, S., Thirumoorthy, K., Palanichamy, K., Harbrecht, M., Chakravarti, A., and Williams, T. M. (2017). Caveolae-Mediated Endocytosis Is Critical for Albumin Cellular Uptake and Response to Albumin-Bound Chemotherapy. *Cancer Research* 77, 5925–5937.

Christianson, H. C., Menard, J. A., Chandran, V. I., Bourseau-Guilmain, E., Shevela, D., Lidfeldt, J., Månsson, A.-S., Pastorekova, S., Messinger, J., and Belting, M. (2017). Tumor antigen glycosaminoglycan modification regulates antibody-drug conjugate delivery and cytotoxicity. *Oncotarget* 8, 66960–66974.

Chuang, E., Wiener, N., Christos, P., Kessler, R., Cobham, M., Donovan, D., Goldberg, G. L., Caputo, T., Doyle, A., Vahdat, L., et al. (2010). Phase I trial of ixabepilone plus pegylated liposomal doxorubicin in patients with adenocarcinoma of breast or ovary. *Ann. Oncol.* 21, 2075–2080.

Comerford, K. M., Wallace, T. J., Karhausen, J., Louis, N. A., Montalto, M. C., and Colgan, S. P. (2002). Hypoxia-inducible factor-1-dependent regulation of the multidrug resistance (MDR1) gene. *Cancer Research* 62, 3387–3394.

Conner, S. D., and Schmid, S. L. (2003). Regulated portals of entry into the cell. *Nature* 422, 37–44.

Connolly, E., Braunstein, S., Formenti, S., and Schneider, R. J. (2006). Hypoxia inhibits protein synthesis through a 4E-BP1 and elongation factor 2 kinase pathway controlled by mTOR and uncoupled in breast cancer cells. *Mol. Cell. Biol.* 26, 3955–3965.

Crosby, M. E., Devlin, C. M., Glazer, P. M., Calin, G. A., and Ivan, M. (2009). Emerging roles of microRNAs in the molecular responses to hypoxia. *Curr Pharm Des.* 15, 3861–3866.

Cummins, E. P., and Taylor, C. T. (2005). Hypoxia-responsive transcription factors. *Pflugers Arch - Eur J Physiol.* 450, 363–371.

Dana, S., Prusty, D., Dhayal, D., Gupta, M. K., Dar, A., Sen, S., Mukhopadhyay, P., Adak, T., and Dhar, S. K. (2014). Potent Antimalarial Activity of Acriflavine In Vitro and In Vivo. *ACS Chem. Biol.* 9, 2366–2373.

Danhier, F., Feron, O., and Préat, V. (2010). To exploit the tumor microenvironment: Passive and active tumor targeting of nanocarriers for anti-cancer drug delivery. *Journal of Controlled Release* 148, 135–146.

Daniels, T. R., Bernabeu, E., Rodríguez, J. A., Patel, S., Kozman, M., Chiappetta, D. A., Holler, E., Ljubimova, J. Y., Helguera, G., and Penichet, M. L. (2012). The transferrin receptor and the targeted delivery of therapeutic agents against cancer. *Biochimica et Biophysica Acta (BBA) - General Subjects* 1820, 291–317.

De Mattos-Arruda, L., and Cortes, J. (2013). Use of Pertuzumab for the Treatment of HER2-Positive Metastatic Breast Cancer. *Adv Ther*. 30, 645–658.

Denison, T. A., and Bae, Y. H. (2012). Tumor heterogeneity and its implication for drug delivery. *Journal of Controlled Release* 164, 187–191.

Depping, R., Steinhoff, A., Schindler, S. G., Friedrich, B., Fagerlund, R., Metzen, E., Hartmann, E., and Köhler, M. (2008). Nuclear translocation of hypoxia-inducible factors (HIFs): Involvement of the classical importin α/β pathway. *Biochimica et Biophysica Acta (BBA) - Molecular Cell Research* 1783, 394–404.

Devic, S. (2016). Warburg Effect - a Consequence or the Cause of Carcinogenesis? *J. Cancer* 7, 817–822.

Dewhirst, M. W., Cao, Y., and Moeller, B. (2008). Cycling hypoxia and free radicals regulate angiogenesis and radiotherapy response. *Nat Rev Cancer* 8, 425–437.

Diaz, J. E., Díaz, N., Leyton, L., and Torres, V. A. (2014). Molecular mechanisms implicated in Caveolin 1 dependent Rab5 activation, migration and invasion of metastatic cancer cells. *Cancer Cell & Microenvironment* 1, e332.

Dings, J., Meixensberger, J., Jäger, A., and Roosen, K. (1998). Clinical Experience with 118 Brain Tissue Oxygen Partial Pressure Catheter Probes. *Neurosurgery* 43, 1082–1094.

Doherty, G. J., and McMahon, H. T. (2009). Mechanisms of Endocytosis. *Annu. Rev. Biochem.* 78, 857–902.

Drab, M., Verkade, P., Elger, M., Kasper, M., Lohn, M., Lauterbach, B., Menne, J., Lindschau, C., Mende, F., Luft, F. C., et al. (2001). Loss of caveolae, vascular dysfunction, and pulmonary defects in caveolin-1 gene-disrupted mice. *Science* 293, 2449–2452.

Duncan, R., and Gaspar, R. (2011). Nanomedicine(s) under the Microscope. *Mol. Pharmaceutics* 8, 2101–2141.

Duncan, R., and Pratten, M. K. (1977). Membrane economics in endocytic systems. *Journal of Theoretical Biology* 66, 727–735.

Duncan, R., and Richardson, S. C. W. (2012). Endocytosis and Intracellular Trafficking as Gateways for Nanomedicine Delivery: Opportunities and Challenges. *Mol. Pharmaceutics* 9, 2380–2402.

Duncan, R., Cable, H. C., Lloyd, J. B., Rejmanová, P., and Kopeček, J. (1982). Degradation of side-chains of N-(2-hydroxypropyl) methacrylamide copolymers by lysosomal thiol-proteinases. *Bioscience reports* 2, 1041–1046.

Dutta, S., Warshall, C., Bandyopadhyay, C., Dutta, D., and Chandran, B. (2014). Interactions between Exosomes from Breast Cancer Cells and Primary Mammary Epithelial Cells Leads to Generation of Reactive Oxygen Species Which Induce DNA Damage Response, Stabilization of p53 and Autophagy in Epithelial Cells. *PLoS ONE* 9, e97580.

Eales, K. L., Hollinshead, K. E. R., and Tennant, D. A. (2016). Hypoxia and metabolic adaptation of cancer cells. *Oncogenesis* 5, e190.

Edgar, R., and Barrett, T. (2006). NCBI GEO standards and services for microarray data. *Nat Biotechnol* 24, 1471–1472.

Elvidge, G. P., Glenny, L., Appelhoff, R. J., Ratcliffe, P. J., Ragoussis, J., and Gleadle, J. M. (2006). Concordant regulation of gene expression by hypoxia and 2-oxoglutarate-dependent dioxygenase inhibition: the role of HIF-1alpha, HIF-2alpha, and other pathways. *J. Biol. Chem.* 281, 15215–15226.

Engelberth, S. A., Hempel, N., and Bergkvist, M. (2014). Development of Nanoscale Approaches for Ovarian Cancer Therapeutics and Diagnostics. *Crit Rev Oncog* 19, 281–315.

Epstein, A. C., Gleadle, J. M., McNeill, L. A., Hewitson, K. S., O'Rourke, J., Mole, D. R., Mukherji, M., Metzen, E., Wilson, M. I., Dhanda, A., et al. (2001). C. elegans EGL-9 and mammalian homologs define a family of dioxygenases that regulate HIF by prolyl hydroxylation. *Cell* 107, 43–54.

Etheridge, M. L., Campbell, S. A., Erdman, A. G., Haynes, C. L., Wolf, S. M., and McCullough, J. (2013). The big picture on nanomedicine: the state of investigational and approved nanomedicine products. *Nanomedicine: Nanotechnology, Biology, and Medicine* 9, 1–14.

Ewer, M. S., Martin, F. J., Henderson, I. C., Shapiro, C. L., Benjamin, R. S., and Gabizon, A. A. (2004). Cardiac safety of liposomal anthracyclines. *Seminars in Oncology* 31, 161–181.

Eyster, C. A., Higginson, J. D., Huebner, R., Porat-Shliom, N., Weigert, R., Wu, W. W., Shen, R. F., and Donaldson, J. G. (2009). Discovery of New Cargo Proteins that Enter Cells through Clathrin-Independent Endocytosis. *Traffic* 10, 590–599.

Ferlay, J., Steliarova-Foucher, E., Lortet-Tieulent, J., Rosso, S., Coebergh, J. W. W., Comber, H., Forman, D., and Bray, F. (2013). Cancer incidence and mortality patterns in Europe: Estimates for 40 countries in 2012. *European Journal of Cancer* 49, 1374–1403.

Fiorentino, I., Gualtieri, R., Barbato, V., Mollo, V., Braun, S., Angrisani, A., Turano, M., Furia, M., Netti, P. A., Guarnieri, D., et al. (2015). Energy independent uptake and release of polystyrene nanoparticles in primary mammalian cell cultures. *Experimental Cell Research* 330, 240–247.

Folkman, J. (2003). Angiogenesis and apoptosis. *Semin. Cancer Biol.* 13, 159–167.

Folkman, J. (1971). Tumor angiogenesis: therapeutic implications. *N Engl J Med.* 285, 1182–1186.

Forsythe, J. A., Jiang, B. H., Iyer, N. V., Agani, F., Leung, S. W., Koos, R. D., and Semenza, G. L. (1996). Activation of vascular endothelial growth factor gene transcription by hypoxia-inducible factor 1. *Mol. Cell. Biol.* 16, 4604–4613.

Franovic, A., Gunaratnam, L., Smith, K., Robert, I., Patten, D., and Lee, S. (2007). Translational up-regulation of the EGFR by tumor hypoxia provides a nonmutational explanation for its overexpression in human cancer. *Proc. Natl. Acad. Sci. U.S.A.* 104, 13092–13097.

Frezza, C., Zheng, L., Tennant, D. A., Papkovsky, D. B., Hedley, B. A., Kalna, G., Watson, D. G., and Gottlieb, E. (2011). Metabolic Profiling of Hypoxic Cells Revealed a Catabolic Signature Required for Cell Survival. *PLoS ONE* 6, e24411.

Gabizon, A., Catane, R., Uziely, B., Kaufman, B., Safra, T., Cohen, R., Martin, F., Huang, A., and Barenholz, Y. (1994). Prolonged circulation time and enhanced accumulation in malignant exudates of doxorubicin encapsulated in polyethylene-glycol coated liposomes. *Cancer Research* 54, 987–992.

Gabizon, A., Shmeeda, H., and Barenholz, Y. (2003). Pharmacokinetics of pegylated liposomal Doxorubicin: review of animal and human studies. *Clin Pharmacokinet.* 42, 419–436.

Gilkes, D. M., and Semenza, G. L. (2013). Role of hypoxia-inducible factors in breast cancer metastasis. *Future Oncology* 9, 1623–1636.

Goldberg, M. S., Hook, S. S., Wang, A. Z., Bulte, J. W., Patri, A. K., Uckun, F. M., Cryns, V. L., Hanes, J., Akin, D., Hall, J. B., et al. (2013). Biotargeted nanomedicines for cancer: six tenets before you begin. *Nanomedicine* 8, 299–308.

Gong, Q., Zhou, L., Xu, S., Li, X., Zou, Y., and Chen, J. (2015). High Doses of Daunorubicin during Induction Therapy of Newly Diagnosed Acute Myeloid Leukemia: A Systematic Review and Meta-Analysis of Prospective Clinical Trials. *PLoS ONE* 10, e0125612.

Gradishar, W. J. (2008). Clinical efficacy and emerging therapeutic utilization of novel taxanes. *European Journal of Cancer Supplements* 6 (10), 12-21.

Gradishar, W. J., Tjulandin, S., Davidson, N., Shaw, H., Desai, N., Bhar, P., Hawkins, M., and O'Shaughnessy, J. (2005). Phase III Trial of Nanoparticle Albumin-Bound Paclitaxel Compared With Polyethylated Castor Oil–Based Paclitaxel in Women With Breast Cancer. *Journal of Clinical Oncology* 23, 7794–7803.

Greer, S. N., Metcalf, J. L., Wang, Y., and Ohh, M. (2012). The updated biology of hypoxia-inducible factor. *EMBO J.* 31, 2448–2460.

Gurevich, E. V., and Gurevich, V. V. (2006). Arrestins: ubiquitous regulators of cellular signaling pathways. *Genome Biol.* 7, 236.

Harney, A. S., Arwert, E. N., Entenberg, D., Wang, Y., Guo, P., Qian, B. Z., Oktay, M. H., Pollard, J. W., Jones, J. G., and Condeelis, J. S. (2015). Real-Time Imaging Reveals Local, Transient Vascular Permeability, and Tumor Cell Intravasation Stimulated by TIE2hi Macrophage-Derived VEGFA. *Cancer Discovery* 5, 932–943.

Harris, A. L. (2002). Hypoxia--a key regulatory factor in tumour growth. *Nat Rev Cancer* 2, 38–47.

Harris, L., Batist, G., Belt, R., Rovira, D., Navari, R., Azarnia, N., Welles, L., and Winer, E. (2002). Liposome-encapsulated doxorubicin compared with conventional doxorubicin in a randomized multicenter trial as first-line therapy of metastatic breast carcinoma. *Cancer* 94, 25–36.

Harrison, J. S., Rameshwar, P., Chang, V., and Bandari, P. (2002). Oxygen saturation in the bone marrow of healthy volunteers. *Blood* 99, 394.

Hashizume, H., Baluk, P., Morikawa, S., McLean, J. W., Thurston, G., Roberge, S., Jain, R. K., and McDonald, D. M. (2000). Openings between defective endothelial cells explain tumor vessel leakiness. *AJPA.* 156, 1363–1380.

Hauptman, P. J., McCann, P., Romero, J. M. R., and Mayo, M. (2013). Reference laboratory values for digoxin following publication of Digitalis Investigation Group (DIG) trial data. *JAMA Intern Med.* 173, 1552–1554.

Hayer, A., Stoeber, M., Ritz, D., Engel, S., Meyer, H. H., and Helenius, A. (2010). Caveolin-1 is ubiquitinated and targeted to intralumenal vesicles in endolysosomes for degradation. *J. Cell Biol.* 191, 615–629.

Helmlinger, G., Yuan, F., Dellian, M., and Jain, R. K. (1997). Interstitial pH and pO2 gradients in solid tumors in vivo: high-resolution measurements reveal a lack of correlation. *Nat. Med.* 3, 177–182.

Hirsilä, M., Koivunen, P., Günzler, V., Kivirikko, K. I., and Myllyharju, J. (2003). Characterization of the Human Prolyl 4-Hydroxylases That Modify the Hypoxia-inducible Factor. *Journal of Biological Chemistry* 278, 30772–30780.

Hoffman, W. E., Charbel, F. T., and Edelman, G. (1996). Brain tissue oxygen, carbon dioxide, and pH in neurosurgical patients at risk for ischemia. *Anesth. Analg.* 82, 582–586.

Holliday, D. L., and Speirs, V. (2011). Choosing the right cell line for breast cancer research. *Breast Cancer Res.* 13, 215.

Howes, M. T., Kirkham, M., Riches, J., Cortese, K., Walser, P. J., Simpson, F., Hill, M. M., Jones, A., Lundmark, R., Lindsay, M. R., et al. (2010). Clathrin-independent carriers form a high capacity endocytic sorting system at the leading edge of migrating cells. *J. Cell Biol.* 190, 675–691.

Höckel, M., and Vaupel, P. (2001). Tumor hypoxia: definitions and current clinical, biologic, and molecular aspects. *J. Natl. Cancer Inst.* 93, 266–276.

Hrkach, J., Hoff, Von, D., Ali, M. M., Andrianova, E., Auer, J., Campbell, T., De Witt, D., Figa, M., Figueiredo, M., Horhota, A., et al. (2012). Preclinical Development and Clinical Translation of a PSMA-Targeted Docetaxel Nanoparticle with a Differentiated Pharmacological Profile. *Science Translational Medicine* 4, 128ra39–128ra39.

Indelicato, M., Pucci, B., Schito, L., Reali, V., Aventaggiato, M., Mazzarino, M. C., Stivala, F., Fini, M., Russo, M. A., and Tafani, M. (2010). Role of hypoxia and autophagy in MDA-MB-231 invasiveness. *J. Cell. Physiol.* 223 359-368.

ISDScotland (2018). Cancer Incidence in Scotland (2016). Available at: https://www.isdscotland.org/Health-Topics/Cancer/Publications/2018-04-24/2018-04-24-Cancer-Incidence-Report.pdf. [accessed 20th September, 2018].

Jacoby, J. J., Erez, B., Korshunova, M. V., Williams, R. R., Furutani, K., Takahashi, O., Kirkpatrick, L., Lippman, S. M., Powis, G., O'Reilly, M. S., et al. (2010). Treatment with HIF-1α Antagonist PX-478 Inhibits Progression and Spread of Orthotopic Human Small Cell Lung Cancer and Lung Adenocarcinoma in Mice. *Journal of Thoracic Oncology* 5, 940–949.

Jain, R. K. (2014). Antiangiogenesis Strategies Revisited: From Starving Tumors to Alleviating Hypoxia. *Cancer Cell* 26, 605–622.

Jain, S., Coulter, J. A., Butterworth, K. T., Hounsell, A. R., McMahon, S. J., Hyland, W. B., Muir, M. F., Dickson, G. R., Prise, K. M., Currell, F. J., et al. (2014). Gold nanoparticle cellular uptake, toxicity and radiosensitisation in hypoxic conditions. *Radiother Oncol.* 110, 342–347.

James, N. D., Coker, R. J., Tomlinson, D., Harris, J. R., Gompels, M., Pinching, A. J., and Stewart, J. S. (1994). Liposomal doxorubicin (Doxil): an effective new treatment for Kaposi's sarcoma in AIDS. *Clin Oncol (R Coll Radiol)* 6, 294–296.

Jiang, B. H., Semenza, G. L., Bauer, C., and Marti, H. H. (1996). Hypoxia-inducible factor 1 levels vary exponentially over a physiologically relevant range of O2 tension. *Am. J. Physiol.* 271, C1172–80.

Johnson, R. W., Sowder, M. E., and Giaccia, A. J. (2017). Hypoxia and Bone Metastatic Disease. *Curr Osteoporos Rep.* 15, 231–238.

Joshua Kaplan, Neeraj Sharma, Sean Dikdan (2018). Hypoxia-Inducible Factor and Its Role in the Management of Anemia in Chronic Kidney Disease. *IJMS.* 19, 389.

Juliano, R. (2013). Nanomedicine: is the wave cresting? *Nat Rev Drug Discov.* 12, 171–172.

Jungermann, K., and Kietzmann, T. (2000). Oxygen: modulator of metabolic zonation and disease of the liver. *Hepatology* 31, 255–260.

Kaelin, W. G., Jr., and Ratcliffe, P. J. (2008). Oxygen Sensing by Metazoans: The Central Role of the HIF Hydroxylase Pathway. *Molecular Cell* 30, 393–402.

Kang, J., Park, J. H., Lee, H. J., Jo, U., Park, J. K., Seo, J. H., Kim, Y. H., Kim, I., and Park, K. H. (2016). Caveolin-1 Modulates Docetaxel-Induced Cell Death in Breast Cancer Cell Subtypes through Different Mechanisms. *Cancer Res Treat.* 48, 715–726.

Kang, Y., Siegel, P. M., Shu, W., Drobnjak, M., Kakonen, S. M., Cordón-Cardo, C., Guise, T. A., and Massagué, J. (2003). A multigenic program mediating breast cancer metastasis to bone. *Cancer Cell* 3, 537–549.

Kelly, B. D. (2003). Cell Type-Specific Regulation of Angiogenic Growth Factor Gene Expression and Induction of Angiogenesis in Nonischemic Tissue by a Constitutively Active Form of Hypoxia-Inducible Factor 1. *Circulation Research* 93, 1074–1081.

Kietzmann, T. (2017). Metabolic zonation of the liver: The oxygen gradient revisited. *Redox Biology* 11, 622–630.

Kim, J.-W., Tchernyshyov, I., Semenza, G. L., and Dang, C. V. (2006). HIF-1-mediated expression of pyruvate dehydrogenase kinase: A metabolic switch required for cellular adaptation to hypoxia. *Cell Metabolism* 3, 177–185.

King, H. W., Michael, M. Z., and Gleadle, J. M. (2012). Hypoxic enhancement of exosome release by breast cancer cells. *BMC Cancer* 12, 421.

Kirtane, A. R., Kalscheuer, S. M., and Panyam, J. (2013). Exploiting nanotechnology to overcome tumor drug resistance: Challenges and opportunities. *Advanced Drug Delivery Reviews* 65, 1731–1747.

Koh, M. Y., Spivak-Kroizman, T., Venturini, S., Welsh, S., Williams, R. R., Kirkpatrick, D. L., and Powis, G. (2008). Molecular mechanisms for the activity of PX-478, an antitumor inhibitor of the hypoxia-inducible factor-1. *Molecular Cancer Therapeutics* 7, 90–100.

Kohler, B. A., Sherman, R. L., Howlader, N., Jemal, A., Ryerson, A. B., Henry, K. A., Boscoe, F. P., Cronin, K. A., Lake, A., Noone, A. M., et al. (2015). Annual Report to the Nation on the Status of Cancer, 1975-2011, Featuring Incidence of Breast Cancer Subtypes by Race/Ethnicity, Poverty, and State. *Journal of the National Cancer Institute* 107, 1197.

Koivunen, P., Hirsilä, M., Günzler, V., Kivirikko, K. I., and Myllyharju, J. (2004). Catalytic Properties of the Asparaginyl Hydroxylase (FIH) in the Oxygen Sensing Pathway Are Distinct from Those of Its Prolyl 4-Hydroxylases. *Journal of Biological Chemistry* 279, 9899–9904.

Konerding, M. A., Malkusch, W., Klapthor, B., van Ackern, C., Fait, E., Hill, S. A., Parkins, C., Chaplin, D. J., Presta, M., and Denekamp, J. (1999). Evidence for characteristic vascular patterns in solid tumours: quantitative studies using corrosion casts. *Br. J. Cancer* 80, 724–732.

Kong, D., Park, E. J., Stephen, A. G., Calvani, M., Cardellina, J. H., Monks, A., Fisher, R. J., Shoemaker, R. H., and Melillo, G. (2005). Echinomycin, a Small-Molecule Inhibitor of Hypoxia-Inducible Factor-1 DNA-Binding Activity. *Cancer Research* 65, 9047–9055.

Korobko, E. V., Palgova, I. V., Kiselev, S. L., and Korobko, I. V. (2006). Apoptotic cleavage of rabaptin-5-like proteins and a model for rabaptin-5 inactivation in apoptosis. *Cell Cycle* 5, 1854–1858.

Kronblad, Å., Jirström, K., Rydén, L., Nordenskjöld, B., and Landberg, G. (2006). Hypoxia inducible factor-1α is a prognostic marker in premenopausal patients with intermediate to highly differentiated breast cancer but not a predictive marker for tamoxifen response. *Int. J. Cancer* 118, 2609–2616.

Kung, A. L., Wang, S., Klco, J. M., Kaelin, W. G., and Livingston, D. M. (2000). Suppression of tumor growth through disruption of hypoxia-inducible transcription. *Nat. Med.* 6 (12), 1335-1340.

Kung, A. L., Zabludoff, S. D., France, D. S., Freedman, S. J., Tanner, E. A., Vieira, A., Cornell-Kennon, S., Lee, J., Wang, B., Wang, J., et al. (2004). Small molecule blockade of transcriptional coactivation of the hypoxia-inducible factor pathway. *Cancer Cell* 6, 33–43.

Lal, S., McCart Reed, A. E., de Luca, X. M., and Simpson, P. T. (2017). Molecular signatures in breast cancer. *Methods* 131, 135–146.

Lambert, J. M., and Berkenblit, A. (2018). Antibody-Drug Conjugates for Cancer Treatment. *Annu. Rev. Med.* 69, 191–207.

Lando, D. (2002). Asparagine Hydroxylation of the HIF Transactivation Domain: A Hypoxic Switch. *Science* 295, 858–861.

Lee, D.-H., Cheul Oh, S., Giles, A. J., Jung, J., Gilbert, M. R., and Park, D. M. (2017a). Cardiac glycosides suppress the maintenance of stemness and malignancy via inhibiting HIF-1α in human glioma stem cells. *Oncotarget* 8, 40233–40245.

Lee, H., Shields, A. F., Siegel, B. A., Miller, K. D., Krop, I., Ma, C. X., LoRusso, P. M., Munster, P. N., Campbell, K., Gaddy, D. F., et al. (2017b). 64Cu-MM-302 Positron Emission Tomography Quantifies Variability of Enhanced Permeability and Retention of Nanoparticles in Relation to Treatment Response in Patients with Metastatic Breast Cancer. *Clinical Cancer Research* 23, 4190–4202.

Lee, K., and Kim, H. M. (2011). A novel approach to cancer therapy using PX-478 as a HIF-1α inhibitor. *Arch. Pharm. Res.* 34, 1583–1585.

Lee, K., Qian, D. Z., Rey, S., Wei, H., Liu, J. O., and Semenza, G. L. (2009a). Anthracycline chemotherapy inhibits HIF-1 transcriptional activity and tumor-induced mobilization of circulating angiogenic cells. *Proceedings of the National Academy of Sciences* 106, 2353–2358.

Lee, K., Zhang, H., Qian, D. Z., Rey, S., Liu, J. O., and Semenza, G. L. (2009b). Acriflavine inhibits HIF-1 dimerization, tumor growth, and vascularization. *Proceedings of the National Academy of Sciences* 106, 17910–17915.

Liao, D., and Johnson, R. S. (2007). Hypoxia: A key regulator of angiogenesis in cancer. *Cancer Metastasis Rev* 26, 281–290.

Lin, J., Denmeade, S., and Carducci, M. A. (2009). HIF-1alpha and calcium signaling as targets for treatment of prostate cancer by cardiac glycosides. *Curr Cancer Drug Targets* 9, 881–887.

Liu, L., Cash, T. P., Jones, R. G., Keith, B., Thompson, C. B., and Simon, M. C. (2006). Hypoxia-induced energy stress regulates mRNA translation and cell growth. *Molecular Cell* 21, 521–531.

Liu, X.-Q., Xiong, M.-H., Shu, X.-T., Tang, R.-Z., and Wang, J. (2012). Therapeutic Delivery of siRNA Silencing HIF-1 Alpha with Micellar Nanoparticles Inhibits Hypoxic Tumor Growth. *Mol. Pharmaceutics* 9, 2863–2874.

Lopez-Lazaro, M. (2009). Digoxin, HIF-1, and cancer. *Proceedings of the National Academy of Sciences* 106, E26–author reply E27.

Low, P. S., Henne, W. A., and Doorneweerd, D. D. (2008). Discovery and Development of Folic-Acid-Based Receptor Targeting for Imaging and Therapy of Cancer and Inflammatory Diseases. *Acc. Chem. Res.* 41, 120–129.

Lundgren, K., Holm, C., and Landberg, G. (2007). Common Molecular Mechanisms of Mammary Gland Development and Breast Cancer. *Cell. Mol. Life Sci.* 64, 3233–3247.

Maeda, H. (2015). Toward a full understanding of the EPR effect in primary and metastatic tumors as well as issues related to its heterogeneity. *Advanced Drug Delivery Reviews* 91, 3–6.

Maeda, H., Nakamura, H., and Fang, J. (2013). The EPR effect for macromolecular drug delivery to solid tumors: Improvement of tumor uptake, lowering of systemic toxicity, and distinct tumor imaging in vivo. *Advanced Drug Delivery Reviews* 65, 71–79.

Mahon, P. C., Hirota, K., and Semenza, G. L. (2001). FIH-1: a novel protein that interacts with HIF-1alpha and VHL to mediate repression of HIF-1 transcriptional activity. *Genes Dev.* 15, 2675–2686.

Majzoub, R. N., Chan, C.-L., Ewert, K. K., Silva, B. F. B., Liang, K. S., and Safinya, C. R. (2015). Fluorescence microscopy colocalization of lipid–nucleic acid nanoparticles with wildtype and mutant Rab5–GFP: A platform for investigating early endosomal events. *Biochimica et Biophysica Acta (BBA) - Biomembranes* 1848, 1308–1318.

Malamas, A. S., Jin, E., Gujrati, M., and Lu, Z.-R. (2016). Dynamic Contrast Enhanced MRI Assessing the Antiangiogenic Effect of Silencing HIF-1α with Targeted Multifunctional ECO/siRNA Nanoparticles. *Mol. Pharmaceutics* 13, 2497–2506.

Mangraviti, A., Raghavan, T., Volpin, F., Skuli, N., Gullotti, D., Zhou, J., Asnaghi, L., Sankey, E., Liu, A., Wang, Y., et al. (2017). HIF-1α-Targeting Acriflavine Provides Long Term Survival and Radiological Tumor Response in Brain Cancer Therapy. *Sci. Rep.* 7, 14978.

Mao, C., Livezey, M., Kim, J. E., and Shapiro, D. J. (2016). Antiestrogen Resistant Cell Lines Expressing Estrogen Receptor α Mutations Upregulate the Unfolded Protein Response and are Killed by BHPI. *Sci. Rep.* 6, 34753.

Masoud, G. N., and Li, W. (2015). HIF-1α pathway: role, regulation and intervention for cancer therapy. *Acta Pharmaceutica Sinica B*. 5 (5), 378-389.

Massagué, J., and Obenauf, A. C. (2016). Metastatic colonization by circulating tumour cells. *Nature* 529, 298–306.

Matsumoto, Y., Nichols, J. W., Toh, K., Nomoto, T., Cabral, H., Miura, Y., Christie, R. J., Yamada, N., Ogura, T., Kano, M. R., et al. Vascular bursts enhance permeability of tumour blood vessels and improve nanoparticle delivery. *Nat. Nano.* 11, 533–538.

Matsumura, Y., and Maeda, H. (1986). A new concept for macromolecular therapeutics in cancer chemotherapy: mechanism of tumoritropic accumulation of proteins and the antitumor agent smancs. *Cancer Research* 46, 6387–6392.

McGuire, S. (2016). World Cancer Report 2014. Geneva, Switzerland: World Health Organization, International Agency for Research on Cancer, WHO Press, 2015. *Adv Nutr.* 7, 418–419.

Michiels, C., Tellier, C., and Feron, O. (2016). Cycling hypoxia: A key feature of the tumor microenvironment. *Biochim. Biophys. Acta* 1866, 76–86.

Miller, M. A., Chandra, R., Cuccarese, M. F., Pfirschke, C., Engblom, C., Stapleton, S., Adhikary, U., Kohler, R. H., Mohan, J. F., Pittet, M. J., et al. (2017). Radiation therapy primes tumors for nanotherapeutic delivery via macrophage-mediated vascular bursts. *Science Translational Medicine* 9, eaal0225.

Milotti, E., Stella, S., and Chignola, R. (2017). Pulsation-limited oxygen diffusion in the tumour microenvironment. *Sci. Rep.* 7, 39762.

Minn, A. J., Gupta, G. P., Siegel, P. M., Bos, P. D., Shu, W., Giri, D. D., Viale, A., Olshen, A. B., Gerald, W. L., and Massagué, J. (2005). Genes that mediate breast cancer metastasis to lung. *Nature* 436, 518–524.

Mitri, Z., Constantine, T., and O'Regan, R. (2012). The HER2 Receptor in Breast Cancer: Pathophysiology, Clinical Use, and New Advances in Therapy. *Chemotherapy Research and Practice* 2012, 1–7.

Moeller, B. J., Richardson, R. A., and Dewhirst, M. W. (2007). Hypoxia and radiotherapy: opportunities for improved outcomes in cancer treatment. *Cancer Metastasis Rev* 26, 241–248.

Mole, D. R., Blancher, C., Copley, R. R., Pollard, P. J., Gleadle, J. M., Ragoussis, J., and Ratcliffe, P. J. (2009). Genome-wide association of hypoxia-inducible factor (HIF)-1alpha and HIF-2alpha DNA binding with expression profiling of hypoxia-inducible transcripts. *Journal of Biological Chemistry* 284, 16767–16775.

Monteith, G. R., Prevarskaya, N., and Roberts-Thomson, S. J. (2017). The calcium-cancer signalling nexus. *Nat Rev Cancer* 17, 367–380.

Mosesson, Y., Mills, G. B., and Yarden, Y. (2008). Derailed endocytosis: an emerging feature of cancer. *Nat Rev Cancer* 8, 835–850.

Motley, A., Bright, N. A., Seaman, M. N. J., and Robinson, M. S. (2003). Clathrin-mediated endocytosis in AP-2–depleted cells. *J. Cell Biol.* 162, 909–918.

Muggia, F. M., Hainsworth, J. D., Jeffers, S., Miller, P., Groshen, S., Tan, M., Roman, L., Uziely, B., Muderspach, L., Garcia, A., et al. (2018). Phase II study of liposomal doxorubicin in refractory ovarian cancer: antitumor activity and toxicity modification by liposomal encapsulation. *J Clin Oncol.* 15, 987–993.

Müller, M., Padberg, W., Schindler, E., Sticher, J., Osmer, C., Friemann, S., and Hempelmann, G. (1998). Renocortical tissue oxygen pressure measurements in patients undergoing living donor kidney transplantation. *Anesth. Analg.* 87, 474–476.

Nagamitsu, A., Greish, K., and Maeda, H. (2009). Elevating Blood Pressure as a Strategy to Increase Tumor-targeted Delivery of Macromolecular Drug SMANCS: Cases of Advanced Solid Tumors. *Japanese Journal of Clinical Oncology* 39, 756–766.

Natfji, A. A., Ravishankar, D., Osborn, H. M. I., and Greco, F. (2017). Parameters Affecting the Enhanced Permeability and Retention Effect: The Need for Patient Selection. *Journal of Pharmaceutical Sciences* 106, 3179–3187.

National Center for Biotechnology Information (2018). Gene Expression Omnibus. Available at : https://www.ncbi.nlm.nih.gov/geo/. [accessed 20th September, 2018].

Nehoff, H., Parayath, N. N., and Taurin, S. (2014). The Influence of Drug Loading on Caveolin-1 Mediated Intracellular Internalization of Doxorubicin Nanomicelles in vitro. *Journal of Nanomedicine and Nanotechnology 5, 197.*

Neshatian, M., Chung, S., Yohan, D., Yang, C., and Chithrani, D. B. (2014). Determining the Size Dependence of Colloidal Gold Nanoparticle Uptake in a Tumor-like Interface (Hypoxic). *Colloids and Interface Science Communications* 1, 57–61.

Neshatian, M., Chung, S., Yohan, D., Yang, C., and Chithrani, D. B. (2015). Uptake of Gold Nanoparticles in Breathless (Hypoxic) Cancer Cells. *j biomed nanotechnol* 11, 1162–1172.

Northfelt, D. W., Dezube, B. J., Thommes, J. A., Miller, B. J., Fischl, M. A., Friedman-Kien, A., Kaplan, L. D., Mond, Du, C., Mamelok, R. D., and Henry, D. H. (1998). Pegylated-liposomal doxorubicin versus doxorubicin, bleomycin, and vincristine in the treatment of AIDS-related Kaposi's sarcoma: results of a randomized phase III clinical trial. *J Clin Oncol* 16, 2445–2451.

O'Brien, M. E. R., Wigler, N., Inbar, M., Rosso, R., Grischke, E., Santoro, A., Catane, R., Kieback, D. G., Tomczak, P., Ackland, S. P., et al. (2004). Reduced cardiotoxicity and comparable efficacy in a phase III trial of pegylated liposomal doxorubicin HCl (CAELYX/Doxil) versus conventional doxorubicin for first-line treatment of metastatic breast cancer. *Ann. Oncol.* 15, 440–449.

O'Byrne, K. J., Thomas, A. L., Sharma, R. A., DeCatris, M., Shields, F., Beare, S., and Steward, W. P. (2002). A phase I dose-escalating study of DaunoXome, liposomal daunorubicin, in metastatic breast cancer. *Br. J. Cancer* 87, 15–20.

Ong, S.-G., Lee, W. H., Theodorou, L., Kodo, K., Lim, S. Y., Shukla, D. H., Briston, T., Kiriakidis, S., Ashcroft, M., Davidson, S. M., et al. (2014). HIF-1 reduces ischaemia–reperfusion injury in the heart by targeting the mitochondrial permeability transition pore. *Cardiovasc. Res.* 104, 24–36.

Onnis, B., Rapisarda, A., and Melillo, G. (2009). Development of HIF-1 inhibitors for cancer therapy. *Journal of Cellular and Molecular Medicine* 13, 2780–2786.

O'Shaughnessy, J., Gradishar, W. J., Bhar, P., and Iglesias, J. (2013). nab-Paclitaxel for first-line treatment of patients with metastatic breast cancer and poor prognostic factors: a retrospective analysis. *Breast Cancer Res Treat.* 138, 829–837.

Palayoor, S. T., Mitchell, J. B., Cerna, D., DeGraff, W., John-Aryankalayil, M., and Coleman, C. N. (2008). PX-478, an inhibitor of hypoxia-inducible factor-1α, enhances radiosensitivity of prostate carcinoma cells. *Int. J. Cancer* 123, 2430–2437.

Palumbo, R., Sottotetti, F., Trifirò, G., Piazza, E., Ferzi, A., Gambaro, A., Spinapolice, E. G., Pozzi, E., Tagliaferri, B., Teragni, C., et al. (2015). Nanoparticle albumin-bound paclitaxel (nab-paclitaxel) as second-line chemotherapy in HER2-negative, taxane-pretreated metastatic breast cancer patients: prospective evaluation of activity, safety, and quality of life. *DDDT*. 9, 2189-2199.

Papandreou, I., Cairns, R. A., Fontana, L., Lim, A. L., and Denko, N. C. (2006). HIF-1 mediates adaptation to hypoxia by actively downregulating mitochondrial oxygen consumption. *Cell Metabolism* 3, 187–197.

Pece, S., Serresi, M., Santolini, E., Capra, M., Hulleman, E., Galimberti, V., Zurrida, S., Maisonneuve, P., Viale, G., and Di Fiore, P. P. (2004). Loss of negative regulation by Numb over Notch is relevant to human breast carcinogenesis. *J. Cell Biol.* 167, 215–221.

Petre, C. E., and Dittmer, D. P. (2007). Liposomal daunorubicin as treatment for Kaposi's sarcoma. *IJN* 2, 277–288.

Place, T. L., Domann, F. E., and Case, A. J. (2017). Limitations of oxygen delivery to cells in culture: An underappreciated problem in basic and translational research. *Free Radical Biology and Medicine* 113, 311–322.

Prabhakar, U., Maeda, H., Jain, R. K., Sevick-Muraca, E. M., Zamboni, W., Farokhzad, O. C., Barry, S. T., Gabizon, A., Grodzinski, P., and Blakey, D. C. (2013). Challenges and Key Considerations of the Enhanced Permeability and Retention Effect for Nanomedicine Drug Delivery in Oncology. *Cancer Research* 73, 2412–2417.

Reider, A., and Wendland, B. (2011). Endocytic adaptors - social networking at the plasma membrane. *Journal of Cell Science* 124, 1613–1622.

Reinhardt, D., Hempel, G., Fleischhack, G., Schulz, A., Boos, J., and Creutzig, U. (2002). Liposomal daunorubicine combined with cytarabine in the treatment of relapsed/refractory acute myeloid leukemia in children. *Klin Padiatr* 214, 188–194.

Rohwer, N., and Cramer, T. (2011). Hypoxia-mediated drug resistance: Novel insights on the functional interaction of HIFs and cell death pathways. *Drug Resistance Updates* 14, 191–201.

Rom, J., Bechstein, S., Domschke, C., Golatta, M., Mayer, C., Heil, J., Thum, J., Smetanay, K., Windemuth-Kieselbach, C., Wallwiener, M., et al. (2014). Efficacy and toxicity profile of pegylated liposomal doxorubicin (Caelyx) in patients with advanced breast cancer. *Anticancer Drugs* 25, 219–224.

Ruas, J. L. (2005). Role of CBP in regulating HIF-1-mediated activation of transcription. *Journal of Cell Science* 118, 301–311.

Sahay, G., Alakhova, D. Y., and Kabanov, A. V. (2010). Endocytosis of nanomedicines. Journal of Controlled Release. 145,182–195

Samanta, D., Gilkes, D. M., Chaturvedi, P., Xiang, L., and Semenza, G. L. (2014). Hypoxia-inducible factors are required for chemotherapy resistance of breast cancer stem cells. *Proceedings of the National Academy of Sciences* 111, E5429–E5438.

Sandin, P., Fitzpatrick, L. W., Simpson, J. C., and Dawson, K. A. (2012). High-Speed Imaging of Rab Family Small GTPases Reveals Rare Events in Nanoparticle Trafficking in Living Cells. *ACS Nano.* 6, 1513–1521.

Santolini, E., Puri, C., Salcini, A. E., Gagliani, M. C., Pelicci, P. G., Tacchetti, C., and Di Fiore, P. P. (2000). Numb is an endocytic protein. *J. Cell Biol.* 151, 1345–1352.

Schmid, E. M., and McMahon, H. T. (2007). Integrating molecular and network biology to decode endocytosis. *Nature* 448, 883–888.

Schnitt, S. J. (2010). Classification and prognosis of invasive breast cancer: from morphology to molecular taxonomy. *Mod Pathol.* 23, S60–S64.

Schodel, J., Oikonomopoulos, S., Ragoussis, J., Pugh, C. W., Ratcliffe, P. J., and Mole, D. R. (2011). High-resolution genome-wide mapping of HIF-binding sites by ChIP-seq. *Blood* 117, e207–e217.

Scita, G., and Di Fiore, P. P. (2010). The endocytic matrix. *Nature* 463, 464–473.

Sehouli, J., Camara, O., Schmidt, M., Mahner, S., Seipelt, G., Otremba, B., Schmalfeldt, B., Tesch, H., Lorenz-Schluter, C., and Oskay-Ozcelik, G. (2009). Pegylated liposomal doxorubicin (CAELYX) in patients with advanced ovarian cancer: results of a German multicenter observational study. *Cancer Chemother Pharmacol.* 64, 585–591.

Seib, F. P., Jones, A. T., and Duncan, R. (2007). Comparison of the endocytic properties of linear and branched PEIs, and cationic PAMAM dendrimers in B16f10 melanoma cells. *Journal of Controlled Release* 117, 291–300.

Semenza, G. L. (2017). A compendium of proteins that interact with HIF-1α. *Experimental Cell Research* 356, 128–135.

Semenza, G. L. (2009). Defining the role of hypoxia-inducible factor 1 in cancer biology and therapeutics. *Oncogene* 29, 625–634.

Semenza, G. L. (2013). HIF-1 mediates metabolic responses to intratumoral hypoxia and oncogenic mutations. *J. Clin. Invest.* 123, 3664–3671.

Semenza, G. L. (2012a). Hypoxia-Inducible Factors in Physiology and Medicine. *Cell* 148, 399–408.

Semenza, G. L. (2012b). Hypoxia-inducible factors: mediators of cancer progression and targets for cancer therapy. *Trends in Pharmacological Sciences* 33, 207–214.

Semenza, G. L. (2015). The hypoxic tumor microenvironment: A driving force for breast cancer progression. *Biochimica et Biophysica Acta (BBA) - Molecular Cell Research* 1863, 382–391.

Semenza, G. L., and Wang, G. L. (1992). A nuclear factor induced by hypoxia via de novo protein synthesis binds to the human erythropoietin gene enhancer at a site required for transcriptional activation. *Mol. Cell. Biol.* 12, 5447–5454.

Semenza, G. L., Jiang, B. H., Leung, S. W., Passantino, R., Concordet, J. P., Maire, P., and Giallongo, A. (1996). Hypoxia response elements in the aldolase A, enolase 1, and lactate dehydrogenase A gene promoters contain essential binding sites for hypoxia-inducible factor 1. *J. Biol. Chem.* 271, 32529–32537.

Seo, K. S., Park, J. H., Heo, J. Y., Jing, K., Han, J., Min, K. N., Kim, C., Koh, G. Y., Lim, K., Kang, G. Y., et al. (2014). SIRT2 regulates tumour hypoxia response by promoting HIF-1α hydroxylation. *Oncogene* 34, 1354–1362.

Seymour, L. W., Ulbrich, K., Steyger, P. S., Brereton, M., Subr, V., Strohalm, J., and Duncan, R. (1994). Tumour tropism and anti-cancer efficacy of polymer-based doxorubicin prodrugs in the treatment of subcutaneous murine B16F10 melanoma. *Br. J. Cancer* 70, 636–641.

Shannon, A. M., Bouchier-Hayes, D. J., Condron, C. M., and Toomey, D. (2003). Tumour hypoxia, chemotherapeutic resistance and hypoxia-related therapies. *Cancer Treat. Rev.* 29, 297–307.

Shi, J., Kantoff, P. W., Wooster, R., and Farokhzad, O. C. (2016). Cancer nanomedicine: progress, challenges and opportunities. *Nat Rev Cancer* 17, 20–37. Available at: http://www.nature.com/articles/nrc.2016.108.

Shim, J. S., and Liu, J. O. Recent Advances in Drug Repositioning for the Discovery of New Anticancer Drugs. *Int. J. Biol. Sci.* 10, 654–663.

Shweiki, D., Itin, A., Soffer, D., and Keshet, E. (1992). Vascular endothelial growth factor induced by hypoxia may mediate hypoxia-initiated angiogenesis. *Nature* 359, 843–845.

Simon, G. R. (2014). nab-Paclitaxel for the treatment of advanced squamous non-small-cell lung cancer: a comprehensive update. *Clin Lung Cancer* 15, 391–397.

Singh, M., Atwal, H., and Micetich, R. (1998). Transferrin directed delivery of adriamycin to human cells. *Anticancer research* 18, 1423–1427.

Smolarczyk, R., Cichoń, T., Pilny, E., Jarosz-Biej, M., Poczkaj, A., Kułach, N., and Szala, S. (2018). Combination of anti-vascular agent - DMXAA and HIF-1α inhibitor - digoxin inhibits the growth of melanoma tumors. *Sci. Rep.* 8, 7355.

Sotiriou, C., Neo, S.-Y., McShane, L. M., Korn, E. L., Long, P. M., Jazaeri, A., Martiat, P., Fox, S. B., Harris, A. L., and Liu, E. T. (2003). Breast cancer classification and prognosis based on gene expression profiles from a population-based study. *Proc. Natl. Acad. Sci. U.S.A.* 100, 10393–10398.

Spencer, J. A., Ferraro, F., Roussakis, E., Klein, A., Wu, J., Runnels, J. M., Zaher, W., Mortensen, L. J., Alt, C., Turcotte, R., et al. (2014). Direct measurement of local oxygen concentration in the bone marrow of live animals. *Nature* 508, 269–273.

Sreeranganathan, M., Uthaman, S., Sarmento, B., Mohan, C. G., Park, I. K., and Jayakumar, R. (2017). In vivo evaluation of cetuximab-conjugated poly(γ-glutamic acid)-docetaxel nanomedicines in EGFR-overexpressing gastric cancer xenografts. *IJN*. 12, 7165–7182.

Sriraman, S. K., Aryasomayajula, B., and Torchilin, V. P. (2014). Barriers to drug delivery in solid tumors. *Tissue Barriers* 2, e29528.

Sullivan, R., and Graham, C. H. (2007). Hypoxia-driven selection of the metastatic phenotype. *Cancer Metastasis Rev* 26, 319–331.

Sun, R. C., and Denko, N. C. (2016). Hypoxic Regulation of Glutamine Metabolism through HIF1 and SIAH2 Supports Lipid Synthesis that Is Necessary for Tumor Growth. *Cell Metabolism* 19, 285–292.

Sundfør, K., Lyng, H., and Rofstad, E. K. (2009). Oxygen Tension and Vascular Density in Adenocarcinoma and Squamous Cell Carcinoma of the Uterine Cervix. *Acta Oncologica* 37, 665–670.

Svensson, A., Azarbayjani, F., Bäckman, U., Matsumoto, T., and Christofferson, R. (2005). Digoxin inhibits neuroblastoma tumor growth in mice. *Anticancer research* 25, 207–212.

Thomlinson, R. H., and Gray, L. H. (1955). The histological structure of some human lung cancers and the possible implications for radiotherapy. *Br. J. Cancer* 9, 539–549.

Torosean, S., Flynn, B., Axelsson, J., Gunn, J., Samkoe, K. S., Hasan, T., Doyley, M. M., and Pogue, B. W. (2013). Nanoparticle uptake in tumors is mediated by the interplay of vascular and collagen density with interstitial pressure. *Nanomedicine: Nanotechnology, Biology, and Medicine* 9, 151–158.

Tosatto, A., Sommaggio, R., Kummerow, C., Bentham, R. B., Blacker, T. S., Berecz, T., Duchen, M. R., Rosato, A., Bogeski, I., Szabadkai, G., et al. (2016). The mitochondrial calcium uniporter regulates breast cancer progression via HIF-1α. *EMBO Mol Med.* 8, 569–585.

Totten, J. D., Wongpinyochit, T., and Seib, F. P. (2017). Silk nanoparticles: proof of lysosomotropic anticancer drug delivery at single-cell resolution. *Journal of Drug Targeting* 25, 865–872.

Trastour, C., Benizri, E., Ettore, F., Ramaioli, A., Chamorey, E., Pouysségur, J., and Berra, E. (2007). HIF-1α and CA IX staining in invasive breast carcinomas: Prognosis and treatment outcome. *Int. J. Cancer* 120, 1451–1458.

Traub, L. M. (2011). Regarding the Amazing Choreography of Clathrin Coats. *PLoS Biol.* 9, e1001037.

U.S. National Library of Medicine (2018a). Study of MBP-426 in Patients With Second Line Gastric, Gastroesophageal, or Esophageal Adenocarcinoma. Available at : https://clinicaltrials.gov/ct2/show/NCT00964080?term=00964080&rank=1. [accessed 20th September, 2018].

U.S. National Library of Medicine (2018b). Phase I Trial of PX-478. Available at : https://clinicaltrials.gov/ct2/show/NCT00522652?term=00522652&rank=1. [accessed 20th September, 2018].

U.S. National Library of Medicine (2018c). A Phase 1, Dose-Escalation Trial of PT2385 Tablets In Patients With Advanced Clear Cell Renal Cell Carcinoma. Available at : https://clinicaltrials.gov/ct2/show/NCT02293980?term=02293980&rank=1. [accessed 20th September, 2018].

U.S. National Library of Medicine (2018d). DIG-HIF1 Pharmacodynamic Trial in Newly Diagnosed Operable Breast Cancer. Available at : https://clinicaltrials.gov/ct2/show/NCT01763931?term=01763931&rank=1. [accessed 20th September, 2018].

van Veldhuisen, D. J., Rienstra, M., and van der Meer, P. (2018). Value of digoxin in patients with heart failure: new pieces to the puzzle. *Eur J Heart Fail.* 20, 1146–1147.

Vasey, P. A., Kaye, S. B., Morrison, R., Twelves, C., Wilson, P., Duncan, R., Thomson, A. H., Murray, L. S., Hilditch, T. E., Murray, T., et al. (1999). Phase I clinical and pharmacokinetic study of PK1 [N-(2-hydroxypropyl)methacrylamide copolymer doxorubicin]: first member of a new class of chemotherapeutic agents-drug-polymer conjugates. Cancer Research Campaign Phase I/II Committee. *Clin. Cancer Res.* 5, 83–94.

Vaupel, P., and Mayer, A. (2014). “Hypoxia in Tumors: Pathogenesis-Related Classification, Characterization of Hypoxia Subtypes, and Associated Biological and Clinical Implications,” in Oxygen Transport to Tissue XXXVI Oxygen Transport to Tissue XXXVI. eds.H. M. Swartz, D. K. Harrison, and D. F. Bruley (New York, NY: Springer New York), vol. 182.

Vaupel, P., Höckel, M., and Mayer, A. (2007). Detection and Characterization of Tumor Hypoxia Using pO 2Histography. *Antioxidants & Redox Signaling* 9, 1221–1236.

Vaupel, P., Kallinowski, F., and Okunieff, P. (1989). Blood flow, oxygen and nutrient supply, and metabolic microenvironment of human tumors: a review. *Cancer Research* 49, 6449–6465.

Vaupel, P., Mayer, A., and Höckel, M. (2004). "Tumor Hypoxia and Malignant Progression," in Methods in Enzymology Oxygen Sensing. (Academic Press), 335–354.

Vaupel, P., Schlenger, K., Knoop, C., and Höckel, M. (1991). Oxygenation of human tumors: evaluation of tissue oxygen distribution in breast cancers by computerized O2 tension measurements. *Cancer Research* 51, 3316–3322.

Vaupel, P., Thews, O., and Hoeckel, M. (2001). Treatment Resistance of Solid Tumors. *Medical Oncology* 18, 243–260.

Venditto, V. J., and Szoka, F. C., Jr. (2013). Cancer nanomedicines: So many papers and so few drugs! *Advanced Drug Delivery Reviews* 65, 80–88.

Ventola, C. L. (2017). Progress in Nanomedicine: Approved and Investigational Nanodrugs. *Pharmacy & Therapeutics* 42, 742–755.

Vercauteren, D., Deschout, H., Remaut, K., Engbersen, J. F. J., Jones, A. T., Demeester, J., De Smedt, S. C., and Braeckmans, K. (2011). Dynamic Colocalization Microscopy To Characterize Intracellular Trafficking of Nanomedicines. *ACS Nano.* 5, 7874–7884.

Vercauteren, D., Vandenbroucke, R. E., Jones, A. T., Rejman, J., Demeester, J., De Smedt, S. C., Sanders, N. N., and Braeckmans, K. (2010). The Use of Inhibitors to Study Endocytic Pathways of Gene Carriers: Optimization and Pitfalls. *Mol Ther.* 18, 561–569.

Verma, S., Miles, D., Gianni, L., Krop, I. E., Welslau, M., Baselga, J., Pegram, M., Oh, D. Y., Diéras, V., Guardino, E., et al. (2012). Trastuzumab Emtansine for HER2-Positive Advanced Breast Cancer. *N Engl J Med* 367, 1783–1791.

Wang, G. L., and Semenza, G. L. (1995). Purification and characterization of hypoxia-inducible factor 1. *J. Biol. Chem.* 270, 1230–1237.

Wang, G. L., Jiang, B. H., Rue, E. A., and Semenza, G. L. (1995). Hypoxia-inducible factor 1 is a basic-helix-loop-helix-PAS heterodimer regulated by cellular O2 tension. *Proc. Natl. Acad. Sci. U.S.A.* 92, 5510–5514.

Wang, T., Gilkes, D. M., Takano, N., Xiang, L., Luo, W., Bishop, C. J., Chaturvedi, P., Green, J. J., and Semenza, G. L. (2014). Hypoxia-inducible factors and RAB22A mediate formation of microvesicles that stimulate breast cancer invasion and metastasis. *Proceedings of the National Academy of Sciences* 111, E3234–E3242.

Wang, X., Lockhart, S. M., Rathjen, T., Albadawi, H., Sørensen, D., O'Neill, B. T., Dwivedi, N., Preil, S. R., Beck, H. C., Dunwoodie, S. L., et al. (2016). Insulin Downregulates the Transcriptional Coregulator CITED2, an Inhibitor of Proangiogenic Function in Endothelial Cells. *Diabetes* 65, 3680–3690.

Wang, X.-L., Xu, R., Wu, X., Gillespie, D., Jensen, R., and Lu, Z.-R. (2009a). Targeted Systemic Delivery of a Therapeutic siRNA with a Multifunctional Carrier Controls Tumor Proliferation in Mice. *Mol. Pharmaceutics* 6, 738–746.

Wang, Y., Roche, O., Xu, C., Moriyama, E. H., Heir, P., Chung, J., Roos, F. C., Chen, Y., Finak, G., Milosevic, M., et al. (2012). Hypoxia promotes ligand-independent EGF receptor signaling via hypoxia-inducible factor-mediated upregulation of caveolin-1. *Proceedings of the National Academy of Sciences* 109, 4892–4897.

Wang, Y., Roche, O., Yan, M. S., Finak, G., Evans, A. J., Metcalf, J. L., Hast, B. E., Hanna, S. C., Wondergem, B., Furge, K. A., et al. (2009b). Regulation of endocytosis via the oxygen-sensing pathway. *Nat. Med.* 15, 319–324.

Wang-Gillam, A., Li, C.-P., Bodoky, G., Dean, A., Shan, Y.-S., Jameson, G., Macarulla, T., Lee, K.-H., Cunningham, D., Blanc, J. F., et al. (2016). Nanoliposomal irinotecan with fluorouracil and folinic acid in metastatic pancreatic cancer after previous gemcitabine-based therapy (NAPOLI-1): a global, randomised, open-label, phase 3 trial. *Lancet* 387, 545–557.

Warburg, O. (1956). On the origin of cancer cells. *Science* 123, 309–314.

Watanabe, S., and Boucrot, E. (2017). Fast and ultrafast endocytosis. *Current Opinion in Cell Biology* 47, 64–71.

Wei, D., Peng, J. J., Gao, H., Li, H., Li, D., Tan, Y., and Zhang, T. (2013). Digoxin Downregulates NDRG1 and VEGF through the Inhibition of HIF-1α under Hypoxic Conditions in Human Lung Adenocarcinoma A549 Cells. *IJMS.* 14, 7273–7285.

Welsh, S., Williams, R., Kirkpatrick, L., Paine-Murrieta, G., and Powis, G. (2004). Antitumor activity and pharmacodynamic properties of PX-478, an inhibitor of hypoxia-inducible factor-1alpha. *Molecular Cancer Therapeutics* 3, 233–244.

Wenger, R. H., Stiehl, D. P., and Camenisch, G. (2005). Integration of Oxygen Signaling at the Consensus HRE. *Science Signaling* 2005, re12–re12.

Wigerup, C., Påhlman, S., and Bexell, D. (2016). Therapeutic targeting of hypoxia and hypoxia-inducible factors in cancer. *Pharmacol. Ther.* 164, 152–169.

Wilhelm, S., Tavares, A. J., Dai, Q., Ohta, S., Audet, J., Dvorak, H. F., and Chan, W. C. W. (2016). Analysis of nanoparticle delivery to tumours. *Nat. Rev. Mater.* 1, 16014.

Wong, C. C. L., Zhang, H., Gilkes, D. M., Chen, J., Wei, H., Chaturvedi, P., Hubbi, M. E., and Semenza, G. L. (2012). Inhibitors of hypoxia-inducible factor 1 block breast cancer metastatic niche formation and lung metastasis. *J Mol Med.* 90, 803–815.

Xia, W., and Low, P. S. (2010). Folate-Targeted Therapies for Cancer. *J. Med. Chem.* 53, 6811–6824.

Yamaguchi, H., Takeo, Y., Yoshida, S., Kouchi, Z., Nakamura, Y., and Fukami, K. (2009). Lipid Rafts and Caveolin-1 Are Required for Invadopodia Formation and Extracellular Matrix Degradation by Human Breast Cancer Cells. *Cancer Research* 69, 8594–8602.

Yamamoto, Y., Ibusuki, M., Okumura, Y., Kawasoe, T., Kai, K., Iyama, K., and Iwase, H. (2007). Hypoxia-inducible factor 1α is closely linked to an aggressive phenotype in breast cancer. *Breast Cancer Res Treat.* 110, 465–475.

Yu, Y. Y., Chang, S. S., and Lee, C. L. (1997). Gold nanorods: electrochemical synthesis and optical properties. *The Journal of Physical Chemistry* 101 (34), 6661-6664.

Yuan, G., Nanduri, J., Bhasker, C. R., Semenza, G. L., and Prabhakar, N. R. (2005). Ca 2+/Calmodulin Kinase-dependent Activation of Hypoxia Inducible Factor 1 Transcriptional Activity in Cells Subjected to Intermittent Hypoxia. *Journal of Biological Chemistry* 280, 4321–4328.

Yuan, Y., Hilliard, G., Ferguson, T., and Millhorn, D. E. (2003). Cobalt Inhibits the Interaction between Hypoxia-inducible Factor- and von Hippel-Lindau Protein by Direct Binding to Hypoxia-inducible Factor. *Journal of Biological Chemistry* 278, 15911–15916.

Zerial, M., and Stenmark, H. (1993). Rab GTPases in vesicular transport. *Current Opinion in Cell Biology* 5, 613–620.

Zhang, H., and Semenza, G. L. (2009). Reply to Lopez-Lazaro: Evidence that digoxin inhibits human cancer. *Proceedings of the National Academy of Sciences* 106, E27–E27.

Zhang, H., Qian, D. Z., Tan, Y. S., Lee, K., Gao, P., Ren, Y. R., Rey, S., Hammers, H., Chang, D., Pili, R., et al. (2008). Digoxin and other cardiac glycosides inhibit HIF-1 synthesis and block tumor growth. *Proceedings of the National Academy of Sciences* 105, 19579–19586.

Łubgan, D., Jóźwiak, Z., Grabenbauer, G., and Distel, L. Doxorubicin-transferrin conjugate selectively overcomes multidrug resistance in leukaemia cells. *Cellular and Molecular Biology Letters* 14, 1423.

Appendix 1 Publications.

1. Brownlee, W.J. & Seib, F.P., 2018. Impact of the hypoxic phenotype on the uptake and efflux of nanoparticles by human breast cancer cells. Scientific Reports, 8(1), p.12318.

Author contribution; WJB designed and performed all experiments; acquired, analysed and interpreted all data; generated and edited the manuscript.

SCIENTIFIC REPORTS

OPEN

Impact of the hypoxic phenotype on the uptake and efflux of nanoparticles by human breast cancer cells

Received: 9 February 2018
Accepted: 30 July 2018
Published online: 17 August 2018

William J. Brownlee[1] & F. Philipp Seib[1,2]

Breast cancer cells adapt to the hypoxic tumoral environment by undergoing changes in metabolism, cell signalling, endo-lysosomal receptor uptake and recycling. The resulting hypoxic cell phenotype has the potential to undermine the therapeutic efficacy of nanomedicines designed for endocytic uptake and specific intracellular trafficking. The aim of this study was to examine the impact of hypoxia and simulated reperfusion on the *in vitro* uptake and release of nanomedicines by human breast cancer cells. Cells were exposed to a hypoxic preconditioning treatment in 1% oxygen for 6 and 24 hours to induce temporal changes in the hypoxic circuit (e.g. HIF-1α expression). The preconditioned cells were then dosed with nanoparticles for 45 or 180 minutes emulating nanomedicine access following tumor reperfusion. Hypoxic preconditioning significantly increased nanoparticle retention by up to 10% when compared to normoxic cultures, with the greatest relative difference between normoxic and hypoxic cultures occurring with a 45 minute dosing interval. Exocytosis studies indicated that the preconditioned cells had a significantly increased nanoparticle efflux (up to 9%) when compared to normoxic cells. Overall, we were able to show that hypoxic preconditioning regulates both the endocytosis and exocytosis of nanomedicines in human breast cancer cells.

Cancer nanomedicines are typically macromolecular drug delivery systems in the nanometer size range that are developed to reduce systemic toxicity but that also have the potential to exploit key features of solid tumor pathophysiology namely, leaky blood vessels and reduced lymphatic drainage to enhance passive tumor accumulation[1,2]. Despite decades of research[2,3], only a few anticancer nanomedicines are currently in routine clinical use; for example, Abraxane® (nanoparticle albumin-bound paclitaxel), Myocet® (liposomal doxorubicin), Doxil® (PEGylated liposomal doxorubicin), marketed as Caelyx® within Europe, Onivyde® (PEGylated liposomal irinotecan) and Daunoxome® (liposomal daunorubicin) are approved for treatment of solid tumors[4]. Specifically, Abraxane®[5], Caelyx®[6] and Myocet®[7] are licensed for the treatment of advanced metastatic breast cancer no longer responsive to estrogen, progesterone and ERBB2 (Her2/neu) targeted therapies. The primary motivation for the development of these nanomedicine formulations has been the improvement in side effect profiles (e.g. reduction in doxorubicin-associated cardio toxicity) enabling the use of these cytotoxic drugs in heavily pre-treated patients[6]. However, the overall small number of this anticancer nanomedicine arsenal generally, reflects the difficulties encountered in the successful development of anticancer nanomedicines from concept through clinical practice[8,9].

Many anticancer nanomedicine designs currently in preclinical and clinical development exploit the leaky vasculature and reduced lymphatic drainage of solid tumors as these tumor features favour the passive accumulation of nanomedicines at the tumor sites. This phenomenon, first described in 1986 and now commonly referred to as the "enhanced permeability and retention" (EPR) effect[10]. This arises due to a number of factors, including intratumoral hypoxia. Hypoxia in turn triggers angiogenesis and neo vascularisation principally via vascular endothelial growth factor[11,12], platelet derived growth factor β and angiopoeitin-2 (ref.[13]). The result is dysregulated and chaotic vascular growth, which commonly lacks stabilising smooth muscle cells. These abnormal blood

[1]Strathclyde Institute of Pharmacy and Biomedical Sciences, University of Strathclyde, 161 Cathedral Street, Glasgow, G4 0RE, UK. [2]Leibniz Institute of Polymer Research Dresden, Max Bergmann Center of Biomaterials Dresden, Hohe Strasse 6, 01069, Dresden, Germany. Correspondence and requests for materials should be addressed to F.P.S. (email: philipp.seib@strath.ac.uk)

vessels are heterogeneous but typically characterised by defective, irregular vascular endothelial cell coverage[14]. These defective endothelial cells exhibit enlarged intercellular fenestrations, which facilitate the (passive) tumorotropic transit and accumulation of nanomedicines (or macromolecules) within solid tumors (i.e. the EPR effect)[15]; acting against this trend is the raised internal tumor pressure[16]. Exploitation of the EPR effect in a clinical setting has proven difficult, and emerging evidence calls for better EPR-positive patient stratification using image-guided approaches; this has now been pioneered in advanced metastatic breast cancer patients[17].

Both tumor vascular development and density[18], as well as perfusion and hypoxia, are key regulators of nanomedicine distribution because nanomedicines are typically administered intravenously and must therefore successfully complete their journey from the injection site to the tumor. Intratumoral hypoxia can be intermittent or transient[19,20], which means that the physical access of a nanomedicine to hypoxic breast cancer tumor cells may be restricted to short, transient periods of vascular reperfusion. During reperfusion, the nanomedicine must navigate physical barriers, such as the extracellular matrix and immune and cancer-associated cells (e.g., fibroblast, macrophages etc.), and must overcome physiological factors (e.g., high interstitial fluid pressure) to reach the core of solid (breast) tumors[21].

Hypoxia within the solid tumor itself is of particular importance. Typically, survival of tumor cells under hypoxic stress requires adaptation via a series of hypoxic induction factors (HIF), principally HIF1[22,23]. These factors consist of a constitutively expressed β subunit (ARNT; aryl hydrocarbon receptor nuclear translocator) and one of three oxygen-labile α subunits (denoted 1, 2 and 3). During periods of hypoxia, HIF1α, rather than undergoing normal proteasomal degradation[24], translocates to the nucleus, where it combines with the HIFβ subunit to act on the conserved consensus sequence 5′-(A/G) CGTG-3′[25], the hypoxic response element, in the promoter region of over 1,000 genes[26,27]. This triggers a cascade of cellular changes, with the overall result being clinically aggressive, highly metastatic[28,29] and treatment resistant[30,31] tumor growth.

However, of potentially greater significance from a nanomedicine perspective is that hypoxic adaptation also alters key cellular processes, including energy metabolism[32–34], endocytic receptor internalisation[35], transmembrane receptor recycling, trafficking[36] and signalling[37]. Nanomedicines designed for intracellular activation in cancer cells rely on endocytosis and correct intracellular trafficking for effective therapeutic payload delivery. The energy dependence of endocytic uptake of nanomedicines means that these hypoxia-induced changes have the potential to directly undermine fundamental nanomedicine design principals. Therefore, an inherent link exists between hypoxic status, re-oxygenation of hypoxic tumor cells and the cellular presentation and internalisation of nanomedicines. However, few if any studies have sought to rigorously quantify the impact of these biological changes upon nanomedicine uptake and retention. Given the dynamic nature of the hypoxic response and the myriad changes observed within hypoxic tumor cells, the aim of this study was to quantify, *in vitro*, the impact of hypoxia exposure, simulated reperfusion and dosing interval on nanomedicine internalisation and retention in triple negative, clinically aggressive human breast cancer cells. The MDA-MB-231 cell line was selected, because it is representative of the most difficult to treat breast cancer subtype (triple negative breast cancer)[38], which is deficient in estrogen, progesterone and ERBB2 (Her2/neu) receptors[39], MDA-MB-231 cells are therefore unresponsive to hormone (e.g., Tamoxifen®) or receptor based therapies (e.g., Herceptin®) which are typical used to treat other breast cancer types. Therefore to make progress with triple negative breast cancer there is the urgent need to better understand the performance of nanomedicines (e.g. nanoparticles) in the presence of hypoxia. This study quantified the uptake and efflux of nanoparticles in hypoxic conditioned MDA-MB-231 breast cancer cells and the bone metastatic subpopulation. In parallel, expression of key biological markers of the hypoxic cell stress response, including HIF1-α, was assessed.

Results

Monitoring the pericellular oxygen concentration. Mean pericellular oxygen was measured at each time point, for wells with media only or media plus MDA-MB-231 cells. Monitoring of pericellular oxygen levels, measured within cell culture wells, allowed an evaluation of the actual oxygen levels cultures were exposed to, as opposed to the regulated 1% oxygen environment in which they were conditioned. Following 30 minutes hypoxic exposure the mean percentage pericellular oxygen level for wells containing cells was lower than those with media only (2.3% versus 6.3% respectively) (Fig. 1, Supplementary Fig. S1). Pericellular oxygen levels reached 1.33%, following 1 hour incubation, ultimately declining to a mean pericellular oxygen level of 0.44% between the 10 and 20 hour hypoxic conditioning period (Fig. 1). Exposure to atmospheric oxygen at 24 hours conditioning, resulted in transient elevation of pericellular oxygen levels, emulating the intermittent reperfusion seen with hypoxic tumors. Values returned to $\leq$ 1% within 50 minutes of resumption of hypoxic conditions.

Impact of fluorescent polystyrene nanoparticles on cell viability and trafficking. The potential confounding effects from reduced cell viability due to nanoparticles (diameter 43.4 nm $\pm$ 4.4) were excluded by assessing cell viability first. We selected this particle size because clinically used nanomedicines are typically within the 10 to 100 nm size range[1,2]. Furthermore, particles with a nominal diameter of 50 nm have no restrictions with respect to uptake routes into cells, which is encountered at larger particle sizes (e.g. >100 nm limited caveola uptake)[2]. Furthermore, polystyrene nanoparticles were selected to minimize any confounding effects (e.g. alternations of plasma membrane/endocytic membrane compositions)[2]. Cell viability over a 48 hour period was similar under either hypoxic or normoxic incubation conditions following exposure to the range of nanoparticle concentrations (Fig. 2a); no biological significant reduction of cell viability was observed ($IC_{50} > 10^{11}$ nanoparticles/ml). Dual wavelength confocal imaging of live MDA-MB-231 cells revealed co-localisation of the fluorescent nanoparticles with acidic intracellular vesicles, indicating endolysosomal uptake for both control and hypoxic cultures (Fig. 2b). The overall trafficking pattern was similar for both normoxic and hypoxic cultures following a 45 minutes and 180 minutes exposure to nanoparticles (Supplementary Fig. S2).

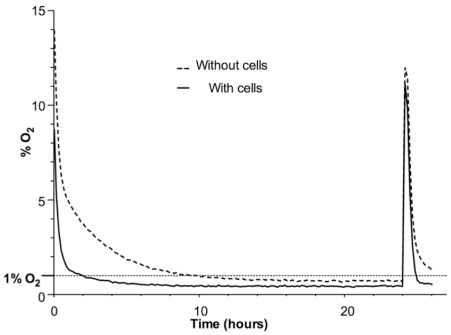

Figure 1. Pericellular oxygen monitoring to emulate transient intratumoral reperfusion of breast tumor. Typical mean pericellular oxygen for cell culture wells with and without MDA-MB-231 cells. Pericellular oxygen monitoring over the entire experimental time course (for magnification see Supplementary Fig. S1). Data average n = 3 (for ± SD see Supplementary Fig. S1).

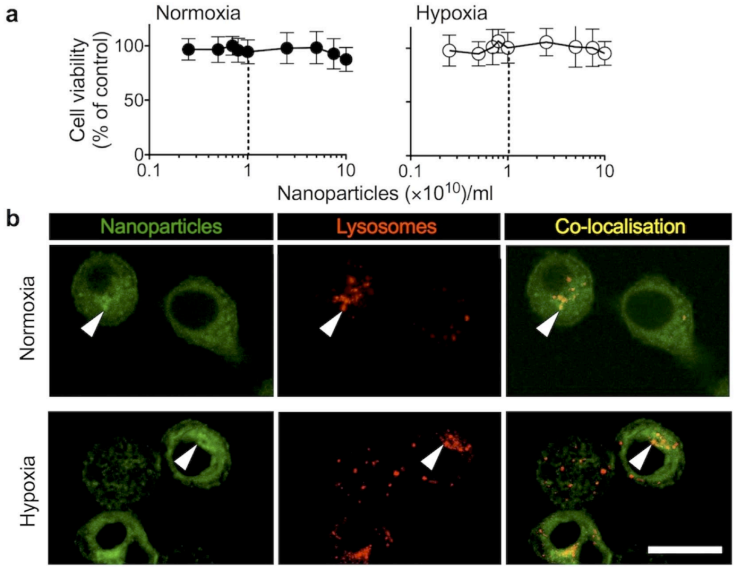

Figure 2. Cytotoxicity and uptake of nanoparticles in response to normoxia and hypoxia. (**a**) *In vitro* cytotoxicity of fluorescent nanoparticles in the MDA-MB-231 human breast cancer cells. Cells were dosed with fluorescent nanoparticles and subsequently cultured in either hypoxia (1% O_2) or normoxia. At 48 hours cell viability was assessed. Dotted lines indicate the nanoparticle dose used for subsequent studies ($n = 18$ at each dosing point, from three biological replicates; ± SD). (**b**) Representative live cell confocal imaging of cells exposed for 24 hours to normoxia or hypoxia and subsequently dosed for 45 minutes with nanoparticles (green). Acidic vesicles were stained using LysoTracker Red. Arrows show nanoparticle co-localisation in acidic vesicles. Scale bar 20 μm.

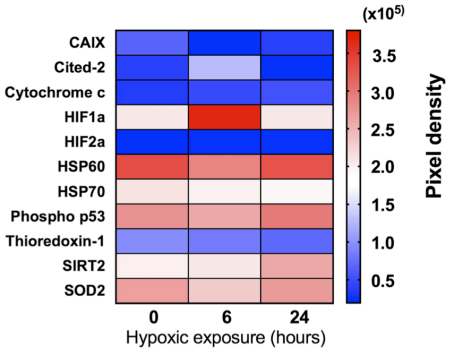

Figure 3. Impact of hypoxia on cell stress related proteins in human MDA-MB-231 breast cancer cells. Cells were conditioned in hypoxia (1% O_2) for either 0, 6 or 24 hours. Relative expression of cell stress related proteins in whole cell lysates using antibody protein arrays (pooled lysates from 3 samples). Full names: *CAIX, carbonic anhydrase 9; Cited-2, CbP/p300 – interacting transactivator – 2; HIF1α, α subunit of hypoxic induction factor 1; HIF2α, α subunit of hypoxic induction factor 2; HSP60, heat shock protein 60; HSP70, heat shock protein 70; Phospho p53 (s46), phosphorylated p53; SIRT2, NAD-dependent deacetylase sirtuin-2; SOD2, mitochondrial superoxide dismutase 2.*

Assessment of the hypoxic phenotype of MDA-MB-231 cells. The phenotypic adaptation of MDA-MB-231 cells exposed to hypoxia was monitored by assessing the expression of 11 cell stress related proteins, including HIF1α, the key effector of hypoxic adaptation, after 0, 6 and 24 hours of hypoxic conditioning (Fig. 3). The protein array results from cell lysates demonstrated differentially regulated cell stress associated proteins. For example, HIF1α levels were highest after 6 hours of hypoxia but remained slightly elevated after 24 hours of hypoxia when compared to normoxic cultures. Carbonic anhydrase 9 expression showed a close to 2 fold increase from 6 hours to 24 hours (relative measured fluorescence 21,003 and 39,116, respectively). CbP/p300 – interacting transactivator -2 (Cited-2) exhibited a similar expression profile, with elevated levels following 6 hours hypoxia, whereas Thioredoxin-1 increased progressively across the 24 hours hypoxic period (Fig. 3).

HIF1α is a master regulator of the hypoxic response; therefore, the protein array results were verified by SDS PAGE and western blotting to determine the relative HIF1α expression in biological replicates (Supplementary Fig. S3a). The immunoblotting results confirmed the HIF1α expression pattern observed with the protein array (Fig. 3, Supplementary Fig. S3b); namely, the HIF1α expression levels were highest after 6 hours of hypoxic incubation (a 4.10-fold increase) and lower at 24 hours (a 1.54-fold increase), whereas the control cultures showed no substantial change in HIF1α (1.0-fold).

Nanomedicine uptake and release by normoxic and hypoxic breast cancer cells. The relative expression of cell stress related proteins, and in particular, the differential expression of HIF1α observed after 6 or 24 hours of hypoxic conditioning led to the choice of these time points for uptake studies in MDA-MB-231 human breast cancer cells (Fig. 4a). Following the respective hypoxia conditioning, MDA-MB-231 cells were exposed to nanoparticles for either 45 or 180 minutes. When compared to the respective normoxic controls, nanoparticle uptake at 45 minutes was significantly increased in cells exposed to 6 hours of hypoxic conditioning. With the same hypoxic conditioning regime nanoparticle uptake was substantially upregulated at 180 minutes (Fig. 4). By contrast, cells conditioned for 24 hours under hypoxia showed significantly increased nanoparticle uptake at both the 45 and 180 minute dosing intervals when compared to normoxic control cultures. The largest overall upregulation of nanoparticle uptake (10.02% ± 5.36) was observed at the 45 minute dosing interval in cells conditioned under hypoxia for 24 hours (Fig. 4b). These observations were verified with the 1833 breast cancer subline (originally derived from MDA-MB-231 via *in vivo* selection[40]). 1833 cells were conditioned for 24 hours in hypoxia and dosed with nanoparticles for 45 minutes also resulting in an increased (7.96% ± 4.35) nanoparticle uptake (Fig. 5a,b).

The observation that hypoxic conditioned MDA-MB-231 and 1833 cells showed consistently increased nanoparticle uptake raised the possibility that this response was due to (i) increased endocytosis (i.e. uptake), (ii) reduced exocytosis (i.e. recycling) or (iii) a combination of both (i) and (ii). This question was addressed by performing pulse chase experiments with normoxic and hypoxic conditioned cells. These studies were conducted with MDA-MB-231 and 1833 cells conditioned for 24 hours to hypoxia and pulse dosed for 45 minutes, as this treatment gave the greatest relative increase in nanoparticle uptake (Figs 4c and 5c). After this treatment, the cells were chased for 30 minutes and then analysed. Comparison of the baseline cell-associated fluorescence with post chase cell-associated fluorescence demonstrated a post-chase drop in the MDA-MB-231 cells which was significantly greater following hypoxic conditioning than following normoxic conditioning (81.13% ± 2.18,

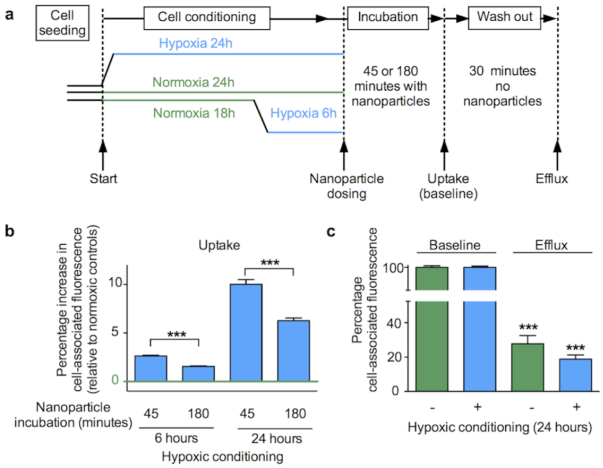

Figure 4. Impact of hypoxic preconditioning on the uptake (endocytosis) and recycling (exocytosis) of nanoparticles by human MDA-MB-231 breast cancer cells. (**a**) Diagram of the experimental approach. Cells were conditioned in hypoxia (1% O_2) for either 6 or 24 hours and then dosed with nanoparticles at an effective concentration of 1×10^{10} nanoparticles/ml for either 45 or 180 minutes. For the recycling studies, cells were preconditioned for 24 hours in either hypoxia (1% O_2) or normoxia. Next, cells were dosed with nanoparticles at an effective concentration of 1×10^{10} nanoparticles/ml for 45 minutes and analysed (baseline), or washed and allowed to exocytose for 30 minutes (exocytosis) (**b**) Cell uptake of fluorescent nanoparticles was assessed by measuring mean single cell-associated fluorescence by flow cytometry. (**c**) Exocytosis of fluorescent nanoparticles of normoxia or hypoxia preconditioned cells. For (**b**,**c**) mean single cell-associated fluorescence was measured by flow cytometry; ≥10,000 events; $n = 15$ for each dosing group and treatment period, 3 independent biological experiments ± SD.

$n = 15$ and 72.14% ± 4.94, $n = 15$, respectively) (Fig. 4). Similarly the post-chase drop in the 1833 cells was also significantly greater following hypoxic conditioning than with normoxic conditioning (52.09% ± 4.75, $n = 10$ and 43.74% ± 10.13, $n = 10$, respectively) (Fig. 5c).

Discussion

We believe this is the first quantitative study on human breast cancer cells that assesses the impact of hypoxic adaptation on both nanomedicine internalisation and recycling whilst also taking into account the temporal changes in key elements of the hypoxic adaptation circuit itself. Recent mechanistic insights into nanomedicine access to tumor cells includes transient vascular bursts[41,42] and a combination of radiotherapy and tumor associated macrophages (TAM) that show the potential to enhance therapeutic delivery of nanomedicines via the characteristically short periodic vascular reperfusion[43] found in tumors. In experimental xenografts these vascular burst were dependent on blood flow, were intermittent and facilitated nanomedicine distribution into large areas of the tumor (100s μ^2) (ref.[42]). We therefore designed our uptake studies so that nanomedicine dosing occurred at the start of short periods of re-oxygenation, followed by hypoxia, to reflect the current understanding of transient tumor vascular reperfusion[44], and the subsequent access of nanomedicines to the intratumoral space.

This study examined the impact of hypoxia on nanoparticle endo- and exocytosis using a simple, but yet effective and well-controlled two-dimensional *in vitro* culture system. The merit of our system is the ability to both monitor pericellular oxygen levels non-invasively and to quantify nanoparticle uptake and efflux. Unlike three-dimensional organotypic culture models our model system reduced the complexity thus eliminating co-founding factors such as mass transport limitations (of both nanoparticles and oxygen) and permitting rapid sample processing and analysis. Rapid sample handling is important to ensure that endocytosis and exocytosis is arrested (here by placing samples on ice). While this study demonstrates the basic role of hypoxia in nanoparticle uptake and efflux, many other factors are likely to impact nanomedicine performance. A number of normoxic studies have considered factors like stability of the carrier, cargo release and particle size and elasticity[45]. However, this study was deigned specifically to exclude as many of these confounding factors as possible.

Our data showed that nanomedicine internalisation is altered in a dynamic fashion in response to varying periods of hypoxic conditioning and dosing intervals. These findings paralleled the altered expression of key proteins within the hypoxic adaptation circuit itself. MDA-MB-231 cells increased their capacity for internalisation of nanoparticles in response to hypoxic conditioning for 6 or 24 hours, with the greatest difference observed

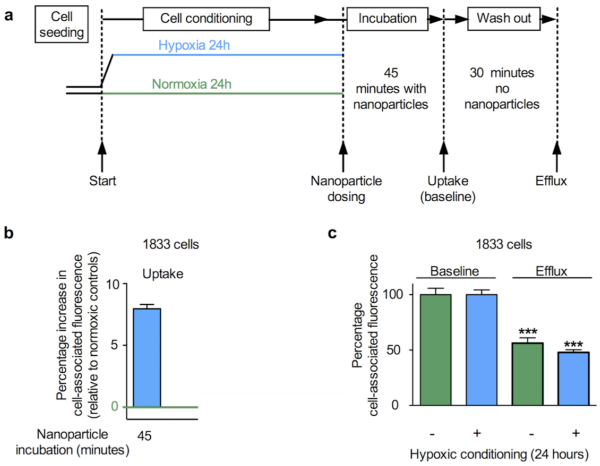

Figure 5. Impact of hypoxic preconditioning on the uptake (endocytosis) and recycling (exocytosis) of nanoparticles by human 1833 breast cancer cells. (**a**) Diagram of the experimental approach. Cells were conditioned in hypoxia (1% O_2) for 24 hours and then dosed with nanoparticles at a concentration of 1×10^{11} nanoparticles/ml for 45 minutes. For the recycling studies, cells were preconditioned for 24 hours in either hypoxia (1% O_2) or normoxia. Next, cells were similarly dosed for 45 minutes and analysed (baseline) or washed and allowed to exocytose for 30 minutes (exocytosis) (**b**) Cell uptake of fluorescent nanoparticles was assessed by measuring mean single cell-associated fluorescence by flow cytometry. (**c**) Exocytosis of fluorescent nanoparticles of normoxia or hypoxia preconditioned cells. Mean single cell-associated fluorescence was measured by flow cytometry, ≥10,000 events per measurement; (**b**) n = 15 from 3 independent biological experiments, (**c**) $n = 20$ for each treatment period, 2 independent biological experiments ± SD.

following 24 hours hypoxia. In addition, following all hypoxic conditioning periods, the greatest relative increase in internalisation was observed over a 45 minute dosing interval. The MDA-MB-231 parent cell line is heterogeneous and contains adapted, highly metastatic sub-populations[40,46]. We therefore examined the performance of nanoparticles in the bone metastatic subline 1833 because bone metastasis is common in triple negative breast cancer[47]. We examined the cellular response in MDA-MB-231 and 1833 cells (classified as mesenchymal-like) to make inroads into the effects of tumor heterogeneity (within the same patient) on nanomedicine uptake and efflux in hypoxia. However, gene expression analysis of triple negative breast cancer has identified six main subtypes (mesenchymal-like cells are one of them)[48]. It thus remains to be seen how all these different subclasses of triple negative cells respond to hypoxia.

Similarly to the parent cell line, 24 hour hypoxic conditioning of 1833 cells followed by a 45 minute dosing interval showed a significant increase in nanoparticle uptake. Furthermore, both the MDA-MB-231 and 1833 cell lines conditioned to hypoxia for 24 hours increased their exocytosis of nanoparticles. We therefore speculate that hypoxic endocytic uptake and recycling are similar in both these mesenchymal-like breast cancer cell lines. However, systematic studies examining these differences have not been reported. Overall, these results demonstrate that intratumoral hypoxia has the potential to alter nanomedicine uptake by tumor cells, thereby modifying intracellular trafficking and confounding effective therapeutic payload delivery.

A key aspect of the hypoxic response is the shift from energy-efficient oxidative phosphorylation to the less productive, yet oxygen conserving, glycolytic pathway[49–51]. As a consequence, hypoxic tumor cells enter a lower energy state associated with reduced ATP synthesis. Because nanomedicine internalisation via endocytosis is an active, energy-dependent process, the expectation would be a reduction in nanomedicine internalisation, yet here, we observed a significant increase. There are however, few studies available for comparison with our work. One study reported a reduction in the cellular uptake of 1.9 nm gold nanoparticles in MDA-MB-231 cells under hypoxic conditions[52]. However, that study employed a very low (0.1%) oxygen environment for hypoxic conditioning and the conditioning was only for 4 hours prior to dosing with nanoparticles. Some cellular hypoxic adaptations would be expected over that short duration of hypoxia, but no validations of molecular changes were reported and pericellular oxygen levels were not determined. In the present study, therefore, we adopted *in situ* pericellular oxygen monitoring and tracked 11 stress related proteins (including the master hypoxic effector, HIF1α) as markers of hypoxic cellular conditioning and the cellular hypoxic response, respectively. By contrast, Neshatian *et al.*[53] demonstrated elevated internalisation of gold nanoparticles (sizes: 15, 50 and 70 nm) in human MCF-7 breast cancer cells following 18 hours of hypoxic pre-conditioning in a very low 0.2% oxygen

environment. For our study, we selected a hypoxic oxygen level of 1% because meta-analysis[54] of *in vivo* ultrasound guided hypoxia measurements within human breast tumors indicated that the median pO_2 was 10 mmHg. Using normobaric assumptions, this approximates to around 1.0 to 1.3% oxygen. As expected, we found lower pericellular oxygen in the presence of cells than in cell-free media (Fig. 1). This suggests that an incubation environment as low as 0.2 or 0.1% O_2, as used in the previous published studies, could lead to anoxic, as opposed to hypoxic, conditions within the cells themselves[55]. This is important, because anoxia is known to trigger alternative cellular responses (e.g. activating transcription factor 3 and 4) that are not mediated via HIF[56,57]. This raises concerns about the relevance of these previously published studies in the context of nanomedicines and limits our ability to compare our work with them.

Overall, nanomedicine retention within cells is the sum of both uptake (i.e. endocytosis) and efflux (i.e. exocytosis)[3] and requires a mechanism for regulation of cellular homeostasis (e.g. cell volume, plasma membrane economics)[58] and for response to and modulation of cell signalling (e.g. receptor recycling versus down regulation). Therefore, assessment of the endocytic index of nanomedicines must include both endocytosis and exocytosis[3]. The current results showed that 24 hour hypoxic preconditioning increased nanomedicine uptake, but it also increased exocytosis (Figs 4 and 5). The degree and speed of recycling under normoxic conditions we have observed here is similar to that noted in previous work (albeit, under differing experimental conditions)[59,60].

The observed upregulation of the energy dependent processes of endo- and exocytosis, in what is ostensibly a low energy hypoxic cellular state, would appear to be counterintuitive. However, tumor cell hypoxic adaptation involves well-established changes to endocytic receptor uptake and signalling[35,61,62] and altered intracellular trafficking[36]. Recent *in vitro* research has shown that MDA-MB-231 and HeLa cells undergo a generalised reduction in overall internalisation of the tumor cell surface proteome in response to hypoxia, with a parallel selective upregulation of specific endocytic pathways, mediated via caveolin 1 (ref.[63]). Further, the recycling of transmembrane proteins may also be influenced by interaction with proteins like Caveolin 1, among others[64]. Interestingly, constitutive *in vitro* expression of Caveolin 1 is markedly higher in MDA-MB-231 cells than in many other tumor cell lines[65,66], suggesting its potential for a greater influence in this cell line. Similarly, upregulation of exocytotic release of exosomes or vesicles from tumor cells during hypoxia is known to play a significant role in tumor development and signaling[37,67], with implications for altered or upregulated exocytosis. Thus, our results may reflect these types of specific upregulated endocytic and exocytic processes, which deserve further investigation.

Our study measured relative expression of HIF1α, the master effector of hypoxic adaptation, to assess how the cellular hypoxic response might change with the duration of hypoxic exposure. Unhydroxylated HIF1α expression was increased approximately four fold when compared to normoxic levels after 6 hours of hypoxia, but returned to near normoxic levels following 24 hours of hypoxia. Similar temporal patterns of HIF1α expression have been demonstrated in MDA-MB-231 cells exposed to similar *in vitro* hypoxic conditions[68]. The regulation of this cyclical HIF1α expression is multifactorial, but it appears to be driven principally by a variety of cellular factors, including REST (repressor element 1- silencing transcription factor)[68]. In the context of our results, it is interesting to note that we observed the greatest differences in nanoparticle internalisation following 24 hours of hypoxic conditioning, where we also found that HIF1α had returned to near normal levels.

We assessed the relative expression of ten other key cell stress proteins in the MDA-MB-231 cells and demonstrated that their altered expression depended on the duration of hypoxia. Whilst all these proteins are relevant to the cellular stress response to hypoxia, of particular note are those known to form part of the HIF1 regulatory circuit. For example, CbP/p300 – interacting transactivator – 2 (Cited 2) is a known HIF1 negative regulatory element that exhibits preferential binding of CBP/p300 co-factors required for HIF1 transcriptional activity[69]. Similarly, the NAD dependent deacetylase Sirtuin2 (SIRT2) has been shown, through deacetylation, to increase proteasomal breakdown of HIF1 via enhanced affinity for PHD2[70]. We found that the relative expression of Cited 2 peaked following six hours of hypoxia, whereas Sirtuin2 exhibited the highest relative expression following 24 hours of hypoxic conditioning. Taken within the context of our studies, these results underline the dynamic nature of hypoxic adaptation within tumor cells and its impact on the uptake and efflux of nanomedicines during hypoxia.

Conclusions

The objective of this work was to quantify the difference that tumor cell hypoxic adaptation might make to *in vitro* nanomedicine uptake and recycling (Fig. 6). We demonstrated that both uptake and recycling of our model nanomedicine were increased following hypoxic incubation in both the MDA-MB-231 and 1833 cell line. Further, we demonstrated with the MDA-MB-231 cell line, that the magnitude of these changes depended on the duration of the hypoxic exposure and the dosing interval. Overall, these results expand the existing knowledge of how the hypoxic tumor microenvironment can potentially alter nanomedicine internalisation, with implications for effective therapeutic delivery and design.

Experimental Section

Cell culture. MDA-MB-231 cells (ATCC® HTB-26™) were purchased from the American Type Culture Collection (Manassas, VA, USA). The 1833 subline was gifted by Dr. Joan Massagué (Memorial Sloan-Kettering Cancer Center, New York, NY, USA) and detailed elsewhere[40]. Cells were cultured as monolayers in RPMI 1640 media (Life Technologies, UK), supplemented with 10% (v/v) foetal bovine serum (FBS), 50 U/mL penicillin and 50 μg/mL streptomycin. Unless otherwise indicated, cells were seeded at 4×10^4 cells/cm^2. For all experimental work, hypoxic or normoxic culture conditions were achieved using a gas mixture of 5% CO_2, 1% O_2 and 87.8% N_2 (hypoxic) or 5% CO_2, 18.6% O_2 and 70.2% N_2 (normoxic) within a humid 37°C incubator. Normobaric conditions were assumed throughout.

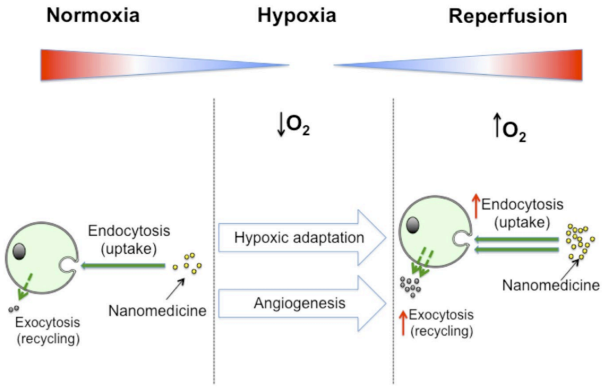

Figure 6. A schematic summary of key findings: Hypoxic conditioning of breast cancer cells increases nanomedicine uptake and efflux.

Fluorescent nanoparticles. Fluoresbrite® spherical fluorescent polystyrene nanoparticles (diameter 43.4 nm ± 4.4 with an excitation/emission maxima at 441/486 nm), suspended in water, were purchased from Polysciences Europe GmbH, Eppelheim, Germany.

***In vitro* cytotoxicity studies.** MDA-MB-231 cells were seeded into 96-well tissue culture treated polystyrene plates (TPP Techno Plastic Products AG, Trasadingen, Switzerland) at a density of 3×10^3 cells/cm^2 in 100 µl complete culture medium. The plates were then incubated in either normoxic or hypoxic conditions for 24 hours. The wells were then aspirated and fresh media containing nanoparticles at a range of concentrations up to 1×10^{11} nanoparticles/ml was added, followed by a further incubation in the respective environment for 44 hours. Next, 20 µl of (3-(4,5- dimethylthiazol-2-yl)-2,5-diphenyltetrazolium bromide (MTT; 5 mg/ml in PBS) was added and incubated for 4 hours. The MTT was aspirated from all wells and formazan crystals were dissolved in dimethyl sulphoxide and absorbance read at 570 nm. Cell viability at each nanoparticle dose was calculated as a percentage of the control (i.e. zero dose).

***In vitro* trafficking of fluorescent nanoparticles.** MDA-MB-231 cells were seeded onto cell culture treated polystyrene Cellstar® cell culture dishes (Greiner Bio-One, Kremsmunster, Austria) for 24 hours in either hypoxic or normoxic conditions (as defined above). Next, cells were dosed with fluorescent nanoparticles for either 45 or 180 minutes, placed on ice and washed twice with PBS at 4 °C, stored on ice and transferred for confocal imaging immediately. Lysosomal staining was achieved using LysoTracker® Red (Invitrogen, Waltham, MA, USA) according to the manufacturer's instructions. Live cell confocal co-localisation imaging was conducted using a Leica TCS SP5 laser scanning confocal microscope equipped with a 40× liquid immersion objective. Confocal slices were assembled into figures, brightness/contrast adjusted using ImageJ v1.0 (National Institutes of Health, Bethesda, Maryland, USA) and imported into Graphpad Prism® v7.0 (GraphPad Software Inc., La Jolla, CA, USA).

Generation of cell lysates. MDA-MB-231 cells were seeded in 75 cm^2 tissue culture treated polystyrene culture flasks and incubated for 24 hours under normoxic conditions to support cell growth. Next, flasks were split into 4 groups and cultured for a further 24 hours using specific conditioning regimes: (i) normoxic control, (ii) 6 hours of hypoxia (i.e. 18 hours normoxia followed by 6 hours of hypoxia conditioning), (iii) 24 hours of hypoxic conditioning and (iv) positive control using 100 µM $CoCl_2$. The $CoCl_2$ dosing served to chemically block HIF1α breakdown in the presence of oxygen. At the end of the conditioning regime, samples were immediately immersed in ice. Within 90 seconds, the culture medium was removed and the cell monolayers were washed twice with 5 ml ice cold PBS, followed by 1.0 ml of ice cold radioimmunoprecipitation (RIPA) buffer containing 40 µl of 25 × Roche Diagnostics Easypack® Protease cocktail (both from Sigma-Aldrich, Dorset, England, UK). The cells were then harvested using a cell scraper. The lysates were pipetted into ice cold centrifuge tubes and, while maintained at 4 °C, vortexed at full power for 1 minute, shaken at full power for 20 minutes and then centrifuged for 20 minutes at 12,000 × g. Following centrifugation, the supernatant was aliquoted and stored at −80°C until further analysis.

Protein separation, western blotting and protein arrays. The total protein concentration of each cell lysate was determined using the Pierce™ bicinchoninic acid protein assay kit (Thermo Scientific, Waltham, MA, USA). Protein samples were denatured in a 1:1 ratio using Laemmli sample loading buffer [65.8 mM Tris-HCl, pH 6.8, 2.1% (w/v) SDS, 26.3% (w/v) glycerol, 0.01% (v/v) bromophenol blue, and 5% (v/v) 14.2 M β-mercaptoethanol

(Bio-Rad Laboratories, Hemel Hempstead, UK)] by heating for 5 minutes at 95 °C. Equivalent protein quantities (25 μg) and a Precision Plus Kaleidoscope™ protein ladder (Bio-Rad Laboratories, Hemel Hempstead, UK) were loaded on to an 8% polyacrylamide gel, and separated at 150 V for 55 minutes. Proteins were blotted onto a polyvinylidene difluoride membrane (Bio-Rad Laboratories, Hemel Hempstead, UK). The following antibodies were used to probe the membrane: Rabbit primary antibodies for β-actin (1:10,000) and unhydroxylated HIF1-α (1:1,000) (monoclonal and polyclonal respectively) as well as monoclonal goat anti-rabbit IgG HRP linked secondary antibody (1:2,000) (all from Cell Signalling Technology, Danvers, MA, USA). Primary antibodies were blocked with 5%w/v bovine serum albumin (Sigma-Aldrich, Dorset, England, UK) in tris-buffered saline Tween (TBST), with secondary antibody blocking achieved with 5% non-fat dry milk powder in TBST. Relevant bands were visualised using Clarity™western ECL substrate and UltraCruz autoradiography film (Santa Cruz Biotech Inc., Dallas, TX, USA). HIF1-α and β-actin bands were digitised (Epson Perfection v600 film flatbed scanner, Epson Europe, B.V., Netherlands), and densitometry scans were completed using Image Studio™ Lite software (LI-COR Biotechnology, Lincoln, NE, USA). The relative expression of 11 cell stress-associated proteins was determined using the R&D Proteome profiler™ (catalogue number #ARY018; R&D Systems, Inc., MN, USA), following the manufacturer's instructions. Triplicates of cell lysates were prepared as detailed above and pooled, with a total of 300 μg protein per sample used. Arrays were imaged and analysed by densitometry, as detailed above.

Normoxic and hypoxic cell cultures and nanoparticle uptake and release. MDA-MB-231 or 1833 cells were seeded into 6-well plates. Plates were then incubated for either (i) 24 hours in hypoxic conditions, (ii) 24 hours in normoxic conditions, or (iii) 18 hours under normoxia followed by 6 hours under hypoxia. Cells were then dosed with nanoparticles at an effective concentration of 1×10^{10} nanoparticles/ml (1×10^{11} nanoparticles/ml for 1833 cells), and the plates were returned to their respective culture environments for either 45 or 180 minutes. For the recycling studies, cells were preconditioned for 24 hours in either hypoxia (1% O_2) or normoxia. Next, cells were dosed with nanoparticles at an effective concentration of 1×10^{10} nanoparticles/ml (1×10^{11} nanoparticles/ml for 1833 cells) for 45 minutes and analysed (baseline), or washed and allowed to exocytose for 30 minutes (exocytosis). Within the next 15 minute time interval, the cells were washed 3 times with ice cold PBS, detached using trypsin and transferred to flow cytometry tubes for analysis. Flow cytometry was performed using a FACS Canto™II FACS analyser (Becton Dickinson, Oxford, England, UK) by assessing mean cell-associated fluorescence with an argon laser (excitation 488 nm, emission 525 nm) and gating 10,000 events. For all hypoxic measurements normoxic control groups were run in parallel. Mean FITC fluorescence values were determined from FCS 3.0 files using FlowJo® v10.3 software (FlowJo LLC, Oregon, USA). Mean FITC fluorescence values (Supplementary Fig. S4) were converted into percentages to calculate relative differences.

Pericellular oxygen monitoring. Three wells of Presens Oxohydrodish® 6 well plates (Presens, Precision Sensing GmbH, Regensburg, Germany) were seeded with MDA-MB-231 cells, as described above. The remaining three wells were filled with an equivalent volume of medium only. Each plate was then placed on the Presens Sensordish® 24-channel plate reader within the hypoxic incubator. Following temperature equilibration, the in-well oxygen percentage was recorded for each well, separately, at frequent intervals, for a period of up to 26 hours.

Statistical analyses. Statistical analyses were performed using GraphPad Prism® v6.0 (Graphpad Software Inc., La Jolla, CA, USA). All significance tests used unpaired two tailed Student's *t* tests, except for cytotoxicity measurements, where a one-way unpaired ANOVA with Sidak multiple comparisons test was used ($\alpha = 0.05$). Asterisks denote statistical significance as follows: $*p < 0.05$, $**p < 0.01$ and $***p < 0.001$. All data are presented as a mean values ± standard deviation (SD), unless otherwise stated.

Data availability section. All data created during this research are openly available from the University of Strathclyde-Pure, at https://doi.org/10.15129/3b637e0e-6b92-4041-bac9-0ed9bc057bfd.

References

1. Shi, J., Kantoff, P. W., Wooster, R. & Farokhzad, O. C. Cancer nanomedicine: progress, challenges and opportunities. *Nat. Rev. Cancer* **17**, 20–37 (2016).
2. Duncan, R. & Gaspar, R. Nanomedicine(s) under theMicroscope. *Mol. Pharmaceutics* **8**, 2101–2141 (2011).
3. Duncan, R. & Richardson, S. C. W. Endocytosis and Intracellular Trafficking as Gateways for Nanomedicine Delivery: Opportunities and Challenges. *Mol. Pharmaceutics* **9**, 2380–2402 (2012).
4. Venditto, V. J. & Szoka, F. C. Jr. Cancer nanomedicines: So many papers and so few drugs! *Adv. Drug Deli. Rev.* **65**, 80–88, https://doi.org/10.1016/j.addr.2012.09.038 (2013).
5. Palumbo, R. *et al.* Nanoparticle albumin-bound paclitaxel (nab-paclitaxel) as second-line chemotherapy in HER2-negative, taxane-pretreated metastatic breast cancer patients: prospective evaluation of activity, safety, and quality of life. *Drug Des. Devel. Ther.* **9**, 2189–2199, https://doi.org/10.2147/DDDT.S79563 (2015).
6. Rom, J. *et al.* Efficacy and toxicity profile of pegylated liposomal doxorubicin (Caelyx) in patients with advanced breast cancer. *Anticancer Drugs* **25**, 219–224, https://doi.org/10.1097/CAD.0000000000000037 (2014).
7. Batist, G. *et al.* Reduced cardiotoxicity and preserved antitumor efficacy of liposome-encapsulated doxorubicin and cyclophosphamide compared with conventional doxorubicin and cyclophosphamide in a randomized, multicenter trial of metastatic breast cancer. *J Clin. Oncol.* **19**, 1444–1454, https://doi.org/10.1200/JCO.2001.19.5.1444 (2001).
8. Goldberg, M. S. *et al.* Biotargeted nanomedicines for cancer: six tenets before you begin. *Nanomedicine* **8**, 299–308 (2013).
9. Barenholz, Y. C. Doxil® — The first FDA-approved nano-drug: Lessons learned. *J. Control. Rel.* **160**, 117–134 (2012).
10. Matsumura, Y. & Maeda, H. A new concept for macromolecular therapeutics in cancer chemotherapy: mechanism of tumoritropic accumulation of proteins and the antitumor agent smancs. *Cancer Res.* **46**, 6387–6392 (1986).
11. Shweiki, D., Itin, A., Soffer, D. & Keshet, E. Vascular endothelial growth factor induced by hypoxia may mediate hypoxia-initiated angiogenesis. *Nature* **359**, 843–845 (1992).

12. Forsythe, J. A. *et al.* Activation of vascular endothelial growth factor gene transcription by hypoxia-inducible factor 1. *Mol. Cell. Biol.* **16**, 4604–4613 (1996).
13. Kelly, B. D. Cell Type-Specific Regulation of Angiogenic Growth Factor Gene Expression and Induction of Angiogenesis in Nonischemic Tissue by a Constitutively Active Form of Hypoxia-Inducible Factor 1. *Circ. Res.* **93**, 1074–1081, https://doi.org/10.1161/01.res.0000102937.50486.1b (2003).
14. Hashizume, H. *et al.* Openings between defective endothelial cells explain tumor vessel leakiness. *AJPA* **156**, 1363–1380, https://doi.org/10.1016/S0002-9440(10)65006-7 (2000).
15. Maeda, H. Toward a full understanding of the EPR effect in primary and metastatic tumors as well as issues related to its heterogeneity. *Adv. Drug Deliv. Rev.* **91**, 3–6, https://doi.org/10.1016/j.addr.2015.01.002 (2015).
16. Jain, R. K., Martin, J. D. & Stylianopoulos, T. The Role of Mechanical Forces in Tumor Growth and Therapy. *Annu. Rev. Biomed. Eng.* **16**, 321–346, https://doi.org/10.1146/annurev-bioeng-071813-105259 (2014).
17. Lee, H. *et al.* 64Cu-MM-302 Positron Emission Tomography Quantifies Variability of Enhanced Permeability and Retention of Nanoparticles in Relation to Treatment Response in Patients with Metastatic Breast Cancer. *Clin. Cancer Res.* **23**, 4190–4202, https://doi.org/10.1158/1078-0432.CCR-16-3193 (2017).
18. Torosean, S. *et al.* Nanoparticle uptake in tumors is mediated by the interplay of vascular and collagen density with interstitial pressure. *Nanomedicine* **9**, 151–158, https://doi.org/10.1016/j.nano.2012.07.002 (2013).
19. Bennewith, K. L. & Durand, R. E. Quantifying transient hypoxia in human tumor xenografts by flow cytometry. *Cancer Res.* **64**, 6183–6189 (2004).
20. Vaupel, P. & Mayer, A. Hypoxia in Tumors: Pathogenesis-Related Classification, Characterization of Hypoxia Subtypes, and Associated Biological and Clinical Implications. *Oxygen Trans. Tissue* **36**, 19–24, https://doi.org/10.1007/978-1-4939-0620-8_3 (2014).
21. Sriraman, S. K., Aryasomayajula, B. & Torchilin, V. P. Barriers to drug delivery in solid tumors. *Tissue Barriers* **2**, e29528, https://doi.org/10.2217/nnm.11.93 (2014).
22. Semenza, G. L. & Wang, G. L. A nuclear factor induced by hypoxia via de novo protein synthesis binds to the human erythropoietin gene enhancer at a site required for transcriptional activation. *Mol. Cell. Biol.* **12**, 5447–5454 (1992).
23. Semenza, G. L. Defining the role of hypoxia-inducible factor 1 in cancer biology and therapeutics. *Oncogene* **29**, 625–634 (2009).
24. Kaelin, W. G. & Ratcliffe, P. J. Jr. Oxygen Sensing by Metazoans: The Central Role of the HIF Hydroxylase Pathway. *Mol. Cell* **30**, 393–402, https://doi.org/10.1016/j.molcel.2008.04.009 (2008).
25. Wenger, R. H., Stiehl, D. P. & Camenisch, G. Integration of Oxygen Signaling at the Consensus HRE. *Sci. STKE.* **2005**, re12–re12 (2005).
26. Bando, H., Toi, M., Kitada, K. & Koike, M. Genes commonly upregulated by hypoxia in human breast cancer cells MCF-7 and MDA-MB-231. *Biomed. Pharmacother.* **57**, 333–340 (2003).
27. Mole, D. R. *et al.* Genome-wide association of hypoxia-inducible factor (HIF)-1alpha and HIF-2alpha DNA binding with expression profiling of hypoxia-inducible transcripts. *J. Biol. Chem.* **284**, 16767–16775, https://doi.org/10.1074/jbc.M901790200 (2009).
28. Brizel, D. M. *et al.* Tumor oxygenation predicts for the likelihood of distant metastases in human soft tissue sarcoma. *Cancer Res.* **56**, 941–943 (1996).
29. Sundfør, K., Lyng, H. & Rofstad, E. K. Oxygen Tension and Vascular Density in Adenocarcinoma and Squamous Cell Carcinoma of the Uterine Cervix. *Acta Oncol.* **37**, 665–670 (2009).
30. Rohwer, N. & Cramer, T. Hypoxia-mediated drug resistance: Novel insights on the functional interaction of HIFs and cell death pathways. *Drug Resist. Updat.* **14**, 191–201, https://doi.org/10.1016/j.drup.2011.03.001 (2011).
31. Mao, C., Livezey, M., Kim, J. E. & Shapiro, D. J. Antiestrogen Resistant Cell Lines Expressing Estrogen Receptor α Mutations Upregulate the Unfolded Protein Response and are Killed by BHPI. *Sci. Rep.* 1–10, https://doi.org/10.1038/srep34753 (2016).
32. Frezza, C. *et al.* Metabolic Profiling of Hypoxic Cells Revealed a Catabolic Signature Required for Cell Survival. *PLoS ONE* **6**, e24411, https://doi.org/10.1371/journal.pone.0024411 (2011).
33. Eales, K. L., Hollinshead, K. E. R. & Tennant, D. A. Hypoxia and metabolic adaptation of cancer cells. *Oncogenesis* **5**, e190, https://doi.org/10.1038/oncsis.2015.50 (2016).
34. Sun, R. C. & Denko, N. C. Hypoxic Regulation of Glutamine Metabolism through HIF1 and SIAH2 Supports Lipid Synthesis that Is Necessary for Tumor Growth. *Cell Metab.* **19**, 285–292, https://doi.org/10.1016/j.cmet.2013.11.022 (2016).
35. Mosesson, Y., Mills, G. B. & Yarden, Y. Derailed endocytosis: an emerging feature of cancer. *Nat. Rev. Cancer* **8**, 835–850, https://doi.org/10.1038/nrc2521 (2008).
36. Wang, Y. *et al.* Regulation of endocytosis via the oxygen-sensing pathway. *Nat. Med.* **15**, 319–324, https://doi.org/10.1038/nm.1922 (2009).
37. King, H. W., Michael, M. Z. & Gleadle, J. M. Hypoxic enhancement of exosome release by breast cancer cells. *BMC Cancer* **12**, 421, https://doi.org/10.1186/1471-2407-12-421 (2012).
38. Brenton, J. D., Carey, L. A., Ahmed, A. A. & Caldas, C. Molecular Classification and Molecular Forecasting ofBreast Cancer: Ready for Clinical Application? *JCO* **23**, 7350–7360 (2005).
39. Lal, S., McCart Reed, A. E., de Luca, X. M. & Simpson, P. T. Molecular signatures in breast cancer. *Methods* **131**, 135–146 (2017).
40. Kang, Y. *et al.* A multigenic program mediating breast cancer metastasis to bone. *Cancer Cell* **3**, 537–549 (2003).
41. Harney, A. S. *et al.* Real-Time Imaging Reveals Local, Transient Vascular Permeability, and Tumor Cell Intravasation Stimulated by TIE2hi Macrophage-Derived VEGFA. *Cancer Discov.* **5**, 932–943, https://doi.org/10.1158/2159-8290.CD-15-0012 (2015).
42. Matsumoto, Y. *et al.* Vascular bursts enhance permeability of tumour blood vessels and improve nanoparticle delivery. *Nat. Nano.* **11**, 533–538, https://doi.org/10.1038/nnano.2015.342 (2016).
43. Miller, M. A. *et al.* Radiation therapy primes tumors for nanotherapeutic delivery via macrophage-mediated vascular bursts. *Sci. Transl. Med.* **9**, https://doi.org/10.1126/scitranslmed.aal0225 (2017).
44. Michiels, C., Tellier, C. & Feron, O. Cycling hypoxia: A key feature of the tumor microenvironment. *Biochim. Biophys. Acta.* **1866**, 76–86, https://doi.org/10.1016/j.bbcan.2016.06.004 (2016).
45. Akinc, A. & Battaglia, G. Exploiting Endocytosis for Nanomedicines. *Cold Spring Harbor Perspectives in Biology* **5**, a016980–a016980, https://doi.org/10.1101/cshperspect.a016980 (2013).
46. Minn, A. J. *et al.* Genes that mediate breast cancer metastasis to lung. *Nature* **436**, 518–524 (2005).
47. Massagué, J. & Obenauf, A. C. Metastatic colonization by circulating tumour cells. *Nature* **529**, 298–306 (2016).
48. Abramson, V. G. & Mayer, I. A. Molecular Heterogeneity of Triple-Negative Breast Cancer. *Curr. Breast Cancer Rep.* **6**, 154–158 (2014).
49. Kim, J.-W., Tchernyshyov, I., Semenza, G. L. & Dang, C. V. HIF-1-mediated expression of pyruvate dehydrogenase kinase: A metabolic switch required for cellular adaptation to hypoxia. *Cell Metab.* **3**, 177–185 (2006).
50. Papandreou, I., Cairns, R. A., Fontana, L., Lim, A. L. & Denko, N. C. HIF-1 mediates adaptation to hypoxia by actively downregulating mitochondrial oxygen consumption. *Cell Metab.* **3**, 187–197 (2006).
51. Semenza, G. L. HIF-1 mediates metabolic responses to intratumoral hypoxia and oncogenic mutations. *J. Clin. Invest.* **123**, 3664–3671 (2013).
52. Jain, S. *et al.* Gold nanoparticle cellular uptake, toxicity and radiosensitisation in hypoxic conditions. *Radiother. Oncol.* **110**, 342–347 (2014).

53. Neshatian, M., Chung, S., Yohan, D., Yang, C. & Chithrani, D. B. Determining the Size Dependence of Colloidal Gold Nanoparticle Uptake in a Tumor-likeInterface (Hypoxic). *Colloids Inter. Sci. Comm.* **1**, 57–61, https://doi.org/10.1016/j.colcom.2014.07.004 (2014).
54. Vaupel, P., Höckel, M. & Mayer, A. Detection and Characterization of Tumor Hypoxia Using pO 2Histography. *Antioxid. Redox Signal.* **9**, 1221–1236 (2007).
55. Place, T. L., Domann, F. E. & Case, A. J. Limitations of oxygen delivery to cells in culture: An underappreciated problem in basic and translational research. *Free Rad. Biol. Med.* **113**, 311–322, https://doi.org/10.1016/j.freeradbiomed.2017.10.003 (2017).
56. Blais, J. D. *et al.* Activating transcription factor 4 is translationally regulated by hypoxic stress. *Mol. Cell. Biol.* **24**, 7469–7482 (2004).
57. Ameri, K. *et al.* Induction of activating transcription factor 3 by anoxia is independent of p53 and the hypoxic HIF signalling pathway. *Oncogene* **26**, 284–289 (2007).
58. Duncan, R. & Pratten, M. K. Membrane economics in endocytic systems. *J. Theor. Biology* **66**, 727–735 (1977).
59. Seib, F. P., Jones, A. T. & Duncan, R. Comparison of the endocytic properties of linear and branched PEIs, and cationic PAMAM dendrimers in B16f10 melanoma cells. *J. Control. Release* **117**, 291–300, https://doi.org/10.1016/j.jconrel.2006.10.020 (2007).
60. Fiorentino, I. *et al.* Energy independent uptake and release of polystyrene nanoparticles in primary mammalian cell cultures. *Exp. Cell Res.* **330**, 240–247, https://doi.org/10.1016/j.yexcr.2014.09.017 (2015).
61. Franovic, A. *et al.* Translational up-regulation of the EGFR by tumor hypoxia provides a nonmutational explanation for its overexpression in human cancer. *Proc. Natl. Acad. Sci. USA* **104**, 13092–13097 (2007).
62. Wang, Y. *et al.* Hypoxia promotes ligand-independent EGF receptor signaling via hypoxia-inducible factor-mediated upregulation of caveolin-1. *Proc. Natl. Acad. Sci. USA* **109**, 4892–4897, https://doi.org/10.1073/pnas.1112129109 (2012).
63. Bourseau-Guilmain, E. *et al.* Hypoxia regulates global membrane protein endocytosis through caveolin-1 in cancer cells. *Nat. Commun.* **7**, 11371, https://doi.org/10.1038/ncomms11371 (2016).
64. Christianson, H. C. *et al.* Tumor antigen glycosaminoglycan modification regulates antibody-drug conjugate delivery and cytotoxicity. *Oncotarget* **8**, 66960–66974, https://doi.org/10.18632/oncotarget.16921 (2017).
65. Nehoff, H., Parayath, N. N. & Taurin, S. The Influence of Drug Loading on Caveolin-1 Mediated Intracellular Internalization of Doxorubicin Nanomicelles *in vitro*. *J. Nanomed. Nanotechnol.* **5**, 197, https://doi.org/10.4172/2157-7439.1000197 (2014).
66. Kang, J. *et al.* Caveolin-1 Modulates Docetaxel-Induced Cell Death in Breast Cancer Cell Subtypes through Different Mechanisms. *Cancer Res. Treat.* **48**, 715–726 (2016).
67. Wang, T. *et al.* Hypoxia-inducible factors and RAB22A mediate formation of microvesicles that stimulate breast cancer invasion and metastasis. *Proc. Natl. Acad. Sci. USA* **111**, E3234–E3242 (2014).
68. Cavadas, M. A. S. *et al.* REST mediates resolution of HIF-dependent gene expression in prolonged hypoxia. *Sci. Rep.* **5**, 17851, https://doi.org/10.1038/srep17851 (2015).
69. Wang, X. *et al.* Insulin Downregulates the Transcriptional Coregulator CITED2, an Inhibitor of Proangiogenic Function in Endothelial Cells. *Diabetes* **65**, 3680–3690 (2016).
70. Seo, K.-S. *et al.* SIRT2 regulates tumour hypoxia response by promoting HIF-1? hydroxylation. *Oncogene* **34**, 1354–1362 (2014).

Acknowledgements

This research was supported by The Royal Society Research Grant RG140331 and Marie Curie FP7 Career Integration Grant 334134 within the 7th European Union Framework Program (F.P.S). W.J.B.'s PhD studentship is supported through the EPSRC Doctoral Training Partnership (EP/M508159/1), University of Strathclyde.

Author Contributions

W.J.B. designed and performed experiments; acquired, analysed and interpreted the data; generated and edited the manuscript. F.P.S. conceived the study, interpreted data and edited the manuscript. Both authors designed the research and discussed the results.

Additional Information

Supplementary information accompanies this paper at https://doi.org/10.1038/s41598-018-30517-3.

Competing Interests: The authors declare no competing interests.

Publisher's note: Springer Nature remains neutral with regard to jurisdictional claims in published maps and institutional affiliations.

Impact of the hypoxic phenotype on the uptake and efflux of nanoparticles by human breast cancer cells

William J. Brownlee[#], *F. Philipp Seib* [#+*]

[#] Strathclyde Institute of Pharmacy and Biomedical Sciences, University of Strathclyde, 161 Cathedral Street, Glasgow, G4 0RE, UK. E-mail: philipp.seib@strath.ac.uk

[+] Leibniz Institute of Polymer Research Dresden, Max Bergmann Center of Biomaterials Dresden, Hohe Strasse 6, 01069 Dresden, Germany

* Corresponding author: Tel. +44 (0) 141 548 2510, E-mail: philipp.seib@strath.ac.uk or philipp.seib@SeibLab.com

Supplementary information

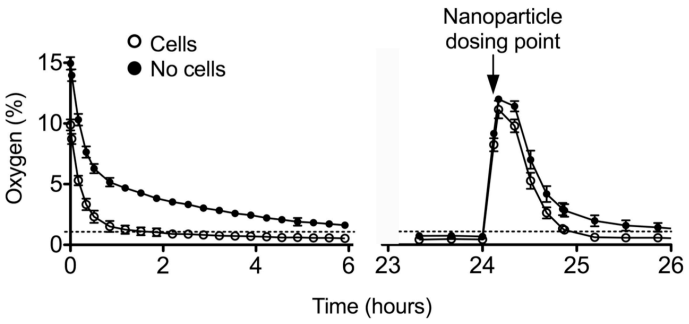

Supplementary Figure S1. Pericellular oxygen monitoring. (a) Magnification of the first 6 hours of culture and (b) oxygen profile during a nanoparticle dosing point emulating re-oxygenation. Data average n=3 ± SD.

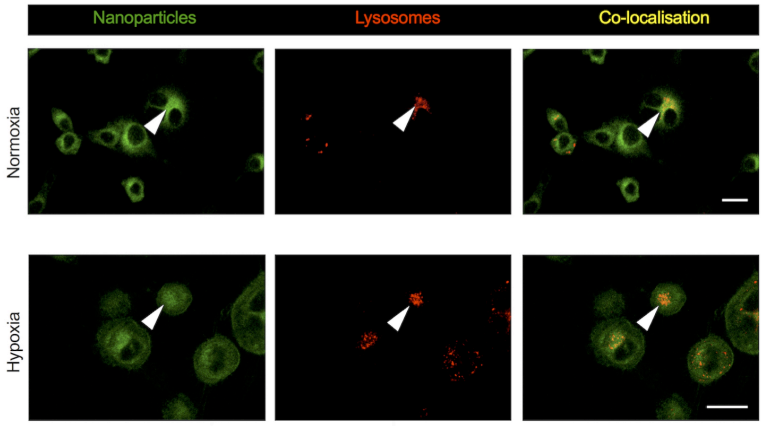

Supplementary Figure S2. uptake of nanoparticles in response to normoxia and hypoxia. Live cell confocal imaging of cells exposed for 24 hours to normoxia or hypoxia and subsequently dosed for 180 minutes with nanoparticles (green). Acidic vesicles were stained using LysoTracker Red. Arrows show nanoparticle co-localisation in acidic vesicles. Scale bar 20 μm

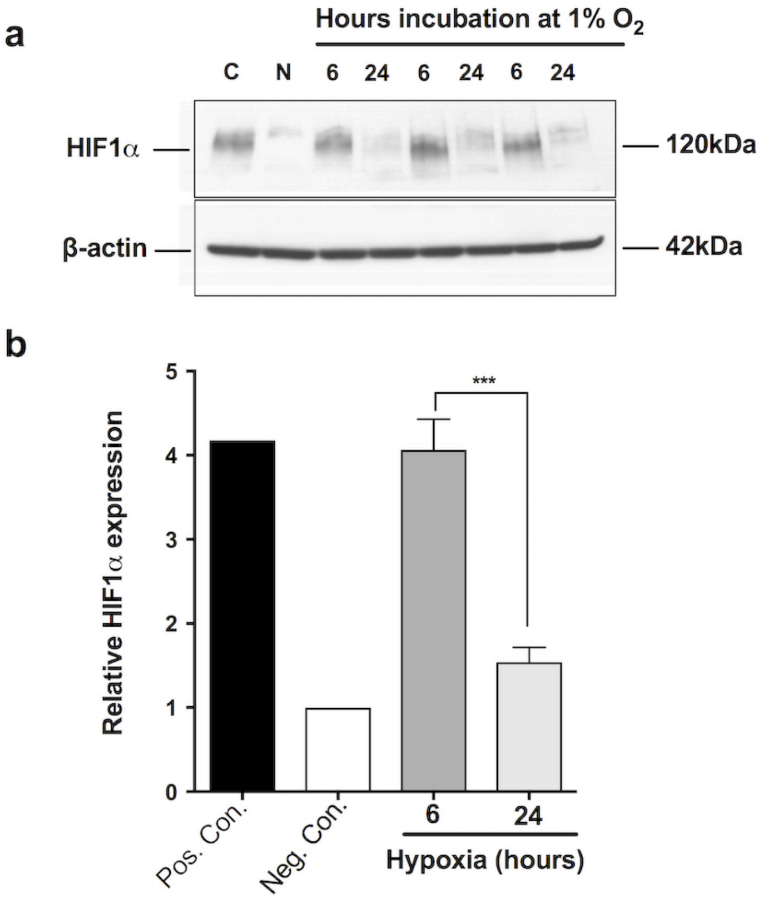

Supplementary Figure S3. SDS PAGE and immunoblotting of cell lysates. (**a**) Blots from 3 independent experiments, stained for unhydroxylated HIF1α (β-actin is loading control); C: positive control; N: normoxic control. (**b**) Densitometry of (a), expressed as fold change relative to normoxia (i.e. set to

1.0); ± SD, *n* = 3 from independent biological experiments. Positive control (Pos Con) cells were treated with 100 μM $CoCl_2$.

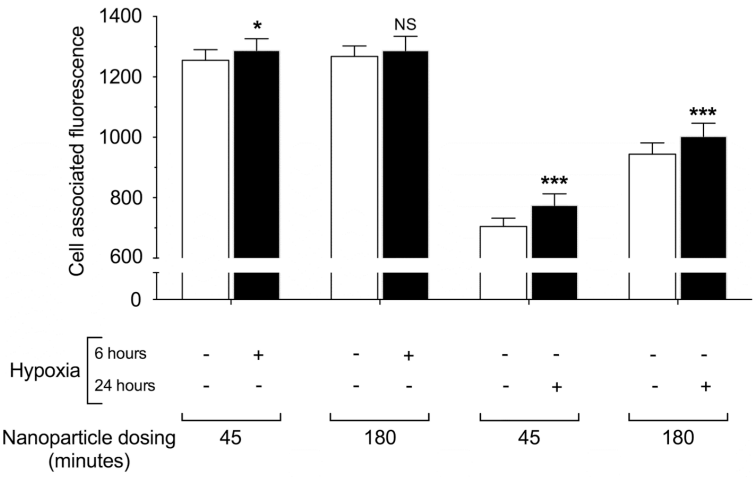

Supplementary Figure S4. Impact of hypoxic preconditioning on the uptake of nanoparticles by human MDA-MB-231 breast cancer cells. Raw data set accompanying Figure 4b. Cells were conditioned in hypoxia (1% O2) for either 6 or 24 hours and then dosed with nanoparticles for either 45 or 180 minutes. Uptake of fluorescent nanoparticles was assessed by measuring mean single cell-associated fluorescence by flow cytometry; ≥10,000 events and n = 15, per treatment group and dosing interval, from 3 independent biological experiments ± SD.

Appendix 2 Accepted conference poster abstracts.

1. United Kingdom and Ireland Controlled Release Society (UKICRS) Annual Symposium and Workshop, University of Strathclyde, Glasgow, Scotland. 30th – 31st May, 2017.

2. Controlled Release Society annual meeting and exposition, Boston, USA. 16th-19th July, 2017. (Unable to attend).

3. Pharmacology 2017. Annual conference of the Pharmacology Society, London, UK. 11th – 13th December, 2017.

Controlled Release Society annual meeting and exposition, Boston, USA, 16th-19th July, 2017. (Unable to attend).

Contribution : Poster presentation abstract (Unable to attend).

In vitro hypoxic pre-conditioning of tumour cells, and nanomedicine internalization.

William Brownlee, Strathclyde Institute of Pharmacy and Biomedical Sciences, University of Strathclyde, Glasgow, SCOTLAND

Abstract Text:

Introduction: Tumour cells adapt to the hypoxic intratumoural environment via a cascade of genomic, proteomic and metabolomic changes. The resulting hypoxic tumour phenotype has been shown to alter cell signaling, endo-lysosomal receptor uptake and recycling. This hypoxic phenotype has potential to undermine the therapeutic potential of nanomedicines, because many nanomedicines are designed for endocytic uptake and require the correct intracellular trafficking in order to release their payload. Tumour cell hypoxic adaptation is mediated via a series of oxygen labile transcription factors, principally hypoxic induction factor 1 (HIF1), which has been shown to exhibit a dynamic expression profile in response to hypoxia. This study was designed to assess the impact which varying time periods of hypoxic exposure had upon the internalization of the model nanomedicine. In parallel, alterations in key cellular stress proteins, including HIF1-alpha, were monitored.

Methods: In vitro modeling of nanomedicine internalisation during hypoxia, was achieved using the human MDA-MB-231 breast cancer cell line, with fluorescent latex nanoparticles (fNP) (diameter 50 nm), as a model nanomedicine. Internalization of fNP at non toxic concentrations was compared following either hypoxic or normoxic incubation (5% CO2, 1% O2 and 87.8% N2, or 5% CO2, 18.6% O2 and 70.2% N2, respectively), for 6 or 24 hours. Cellular oxygen levels were monitored using pericellular oxygen measurement. In tandem, the dynamic changes to key cellular stress proteins in response to the same periods of hypoxic exposure, were assessed using protein arrays. Changes to HIF1-alpha were then confirmed using SDS-PAGE and Western blotting.

Results: Results showed that 24 hour exposure to hypoxia (1% O2, 5% CO2), led to an significant increased in endocytic uptake of fNP at 45 and 180 minutes post dosing, whereas six hours exposure to hypoxia did not. HIF1-alpha expression was found to be elevated following six hours hypoxic exposure, but not elevated following 24 hours hypoxic expression.

Conclusions: This study demonstrates how duration of intratumoral hypoxic conditioning, alters key elements of the hypoxic tumor cell proteome, with parallel altered internalization of a model nanomedicine.

Pharmacology 2017. Annual conference of the Pharmacology Society, London, UK. 11th – 13th December, 2017.

Contribution : Poster presentation.

Impact of hypoxia upon nanomedicine uptake and efflux in a human breast cancer cell line

Biography:
Currently undertaking research as PhD candidate in the Seib Laboratory, Strathclyde Institute of Pharmacy and Biomedicial Sciences, University of Strathclyde, Glasgow, UK.

Author Block: W. J. Brownlee[1], F. P. Seib[1,2]. *[1]Seib Laboratory, Strathclyde Institute of Pharmacy and Biomedical Sciences, University of Strathclyde, Glasgow, United Kingdom, [2]Leibniz Institute of Polymer Research, Dresden, Germany,*

Abstract:

Introduction

Breast cancer cells adapt to the hypoxic tumoral environment via a cascade of significant cellular changes affecting cell signalling, metabolism, endo-lysosomal receptor uptake and recycling[1]. This hypoxic phenotype has the potential to undermine the therapeutic potential of nanomedicines, since many nanomedicines are designed for endocytic uptake and require the correct internalization and intracellular trafficking for effective therapeutic payload delivery. This study was designed to quantify the impact of hypoxic pre-conditioning and simulated reperfusion upon the uptake and release of nanomedicines in the human MDA-MB-231 breast cancer cell line. In parallel, key biological markers of the hypoxic cellular stress response were assessed in response to varying periods of hypoxic exposure.

Method

Modeling of nanomedicine internalisation following hypoxic pre-conditioning and reperfusion, *in vitro*, was achieved using the human MDA-MB-231 breast cancer cell line, with fluorescent latex nanoparticles (diameter 50 nm). Cellular internalization and efflux of nanoparticles at non toxic concentrations was compared following either hypoxic (1% O_2) or normoxic (18.6% O_2) incubation for 6 or 24 hours. Pericellular oxygen measurement was used to confirm cellular hypoxia. In tandem, dynamic changes to key cellular stress proteins in response to the same periods of hypoxic exposure, were assessed using protein arrays. Temporal changes to HIF1α were then confirmed using SDS-PAGE and Western blotting.

Results

Results showed *in vitro* nanoparticle internalisation by our human breast cancer cell line, was increased following 24 hours hypoxic preconditioning, when compared to that following normoxic incubation. Interestingly, the increase was found to be significant for both 45 or 180 minute dosing periods (110.02 ± 1.38 *vs*. 100.0 ± 1.01, $p < 0.001$; 106.3 ± 1.19 *vs*. 100.0 ± 1.01, $p < 0.001$), respectively. $n = 15$, from three separate biological experiments at each dosing interval.

Impact of hypoxia upon nanomedicine uptake and efflux in human breast cancer cells

William. J. Brownlee* and F. P. Seib.

Strathclyde Institute of Pharmacy and Biomedical Sciences, University of Strathclyde, Glasgow, Scotland, UK. *E-mail: william.brownlee@strath.ac.uk

Introduction

- Rational cancer nanomedicine design often depends upon effective endocytic internalisation, and intracellular trafficking for effective therapeutic payload delivery into tumour cells. However, solid tumours are characteristically hypoxic compared to surrounding tissues, and to ensure survival and proliferation, tumour cells undergo a cascade of substantial genomic, proteomic and metabolomic cellular adaptations. Mediated via a family of oxygen labile transcription factors, termed hypoxic induction factors (HIF), this dynamic adaptation to reducing oxygen levels, is also known to disrupt cellular receptor endocytosis, intracellular trafficking and recycling[2]. As a consequence, cancer nanomedicine internalisation and therapeutic payload delivery may be disrupted.

This study was therefore designed to quantify the impact *in vitro* hypoxic exposure and duration has upon effective nanomedicine endocytosis (uptake) and exocytosis (efflux).

Graphical abstract

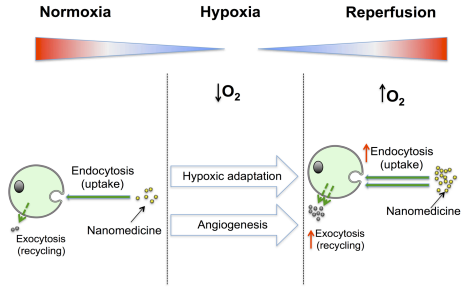

Results

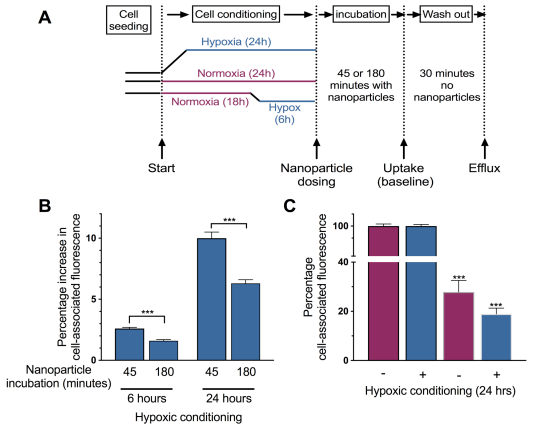

Figure 1. Impact of hypoxic preconditioning on the uptake (endocytosis) and efflux (exocytosis) of nanoparticles by human MDA-MB-231 breast cancer cells.

(A) Outline study scheme
(B) The *In vitro* uptake (endocytosis) of nanoparticles by MDA-MB-231 cells was increased, following 6 or 24 hours hypoxic pre-conditioning.
(C) The *In vitro* efflux of nanoparticles by MDA-MB-231 cells was increased, following 24 hours hypoxic pre-conditioning. Results were normalized to the normoxic treatment mean.

For **(A)** and **(B)** mean single cell-associated fluorescence was measured by flow cytometry; ≥ 10,000 events gated; *n* = 15 for each dosing group and treatment period, 3 independent biological experiments ± SD.

Results

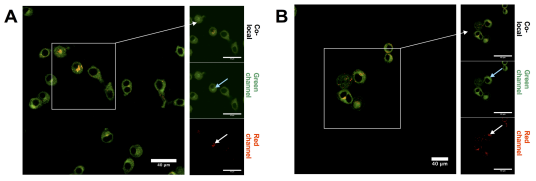

Figure 2. Endolysosomal uptake of nanoparticles.
Confocal microscopy of MDA-MB-231 cells, cultured under normoxic **(A)** or hypoxic **(B)** conditions as monolayers *in vitro*, revealed co-localisation of nanoparticles with lysosomes, indicating endo-lysosomal uptake. Lysosomes were stained using Lysotracker Red. Nanoparticles (blue arrow), lysosomes (white arrow)

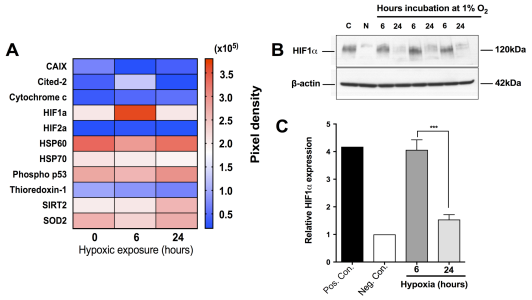

Figure 3. MDA-MB-231 cells exhibited a dynamic HIF1α expression profile, in response to varying periods of hypoxia *in vitro*. Relative expression of key cell stress proteins from MDA-MB-231 cell lysates was determined following *in vitro* hypoxic incubation for either 6 or 24 hours. **(A)** Relative cell stress protein expression heat map. **(B)** SDS PAGE and immunoblotting of MDA-MB-231 cell lysates, stained for unhydroxylated HIF1α, with β actin as internal loading control. **(C)** Densitometry of **(B)**. For both hypoxic exposure periods, *n* = 3 from three separate biological experiments. Results were normalised to the mean, with normoxia set as 1.0. 24 hours normoxic incubation alone, or in the presence of 100μM $CoCl_2$, were used as negative (**N**) and positive (**C**) controls respectively.

Discussion & Summary

- 24 hours hypoxic pre-conditioning of the MDA-MB-231 cell line, significantly increased endocytosis (uptake) and exocytosis (efflux) of our model nanomedicine, compared to normoxic controls.
- Uptake difference, was greater, following 24 hours hypoxia, rather than 6 hours hypoxia
- HIF1α expression was found to be highest following 6 hours hypoxia, falling back to near normoxia levels following 24 hours hypoxia.
- These results are important in developing an understanding of the extent of change induced in nanomedicine uptake within the hypoxic tumour micro-environment.

References

1. Semenza, G. L. The hypoxic tumor microenvironment: A driving force for breast cancer progression. Biochimica et Biophysica Acta (BBA) - Molecular Cell Research 1863, 382–391 (2015).
2. Wang, Y. et al. Regulation of endocytosis via the oxygen-sensing pathway. Nat. Med. 15, 319–324 (2009).

Acknowledgements

This research was supported by a Royal Society Grant RG2014R2 and Marie Curie FP7 Career Integration Grant 334134 within the 7th European Union Framework Program (F.P.S). W.J.B's PhD studentship is supported through the EPSRC Doctoral Training Partnership, University of Strathclyde. Conference travel supported by Fitzpatrick family and Biochemical Society grants.

United Kingdom and Ireland Controlled Release Society (UKICRS) Annual Symposium and Workshop, University of Strathclyde, Glasogw, Scotland. 30th – 31st May, 2017.

Contribution : Poster presentation.

***IN VITRO* NANOMEDICINE INTERNALISATION IN A BREAST CANCER CELL LINE, FOLLOWING HYPOXIC PRE-CONDITIONING.**
William J. Brownlee [1], F. Philipp Seib[1].
[1] Strathclyde Institute of Pharmacy and Biomedical Sciences, University of Strathclyde, Glasgow G4 0RE, United Kingdom.
Background: Tumour cells adapt to the hypoxic intratumoural environment via a cascade of genomic, proteomic and metabolomic changes. The resulting hypoxic tumour phenotype has been shown to alter cell signaling, endo-lysosomal receptor uptake and recycling. This hypoxic phenotype has potential to undermine the therapeutic potential of nanomedicines, because many nanomedicines are designed for endocytic uptake and require the correct intracellular trafficking in order to release their payload. Tumour cell hypoxic adaptation is mediated via a series of oxygen labile transcription factors, principally hypoxic induction factor 1 (HIF1), which has been shown to exhibit a dynamic expression profile in response to hypoxia. This study was designed to assess the impact hypoxic exposure had upon the endocytic uptake of a model nanomedicine. In parallel, alterations in key cellular stress proteins, including HIF1α, were monitored.
Methods: *In vitro* modeling of nanomedicine internalisation during hypoxia, was achieved using the human MDA-MB-231 breast cancer cell line, with fluorescent latex nanoparticles (fNP) serving as a model nanomedicine. Internalization of fNP at non-toxic concentrations was compared following either hypoxic or normoxic incubation (5% CO_2, 1% O_2 and 87.8% N_2, or 5% CO_2, 18.6% O_2 and 70.2% N_2, respectively), for 6 or 24 hours. Cellular oxygen levels were monitored using pericellular oxygen measurement. In tandem, the dynamic changes to key cellular stress proteins in response to the same periods of hypoxic exposure, were assessed using protein arrays. Changes to HIF1α were then confirmed using SDS-PAGE and Western blotting.
Results: Results showed that 24 hour exposure to hypoxia (1% O_2, 5% CO_2), led to a significant increase in internalisation of fNP at 45 and 180 minutes post dosing, whereas six hours exposure to hypoxia did not. HIF1α expression was found to be elevated following six hours hypoxic exposure, but had fallen to near normoxic levels following 24 hours hypoxic exposure.
Conclusions: This study demonstrates how duration of intratumoral hypoxic conditioning alters key elements of the hypoxic tumor cell proteome, with parallel altered internalization of a model nanomedicine.

Hypoxia alters *in vitro* nanomedicine uptake in a breast cancer cell line.

William. J. Brownlee* and F. P. Seib.

Strathclyde Institute of Pharmacy and Biomedical Sciences, University of Strathclyde, Glasgow, UK. *E-mail: william.brownlee@strath.ac.uk

Introduction

- Many nanomedicines depend upon effective endocytic internalisation, and trafficking for effective therapeutic payload delivery into tumour cells.
- Solid tumours are characteristically hypoxic to varying degrees, compared to surrounding normal tissue. Tumour cell survival in this stressful hypoxic environment is therefore dependent upon a cascade of substantial genomic, proteomic and metabolomic cellular adaptations mediated by a family of oxygen labile transcription factors, termed hypoxic induction factors (HIF).
- Tumor cell hypoxic adaptation is also known to disrupt cellular receptor endocytosis, intracellular trafficking and recycling – with potential impact upon successful nanomedicine payload delivery.
- This study was designed to **quantify** the impact *in vitro* hypoxic exposure has upon effective nanomedicine endocytosis, and determine if dosing interval or duration of hypoxia could influence results.

Methods and Materials

- *In vitro* modeling of nanomedicine internalisation, was achieved using the human MDA-MB-231 breast cancer cell line, with fluorescent (FITC) labelled latex nanoparticles (**fNP**) serving as a model nanomedicine.
- Internalization of fNP at non-toxic concentrations was compared following either hypoxic or normoxic incubation (5% CO_2, 1% O_2 and 87.8% N_2, or 5% CO_2, 18.6% O_2 and 70.2% N_2, respectively), for 6 or 24 hours, in a humid 37°C environment .
- In tandem, dynamic changes to key cellular stress proteins in response to hypoxia, were assessed. Changes to HIF1α were confirmed using SDS-PAGE and Western blotting.
- Statistical significance was tested in figures 2 and 3 using Students' *t* test, where *, **, *** and **** denote p<0.05, 0.01, 0.001 and 0.0001 respectively. unpaired ANOVA, with Sidak multiple comparisons test (α = 0.05) was used in figure1. In all cases error bars denote SD, unless indicated otherwise.

Results

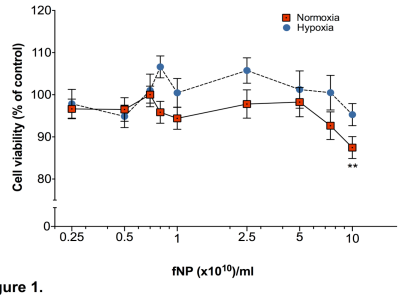

Figure 1.
In vitro MDA-MB-231 cell viability measured by MTT assay over a 48 hour period at the fNP doses shown, as percentage of viability at zero fNP dose, in either hypoxic or normoxic conditions. For each data point n = 18 from three biological replicates. Error bars denote SEM. Significance at each dosing point was compared to zero dose, under respective conditions.

Acknowledgement

This research was supported by a Royal Society Grant RG2014R2 and Marie Curie FP7 Career Integration Gran 334134 within the 7th European Union Framework Program (F.P.S). B.J.W's PhD studentship is supported through the EPSRC Doctoral Training Partnership, University of Strathclyde.

Results

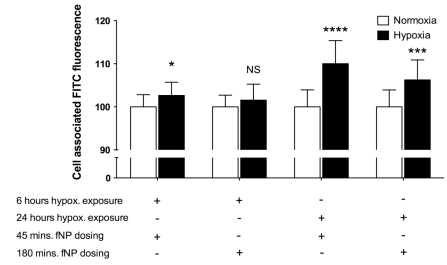

Figure 2.
Hypoxia of 6 or 24 hours duration increases *in vitro* fNP internalisation by MDA-MB-231 cells. *In vitro* comparison of fNP uptake by MDA-MB-231 cells over either 45 or 180 minutes, following exposure to either normoxic or hypoxic incubation for 6 or 24 hours, as measured by cell associated FITC fluorescence. Results were normalized to the normoxic treatment mean in each comparison, with n = 30 from three separate biological experiments for each treatment group and dosing interval.

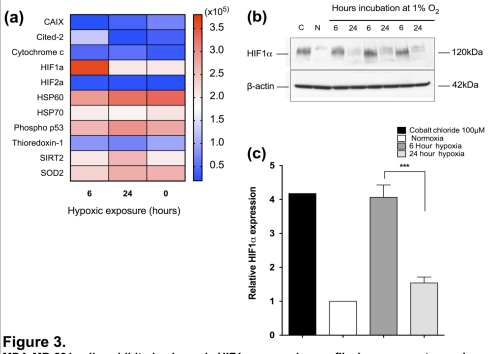

Figure 3.
MDA-MB-231 cells exhibited a dynamic HIF1α expression profile, in response to varying periods of hypoxia *in vitro*. Relative expression of key cell stress proteins from MDA-MB-231 cell lysates was determined following *in vitro* hypoxic incubation for either 6 or 24 hours. **(a)** Relative cell stress protein expression heat map. **(b)** SDS PAGE and immunoblotting of MDA-MB-231 cell lysates, stained for unhydroxylated HIF1α, with β actin as internal loading control. **(c)** Densitometry of **(b)**. For both hypoxic exposure periods, n = 3 from three separate biological experiments. Results were niormalised to the mean, with normoxia set as 1.0. 24 hours normoxic incubation or in the presence of 100μM $CoCl_2$, were used as negative (**N**) and positive (**C**) controls respectively.

Discussion & Summary

- This study demonstrated 24 hours, and to a lesser degree, 6 hours hypoxia, increased nanomedicine internalisation.
- The results also showed uptake was greatest over a 45 minute dosing period, rather than 180 minutes.
- In the MDA-MB-231 cell line, HIF1α expression was found to be highest following 6 hours hypoxia, falling back to near normoxia levels following 24 hours hypoxia.
- These results are important in developing an understanding of the extent of change induced in nanomedicine uptake within the hypoxic tumor micro-environment.

Appendix 3 Competitive grants and prizes awarded.

Competitive funding

1. Awarded 445 GBP of competitive funding as travel grant from The Biochemical Society, to present a poster at Pharmacology 2017.

2. Awarded 345 GBP of competitive funding as travel grant from the Fitzpatrick travel award, to present a poster at Pharmacology 2017.

Academic prizes

1. Awarded First Prize, from over 120 presentations, for best research presentation at annual Strathclyde Institute of Pharmacy and Biomedical Sciences postgraduate study conference.